Distribution Agreement

In presenting this thesis or dissertation as a partial fulfillment of the requirements for an advanced degree from Emory University, I hereby grant to Emory University and its agents the non-exclusive license to archive, make accessible, and display my thesis or dissertation in whole or in part in all forms of media, now or hereafter known, including display on the world wide web. I understand that I may select some access restrictions as part of the online submission of this thesis or dissertation. I retain all ownership rights to the copyright of the thesis or dissertation. I also retain the right to use in future works (such as articles or books) all or part of this thesis or dissertation.

Signature:

_____ _____

Katherine E Squires

Human RGS14: Relationship Between Sequence Variation, Brain Distribution, and Protein Function

By

Katherine Elizabeth Squires
Doctor of Philosophy

Graduate Division of Biological and Biomedical Sciences
Molecular and Systems Pharmacology

_____

John R Hepler, Ph.D.
Advisor

_____

David Weinshenker, Ph.D.
Committee Member

_____

Randy A Hall, Ph.D.
Committee Member

_____

Eric A Ortlund, Ph.D.
Committee Member

Accepted:

_____

Lisa A Tedesco, Ph.D.
Dean of the James T. Laney School of Graduate Studies

_____
Date

Human RGS14: Relationship Between Sequence Variation, Brain Distribution, and Protein Function

By

Katherine Elizabeth Squires
Bachelor of Science, North Carolina State University, 2011

Advisor: John R Hepler, Ph.D.

An abstract of a dissertation submitted to the Faculty of the James T. Laney School of Graduate Studies of Emory University in partial fulfillment of the requirements for the degree of Doctor of Philosophy in Graduate Division of Biological and Biomedical Sciences

Molecular and Systems Pharmacology
2018

Abstract

Human RGS14: Relationship Between Sequence Variation, Brain Distribution, and Protein Function

By

Katherine Elizabeth Squires

Regulators of G protein signaling (RGS) proteins have become appreciated for their diverse and defining roles in the regulation of an array of human physiological processes, including those that manifest as both diseases and traits. While our understanding of the roles of RGS proteins in disease propensity and progression is based largely on knockout studies, our understanding of the diversity of genetic variation reflected in the human population, and whether these genetic variants recapitulate knockout mouse models in the lab, has remained largely unexplored. Population genome/exome sequencing has provided a wealth of human genetic variant data, with which we can mine for functionally-relevant variants in RGS proteins. While loss or mutation of some proteins triggers profound phenotypes and devastating monogenic diseases, loss/mutation of RGS proteins yields more subtle phenotypes, making their contribution to disease harder to study. In this body of work, I define new analytical methods for predicting functionally-relevant variants in human RGS proteins, which participate in complex, polygenic diseases. I then extend these analyses to RGS14, a regulator of long term potentiation and spatial learning. I uncover two human RGS14 variants that disrupt its nuclear-cytoplasmic compartmental balance, and impede its capacity to suppress long term potentiation. To further explore the unique cellular and subcellular localization of human RGS14, we immunolabeled native RGS14 in monkey and human brain, and found broader expression compared to rodents, in brain regions including the basal ganglia (striatum, globus pallidus, and substantia nigra), amygdala, and hippocampus. At the subcellular level, a population of nuclear RGS14 was found, corroborating my findings in neuronal cultures. These studies, combined with my work examining the contribution of human variants tipping the nucleo-cytoplasmic balance, suggest that human carriers may see a loss-of-function of RGS14 in cytosolic compartments such as spines and dendrites, and/or a gain-of-function of RGS14 in the nucleus. The widespread distribution of RGS14 in human brain further suggests that this disequilibrium may have detrimental effects in previously unexplored ways within the basal ganglia and beyond. Overall, I propose RGS14 is a native nucleo-cytoplasmic shuttling protein in the brain, and that human RGS14 has unique localization and sequence diversity uncaptured by previous mouse studies.

Human RGS14: Relationship Between Sequence Variation, Brain Distribution, and Protein Function

By

Katherine Elizabeth Squires
Bachelor of Science, North Carolina State University, 2011

Advisor: John R Hepler, Ph.D.

A dissertation submitted to the Faculty of the James T. Laney School of Graduate Studies of Emory University in partial fulfillment of the requirements for the degree of Doctor of Philosophy in Graduate
Division of Biological and Biomedical Sciences

Molecular and Systems Pharmacology
2018

TABLE OF CONTENTS

List of Figures and Tables

CHAPTER 1:

INTRODUCTION: REGULATORS OF G PROTEIN SIGNALING ARE CRITICAL MEDIATORS OF HUMAN PHYSIOLOGY, TRAITS, AND DISEASE[1]

[1] This chapter has been assembled in part or in whole from the submitted manuscript: Squires KE, Montañez-Miranda C, Pandya RR, Torres MP, and Hepler JR (2017) Genetic Analysis of Rare Human Variants of Regulators of G Protein Signaling (RGS) Proteins and Their Role in Human Physiology and Disease. *Pharmacol Rev*.

1.1. G PROTEIN SIGNALING

Cells communicate by releasing chemical messengers that dictate cell and organ physiology. These messengers include many natural ligands such as hormones, neurotransmitters, cytokines, nutrients, sensory input and other natural molecules. Since most of these messengers cannot cross the outer cell (plasma) membrane, membrane-bound receptors and their cognate heterotrimeric G proteins (Gαβγ) act as cellular transducers. At rest, G protein coupled receptors (GPCRs) are in close proximity with an inactive Gαβγ protein complex, with guanosine diphosphate (GDP) bound to Gα. Upon receptor activation by ligand binding, the chemical message is transduced across the plasma membrane through the receptor to promote the release of GDP from the associated Gα. Due to the high concentration of guanosine triphosphate (GTP) in the cytosol, Gα quickly binds a GTP to form Gα-GTP, which has reduced affinity for both receptor and Gβγ, and thus dissociates. The free Gα-GTP and Gβγ are then able to relate the chemical message to an intracellular cascade of effectors and second messengers that dictate all aspects of cell and organ physiology. The duration of signaling by Gα-GTP and Gβγ is governed by the intrinsic GTPase activity of the Gα subunit (1-5). Upon hydrolysis of the GTP to GDP, Gα-GDP reassociates with Gβγ to terminate signaling. Under normal physiological conditions, a Gα acts as a "molecular switch" capable of turning itself off by GTP hydrolysis. However, researchers noted early on that the rate of GTP hydrolysis by purified Gα proteins *in vitro* was much slower than that observed by Gα in cells, hinting at a missing piece of a the puzzle: cellular factor(s) that govern the off rate of G protein signaling (6, 7).

1.2 A (VERY) BRIEF HISTORY OF REGULATORS OF G PROTEIN SIGNALING

The missing piece was identified based on foundational observations dating back to the early 1980s. SST2, a yeast protein important for mating, was found to regulate sensitivity to pheromones

(8). Later it was shown that SST2 does so via regulation of (9) and physical association with (10) yeast Gα proteins, which share homology to mammalian systems. These findings followed the discovery of a class of mammalian proteins that could enhance the GTPase activity of Ras and Ras-like small G proteins (11), speeding up the turnover of GTP and accordingly the termination of signaling (termed GTPase accelerating proteins, or GAPs). The postulated missing piece, a mammalian GAP for heterotrimeric Gα proteins, was discovered soon thereafter as a family of novel proteins very similar to the yeast SST2 (12-14). These specialized Gα GAPs were named regulators of G protein signaling (RGS), and thus the RGS field was born.

Since their initial discovery, 20 canonical RGS (Figure 1.1) and 19 RGS-like proteins have been identified, and extensive characterization of these proteins has revealed multifunctional roles (15-18). All canonical RGS proteins share a conserved, approximately 120 amino acid RGS domain, which binds active Gα-GTP and catalyzes the transition state of GTP hydrolysis by Gα, demonstrated by the fact that the RGS domains bind preferentially to Gα-GDP activated with the transition state mimetic, AlF_4^- (19). While RGS proteins are classified according to the presence of an RGS domain, we now understand that RGS proteins encompass a wide diversity of multi-domain signaling and scaffolding proteins that are categorized by sequence similarity (Figure 1.1). Further, we have come to appreciate that regulation of G protein signaling is crucial for normal cellular function, and improperly regulated G protein signaling underlies many disease states (20, 21), signifying the potential for RGS proteins as therapeutic targets.

1.3 RGS PROTEIN RARE HUMAN VARIANTS IN COMPLEX DISEASES

Recent genetic analysis of human exomes indicates that an explosion of variants within protein coding regions arose between 5,000-10,000 years ago, leading to diverse human traits and a broad range of potential disease determinants (22). Population and clinical genome sequencing has generated new information regarding the etiology of disease, and the recent release of large-scale genome and exome sequencing data (Genome Aggregation Database, GnomAD, of the Broad

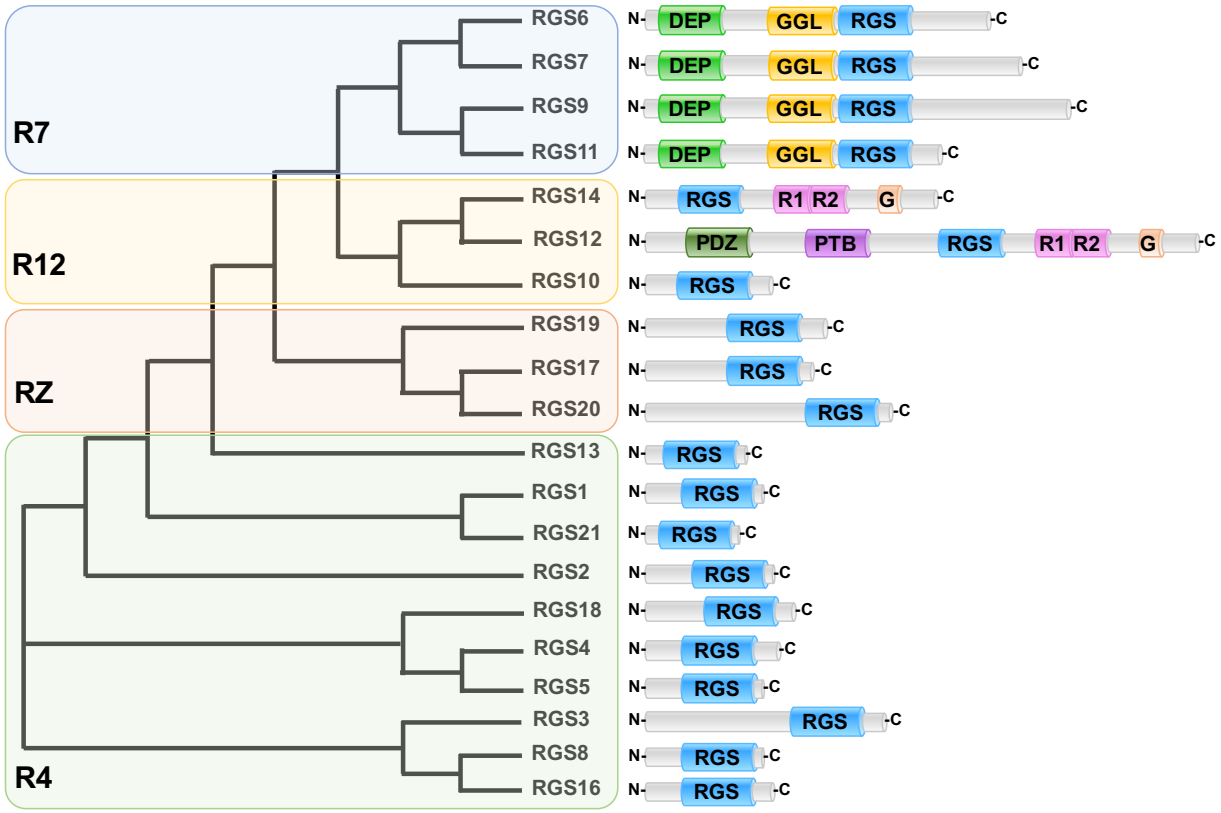

Figure 1.1. Phylogenetic tree of the human Regulator of G protein Signaling (RGS) protein family.

RGS proteins (human sequence) was phylogenically mapped using Clustal W, and each subfamily highlighted by color. The R7 subfamily is labeled in blue, followed by the R12 subfamily in gold, the RZ subfamily in red, and finally the R4 family in green. Protein domains are indicated by color: Blue "RGS" are Regulator of G protein signaling domains, green "DEP" are disheveled EGL10-Pleckstrin homology domains, yellow "GGL" are G protein γ subunit-like domains, pink "R1" and "R2" are Ras/Rap-binding domains, orange "G" are G protein regulator motifs, and lavender "PTB" is phosphotyrosine binding domain.

Institute (23)) has allowed for the analysis and possible discovery of new disease-linked rare variants. While some proteins are functionally well-positioned to participate in monogenic diseases (24, 25), others such as RGS proteins are likely involved in more complex pathways that contribute to disease progression (21, 26, 27). Whereas genetic deletion of the ubiquitously expressed heterotrimeric G proteins can result in severe defects or embryonic lethality (28-34), genetic loss of their more discretely expressed modulators, the RGS proteins, results (broadly speaking) in subtle and less detrimental phenotypes with only a few exceptions (see below). RGS proteins therefore participate in complicated multifactorial physiological processes and disease states (16, 35-38), and large-scale genomic association studies may not be able to detect disease-associated polymorphisms (39). Due to the purifying drive of natural selection, very rare variants (1-2% or less) in fact seem to play a far greater role as genetic determinants of disease compared to the more common and less deleterious polymorphisms (40, 41), an idea supported by the observed inverse relationship between minor allele frequency and disease risk (42). The rarity of these variants means that most carriers are heterozygous, as the likelihood of inheriting the same single nucleotide variant (SNV) from each parent is incredibly low. However, both diseases and traits can arise from heterozygosity. For instance, a single variant allele can cause a dominant negative phenotype (43), an intermediate phenotype (as compared to wild type or knockout) (44), mislocalization to cellular compartments leading to aberrant singling (45), or a change-of-function in other ways.

Given this context, my thesis describes an approach to identify likely deleterious rare human variants (defined here as less than 2% prevalence) in functionally sensitive regions of RGS proteins, with an emphasis on the well-defined RGS domain. Due to the likely involvement of RGS proteins in complex disease states (20), these variants may contribute to a "first hit," leaving the carrier more vulnerable to disease given a secondary insult (e.g. environmental, subsequent mutation of a protein in related signaling pathway, or otherwise). Furthermore, both a loss-of-function (LoF) as well as a gain-of-function (GoF) variant could equally disrupt cellular systems in delicate equilibrium. Thus, I emphasize an un-biased approach that measures a *change-of-function* (CoF),

which encompasses both variant forms. Finally, it is important to consider that, due to cultural practices (and genetic drift), variants may be expressed more commonly or exclusively within a single ethnic group, and may give rise to unique human *traits*, rather than the more obvious and deleterious disease states.

Combined functional analysis

My analysis here takes advantage of cutting-edge bioinformatics, proteomic and structural tools, including combined annotation dependent depletion (CADD) (46), missense tolerance ratio (MTR) (47), and post-translational modification cluster analysis (48, 49). CADD combines multiple *in silico* measurements of conservation, functional protein metrics, regulatory metrics, and more to generate a single quantitative score known as a C-score (46). This C-score measures "deleteriousness" and ranges from 1 to 99, with rankings amongst all 8.6 billion SNVs analyzed by Kircher et. al. C-scores that fall above 10 are within the top 10% of SNVs in their curated dataset, while C-scores above 20 are within the top 1%, and C-scores above 30 are in the top 0.1%, in terms of deleteriousness. Importantly, C-scores correlate well with molecular functionality, disease severity, complex trait associations, and pathogenicity (46). A complimentary score, MTR, is a newly described ratio comparing how much variation exists within a population compared to how much is expected, given intrinsic mutability properties of each codon (47). This score, while similar to d_N/d_S ratios (50), is optimized for intra-species comparison and can identify regions or even individual residues that are likely sensitive to missense mutation, given a very low MTR.

Post-translational modifications (PTMs) play critical roles in regulating and determining protein function, the disruption of which can cause disease (48, 49, 51-53). Inherently, PTMs alter the structure of proteins and therefore have the potential to alter their function as well. In addition, PTMs can have pronounced effects on protein-protein interactions, serving in many cases as "handles" for PTM-specific binding domains (54). There are hundreds of distinct PTMs known to impact eukaryotic proteins (55-57), but only a handful are reported in human RGS proteins (58), including phosphorylation, ubiquitination, acetylation, methylation, and palmitoylation. Reversible

phosphorylation of proteins, the most common form of PTM in eukaryotes, is mediated by kinases and phosphatases (54). A phosphate moiety is typically added covalently to serine, threonine, or tyrosine residues, which alters the structural and chemical nature of the modified residue through the addition of bulk as well as negative charge. Though subtle differences are known to exist between each type of phosphorylation, in general, the PTM can mediate intra-protein conformational changes that can affect protein function (e.g. catalytic activity) (59, 60), but also inter-protein interactions that can facilitate yet additional modification (e.g. ubiquitination) (61), changes in subcellular localization (62), among several other functional effects (63). Ubiquitination, the reversible covalent attachment of the ubiquitin protein to lysine residues and the second most commonly observed PTM to date, is mediated by ubiquitin ligating and deubiquitinating enzymes that can introduce or remove monomeric or polymeric ubiquitin PTMs that often dictate protein fate (64). Whereas polyubiquitination of proteins is a ubiquitous marker for proteasomal degradation, monoubiquitination is often found to control protein trafficking, as in the case of GPCR endocytosis and lysosomal trafficking (65-67). Protein acetylation, like ubiquitination, results from the covalent modification of the epsilon amine of lysine sidechains and is mediated by acetyl transferases and de-acetylases (68). Acetylation is somewhat analogous to reversible phosphorylation, but alters the chemistry of the modified lysine by neutralizing its positive charge. Unlike phosphorylation or ubiquitination, acetylation very commonly also occurs at the amino-terminal ends of proteins (69). Beyond its effects on protein structure and function, modification at lysine sidechains is also known to be important for crosstalk between other modifying enzymes (70) and for regulating protein-protein interactions (71), while N-terminal acetylation serves more generalized roles in regulating protein half-life (72, 73), including that of RGS2 (74). Palmitoylation is another form of reversible acylation, like ubiquitination and acetylation, but occurs on cysteine residues catalyzed by palmitoyl acyl transferases (PATs) and removed by palmitoyl thioesterases (75). In general, the addition of palmitate to proteins serves to regulate their stability, trafficking, and membrane localization. Within G protein signaling systems,

palmitoylation-targeted membrane localization serves essential roles for Gα subunit localization (76, 77), may be involved in GPCR dimerization (78), and has also been shown to regulate the GAP activity of certain RGS proteins (79). Finally, methylation results from the alkylation of arginine or lysine residues catalyzed by residue-specific methyltransferases. Not solely a histone modification, methylation of either lysine or arginine can occur to different degrees resulting in mono-, di-, or tri-methylated states that can further be classified as symmetric or asymmetric in the case of arginine (80, 81). Importantly, the degree to which a residue is methylated can dictate several differences in functional effect (80, 82). Thus, in the following sections I review and discuss the canonical 20 RGS proteins, their noted and crucial PTMs, associated human variants, and their roles in physiology and disease.

1.4 RGS PROTEINS IN PHYSIOLOGY AND HUMAN DISEASE

A. *The R4 Family*

1. R4 Family Overview

Members of the R4 subfamily compose the largest and best characterized of the RGS proteins due to their early discovery and simplicity in structure. R4 family RGS proteins include: RGS1, RGS2, RGS3, RGS4, RGS5, RGS8, RGS13, RGS16, RGS18, and RGS21 (Figure 1.1). All R4 family members exhibit capacity to bind and act as GAPs for both Gαi/o and Gαq (18) proteins, although with varying specificity (83-86) based, in some cases, on subtle structural differences (87). For example, RGS2 demonstrates much greater selectivity for Gαq (83), whereas RGS4 demonstrates greater selectivity for Gαi (84, 88). In addition to the canonical RGS domain, these small RGS proteins also share an N-terminal amphipathic α helix which, in coordination with N-terminal palmitoylation (89), facilitates plasma membrane localization (90-92) and consequent actions on Gα proteins. Outside of this, the N-termini of certain R4 RGS proteins show considerable diversity which determine their specificity for receptor coupling (93, 94) and regulation by cellular protein degradation pathways (95, 96). Thus, although this review focuses

primarily on the conserved RGS domain, it is important for readers to note that human variants in these other protein regions can cause a profound change-of-function phenotype. Table 1.1 contains a brief overview of each protein within the R4 family, its tissue distribution, and its reported links to physiology and disease. Figure 1.1 shows a phylogenetic map of all RGS family proteins, with R4 family proteins highlighted in green.

2. R4 Family Proteins in Human Physiology and Disease

Although not initially recognized as an RGS protein, RGS1 was cloned from activated B lymphocytes as an early activation gene, and designated BL34 (97) shortly before the RGS domain was characterized. Since its discovery, much has been learned about the role of RGS1 in immune physiology and pathology (26). In B and T lymphocytes, RGS1 controls Gαi2-mediated chemotaxis and migration (98, 99). RGS1 knockout mice exhibited abnormal B cell migration, exaggerated germinal center formation, and atypical spleens (100). Unsurprisingly, RGS1 has been linked with multiple T- and B-cell related diseases such as inflammatory bowel disease, multiple sclerosis (101), type 1 diabetes (102) and celiac disease (102, 103). RGS1 has also been implicated in atherosclerosis, and is upregulated in atherosclerotic plaques and aortic aneurysms, where it regulates monocyte and macrophage chemotaxis (104). A recent report demonstrated that elevated RGS1 expression in diffuse large B cell lymphoma was associated with poor overall survival (105). In this light, loss of function variants may play a role in RGS1-mediated immune disorders, or susceptibility to these disorders.

RGS2 is a widely expressed (106) immediate early gene that is induced by various stimuli (107), though it is best understood for its roles in the vasculature and the brain. In the hippocampus, a brain region related to learning and memory, high frequency stimulation (a method used to produce synaptic plasticity and long-term potentiation) induces RGS2 expression (108), and RGS2 knockout mice exhibit impaired basal neuronal activity (109), supporting a role for RGS2 in synaptic plasticity and memory (21). Due to its widespread expression throughout the brain, RGS2

has been linked to many neurological diseases and affective disorders including anxiety, post-traumatic stress disorder, and suicide (110-115). In particular, a variant in the 3' untranslated region of RGS2, rs4606, is associated with reduced mRNA expression of RGS2 (116), and is linked to anxiety (113, 117) and suicide (114, 118). In the periphery, RGS2 is expressed in vascular smooth muscle cells, where it is regulated by nitric oxide and controls vascular relaxation (119, 120). RGS2 knockout mice are hypertensive (121), and hypertensive human patients have reduced RGS2 mRNA compared to controls (116). Further, hypertensive patients were more likely to have a single nucleotide variant (SNV) in the 3' untranslated region, which correlated with RGS2 expression. In a Japanese cohort, several N-terminal coding mutations (Q2L, M5V, and R44H) were associated with hypertension (122). In a subsequent study, it was found that the Q2L mutation destabilized RGS2 protein (but was reversed by proteasomal inhibition), whereas Q2R (another SNV found in both cases and controls) did not (96). A more recent study demonstrated that four human variants including Q2L, R188H, R44H, and D40Y, showed reduced capacity to inhibit Ca^{2+} release by the angiotensin II receptor (123). For further review of RGS2 function in physiology, see Bansal et al (27). Altogether, RGS2 expression has been found to regulate multiple aspects of normal and pathophysiology, and loss-of-function variants would likely generate similar phenotypes to loss of protein. Finally, RGS2 also has been shown to negatively regulate protein translation by binding directly to the eukaryotic initiation factor 2Bε (eIF2Bε) subunit via a 37-amino acid segment within the RGS domain (124), suggesting variants in this region could impact protein translation.

In contrast to RGS2, less is known about RGS3. RGS3 is found in the heart (125), and mouse overexpression studies have shown that it protects against cardiac hypertrophy (126) and also regulates the survival/differentiation responses in multiple cell types (127, 128). In humans, the longest splice variant (and canonical PDZ-containing isoform) RGS3-1 may promote epithelial-mesenchymal transition via WNT signaling (129), and have a role in docetaxel-resistant breast cancer (130). Other reports link RGS3 expression to various types of cancers, mediated by microRNAs which bind the 3' untranslated region to regulate RGS3 expression (131, 132).

RGS4 is selectively expressed in the heart and the brain (125, 133), where its expression and protein stability is tightly controlled by its N-terminus (96, 134). While RGS4 protein in the heart is found at very low levels under normal cardiac physiology (135), it can be upregulated during pathophysiology and cardiac remodeling (136-140). Additionally, RGS4 knockout mice are susceptible to atrial fibrillation (141). A great deal is known about RGS4 in the brain. First, RGS4 mRNA is decreased in the frontal cortex of schizophrenic patients, whereas other R4 family transcripts were not (142). Further, several non-coding SNVs ("SNP1", "SNP4", "SNP7", and "SNP18") are found to be associated with RGS4 expression and schizophrenia diagnosis in multiple populations (35, 143-149). Aside from schizophrenia, RGS4 mRNA levels and SNVs have been linked with Alzheimer's Disease (150) and alcoholism (151). RGS4 is associated with Parkinson's Disease development, via decreased regulation of dopamine receptors and/or muscarinic acetylcholine receptors (152-154), although results are varied (155). In dopamine-depleted mice, a mouse model for Parkinson's Disease, RGS4 is upregulated and inhibits M4 muscarinic auto receptors, an effect which is mimicked by RGS4 infusion onto untreated cells (154). Remarkably, in that study, infusion of an RGS4 construct which lacks the N-terminus (and is less potent at M4 receptors) reversed *native* RGS4-mediated attenuation of M4 signaling in dopamine-depleted mice. That is to say, this dysfunctional RGS4 demonstrated a dominant negative effect on RGS4-mediated cell signaling, *suggesting that fully functional knockouts may arise from only one LoF allele.* This supports the prediction that, while rare variants overwhelmingly occur in a heterozygous manner (as discussed above), diseases and traits can still arise from one minor allele, in this case as a dominant negative effect.

RGS5 is found broadly in tissues including but not limited to the cardiovascular system and brain (156). Although there have been several genome-wide association studies suggesting a link between RGS5 variants and neurological disorders, such as schizophrenia and bipolar disorder (157, 158), it's role is best defined in the vasculature. Here, RGS5 is expressed in arterial smooth muscle cells, and its expression is correlated with protection from hypertension and atherosclerosis

(159-161). Specifically, RGS5 is downregulated in various hypertensive animal models (162, 163) as well as atherosclerotic plaques in non-human primates (164) and humans (165). Further, RGS5 seems to be an important regulator of vascular remodeling, under both normal and pathophysiological conditions (166-168). For example, vascularization of tumors is normalized in RGS5 knockout mice, and immune-mediated destruction of solid tumors was more effective, resulting in greatly improved survival (169). Mouse models also show that blood pressure is reduced in RGS5-null mice (170, 171). Accordingly, a human genome wide screen found RGS5 expression was linked to blood pressure regulation (172). The role of RGS5 in vascular physiology and pathophysiology was recently reviewed (37).

RGS8 appears to be enriched throughout the brain (173), especially in Purkinje cells of the cerebellum (174-176). Interestingly, when RGS8 cDNA is expressed in non-neuronal cells, it accumulates in the nucleus, while in Purkinje neurons RGS8 is found within the soma and dendrites (177). Co-expression with constitutively active Gαo protein, or expression of RGS8 lacking the N-terminus reversed the nuclear localization (175, 178), suggesting either robust nuclear export in Purkinje neurons of RGS8, or a cytosolic-localizing binding partner of RGS8 that is specific to Purkinje neurons versus non-neuronal cells. Further, unlike canonical RGS function on G protein gated potassium channels which accelerate channel desensitization (179-181), RGS8 speeds up both the "on" rate as well as the "off" rate channel kinetics (182). RGS8 knockout mice have been generated, but no overt phenotype or histological abnormality was found (183). Thus, RGS8's role in physiology remains uncertain though likely important for key regulatory processes. While not much is known regarding RGS8 links to human disease, one study found that electroconvulsive seizures in rats caused an increase in RGS8 mRNA in the prefrontal cortex two hours following acute shock, and significantly reduced RGS8 mRNA in hippocampus 24 hours following both acute and chronic shock (184), suggesting a potential role for RGS8 in seizures.

RGS13 is another immune-specific modulator that is expressed in B and T lymphocytes (185, 186), as well as mast cells (187, 188). In B and T cells, RGS13 acts to desensitize chemokine

receptor signaling (185, 186, 189) similar to RGS1, and RGS13 knockout mice have enhanced B cell responses (190). In mast cells, RGS13 constrains allergic responses generated by immunoglobulin E (187, 188), and RGS13 knockout mice exhibit enhanced immunoglobulin E-mediated anaphylaxis. RGS13 transcript is greatly increased in adult T cell leukemia/lymphoma (191, 192) and asthma (193), underscoring both its role in immune cells and the importance of homeostatic balance of RGS13 signaling.

Originally cloned from the retina (194, 195), RGS16 has a relatively broad expression pattern including the heart (196), brain (197), liver (198), and immune system (199-202). RGS16 localization and GAP activity is regulated by addition of a palmitate at multiple cysteine residues (203, 204). As with many R4 family members, one of the most well-defined functions for RGS16 has been its role in adaptive immunity. RGS16 is involved in trafficking and migration of T lymphocytes (185) in response to an allergen challenge (205), and RGS16 knockout mice have an enhanced inflammatory response in the lung (206). Apart from its defined roles in allergic responses, RGS16 also has an intriguing role in regulating circadian systems (207). Within the brain, RGS16 is expressed in both the suprachiasmatic nucleus (SCN) and the thalamus (197, 208). The SCN sets the global circadian clocks through cyclical signaling pathways, where RGS16 expression is cyclical. Loss of RGS16 causes dysregulation in circadian signaling in the SCN as well as delayed, shorter circadian behavioral activity in mice (209, 210). Another component of SCN circadian regulation is feeding behavior, which is synchronized with circadian rhythms co-regulated by the liver. In mice, food anticipatory activity was found to be attenuated in RGS16 knockdown mice during a restricted feeding schedule (209). Complementary studies in the liver showed that RGS16 knockout mice had higher rates of fatty acid oxidation, while mice that overexpress RGS16 had lower rates of fatty acid oxidation and higher blood triglyceride levels (211). Interestingly, in humans noncoding variants in RGS16 have been linked with self-reported “morning people” (212, 213). Finally, RGS16 expression has been linked with various cancers (214-216).

RGS18 expression is mostly confined to bone marrow-derived cells (217-219), more specifically in platelets (220). Though very little is known about RGS18 beyond its expression, mechanistically it seems to be important for regulating platelet activation (221, 222). RGS18 knockout mice have reduced bleeding compared to wild type mice, hyper-responsive platelet activation (223), and reduced platelet recovery following acute thrombocytopenia (224). In humans, RGS18 mRNA is elevated in aspirin-resistant platelets (225), and RGS18 protein was elevated in amyotrophic lateral sclerosis patients (226). Beyond its role in platelets, human SNVs near the RGS18 gene were associated with suicide attempts (227), though no clear mechanism for this is known.

Among the R4 family, RGS21 is the smallest and most recently cloned RGS protein (228). It was originally cloned from bitter and sweet taste cells, although the protein may be expressed much more broadly (229). In bitter taste cells, RGS21 was found to inhibit bitter taste signaling to cAMP, suggesting a role of RGS21 in the gustatory system (230). Since then, human SNVs have linked RGS21 with Celiac Disease (231). Nonetheless, roles for RGS21 in physiology and disease remain largely unexplored.

B. The R7 Family

1. R7 Family Overview

The R7 family of RGS proteins is composed of RGS6, RGS7, RGS9 and RGS11 (Figure 1.1). These are highly homologous proteins mostly expressed in the nervous system where they have a role in neuronal G protein signaling controlling nociception, reward behavior, motor control, and vision (21, 176, 232). The R7 RGS proteins contain distinctive domains that form stable stoichiometric heterotrimeric complexes with accessory binding partners that control protein-protein interaction, subcellular localization, and protein stability (232, 233). Besides the canonical RGS domain, other domains include the disheveled EGL10-Pleckstrin homology (DEP) domain, an R7 homology domain, and a G protein γ subunit-like (GGL) domain (21, 38, 176, 233). The

RGS domain is located at the C terminus, where it stimulates GTP hydrolysis on Gαi/o protein subunits (232, 234-240). The GGL domain, located upstream from the RGS domain, is structurally homologous to conventional γ subunits of G proteins (232, 237) and binds Gβ5 (type 5 G protein β subunit) as an obligatory partner (232), which is crucial for protein stability (21, 232-234). Consistent with the brain expression patterns of R7 family members, various neurological conditions such as anxiety, schizophrenia, drug dependence, and visual complications have been linked with the function of these proteins. Table 1.1 contains a brief overview of each protein within the R7 family, its tissue distribution, and its reported links to physiology and disease. Figure 1.1 shows a phylogenetic map of all RGS family proteins, with R7 family proteins highlighted in blue.

2. R7 Family Proteins in Human Physiology and Disease

RGS6 is highly expressed, at both the mRNA level and protein level, in brain tissue and in the heart (38, 176), with mRNA reported elsewhere. Within heart, RGS6 functions as an essential modulator of parasympathetic activation to prevent parasympathetic override and severe bradycardia (241). Studies relating RGS6 to human diseases are limited, though literature suggests that RGS6-specific modulation of Gα may be involved in regulating several central nervous system diseases such as alcoholism (236), anxiety and depression (242), Parkinson's disease (243), Alzheimer's disease (244), schizophrenia (245) and vision (246). Prolonged exposure to alcohol upregulates RGS6 protein in a brain region known as the ventral tegmental area of wild type mice. RGS6 knockout mice have reduced striatal dopamine, ameliorated alcohol-seeking behavior, and a reduction in alcohol-conditioned reward and withdrawal. RGS6 knockout mice also showed protection from pathological effects of chronic alcohol consumption on peripheral tissues, believed to be due to direct or indirect regulation by RGS6 of reactive oxygen species (38, 236). RGS6 is also enriched in dopaminergic neurons of the substantia nigra pars compacta, which are characteristically lost in Parkinson's disease (38). Studies have shown that RGS6 knockout mice, but not wild type mice, suffered from age-onset neurodegeneration of these neurons by the first

year. These results also correlate with a decrease in gene products associated with differentiation, and maintenance of dopamine neurons during development (38, 247), and whose expression is dysregulated in RGS6 knockout mice (38). Within mouse brain, RGS6 is also expressed in cortical and hippocampal neurons, where it mediates anxiety and depression (236). RGS6 knockout mice displayed spontaneous anxiolytic and antidepressant behaviors that are sensitive to 5-HT1A receptor antagonism (38). Several studies have suggested RGS6 SNVs are significantly associated with multiple central diseases, including Alzheimer's Disease (rs4899412) (38, 244) and schizophrenia (rs2332700) (38, 245). Accordingly, the RGS6 gene can influence the pathophysiological processes underlying Alzheimer's Disease (244, 248, 249). Outside of the brain, atypical RGS6 protein expression is linked to several forms of cancer. A C→T SNV located in the 3' UTR of the RGS6 gene was associated with a 34% reduction in bladder cancer, and an increase in RGS6 protein (rs2074647) (38, 250). RGS6 expression was found to be negatively correlated with human pancreatic cancer (38), human breast cancer progression (38, 251, 252) and resistance to chemotherapies (251). Finally, in roles unrelated to cancer, a splice mutation in RGS6 was identified as a genetic cause of autosomal recessive congenital cataract (ARCC), mental retardation, and microcephaly in two Tunisian siblings (246).

RGS7 is highly expressed in brain, in particular regions linked to anxiety such as the amygdala, hippocampus, brain stem and hypothalamus (173, 253). RGS7 mRNA is found in abundance in neurons of ventral tegmental area and nucleus accumbens (254), which have roles in drug reward and reinforcement. Within this circuit, the euphoric and analgesic effects of morphine are mediated by the μ-opioid receptor. RGS7 knockout mice showed an enhancement in reward behavior, increased analgesia, delayed tolerance, and heightened withdrawal in response to morphine administration (254). Further, chromosome 1q43, which contains the RGS7 gene, has been reported as a risk loci for panic disorder (253), and RGS7 SNV rs11805657 is associated with panic disorder (253, 255, 256). Outside of the brain, GWAS shows modest evidence for the involvement of RGS7 intron variants (rs4660010 and rs261809) in multiple sclerosis. Accordingly, it has been suggested

that alteration in RGS7 function could potentially impair the normal dampening of the inflammatory response, leading to multiple sclerosis (257). Overall, less is known about RGS7's link to physiology and pathophysiology relative to other RGS, and the human variant information provided in this review may prove helpful in defining RGS7's involvement in potential traits or disease.

The RGS9 gene forms two products: a short retina specific transcript variant (RGS9-1) where it acts as a GAP on mammalian photoreceptor-linked G proteins (258), and a long brain-specific transcript variant (RGS9-2) enriched in the striatum (259). The full-length human RGS9-1 consist of 484 amino acids, while RGS9-2 contains almost 200 extra amino acids at its C terminus (259). Both RGS9 variants have an RGS domain and a DEP domain that binds to adaptor proteins such as R9AP (RGS9-1 anchor protein) in the retina, and R7BP (R7 binding protein) in the brain (260). RGS9-1 accelerates the GTPase activity of transducin and co-localizes with other members of the phototransduction cascade (258, 259). During the recovery phase of visual transduction, RGS9 is anchored to a photoreceptor outer segment by R9AP, and mutations in both proteins have been associated with stationary retinal dysfunction syndrome, including RGS9 W299R (261-265). RGS9-1 loss of function in the retina leads to bradyopsia, an inability to see moving objects during sudden changes in light intensity (262). Importantly, variants such as R128X (a nonsense mutation) in RGS9-1 create a truncated gene product lacking important domains crucial for a functional protein (261). RGS9-2 is expressed in the striatum of rat (176, 259), and human brain (259, 266-268), a region highly involved in antipsychotic-induced tardive dyskinesia. Genetic differences in RGS9-2 may play a role in patients developing tardive dyskinesia after antipsychotic treatment, because of RGS9-2 regulation of the D2 dopamine receptor (267, 269-272). Intronic SNVs rs8077696, rs8070231, and rs2292593 were reported to likely alter binding efficiency of RGS9-2 to D2DR and play an important role in the development of tardive dyskinesia (268). RGS9-2 also regulates the μ-opioid receptor (272-275) and modulates reward responses through both opioid and dopamine receptors (272, 276). These neurotransmitter systems regulate feeding behavior and body

weight (272, 277, 278) in addition to reward response (272, 279, 280). A study showed an association between rs3215227 (an intronic variant) and significant higher body mass index in East Asian subjects (272). RGS9-2 involvement in the dopamine reward pathway has suggested its involvement in addiction behavior. Cocaine self-administration in rats shows decreased RGS9-2 levels in the striatum compared with controls (260, 267). RGS9 knockout mice have distinct locomotor-activating actions of dopaminergic or opioidergic agents such as cocaine, amphetamine, or morphine when compared to wild type mice (260, 267, 281). The absence of RGS9 also shows accelerated locomotor sensitization and increased reward sensitivity (260, 274, 281).

RGS11 is highly expressed in the brain, especially in retinal bipolar and nerve cells (282-284), as well as outside the brain (285). RGS11 interacts with mGluR6 at the dendritic tips of ON bipolar cells to regulate light-evoked responses (284). Gβ5 knockout mice have greatly reduced RGS11 expression in the retina, resulting in dysfunctional photoreceptor signaling (282-284). Beyond the brain, recent studies have shown that upregulation of RGS11 might play a role in cancer. RGS11 is highly overexpressed in multiple tumors and associated with increased primary tumor status, nodal metastasis, and disease stage (285). In colorectal cancer, RGS11 is upregulated and involved in chemotherapy resistance (285, 286). While RGS11's role in retinal bipolar and nerve cells has been described, its role in cancer and other diseases remains yet to be fully defined (285).

C. The R12 Family

1. R12 Family Overview

The R12 family is a diverse group of RGS proteins, consisting of three members: RGS10, RGS12, and RGS14. Each has its own unique structure and function, but share a conserved RGS sequence and dynamic nuclear shuttling (62, 287-290). While RGS10 is a small, simple RGS protein that resembles the R4 family members, RGS12 and RGS14 have larger and more complex structures that share homology. Both RGS12 and RGS14 contain accessory domains, including two tandem Ras/Rap-binding domains (R1 and R2) and a G protein regulatory (GPR) motif. The R1

domains of RGS12 and RGS14 each interact with small G proteins such as Rap2 and H-Ras to regulate MAPK signaling (291-294). The GPR motif binds inactive (as opposed to active GTP-bound) Gα proteins and serves as an inhibitor of GDP release (295-298) and also a regulator of RGS protein subcellular localization and membrane attachment (288, 299). RGS12 is expressed in humans as multiple splice variants (300), the longest of which (called Trans-Spliced, "RGS12-TS") contains two additional domains: a PDZ domain and a PTB domain. PDZ domains are important regulators of localization and interaction with binding partners (301). For example, RGS12-TS binds to CXCR2 via its PDZ domain (302) as a means of directing to its target signaling partners. The PTB domain binds phosphotyrosines, and one report demonstrated that the PTB domain of RGS12 can attenuate PDGF-induced pERK (303). The demonstrated roles of these accessory domains are important to consider in RGS protein function/regulation beyond the canonical RGS domains highlighted in our review here. Table 1.1 contains a brief overview of each protein within the R12 family, its tissue distribution, and its reported links to physiology and disease. Figure 1.1 shows a phylogenetic map of all RGS family proteins, with R12 family proteins highlighted in gold.

2. R12 Family Proteins in Human Physiology and Disease

RGS10, at 20 kDa, is one of the smallest RGS family proteins, and is highly expressed in the brain and immune system (176, 304). In humans, there are three splice variants of RGS10, differing by only a few amino acids at the N-terminus. However, these small differences can have a substantial effect on RGS10 function, as the shortest splice variant (lacking only 14 amino acids) has impaired GAP activity (305). RGS10 is also dynamically regulated within the cell. Palmitoylation of an N terminal cysteine targets RGS10 to the plasma membrane and enhances its GAP activity (79), while phosphorylation of a C terminal serine targets RGS10 to the nucleus and impedes its GAP activity (62). RGS10 has been documented in the nuclei of microglia and neurons (287), where it may serve to regulate neuroinflammation. Indeed, RGS10 has been shown to

promote survival of dopaminergic neurons via regulation of neuroinflammatory pathways in nigrostriatal circuits (306, 307), implicating a neuroprotective role for RGS10 in dopaminergic disorders such as Parkinson's Disease (308). Interestingly, a polymorphism (V38M or V44M in canonical sequence) in RGS10 was found in Japanese patients with Schizophrenia, but it was not found to be significantly associated with disease due to sample size (309). In peripheral immune cells, RGS10 regulates macrophage activation (310) and platelet activation (311) and T lymphocytes (312), with potential roles in clotting or autoimmune diseases. Additionally, loss of RGS10 in aged mice is linked with dysregulated peripheral immune cells and inflammatory cytokines (313). Last, there is a curious link between RGS10 and chemoresistant ovarian cancer (314-317), potentially via a Rheb-GTP/mTOR pathway (318). A comprehensive review of the roles of RGS10 in neurons and immune cells was recently published (319).

RGS12, in contrast to RGS10, is the largest RGS protein family member, with multiple splice variants ranging in size from 55 kDa to 155 kDa. As outlined above, RGS12 contains additional signaling domains other than an RGS domain (302, 320, 321) that interact with various proteins. Beyond this, RGS12 also has been shown to interact with calcium channels in neurons (322, 323) and *de novo* mutations have been linked with schizophrenia (324). RGS12 expression has been reported throughout the body, including the brain, lung, testis, heart, and spleen (320, 325). Like RGS10, RGS12 also shuttles in and out of the nucleus where it has been shown to repress transcription (290, 326). RGS12 is also expressed in osteoclasts, and regulates differentiation (327). Accordingly, RGS12 knockout mice have aberrant bone mass (328, 329), suggesting a potential role in osteoporosis. Finally, RGS12 has been linked with cardiac hypertrophy (330) and various cancers (331, 332).

RGS14 is a ~60 kDa protein within the R12 family that is expressed in brain, heart, and spleen of rodents (320, 333, 334). Although its brain expression pattern in adult rodents is largely limited to hippocampal area CA2, RGS14 has a wider brain distribution pattern in monkey and human brain (335), including multiple nuclei of the basal ganglia. Of note, within striatum of monkey

brain, RGS14 appears to express several shorter splice variants not observed in rodent (335). Although RGS14 has not been conclusively linked with any specific diseases in the brain, GWAS identified RGS14 as a risk factor for multiple sclerosis (336), and a follow-up mouse study confirmed differential expression in a mouse model of multiple sclerosis (337). RGS14 also suppresses hippocampal-based synaptic plasticity and learning in the CA2 region of the hippocampus in mice (338), which has been linked to social and contextual memory (339-342). While RGS14's role in these behaviors has not yet been fully elucidated (16), its high level of expression in area CA2 suggests it may be a key regulator of hippocampal-based learning and memory. Outside of the hippocampus, RGS14's role within the basal ganglia suggests a link to movement disorders, such as Parkinson's Disease, and transcriptional studies of Parkinson's patients showing decreases in RGS14 mRNA support a possible role in this process (343). In the periphery, RGS14 expression is down-regulated in failing human hearts, which suppresses cardiac remodeling through regulation of the MEK/ERK pathway (334). RGS14 interacts with active H-Ras-GTP and Raf-1 and to block ERK signaling (291-293), and RGS14 actions on cardiac remodeling presumably are mediated through one or both Ras/Rap-binding domains on RGS14 (334), highlighting the importance of accessory domains on RGS protein functions independent of the canonical RGS domain. Finally, multiple genetic studies have found variants in the proximity of the RGS14 gene that are associated with kidney disease (344-346) and altered serum concentrations of both parathyroid hormone (347) and phosphorous (348), implicating a potential role for RGS14 in regulating the homeostasis of serum phosphate and other ions.

D. The RZ Family

1. RZ Family Overview

The RZ family is composed of RGS17, RGS19 and RGS20. These all are small simple RGS proteins similar to the R4 family members. However, unique to the RZ family members is a conserved string of cysteine residues found near their N-termini that is palmitoylated and regulates both their membrane localization and interaction with binding partners (349, 350). RZ proteins also

function as adapter proteins for Gα subunit degradation, and play important roles in the regulation of signaling and cytoskeletal events in the brain (351). They are also highly conserved in metazoans, and most closely related to the R4 RGS family (349, 352). All members of this family can bind to certain members of the Gαi and Gαq subfamily, but with some selectivity (351, 353, 354). Table 1.1 contains a brief overview of each protein within the RZ family, its tissue distribution, and its reported links to physiology and disease. Figure 1.1 shows a phylogenetic map of all RGS family proteins, with RZ family proteins highlighted in red.

2. RZ Family Proteins in Human Physiology and Disease

RGS17, also known as RGSZ2, demonstrates GAP activity for Gαi/o, Gαz and Gαq (355). In humans, RGS17 is expressed in the nucleus accumbens, hippocampus, and putamen, with highest expression found in the cerebellum (351, 356). However, outside the brain, RGS17 has been reported to be overexpressed in human lung adenocarcinomas and prostate cancer (351, 355, 357). In lung, colon, and prostate tumor cell lines, knocking down RGS17 results in decreased tumor growth and tumor cell proliferation; conversely, overexpression of RGS17 in these cell lines resulted in increased tumor growth (355, 357). Underscoring this, SNVs in the first intron of the RGS17 gene (rs6901126, rs4083914, and rs9479510) are associated with lung cancer (357). RGS17 also is overexpressed in human liver cancer (356). Further, when ovarian cancer cells are treated with chemotherapeutic agents, there is a loss of RGS17 expression, suggesting a role for RGS17 in chemoresistance, perhaps by promoting cell survival via PI3K/AKT signaling in these cells (317, 356). Outside of RGS17 links to cancer, postmortem brain samples from patients with clinical depression show a decrease in RGS17 expression (356, 358). Furthermore, SNVs in RGS17 found in the promoter region (rs596359) and introns (rs6931160, rs9397585, rs1933258, rs9371276, rs516557, and rs545323) are associated with substance dependence (356, 359). Finally, two intronic RGS17 SNVs are associated with smoking initiation, rs7747583 and rs2349433 (356, 360). While possible mechanisms are unknown, expression of RGS17 in brain regions known to be linked

to substance dependence support the relationship between SNVs and these diseases.

Comparatively less is known about RGS19, which is highly expressed (by mRNA) in the heart, lung, and liver, but very low in brain, and seems to regulate proliferation of embryonic stem cells (13, 361). Unlike the other two RZ family members, RGS19 preferentially interacts with Gαi3 (13). One report showed loss of RGS19 slightly enhances opioid-induced analgesia at μ-opioid receptors (362), a brain-specific function that suggests even low expression can have a functional impact. RGS19 expression levels are reportedly upregulated in several disease states including multiple sclerosis (363) and ovarian cancers (364). RGS19 is also highly expressed in human neuroblastoma SH-SY5Y cells (365). However, in other instances, RGS19 has been reported to inhibit Ras activation by upregulating Nm23, a tumor metastasis suppressor (366). Transgenic mice overexpressing RGS19 exhibited multiple heart defects during development, and increased expression of heart failure-related biomarkers including B-type natriuretic peptide and beta-MHC (367). While there are few reports thus far defining RGS19 in human disease, the overexpression studies in mice highlight the potential heart disease contribution of gain-of-function variants.

RGS20, also known as RGSZ1 and Ret RGS, selectively interacts with Gαz and Gαi2 subunits (368, 369). The RGS20 transcript is highly expressed in human caudate nucleus and temporal lobe (368), and RGS20 splice variants are detectable in the eye (370, 371). Loss of RGS20 in mice leads to enhanced μ-opioid induced analgesia and tolerance to morphine (362). Outside the brain, RGS20 is found at significantly high levels in melanoma and metastatic breast cancer cells (370). Furthermore, expression of RGS20 in HeLa, breast adenocarcinoma MDA-MB-231, non-small cell lung carcinoma H1299, and A549 cells results in enhanced cell aggregation, migration, invasion, and adhesion, suggesting a role for RGS20 in tumor metastasis (370). A recent study on triple-negative breast cancer reported RGS20 was overexpressed in those tissues, and that protein expression correlated with disease progression/prognosis, suggesting a novel target for therapy (372). Finally, RGS20 is reported to be significantly associated with hypertension, where it may

synergistically interact with other genes to predispose patients to hypertension (373).

1.5 PHARMACOLOGICAL IMPACT OF HUMAN VARIANTS IN RGS PROTEINS

G protein coupled receptors (GPCRs) have dominated the field of drug discovery for decades, and resulting new therapeutics have revolutionized modern medicine (374). However, despite their success in ameliorating many diseases, drugs that target GPCRs often have off-target effects, making their therapeutic utility less than ideal. In more recent years, drug discovery efforts have turned to new ways of modulating GPCR signaling, including but not limited to such novel approaches as biased agonism (375), positive and negative allosteric modulators (i.e. PAMs and NAMs) (43), and targeting the regulation of G protein signaling via RGS proteins (376). The rationale (377) for targeting RGS proteins would be to: 1) potentiate the effects of "dirty" GPCR agonists, thereby lowering the requisite therapeutic dose and off-target actions; and 2) enhancing specific tissue and/or receptor signaling output when confronted with reduced natural agonist (e.g. depression, neurodegenerative diseases, others). Currently available small molecule modulators that target RGS proteins do so by binding to and blocking RGS domain interactions with Gα (378). The emergence of personal genomics raises the realistic prospect of precision personalized medicine (379). Understanding the specific drug and target mechanism of action, and how that is intertwined with genetic variation, could lead to better predictions of therapeutic efficacy.

As we edge closer to a world with precision medicine, the benefits of understanding the effects of genetic variation on target protein gain-of-function versus loss-of-function will be of great value. If a complex disease is found to be impacted by an RGS protein, particularly by enhancement of the RGS domain/GAP activity, an RGS inhibitor may prove to be a superior target compared to a drug that targets a GPCR upstream of the RGS. For example, RGS5 mediates angiogenesis and, remarkably, vascularization of tumors is normalized in RGS5 knockout mice (169). Thus, normal or gain-of-function variants of RGS5 would promote tumor angiogenesis and, in this case, a

selective targeted inhibitor of RGS5 may make immune-mediated destruction of solid tumors more effective, greatly improving survival. Similarly, if a gain-of-function mutation in the RGS domain of RGS4 for instance (380) is found to underlie an individual's cardiovascular disease, an RGS inhibitor that selectively blocks RGS4 actions such as CCG-203769 (381) may offer therapeutic benefit. By contrast, if a loss-of-function in RGS4 or other RGS protein is found to contribute to disease progression, such an RGS inhibitor may exacerbate the disease and should thus be avoided. A prime example of the power of this analysis is a recent report on RGS2 human variants (123) that are linked to hypertension (122). The authors found that these RGS2 human variants, located in the N terminus, reduced RGS2-mediated inhibition of Ca^{2+} signaling via protein degradation and mislocalization, and provided a mechanism for their association with hypertension. Simply knowing a link between a variant and a disease does not account for functional directionality. Instead, one would rather know whether or not the variant enhances or reduces protein function. Knowing this information becomes important in the case of RGS proteins since they regulate the timing of G protein on/off rates; thus, a drug that stimulates a GPCR may exacerbate the disease state in a patient with a loss-or-gain-of-function variant in a downstream regulatory RGS. Just as mutations in a metabolic enzyme dysregulate intended bioavailability or half-life of a drug, dysregulated RGS proteins may lead to extended or exaggerated drug actions. Therefore, it will be critical to understand how natural genetic variation may affect druggable targets, both current and future.

Although I have focused on the effects of rare human variants within the canonical RGS domain, we must note that other domains and regions on RGS proteins are, in many ways, equally important for RGS protein function. Other RGS protein domains/regions dictate subcellular localization, modify GAP activity, stabilize the protein and engage additional signaling pathways independent of G protein signaling. For example, RGS4 is robustly degraded by an N terminal cysteine degradation signal (96), and genetic modification (C→S) of this N terminal cysteine increases RGS4 protein expression by nearly 50-fold. This could have major implications in

diseases linked with RGS4 expression, such as schizophrenia and alcoholism (142, 151). The subcellular localization of RGS14 is regulated by a C terminal G protein regulatory (GPR) motif (288, 299), which binds an inactive Gα-GDP. Ablation of this interaction may have consequences for the role of RGS14 as a regulator of hippocampal-based learning and synaptic long-term potentiation (338). RGS7 family members all contain DEP domains (binds R7BP) that are important for plasma membrane localization (382), and GGL domains (binds Gβ5) that are essential for protein stability (383). Loss of interaction with either of these critical binding partners would disrupt the function of RGS7 completely independent of the RGS domain, but the DEP domain could, in theory, serve as a beneficial drug target. Indeed, information gained from loss- or gain-of-function genetic variation throughout each of the functional domains of these heterogeneous RGS proteins may provide key insight into the etiology of disease and, should drug modulators become available, may be the best course of treatment. The widespread accessibility of genome sequencing and parallel improvements in *in-silico* predictions of protein functions brings precision medicine and pharmacogenomics much closer to reality. Within this context, modern drug development and usage should take into account whether, and how, natural genetic variation may affect patient responses to therapies targeting complex disease states.

Overview of RGS Protein Distribution and Function						
RGS Family	**RGS**	**Major Tissue Distribution**	**Function**	**Knockout Phenotype**	**Proposed Disease Links**	**Refs**
R4 Subfamily	RGS1	Immune system (B and T lymphocytes, monocytes, natural killer cells, etc)	Suppress chemotaxis	Abnormal B cell migration, exaggerated germinal center formation, and atypical spleens	Diseases of the immune system (inflammatory diseases, B cell lymphomas, etc.)	(100-104)
	RGS2	Cardiovascular system and brain	Vascular relaxation	Impaired basal neuronal activity and hypertension	Anxiety, PTSD, suicide, hypertension	(109-117, 121, 122)
	RGS3	Heart	Still under investigation	Overexpression protects against cardiac hypertrophy	Possible link to cancers	(126, 130-132)
	RGS4	Heart and brain	Respond to cardiovascular stress and modulate neuronal signaling	Susceptible to atrial fibrillation	Schizophrenia, alcoholism	(35, 136-141, 143-151, 384)
	RGS5	Vasculature	Control vascular remodeling	Reduced blood pressure, improved immune-mediated destruction of solid tumors and survival	Hypertension, atherosclerosis, cancer angiogenesis	(159-161, 169-172)
	RGS8	Brain (Cerebellum)	Still under investigation	None noted	Possible link to seizures	(184)
	RGS13	Immune system (B and T lymphocytes, mast cells, etc)	Suppress immune response	Enhanced B cell responses and anaphylaxis	Leukemia/lymphoma, asthma	(187, 188, 190-193)
	RGS16	Retina, heart, brain, liver, immune system	Regulate inflammatory response and circadian rhythms	Enhanced inflammatory response in the lung and dysregulated circadian signaling	Circadian clocks/morning wakefulness	(206, 209, 210, 212, 213)
	RGS18	Platelets	Regulation of hemostasis	Reduced bleeding and hyper-responsive platelet activation	Aspirin resistance, ALS, suicide	(223, 225-227)
	RGS21	Bitter and sweet taste cells	Gustatory sensation	Unknown	Still under investigation	(231)
R7 Subfamily	RGS6	Brain and heart	Regulate drug reward, anxiety, and depression	Protection from alcohol seeking behaviors, anxiety and depression-like behavior; Enhanced dopamine neurodegeneration	Alcoholism, anxiety and depression, Parkinson's disease, Alzheimer's disease, and schizophrenia	(38, 236, 242-245)
	RGS7	Brain	Regulates anxiety and drug reward	Enhanced reward, withdrawal and analgesia, and delayed tolerance to morphine	Panic Disorder and Multiple Sclerosis	(253, 255-257)
	RGS9	Retina; brain striatum	Regulation of photoreceptor	Disrupted striatal dopamine signaling	Retinal dysfunction	(261-265)

			and striatal signaling	related to stimulants and motor deficits		
	RGS11	Retina	Regulation of photoreceptor signaling	Unknown	Retinal dysfunction	(282-284)
R12 Subfamily	RGS10	Brain and immune system	Suppression of neuroinflammation	Enhanced neuroinflammation and neurodegeneration	Parkinson's Disease, possible link to Schizophrenia and chemoresistant ovarian cancer	(306-309, 314-317)
	RGS12	Brain, lung, testis, heart, bone and spleen	Regulates osteoclast differentiation	Growth retardation and increased bone mass	Potential role for osteoporosis	(328, 329)
	RGS14	Brain, spleen, and heart	Regulation of blood calcium homeostasis, LTP regulation	Improved spatial learning	Kidney Disease, possible link to social memory	(338, 344-346)
RZ Subfamily	RGS17	Brain	Regulation of drug dependence	Decreased tumor growth and proliferation	Smoking and substance dependence	(355, 356, 359, 360)
	RGS19	Heart, lung, brain and liver	Potential links to cardiac development and regulation of cell proliferation	Enhanced analgesia and heart defects	Multiple Sclerosis, ovarian cancers	(363, 364, 385)
	RGS20	Brain and eye	Still under investigation	Enhanced analgesia and tolerance to morphine	Hypertension and breast cancer	(362, 370, 373)

Table 1.1. Summary of RGS distribution, function, disease links, and predicted loss of function effects on human physiology.

Here we summarize the broad tissue distribution and characterized function on physiology for each RGS family member. Note that this is not an all-encompassing list, but rather where each RGS is best defined. Disease links are sourced from human studies when available and animal studies otherwise, usually correlative data between disease phenotype and protein or transcript expression, and are described in the text.

CHAPTER 2:

GENETIC ANALYSIS OF REGULATORS OF G PROTEIN SIGNALING (RGS) PROTEINS[2]

[2] This chapter has been assembled in part or in whole from the submitted manuscript: Squires KE, Montañez-Miranda C, Pandya RR, Torres MP, and Hepler JR (2017) Genetic Analysis of Rare Human Variants of Regulators of G Protein Signaling (RGS) Proteins and Their Role in Human Physiology and Disease. *Pharmacol Rev*.

2.1 ANALYSIS OF RARE HUMAN VARIANTS OF RGS PROTEINS

As outlined above, RGS proteins play key roles in human physiology and disease, and rare human variants are thought to underlie many complex human diseases and traits. Therefore, we took advantage of recently available human exome sequencing databases and newly described bioinformatics/proteomic analytical tools to identify rare human variants in canonical RGS proteins that we predict will have a marked change-of-function phenotype. Using knowledge (published structural protein data bank, PDB files) of the binding interface between the RGS domain and partner Gα gained by crystallography and sequence conservation, we focus on individual variants of interest derived from these massive datasets that are likely to disrupt RGS-Gα interactions. Whereas a loss-of-function (LoF) or gain-of-function (GoF) may lead to disease states, a GoF in one pathway may in fact lead to a LoF in a completely separate pathway. Thus, as described above, we consider a change-of-function (CoF) that accounts for either LoF or GoF. We postulate that these variants may be missed by genome association studies due to their rarity (1-2% or less), but nonetheless confer the same phenotype (i.e. multiple genotypes may have the same phenotype), or may redirect the RGS function (e.g. by mislocalization) to affect atypical pathways. Given these caveats, here we analyze the entire coding sequence for all 20 canonical RGS proteins (available as supplemental data for the submitted review [Squires KE, Montañez-Miranda C, Pandya RR, Torres MP, and Hepler JR (2017) Genetic Analysis of Rare Human Variants of Regulators of G Protein Signaling (RGS) Proteins and Their Role in Human Physiology and Disease. *Pharmacol Rev*.]), and provide a detailed case study of a representative RGS protein from each subfamily highlighted below (RGS4 from R4, RGS9 from R7, RGS10 from R12, and RGS17 from RZ) (Figures 2.1-2.4).

Selection of rare variants that have potential to produce CoF phenotypes was based on several factors described here. First and foremost, we identified rare variants as those for which prevalence is well below 2% in a given population (for this dataset: min = 0.0009%, max = 1.92%, median =

0.0032%). Second, we used Combined Annotation Dependent Depletion (CADD) analysis, presented as a C-score (Table 2.1), to estimate the potential "deleteriousness" of each variant – a feature that strongly correlates with both molecular functionality and pathogenicity (46). A CADD C-score above 20 (top 1%), which we used as a hard filter, indicates a very high likelihood of deleteriousness (for this dataset: min = 23, max = 35, median = 29.4). Third, we considered structural data and sequence conservation when available (Panel A for Figures 2.1-2.4). Variants that overlap with identified contact points between the RGS domain and Gα provide a strong case for CoF and were selected. Similarly, variants that overlap with highly conserved residues (particularly those that reside in critical regions of the RGS domain as determined by high-resolution structural data) were selected. This criterion was particularly important for eliminating variants that fall on highly variable residues within the family (i.e. if the amino acid properties are not conserved within the family it is likely a noncritical residue). Fourth, we utilized a newly described bioinformatics tool to measure the tolerance of each position in each RGS protein for mutation, expressed as a missense tolerance ratio (MTR) (Panel B for Figures 2.1-2.4, Table 2.1), which estimates the functional sensitivity of a given residue to mutation (47). MTR represents a novel measure of purifying selection acting on missense variants in a 31-codon sliding window across the sequence of a gene. Neutrality, or an MTR of 1.0, represents the point at which the observed number of missense variants is equivalent to the expected number in the sliding window. MTR is a useful tool for interpreting missense variants in the context of monogenic diseases (47), and although may be less predictive in polygenic diseases, is nonetheless reported here (for this dataset: min = 0.5, max = 1.19, median = 0.94) (Table 2.1).

As a further level of analysis, we consider sites of post translational modification (PTM) found in human RGS proteins that, in many cases, overlap with rare variants that exhibit high C-scores (Panel B for Figures 2.1-2.4). As outlined above, PTMs serve critical regulatory roles in protein function and are often overlooked or missed in disease assessment (49). A recent advance in the analysis of PTMs (48, 49, 386) offers a powerful bioinformatics/proteomics tool for characterizing

experimentally verified PTMs in the context of their alignment within protein or domain families (i.e. Modified Alignment Positions, MAPs), and provides a functionally impactful analysis that is complimentary to CADD and MTR data. This approach has shown further promise in the discovery of PTMs associated with disease-linked mutations (49). Therefore, we surveyed the coincidence of PTMs/MAPs and mutations within each RGS protein, with the goal of highlighting positions where CoF might be attributable to a change in PTM status. For this purpose, PTMs unique to each human RGS protein are superimposed onto the MTR plots where the specific type of modification (Ph = phosphorylation, Ub = ubiquitination, Ac = acetylation, Pm = palmitoylation) is noted above the graph and the median, 25%, and 5% MTR values are indicated by a horizontal red, grey, and green lines, respectively, for representative family members (Panel B for Figures 2.1-2.4). In each case, only positions found to be modified in the given human RGS protein are shown (Figures 2.1-2.4, red circles). Within the RGS domain of each protein, the size of each PTM site reflects the total number of PTMs observed within the domain MAP, whereas positions outside the RGS domain simply indicate the position of a single PTM for the given protein. Each PTM site is further annotated to indicate when there is evidence of function for the PTM in the given protein (green outer ring) or evidence for function within the MAP for the domain family (red outer ring). Disease-linked variant positions are also indicated (orange circles). Although not included in our primary analysis, we also report "neighboring PTM" count (Table 2.1), which is a summation of reported PTMs found within a +/-7 residue window surrounding the human variant. Variants that fall within this window may in fact conflict with the ability of a modifying enzyme to dock on the target protein. We therefore indicate in our analysis below when this occurs, and propose this may be one mechanism for a CoF phenotype. Notably, in each RGS protein case study we present, the RGS domain is both under mutational selective pressure and is a hotbed for PTM activity, supporting the idea that disruption of these domains by mutation is likely to alter critical cellular functions.

Taking all of this information into account, we plot the genic distribution of both missense (Top of Panel C for Figures 2.1-2.4) and silent (Bottom of Panel C for Figures 2.1-2.4) variants for each

RGS protein, along with a mapping of the selected rare variants of interest onto the protein sequence (Panel D for Figures 2.1-2.4). These selected variants, identified from the predictive criteria, are finally placed onto the reported crystal structure of the RGS protein (Panel E for Figures 2.1-2.4) and listed in Table 2.1. Importantly, while our focus and discussion is centered on the RGS domain of each protein subfamily, we present the comprehensive set of missense variants, MTR, CADD C-score, and PTMs for the entire sequence of all 20 canonical RGS proteins (supplemental data in submitted manuscript). Lastly, we validate this overall approach by testing one of the selected variants for RGS4 to show that this variant, as predicted, results in a profound CoF phenotype (Figure 2.5). I propose that this overall approach and dataset can be used and expanded to other individual RGS proteins across each family (and any protein family in general), as well as other functional domains (described in Chapter 3) to prioritize rare variants and PTMs for CoF studies and improved understanding of human pathophysiology.

2.2 METHODS

Immunoaffinity capture of the RGS4:Gαi1 complex from cells

HEK293 cells were transfected with Venus-RGS4 (WT or R134W) and Gαi1-Luciferase. Cells were washed with ice cold PBS, and then lysed with AlF_4^- lysis buffer (50mM Tris, 150mM NaCl, 1mM EDTA, 2mM DTT, 5mM $MgCl_2$, 1% Triton X-100, protease inhibitors, 10mM NaF, 9mM $MgCl_2$, 30μM $AlCl_3$). Cells rotated end-over-end for 1.5 hours at 4°C. Samples were then centrifuged for 10 minutes at 13,000 RPM at 4°C, and 30μL of cell lysate was collected for input. Protein G sepharose (GE Healthcare) (50μL) was washed 3x with 1mL of ice cold PBS, and then incubated for an hour with 3% BSA (bovine serum albumin) rotating at 4°C. Beads were spun down, 3% BSA was removed, and lysates were added to beads with 2μL anti-GFP (MBL) to rotate for 1.5 hours at 4°C. Beads were then centrifuged for 30 seconds at 3000 RPM at 4°C, washed 4x with 1mL of ice cold wash buffer (0.1% Tween-20 in 1x PBS with AlF_4^-), and boiled in Laemmli buffer for 5 minutes. 13% SDS-PAGE separated samples and nitrocellulose membranes were

blotted with anti-Renilla Luciferase (Millipore, 1:1000) and anti-GFP (MBL, 1:1000). Secondary antibodies used were goat anti-mouse (1:5000) and goat anti-rabbit (1:25000), respectively.

Bioluminescence Resonance Energy Transfer (BRET)

For variant and wild type RGS4, we generated RGS4-Luciferase (RGS4-Luc) fusion constructs, a tag suitable for bioluminescence resonance energy transmission (BRET) which emits light at 485nm in the presence of 5 μM coelenterazine H (CTZ) (387). In combination with a YFP-tagged Gαi1 (Gα-YFP), RGS4-Luc will transfer energy to Gα-YFP upon binding, thereby producing a 535nm emission BRET signal. We incubated AlF4- with cells expressing RGS4-Luc and Gα-YFP to mimic the transition state of Gα and recruit RGS4 binding for 30 minutes and then recorded emissions at 485nm and 535nm following CTZ activation. Net BRET was calculated by dividing the emission at 535nm by the emission at 485nm, and then subtracting background signal of 485nm alone.

Missense Tolerance Ratio

We calculated missense tolerance ratio as recently described (47). Briefly, we used a 31-codon sliding window using the following calculation:

$$MTR = \frac{\sum[missense_{obs}] \,/\, \sum[missense_{obs} + synonymous_{obs}]}{\sum[missense_{expected}] \,/\, \sum[missense_{expected} + synonymous_{expected}]}$$

where observed variants ("obs") were reported variants from the GnomAD database and expected variants were calculated from all possible codon variations.

Post-Translational Modification Alignment Analysis

PTM alignment analysis is based on the SAPH-ire model as described previously (49) but was restricted to report only PTM count as described below. To account for the diverse domains observed across the different proteins of the RGS protein family, a domain specific analysis was performed for all domain families observed within the RGS superfamily. Seven domains seen across RGS proteins were analyzed, namely DEP: disheveled, EGL-10, pleckstrin homology domain; DHEX, DEP helical extension (IPR000591), GGL: Gγ subunit-like domain (IPR015898),

GPR/GoLoco: G protein regulatory motif (IPR003109), PDZ: domain present in PSD-95, Dlg, and ZO-1/2 (IPR001478), PTB: phospho-tyrosine binding domain (IPR006020), RBD: Raf-like Ras binding domain (IPR003116), and RGS domain (IPR016137; the focus of this review). The domain sequences for all RGS proteins belonging to each of these domain families were obtained from Interpro (388). The multi-FASTA files generated for each domain family were subsequently aligned using MUSCLE using default parameters (389). Modified Alignment Positions (MAPs), domain family alignment positions that harbor at least one experimentally verified PTM specific to human RGS proteins, were coalesced and the PTM count within each determined by the sum of human family members for which experimental PTM has been observed and curated in the public domain via dbPTM and Phosphosite Plus (55, 390). PTMs outside the RGS domain and specific to each given RGS protein are reported as single observations though may, in many cases, coalesce into MAPs of other domain families (data not shown). Non-domain PTMs and RGS domain MAPs were related directly to mutation data based on UniProt ID and native position anchor sequences (391), and plotted with respect to the MTR value at each native position.

2.3 R4 FAMILY: RGS4 RARE VARIANTS

Among the R4 subfamily of RGS proteins, RGS4 is perhaps the best characterized with abundant functional information including the first solved RGS protein crystal structure (19). Therefore, RGS4 is well suited as a "case study" for analyzing and predicting change-of-function (CoF) human variants within the R4 family. Consistent with this idea, a human mutation in RGS4, S30C, has previously been reported to display a gain-of-function phenotype (enhanced GAP activity) that translated to RGS16 when an analogous mutation was made (380). This demonstrates the idea that insights gained from mutational analysis in one RGS protein may extend to other close family members, though here we emphasize variants unique to each individual RGS protein.

Human RGS4 has five reported splice variants with predicted sizes ranging from 93-304 amino acids (392). The RGS4 variants in the GnomAD database (23) are reported with respect to the

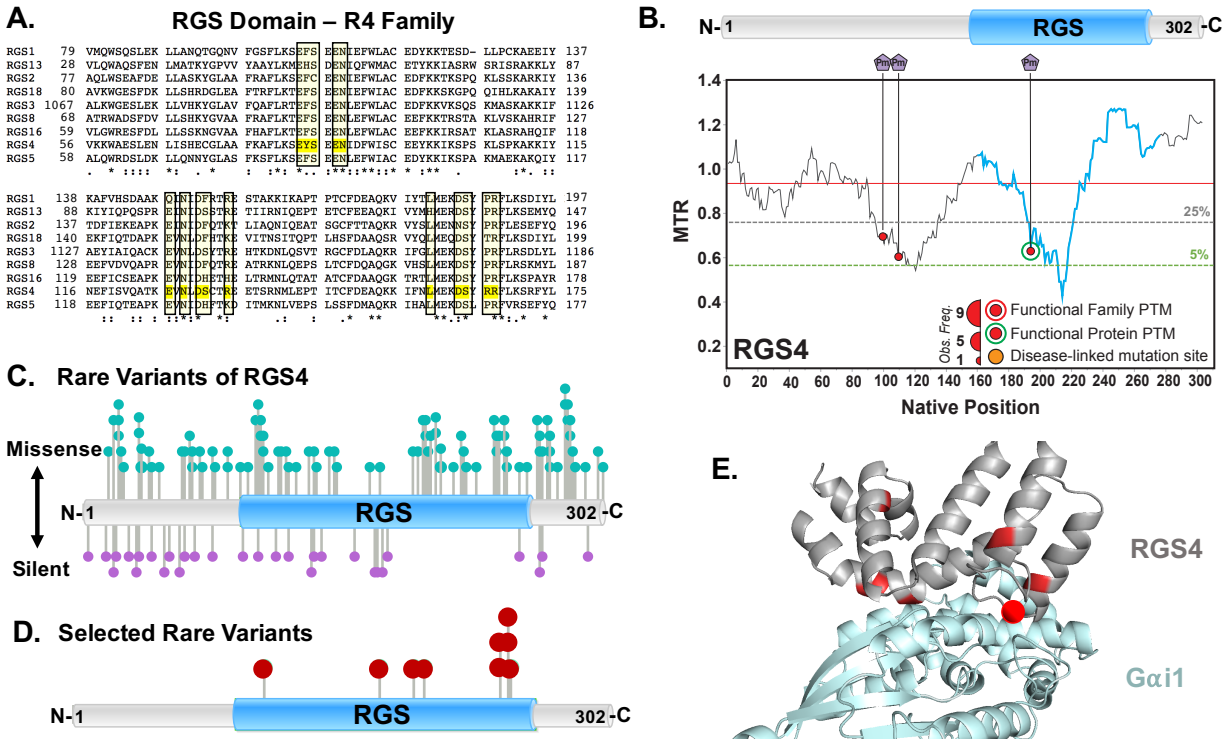

Figure 2.1. The R4 Subfamily of RGS proteins: Analysis of RGS4 human variants.

A) *Clustal W was used to align sequences of the RGS domains within the R4 subfamily of human RGS proteins. The RGS4:Gαi1-AlF_4^- crystal structure (PDB: 1AGR) was used to extract residues on RGS4 critical for interaction with Gαi1 (highlighted in yellow). We then added pale yellow-filled boxes to extend this information to all R4 subfamily members.* ***B)*** *Missense Tolerance Ratio (MTR) and Post-Translational Modification (PTM) cluster analysis plot for RGS4 (see text for details). The RGS domain of RGS4 (highlighted in blue) is under selective pressure, indicated by a low MTR (median, red line; 25%, grey dashed line; 5%, green dashed line). RGS4 is palmitoylated on three residues, and although one is found to be mutated in the human population (GnomAD version 2.0), it is not located within the RGS domain and therefore not highlighted in this analysis (but see Table S1, Supplemental data)* ***C)*** *Rare Human Variants of RGS4 plotted along the sequence using Lollipops (https://github.com/pbnjay/lollipops). Missense (amino acid change) variants are displayed on top in teal, while silent (no amino acid change) variants are displayed on the bottom in purple.* ***D)*** *From our analyses, we selected nine variants in the RGS domain predicted to have a change-of-function phenotype, and mapped them onto the RGS4 sequence using Lollipops (https://github.com/pbnjay/lollipops).* ***E)*** *These selected variants are mapped onto the reported crystal structure (PDB: 1AGR) of RGS4 (grey, selected residues in red) in complex with Gαi1-AlF_4^- (light blue).*

longest splice variant (RGS4-3), which adds almost one hundred amino acids to the N terminus of the commonly used canonical human RGS4 reference sequence (RGS4-1; 205 amino acids) (392). Therefore, for our purposes here, we list first the reported variant amino acid location within the longer RGS4-3 sequence followed by the canonical residue position in parentheses (Table 2.1). In our analysis of RGS4, we first compare an alignment of all R4 family members and identify residues that are contact points for Gα highlighted in yellow, as determined by x-ray crystallography (19) (Figure 2.1A). Conserved RGS:Gα interface contact regions across R4 family members are highlighted by boxes. Next, we examine MTR for our case study protein, RGS4 (Figure 2.1B), with reported PTMs unique to human RGS4 plotted onto the MTR data and identified above. From this analysis, it is clear that the RGS domain of RGS4 is under selective pressure, suggesting that human variants in this region are likely to change the function of the protein. Thus, we take advantage of the reported crystal structure for RGS4 in complex with Gαi1 (19), extracting information about contact points between the two proteins. From these structural, PTM, and CADD analyses, we identified nine variants including: E214(117)K, D227(130)G, D260(163)N, D260(163)G, R264(167)C, L170(73)P, R231(134)W, R263(166)C, and R263(166)H (Figure 2.1C-D, Table 2.1). Of these, E214(117)K (C-score 27.3), D227(130)G (C-score 29.6), D260(163)N (C-score 32), D260(163)G (C-score 29.4), and R264(167)C (C-score 35) are all highly or completely conserved residues among the R4 family (Figure 2.1A) and participate in salt bridge interactions. Mutation of these residues to a non-charged (as with variants D227(130)G and D260(163)G), or opposite charge (as with variants D260(163)N and E214(117)K) residue is predicted to decrease the stability of an RGS4:Gαi1 complex. L170(73)P (C-score 23) is located within an α helix and is, therefore, predicted to disrupt secondary structure of the RGS domain. Amino acid R231(134) is another highly conserved residue within the family that participates in stabilizing switch III on the Gα subunit, an important interaction for promoting GTP hydrolysis. As such, the R231(134)W (C-score 29.8) variant very likely disrupts RGS4 capacity to interact

with Gα (see below). Finally, R263(166)C (C-score 28.4) and R263(166)H (C-score 24.5) are predicted to disrupt contact between the RGS domain and the all helical domain of Gα. In these cases, disruption of binding to Gα, or disruption of RGS4 capacity to stabilize switch regions on Gα, should similarly affect downstream G protein signaling events and disease states. Table 2.1 lists human variants in RGS4 that are predicted to disrupt RGS4 interaction with Gα, and/or GAP activity.

Further analysis of the RGS4 sequence using PTM alignment analysis identified three residues in human RGS4 that undergo PTM. C99 and C109, both located outside the RGS domain, are palmitoylated. Of note, C109 corresponds to reported human variant C109(12)R and is an important regulator of RGS4 subcellular localization and GAP activity (134). Therefore, this human variant, although not within our focus here on the RGS domain, is predicted to disrupt the function of RGS4 and thus may mimic loss of RGS4 as is the case for multiple diseases described above. In addition, C192(95) located within the RGS domain of RGS4 is palmitoylated, and serves an important role in regulating RGS4 membrane localization and its GAP activity (79). However, this cysteine residue does not correspond with a reported human variant from this dataset. Thus, we mapped our selected rare variants for RGS4 onto the sequence (Figure 2.1D) and structure (Figure 2.1E) of RGS4. In all, we identified nine variants (corresponding to seven residues) within the RGS domain of RGS4 that are predicted to exhibit CoF phenotypes. Below, we take a similar approach to extend our analyses to other RGS subfamilies.

2.4 R7 FAMILY: RGS9 RARE VARIANTS

Unlike the R4 family, the R7 family of RGS proteins are all larger multi-domain proteins (Figure 1.1). Among the R7 subfamily of RGS proteins, RGS9 was chosen as a representative family member to analyze because of its solved protein crystal structure in complex with Gα and known RGS9 links to disease (261-265, 393). Structural insight for the RGS9 RGS domain co-crystallized in complex with a Gαi1/t chimera reveals a mostly charged interface (393), similar to

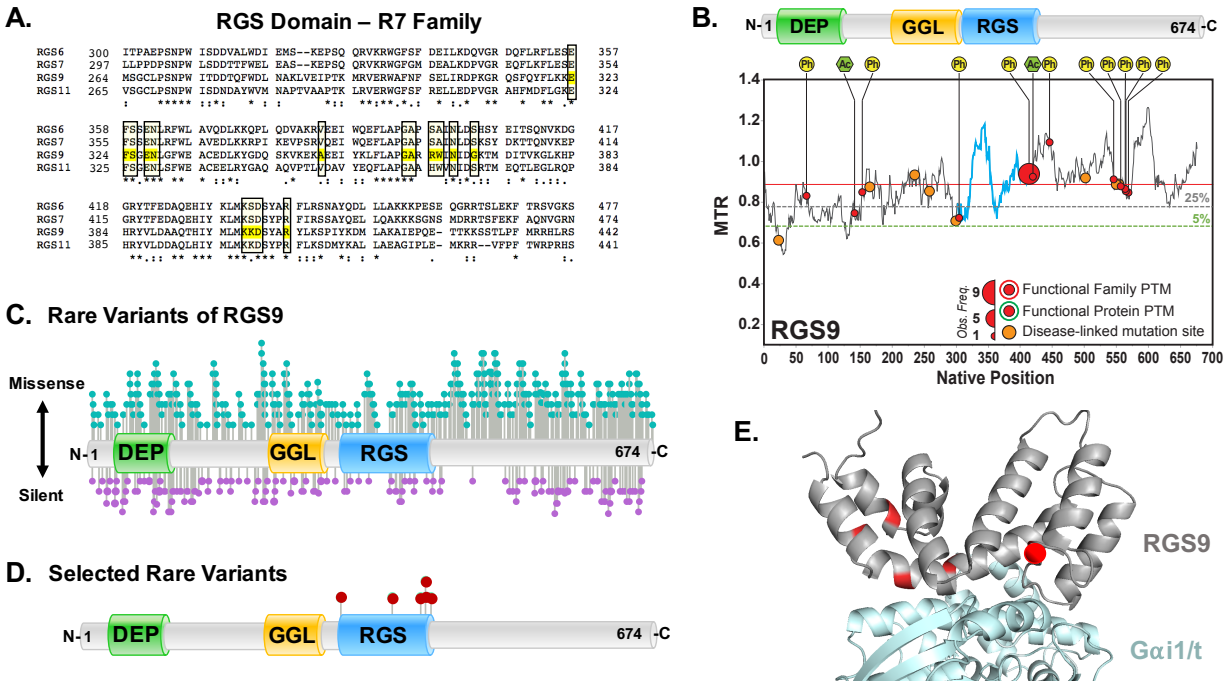

Figure 2.2. The R7 Subfamily of RGS proteins: Analysis of RGS9 human variants.

A) *Clustal W was used to align sequences of the RGS domains within the R7 subfamily of human RGS proteins. The RGS9:Gαi1/t-AlF_4^- crystal structure (PDB: 1FQK) was used to extract residues on RGS9 critical for interaction with Gαi1/t (highlighted in yellow). We then added pale yellow-filled boxes to extend this information to all R7 subfamily members.* ***B)*** *Missense Tolerance Ratio (MTR) and Post-Translational Modification (PTM) cluster analysis plot for RGS9 (see text for details). The RGS domain of RGS9 (highlighted in blue) is under selective pressure, indicated by a low MTR (median, red line; 25%, grey dashed line; 5%, green dashed line). Human RGS9 contains many reported post-translational modifications, including multiple acetylations and phosphorylations, one of which (phosphorylation) is found to be mutated in the RGS domain (GnomAD version 2.0) and met our criteria for inclusion (Table 2 and Table S1).* ***C)*** *Rare Human Variants of RGS9 plotted along the sequence using Lollipops (https://github.com/pbnjay/lollipops). Missense (amino acid change) variants are displayed on top in teal, while silent (no amino acid change) variants are displayed on the bottom in purple.* ***D)*** *From our analyses, six variants in the RGS domain of RGS9 were predicted to have a change-of-function phenotype, and mapped onto the RGS9 sequence using Lollipops (https://github.com/pbnjay/lollipops).* ***E)*** *Selected variants were mapped onto the crystal structure (PDB: 1FQK) of RGS9 (grey, selected residues in red) and Gαi1/t-AlF_4^- (light blue).*

other RGS:Gα interfaces, and provides information about residues that are both highly conserved and crucial for interaction (highlighted in Figure 2.2A). The RGS9 MTR plot (Figure 2.2B) demonstrates that the RGS domain, particularly the C terminal half of the domain, is under selective pressure. This information indicates that the latter half of the domain is predicted to be sensitive to missense variation.

We next examined whether reported human PTMs aligned with human variants (Figure 2.2B). While there are many PTMs outside of the RGS domain, two rare-variant phosphorylation sites were found within the RGS domain, S304R and Y413C. Whereas Y413C has a CADD C-score of 27.2, S304R has a CADD C-score of 3.7, which did not meet our cutoff. We mapped the rare human variants to the sequence of RGS9 (Figure 2.2C), and noticed a large degree of variation across the gene, suggesting a great deal of sequence diversity. Based on the PTM, CADD, and structural analyses, we selected six variants of interest (W299R, R364C, K400Q, R406C, R406H, and Y413C; Table 2.1) and mapped them onto the RGS9 sequence (Figure2.2D) and structure (Figure 2.2E). Most variants map to the C terminal half of the RGS domain (Figure 2.2B), with the exception of W299R, which was found in the literature to underlie some cases of retinal dysfunction (261-265). Based on the crystal structure of RGS9 (393), W299 participates in an electrostatic interaction with a nearby lysine (K311) to stabilize the tertiary structure of the RGS domain, and mutation to a positively charged arginine in the W299R variant (C-score 29.1) could disrupt this tertiary structure. As noted above, we report human variants that fall within a +/- 7 residue window of PTM. As such, W299R has 1 neighboring PTM, a phosphorylation on S304. Thus, one possibility is that the W299R variant leads to retinal dysfunction by disrupting phosphorylation of S304, a prospect that must be further explored. Y413C, while modified itself, also falls within a neighboring PTM window, an acetylation on K419. R364C (C-score 29.5) makes a water-mediated contact with Gαi1/t and stabilizes the α5-α6 loop, which undergoes the greatest conformational change when serving as a GAP for Gα. K400Q (C-score 28.1) is perfectly conserved within the R7

family and makes a contact with the α helical domain of Gα, which is important for RGS:Gα specificity (394). Finally, R406C and R406H, also perfectly conserved within the family, form a cis salt bridge with a nearby aspartate (D402) on RGS9 to help stabilize Gα switch I, and these variants have very high CADD C-scores (35 and 34, respectively). R406C/H also fall within a neighboring PTM, that of Y413C.

Due to the known link between W299R and retinal dysfunction, we propose that these as-yet undefined variants listed here may have a similar role in retinal or other RGS9-linked diseases. Elsewhere within the CNS, RGS9-2 has a role in the striatum (395) regulating dopamine signaling, which has consequences for addiction, Parkinson's Disease, and Schizophrenia (267, 269, 396). Notably, these phenotypes, such as enhanced sensitivity to stimulants, arise from a loss of RGS9-2 protein. Thus, LoF variants described in this dataset may contribute to susceptibility of these diseases in carriers. Further, as the R7 subfamily proteins contain additional signaling domains that are critical for protein stability and proper subcellular localization (232, 397), LoF variants in those domains could also cause LoF phenotypes that should be explored further. Table 2.1 lists human variants in the RGS domain of RGS9 that we predict disrupt RGS9 interaction with Gα and/or GAP activity.

2.5 R12 FAMILY: RGS10 RARE VARIANTS

Among the R12 subfamily of RGS proteins, RGS10 is the smallest and simplest, and is the only family member that has been crystallized in complex with a Gα, Gαi3 (398), providing an excellent case study for the R12 family. We first compared amino sequence conservation and highlighted contact points between RGS10 and Gαi3 (Figure 2.3A). As with RGS4, human RGS10 has three splice variants which range in size from 167 to 181 amino acids (316, 319, 399). The RGS10 variants in the GnomAD database (23) are reported with respect to the longest splice variant (RGS10-3 and mapped onto this sequence in Figure 2.3C), which adds only eight amino acids to the N terminus of the commonly used canonical human RGS10 reference sequence (RGS10-1; 173

amino acids).

Compared to other solved RGS domain-Gα crystal structures (19, 393), the RGS domain of RGS10 makes fewer contact points with Gα (compare to highlighted regions in Figures 2.1A and 2.2A), yet five variants were found in our predictive CADD/PTM/structural analysis: L46(38)P, V52(44)M, D141(133)N, R145(137)C, and K148(140)R (mapped onto the RGS10 sequence in Figure 2.3D and RGS10 structure in Figure 2.3E). The RGS10 MTR plot shows a high degree of selective pressure across the entire RGS domain (Figure 2.3B). Furthermore, there are several reported human PTMs within the RGS domain, including K53 and K148 (ubiquitination), K78 (acetylation), Y94 and Y143 (phosphorylation). Of these, only K148 is included in the GnomAD dataset as K148(140)R (Figure 2.3B and Table 2.1). Of note, K148(140)R has a CADD C-score of 25, which met our criteria for a CoF candidate.

In addition to the highlighted variant residues above, D141(133)N, R145(137)C, and L46(38)P met our structural and sequence analysis criteria. Residues D141(133)N and R145(137)C both have very high CADD C-scores of 35 and are close to two reported PTMs, a phosphorylation on Y143(135) and a ubiquitination on K148(140), indicating that these variants are likely to be deleterious to protein function. Consistent with this idea, both variants occur at highly conserved residues that are important for ionic stabilization. Changing the charge of the side chain from negative to uncharged, as is the case for D141(133)N and R145(137)C, is likely to disrupt efficient binding of the RGS domain to the Gα protein. L46(38)P (C-score 29.6) inserts a proline into an α helix, which we predict will cause disruption of the secondary structure. Furthermore, L46(38)P falls within two neighboring PTMs, a phosphorylation on S41(33) and a ubiquitination on K53(45). We postulate that disrupting secondary structure via insertion of a proline into an α helix would greatly inhibit the ability of a modifying enzyme to dock.

Finally, V52(44)M has a high CADD C-score of 34 and is next to a modified residue, K53(45), suggesting that this mutation could lead to LoF. In support of this evidence, we observed that

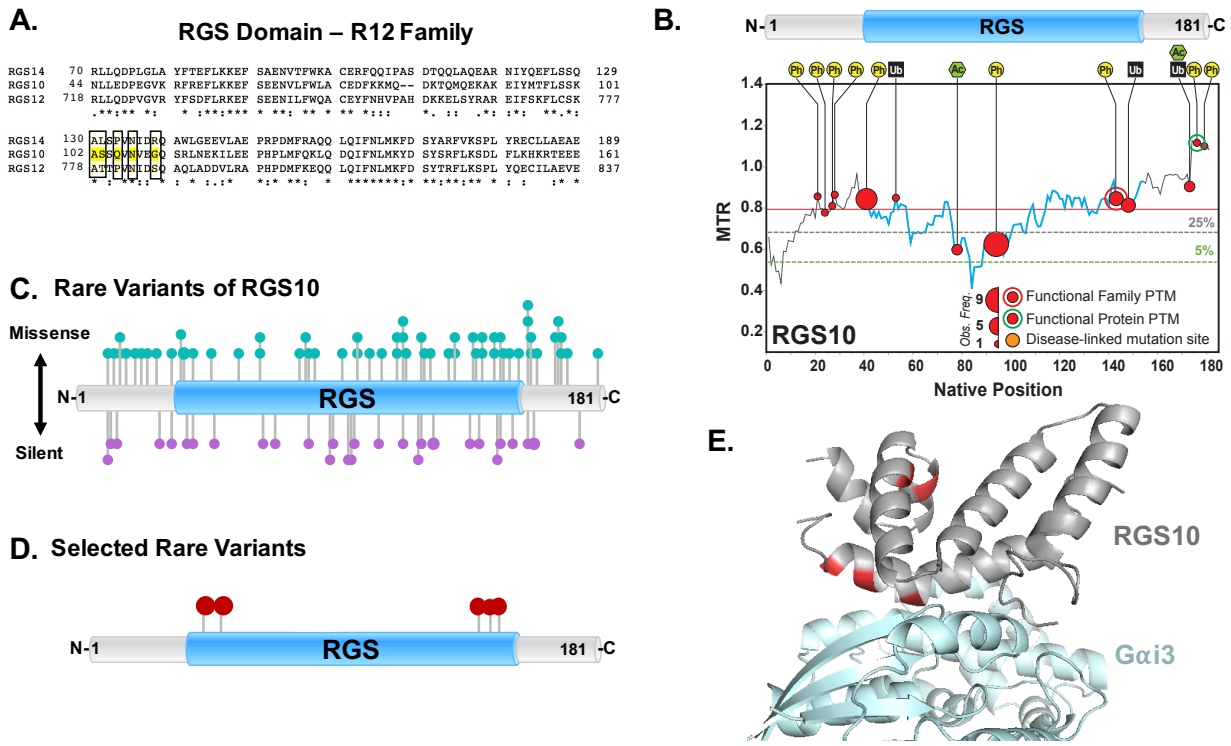

Figure 2.3. The R12 Subfamily of RGS proteins: Analysis of RGS10 human variants.

A) *Clustal W was used to align sequences of the RGS domains within the R12 subfamily of human RGS proteins. The RGS10:Gαi3-AlF_4^- crystal structure (PDB: 2IHB) was used to extract residues on RGS10 critical for interaction with Gαi3 (highlighted in yellow). We then added pale yellow-filled boxes to extend this information to all R12 subfamily members.* ***B)*** *Missense Tolerance Ratio (MTR) and Post-Translational Modification (PTM) cluster analysis plot for RGS10. The RGS domain of RGS10 (highlighted in blue) is under selective pressure, indicated by a low MTR (median, red line; 25%, grey dashed line; 5%, green dashed line). Human RGS10 contains many reported post-translational modifications, including multiple ubiquitinations, acetylations and phosphorylations, one of which is found to be mutated in the RGS domain (GnomAD version 2.0) and met our criteria for predicted change-of-function phenotype (Table 2 and Table S1).* ***C)*** *Rare Human Variants of RGS10 plotted along the sequence using Lollipops (https://github.com/pbnjay/lollipops). Missense (amino acid change) variants are displayed on top in teal, while silent (no amino acid change) variants are displayed on the bottom in purple.* ***D)*** *From our analyses, we selected six variants in the RGS domain with predicted change-of function phenotype, and mapped them onto the sequence of RGS10 using Lollipops (https://github.com/pbnjay/lollipops).* ***E)*** *Finally, we mapped these selected variants onto the crystal structure (PDB: 2IHB) of RGS10 (grey, selected residues in red) and Gαi3-AlF_4^- (light blue).*

V52(44)M is putatively linked to schizophrenia (309). V52(44) appears to participate in a hydrophobic core of the RGS domain, thus a mutational change to methionine will likely disrupt this interaction. Interestingly, V52(44)M is found in nearly 2% of the East Asian population, and as such, we speculate that it could be an attractive target for deeper study. Furthermore, as loss of RGS10 protein in mice is linked with an increase in neuroinflammation (306, 307, 312, 319), LoF variants highlighted here may lead to susceptibility for neurodegenerative diseases such as Parkinson's Disease. Table 2.1 lists human variants in RGS10 that are predicted to disrupt RGS10 interaction with Gα and/or GAP activity.

2.6 RZ FAMILY: RGS17 RARE VARIANTS

Unlike the other RGS subfamilies, no member of the RZ subfamily (RGS17, RGS19, or RG20) has been crystalized in complex with a Gα partner. However, a crystal structure of RGS17 alone has been reported (398), allowing us to utilize this structure and conserved sequence alignments with other RGS family members to determine predicted CoF variants. RGS17 also has been linked to a number of diseases (351, 355-357), and therefore provides an attractive "case study" example for the RZ subfamily. For this, we first aligned the RGS domain of RGS17 with each of the case study proteins (RGS4, RGS9, RGS10, Figures 2.1-2.3) and highlight in yellow the residues that are indicated as contact points with Gα, based on their respective crystal structures (Figure 2.4.1). We noted a great deal of conservation for residues that participate in Gα interaction. For example, residues 145-155 correspond to the α5-α6 loop on each of the comparison family members (19, 393, 398), a region found within RGS domains that is critical for stabilization of switch II in Gα and GAP activity. We then used this information to predict contact points between RGS17 and Gα, and highlighted in yellow those *predicted* contact points in Figure 2.4A for all members of the RZ family. Each of those predicted contact points is either highly or completely conserved (highly conserved denoted by ":", completely conserved denoted by "*", yellow boxes). Again, MTR analysis for RGS17 (Figure 2.4B) indicates that the RGS domain is under selective pressure, with

the exception of residues 134-143 which immediately precede the highly conserved α5-α6 loop. Using PTM alignment analysis, we identified two phosphorylation sites reported in the RGS domain of human RGS17, Y137 and Y171. Whether either phosphosite is functional for the protein is yet unknown. Although Y171 is a known variant site (Y171F), its low PTM observation frequency and CADD C-score (9.1) exclude this variant from our selected dataset. Y134 contributes to a MAP that is one of the most frequently observed phosphorylation sites in the RGS domain, but whose function is currently unknown. Thus, while not aligned with a genetic variant, PTM at this position appears to be very common in the RGS domain of several RGS proteins, a highly predictive feature for functional significance (48, 49, 386). Indeed, the lack of genetic variance at or near this position suggests that it is of critical importance, and any future variant at this position would be a prime target for functional analysis.

Based on our combined structural, conservation, CADD, and PTM analysis, three variants met our predictive criteria: E148G, P166L and R189T (Figure 2.4D). Amino acid E148 in RGS17 is a charged residue found in the highly conserved α5-α6 loop that serves as a key Gα contact point for each of the representative RGS (Figures 2.4A and 2.4.1). E148 in RGS17 is also 100% conserved within the RZ family. The charged residues analogous to E148 in other RGS protein crystal structures participate in ionic bonding with opposite charge residues to stabilize this α5-α6 loop, thus this negatively charged glutamate in RGS17 is a likely ionic binding partner serving the same role. As such, the E148G variant (C-score 28.2) of RGS17 could disrupt RGS17 interactions with target Gα subunits. We also identified P166L (C-score 28.3), which is 100% conserved both within the RZ family (Figure 2.4A) and across the other RGS subfamilies (Figure 2.4.1). This conserved proline appears to mediate the critical turn in the α6-α7 loop that is present in all RGS domains. Furthermore, it is located near a neighboring PTM, a phosphorylation on Y171. Due to the drastically different side chain properties of leucine versus proline, we speculate that P166L could result in CoF. Residue R189T (C-score 28.1), which was also identified as a potential CoF

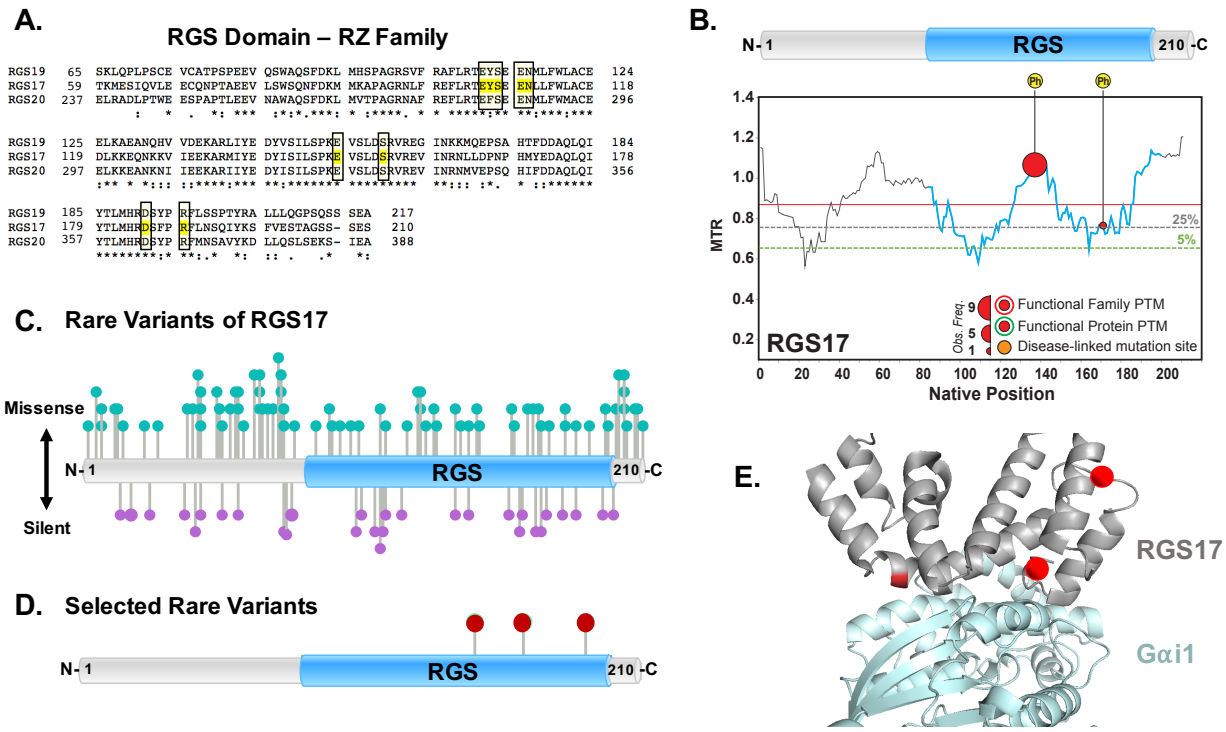

Figure 2.4. The RZ Subfamily of RGS proteins: Analysis of RGS17 human variants.

A) *Clustal W was used to align sequences of the RGS domains within the RZ subfamily of human RGS proteins. A crystal structure for RGS17 in complex with a Gα is not yet available, although a crystal structure of RGS17 alone has been reported (PDB: 1ZV4). We therefore compared critical residues across all RGS subfamilies and highlighted residues in RGS17 that are, based on conservation, predicted to be contact points for Gα interaction. We then added pale yellow-filled boxes to extend this information to all RZ subfamily members.* ***B)*** *Missense Tolerance Ratio (MTR) and Post-Translational Modification (PTM) cluster analysis plot for RGS17. The RGS domain of RGS17 (highlighted in blue) is under selective pressure, indicated by a low MTR (red line is median MTR for gene). RGS17 contains two phosphorylations, both within the RGS domain (Table 2 and Table S1). While one is found to be mutated in humans (GnomAD version 2.0), it did not meet our criteria for inclusion in our change-of-function table, but nonetheless should be noted for study.* ***C)*** *Rare Human Variants of RGS17 plotted along the sequence using Lollipops (https://github.com/pbnjay/lollipops). Missense (amino acid change) variants are displayed on top in teal, while silent (no amino acid change) variants are displayed on the bottom in purple.* ***D)*** *From our analyses, we selected three variants in the RGS domain with predicted change-of function phenotype, and mapped them onto the RGS17 sequence using Lollipops (https://github.com/pbnjay/lollipops).* ***E)*** *Finally, we structurally aligned the apo RGS17 structure (PDB: 1ZV4) with the RGS4:Gαi1-AlF_4^- structure (PDB: 1AGR), and mapped these selected variants onto the model of RGS17 (grey, selected residues in red) and Gαi1 (light blue).*

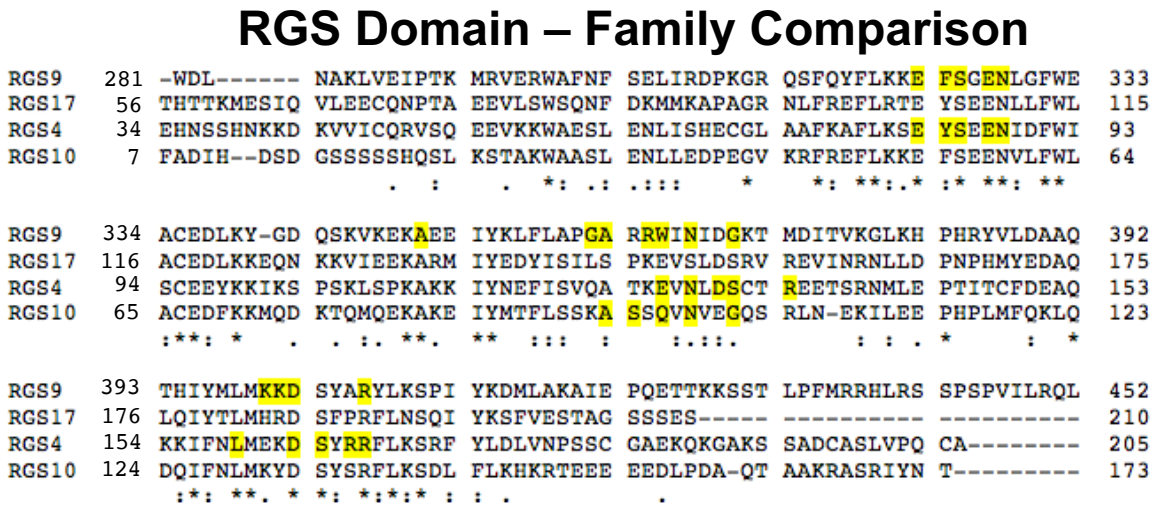

Figure 2.4.1. Family alignment of RGS domains.

To identify conserved residues critical for Gα interaction, we used Clustal W to align each of the representative subfamily members (RGS4, RGS9, RGS10) with RGS17. We highlighted residues that were noted as important for binding (Figures 2, 4, 5) to compare against RGS17. From this information, we identified residues in RGS17 that are predicted contact points with Gα.

candidate, like P166, is 100% conserved within the RZ subfamily and across all other RGS subfamilies. We predict this variant could disrupt RGS17 ionic interactions with target Gα subunits, as shown in a structural homology model based on the solved crystal structure of the RGS4:Gαi1-AlF_4^- complex (19) (Figure 2.4E).

2.7 RGS4 HUMAN VARIANT: PROOF-OF-PRINCIPLE

To validate our approach, we selected one human variant in RGS4 from our list, R231(134)W, to test for a CoF phenotype. Compared to wild type RGS4, R231(134)W (Figure 2.5A) exhibited a loss of direct Gαi1-AF_4^- binding (Figure 2.5B), as well as a dramatic decrease in Gα-YFP binding in live cells by BRET analysis, indicating a profound LoF phenotype (Figure 2.5C). This data suggests that the capacity of the RGS domain of RGS4 to bind Gα, and thus serve as a GAP, is disrupted by this naturally-occurring human variant, and may therefore be a determinant in RGS4-linked diseases found in carriers. For example, multiple neurological diseases, including Schizophrenia and alcoholism, correlate with low RGS4 expression (142, 151), a phenotype that would also be expected for a loss-of-function variant in the RGS domain of RGS4. Therefore, one possible hypothesis is that LoF variant R231(134)W is a risk factor for Schizophrenia – a classification that could be difficult to make through unbiased genome-wide studies due to the extremely low prevalence of the variant in the population (0.0065% of the African population). Indeed, we propose that hypotheses generated through an integrated bioinformatics analysis such as this one could reveal several such cases wherein disease states can be more confidently linked to discrete changes in protein structure and function. Other LoF variants listed in Table 2.1 are predicted to share the same phenotype and outcome.

2.8 DISCUSSION

RGS proteins participate in many complex diseases and traits, ranging from hypertension to cancer to morning wakefulness (116, 122, 163, 213, 314, 316). Due to their important functional

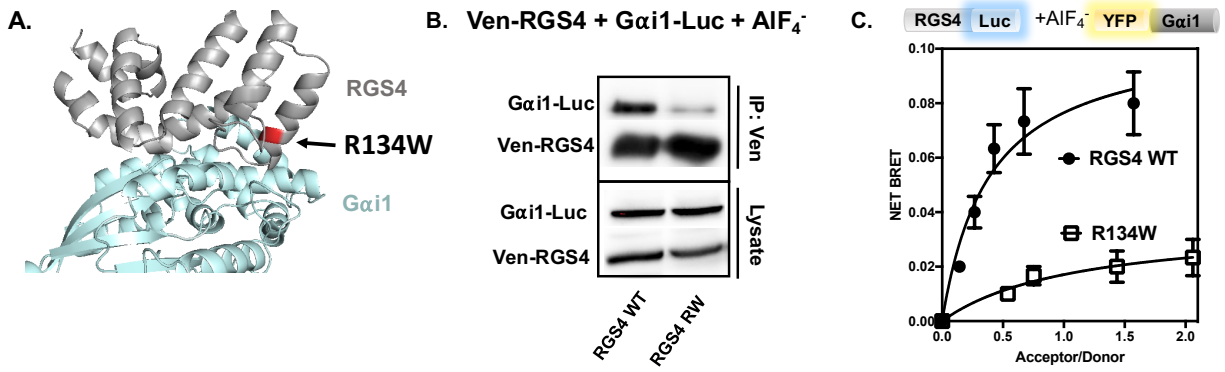

Figure 2.5. RGS4 human variant R231(134)W disrupts RGS domain interaction with activated Gαi1.

To validate our methods, we selected one variant from the list to generate a mutation and test binding between RGS4 (WT or mut) and Gαi1-AlF4-. We chose R231(134)W and highlighted this residue on the structure of RGS4: Gαi1-AlF4- in red ***(A)****. This arginine residue is positively charged and interacts with the carbonyl oxygen of glutamate 236 on Gαi1 in the switch III region. Disruption of this interaction by mutation to a tryptophan (uncharged) is predicted to reduce RGS4 binding to Gαi1.* ***B)*** *We generated this mutation and performed an immunoprecipitation of RGS4 (WT or RW) and found that the mutation greatly reduced Gαi1-AlF4- co-immunoprecipitation.* ***C)*** *We next examined this interaction in live cells and found that again, the RW mutant greatly reduced Net BRET signal between RGS4 RW and Gαi1-AlF4-, compared to wild type RGS4, indicating that the mutant is not interacting with Gαi1-AlF4-.*

roles, I identified and reported a comprehensive list of missense variants for each RGS protein, alongside their MTR values (47) and publically curated human PTMs using PTM alignment analysis (48, 49). I then mapped each with respect to their sequence and structure. Using all of this information (human variants, CADD and PTMs) in combination, I have prioritized a narrow list of select variants that I predict will disrupt human RGS protein function. As a proof-of-principle to validate the approach, I tested one of these selected variants to demonstrate a profound change-of-function phenotype, and highlighted others for future study. While the focus here is on the RGS domain, I recognize that other RGS protein regions and domains are also essential for RGS protein function, as explored in the following chapter. As such, the comprehensive dataset examining these measures for the entire exome sequence for each canonical RGS protein is also provided as a supplement to the submitted review [Squires KE, Montañez-Miranda C, Pandya RR, Torres MP, and Hepler JR (2017) Genetic Analysis of Rare Human Variants of Regulators of G Protein Signaling (RGS) Proteins and Their Role in Human Physiology and Disease. *Pharmacol Rev*.]. I reason that if rare variants occur in functionally sensitive regions of RGS proteins (e.g. the RGS domain) such that they confer a profound change-of-function phenotype, then these variants likely make important (and previously unappreciated) contributions to complex human disease states and/or unique human traits. As such, I believe that computationally-identified rare variants, combined with experiments that validate a change-of-function for such variants, can provide a deeper understanding of the etiology of complex disease states and the evolution of human traits.

Selected Human RGS Protein Rare Variants							
RGS Protein	**Residue Mutation**	**LoF Rationale**	**CADD**	**MTR**	**PTM**	**Neighboring PTMs**	**Prevalence**
RGS4	L170(73)P	Proline in α helix	23	1.01	0	0	0.0043% (South Asian)
	E214(117)K	Salt bridge partner	27.3	0.50	0	0	0.0063% (Latino)
	D227(130)G	100% conserved, salt bridge partner	29.6	0.90	0	0	0.0065% (African)
	R231(134)W	Highly conserved, stabilizes switch III	29.8	1.04	0	0	0.0065% (African)
	D260(163)N	Highly conserved, salt bridge partner, very high CADD	32	1.19	0	0	0.0065% (African)
	D260(163)G	Highly conserved, salt bridge partner	29.4	1.19	0	0	0.0009% (European)
	R263(166)C	Contact with α helical domain of Gαi1	28.4	1.07	0	0	0.0116% (East Asian)
	R263(166)H	Contact with α helical domain of Gαi1	24.5	1.07	0	0	0.0032% (Global)
	R264(167)C	Highly conserved, salt bridge partner, very high CADD	35	1.06	0	0	0.0009% (European)
RGS9	W299R	Link to disease, participates in electrostatic interaction	29.1	0.71	0	1	0.0229% (European)
	R364C	Stabilizes α5-α6 loop of RGS domain	29.5	0.78	0	0	0.0018% (European)
	K400Q	100% conserved, contact with α helical domain	28.1	0.97	0	0	0.0018% (European)
	R406C	100% conserved, salt bridge partner, very high CADD	35	0.98	0	1	0.0030% (Latino)
	R406H	100% conserved, salt bridge partner, very high CADD	34	0.98	0	1	0.0009% (European)
	Y413C	Phosphorylation	27.2	0.94	1	1	0.0032% (South Asian)

RGS10	L46(38)P	Proline in α helix	29.6	0.78	0	2	0.0032% (South Asian)
	V52(44)M	Possible link to schizophrenia, hydrophobic core partner	34	0.78	0	1	1.9239% (East Asian)
	D141(133)N	Highly conserved, ionic stabilization, very high CADD	35	0.90	0	2	0.0183% (Other)
	R145(137)C	Highly conserved, ionic stabilization, very high CADD	35	0.86	0	2	0.0617% (East Asian)
	K148(140)R	Ubiquitination	25	0.81	1	1	0.0009% (European)
RGS17	E148G	100% conserved, likely ionic interaction	28.2	0.87	0	0	0.0010% (European)
	P166L	100% conserved within and across family, high CADD	28.3	0.73	0	1	0.0009% (European)
	R189T	100% conserved, likely ionic interaction	28.1	1.03	0	0	0.0009% (European)

Table 2.1. Human rare variants in each representative family member's RGS domain are predicted to disrupt function due to structural changes or inability to bind/GAP Gα.

Residues were selected based on our criteria (outlined in the text) of CADD>20, residues that overlap with conserved sites important for Gα interaction (determined by structural insights), and PTM alignment analysis. Each residue mutation (native, residue position, mutation) has a description as to why it is predicted to disrupt function ("LoF Rationale"), its associated combined annotation dependent depletion score ("CADD"), associated genic intolerance score ("MTR Ratio"), number of reported PTMs, number of neighboring PTMs (where a PTM is found within 7 amino acids before/after), and prevalence in the population ("Prevalence"). Note that if the human variants are reported in the non-canonical transcript, the analogous residue position for the canonical sequence is coded in grey.

CHAPTER 3:

RARE HUMAN VARIANTS IN REGULATOR OF G PROTEIN SIGNALING 14 (RGS14) DISRUPT NUCLEO-CYTOPLASMIC EQUILIBRIUM AND INHIBITION OF LONG TERM POTENTIATION IN HIPPOCAMPAL NEURONS

3.1 ABSTRACT

Regulator of G protein signaling 14 (RGS14) is a mediator of long term potentiation (LTP) in mouse hippocampal area CA2 and mice lacking RGS14 (RGS14 knockout) have enhanced spatial learning, although the precise mechanism for this remains a mystery. RGS14 is a dynamically regulated protein, and rapidly translocates into and out of the nucleus of mammalian cells with equilibrium predominantly in the cytosol. However, recent evidence points to a nuclear pool of RGS14 in the primate brain, suggesting that nuclear import and export is an active part of RGS14's life cycle in neurons. While human and rodent RGS14 sequences are over 90% conserved (with nearly 100% identity in functional domains), canonical protein sequences do not represent the great genetic diversity among human sequences. The vast majority of these genetic deviations from the "norm" (i.e. the defined major allele) are rare or very rare (1-2% or less in the population), yet constitute a great deal of sequence heterogeneity. We thus sought to define: 1) RGS14 subcellular dynamics in neurons; and 2) the contribution of human-derived sequence variants on this nucleo-cytoplasmic balance. Here we report that cytosolic RGS14 moves into the nuclei of neurons (as opposed to a nuclear-specific pool) and its export is governed by interaction with CRM1/Exportin 1. Next, we screen and identify unique human variants from multiple ethnic populations that disrupt this delicate nucleo-cytoplasmic equilibrium. We identified two human RGS14 variants (L/R and R/Q) that each had distinct nuclear localization properties. Whereas the RGS14 R/Q variant occupies both the nucleus and the cytoplasm, the L504R variant accumulates in the nucleus irreversibly. We structurally aligned these variants onto the CRM1 crystal structure to provide a mechanism for the gradient of nuclear sequestration. As RGS14 is a critical mediator of LTP, we finally tested the effects of these variants on RGS14-mediated suppression of LTP in CA1 hippocampal neurons. We found that, unlike wild-type RGS14, each variant failed to inhibit LTP. While suppression of LTP recovered after ten minutes with the R/Q variant, the L/R variant failed to suppress LTP for the duration of recording, indicating that the degree of mislocalization has a direct effect on RGS14 function. These data provide novel insight into human variants that may

have previously unappreciated functional effects in LTP, learning, and beyond.

3.2 INTRODUCTION

G protein coupled receptors control many aspects of cognition (400), including synaptic plasticity and learning (401, 402), and their signaling is tightly regulated by the Regulators of G protein Signaling (RGS) protein family. Upon activation of a Gαi/o-linked receptor, Gαi/o is released, binds GTP, and signals to downstream effectors. The duration of Gαi/o-GTP signaling is controlled by the Gαi/o internal GTPase "clock." Upon binding to an RGS domain, GTPase activity is catalyzed, thus speeding up the termination of Gαi/o signaling (17). In this way, RGS proteins are gaining appreciation for their own roles in regulating many aspects of synaptic plasticity (21) and disease (20).

The RGS protein family consists of 20 classical RGS proteins, which all share a conserved ~120 amino acid RGS domain, and as such their canonical role is to facilitate the GTPase activity of Gαi/o-GTP. However, several RGS proteins contain additional signaling domains, which act to regulate different aspects of cellular signaling, unique from its actions on Gαi/o-GTP. One such family member, RGS14, has additional signaling domains including two tandem Ras/Rap binding domains which bind active H-Ras-GTP and Rap2A-GTP to regulate MAP kinase signaling (292-294) and a G protein regulatory (GPR) motif. While the RGS domain binds active Gαi/o-GTP to catalyze GTPase activity, the GPR motif binds inactive Gαi-GDP to inhibit guanine dissociation (298, 333). Furthermore, the GPR motif recruits RGS14 to the plasma membrane where RGS14 can exert its actions on downstream effectors (299). In this way, while the canonical GAP functions of RGS14 may be dependent on its RGS domain, its localization is dependent on its GPR motif.

We previously reported that RGS14 is specifically and strongly expressed in pyramidal neurons within a small enigmatic subregion of the hippocampus, Cornu Ammonis 2 (CA2), but not neighboring region CA1 in mouse brain (338). While CA1 neurons can be induced to undergo robust long-term potentiation (LTP), the molecular correlate to learning and memory, LTP is

curiously absent from CA2, where RGS14 is naturally expressed (403). Further, RGS14 was found at spines and dendrites in CA2 neurons, positioning it to modulate LTP. Upon genetic ablation of RGS14, we reported robust LTP in CA2, mirroring that of CA1, with no changes in CA1, consistent with RGS14's expression patterns. RGS14 ablation further conferred an enhancement in spatial learning, a hippocampal-dependent task (338), leading us to conclude that RGS14 is a natural suppressor of LTP and learning.

While previous studies were carried out in rodents, we recently published a report describing in detail the cellular and subcellular localization of RGS14 in the primate brain (335). Not only was RGS14 expression more widespread in humans and monkeys compared to rodents (404), but we found evidence of splice variants, as well as native expression of RGS14 in the nuclei of a subpopulation of neurons. This is consistent with earlier reports demonstrating recombinant RGS14 is a dynamic protein that can traverse the nuclear membrane (288, 289), but was the first time that RGS14 had been found *natively* in the nuclei of neurons. This prompted us to explore the effects of nuclear shuttling on the function of RGS14 as a suppressor of LTP. Finally, due to our exciting findings in primate brain, we took advantage of the recent release of human genetic variant data encompassing over 130,000 individuals (23) to explore the contribution of naturally occurring (non-disease) mutations on the subcellular distribution of RGS14 and its ability to suppress LTP.

Here we report that RGS14 shuttles into and out of the nucleus in neurons, that the nuclear export sequence (NES) overlaps with the GPR motif in RGS14, and binds nuclear export receptor CRM1/XPO1 (Exportin 1). Further, rare human variants in RGS14 are found throughout the gene, including in close proximity to the NES. Two human variants within the NES were found in the Ashkenazi Jewish and East Asian populations, and conferred a shift in the nucleo-cytoplasmic equilibrium from the cytosol to the nucleus, and a reduction in binding to Gαi1-GDP, an indicator of dynamic subcellular mobilization (299). Finally, we report for the first time that virally-expressed wild type RGS14 is able to fully block LTP, while both the East Asian and Ashkenazi mutants fail to block LTP in CA1 neurons. Our findings suggest that naturally occurring rare

variants in these two populations may disinhibit LTP and learning in the carriers, and give rise to traits involving spatial, social, and contextual memory (339-342). Finally, given the exciting new findings from our recent report showing broad expression of RGS14 in the hippocampus and basal ganglia in human and monkey brain, these variants may confer as yet unknown diseases, traits, or phenotypes on the carriers, distinct from their role in the hippocampus.

3.3 METHODS

Constructs and Reagents

Leptomycin B was obtained from Sigma and cells were treated at 20nM for 2 hours. RGS14 was cloned into phRLucN2 as described previously (293), pLic-GST as described previously (335), and pAAV-hSyn-YFP using restriction sites AgeI and HinDIII. pET-hRan-GTP was acquired from AddGene (catalog #42048) and pGEX-TEV-hCRM1 was kindly provided by Dr. YuhMin Chook (UT Southwestern) (405). Isopropyl β-D-1-thiogalactopyranoside (IPTG) was purchased from Fisher Scientific. Primers for mutagenesis are provided in Table 3.1.

Purification and Pure Protein Interactions

RGS14 was purified as described previously (335). Briefly, GST-RGS14 was expressed in BL21 (DE3) *Escherichia coli* (E. Coli), pellets were resuspended in 50 mM HEPES, 200mM NaCl, 10% glycerol, and 2mM BME. Bacterial lysate was passed over a glutathione affinity column, washed with PBS, eluted with 10mM reduced glutathione in 50mM Tris (pH 8), and cleaved overnight with TEV protease. Purity was verified by coomassie. His-Ran Q69L was purified as follows. BL21 bacterial cells were transformed with His-Ran Q69L and protein expression was induced with IPTG at 37°C for 2 hours. Bacterial pellets were resuspended in 50mM HEPES, 150mM NaCl, 10% glycerol, 10mM GTP, 2mM BME, 20mM imidazole, 2mM $MgCl_2$, and PMSF. Lysates were then passed over a Ni^{2+} affinity column, washed with resuspension buffer and finally eluted with resuspension buffer containing 200mM imidazole. Purity was verified by coomassie. GST-CRM1 was purified as described by the Chook Lab (405) as follows. BL21 bacterial cells

expressing GST-CRM1 were induced with IPTG overnight at 25°C. Lysate (40 mM HEPES pH 7.5, 2 mM $MgSO_4$, 200 mM NaCl, 5 mM dithiothreitol (DTT), 10% glycerol, and protease inhibitors) was then passed over a glutathione affinity column (Sepharose 4B, GE Healthcare), washed with buffer (40 mM HEPES, 2 mM $MgSO_4$, 150 mM NaCl, 2 mM DTT) and beads were resuspended in PBS. CRM1 was cleaved from the beads by incubating with TEV protease overnight at 4°C. Purity was verified by coomassie.

Structural Modeling

The RGS14-NES/CRM1 model was generated in PyMol (The PyMOL Molecular Graphics System, Version 2.0 Schrödinger, LLC.) through structurally aligning the RGS14 GPR peptide/Gαi1 structure (PDB code 1KJY) with the CRM1/mDia2 structure (PDB code 5UWP). Figures were constructed using PyMol.

Human Genetic Variants and Lollipop Plot

Human variant information was obtained from the Genome Aggregation Database (GnomAD version 2.0) at the Broad Institute (http://gnomad.broadinstitute.org) (23). Data was sorted by missense and synonymous annotation. The lollipop plot was then generated by open source code available on GitHub (406). Human variants were generated in rRGS14 (of which the GPR motif shares 100% identity compared to human but the amino acid number is less one) and are reported in this manuscript as such. Primers used to make the human variants are listed in Table 3.1.

Bioluminescence Resonance Energy Transfer (BRET)

BRET was performed as described previously (293, 299, 387). Briefly, HEK293 cells were maintained in 1x Dulbecco's Modified Eagle Medium (Mediatech, Inc) without phenol red and supplemented with 10% Fetal Bovine Serum (FBS), 2mM L-Glutamine, and 1% penicillin/streptomycin (VWR, Calbiochem, and Invitrogen, respectively). Cells were transiently transfected with polyethyleneimine and RGS14-Luciferase(Luc) plus Gαi1-YFP (407) for 40 hours. Cell were resuspended in Tyrode's Solution (140 mM NaCl, 5 mM KCl, 1 mM $MgCl_2$, 1

mM $CaCl_2$, 0.37 mM NaH_2PO_4, 24 mM $NaHCO_3$, 10 mM HEPES, and 0.1% glucose, pH 7.4) and plated at 10^5 cells per well in a 96-well Optiplate (PerkinElmer Life Sciences). YFP expression was quantified using a TriStar LB 941 plate reader (Berthold Technologies) at 485 nm excitation and 530 nm emission. Next, 5 μM coelenterazine H (Nanolight Technologies) was incubated for 2 minutes and BRET measurements were taken at 485 nm (Luc emission) and 530 nm (YFP emission). The Net BRET ratio was quantified as follows: (530 nm signal / 485 nm signal) – (485 nm signal from Luc alone). Acceptor/Donor ratios were calculated as follows: (530 nm signal from YFP measurement)/(485 nm signal from BRET measurement). Each experiment was repeated 3 times.

Co-immunoprecipitation

Purified proteins were incubated together for one hour at 4°C, rotating end over end. Protein G sepharose (GE Healthcare) was blocked in 3% BSA for one hour, and then added to incubated proteins, along with 2μL RGS14 antibody (Proteintech). The beads, antibody, and proteins were incubated for two hours at 4°C, rotating end over end. Beads were then centrifuged, washed with Triton X in PBS, boiled for 5 minutes, and samples were immunoblotted with RGS14 antibody (Proteintech), CRM1 antibody (Santa Cruz), and Ran antibody (Santa Cruz).

Dissociated Hippocampal Neuronal Culture

Our protocol for culturing neurons was adapted from Beaudoin et al. 2012 *(408)*. Brains were removed from E18-19 embryos obtained from a timed pregnant Sprague-Dawley rat (Charles River). The meninges were removed and the hippocampi were isolated in calcium and magnesium free HBSS (Invitrogen) supplemented with 1x sodium pyruvate (Invitrogen), 0.1 percent glucose (Sigma-Aldrich), and 10 mM HEPES (Sigma-Aldrich) pH 7.3. Isolated hippocampi were washed with the HBSS solution then dissociated using the same buffer containing 0.25 percent trypsin (Worthington) for minutes at 37°C. Trypsinized hippocampi were washed two times with the same HBSS buffer before being triturated 5-6 times with a fire-polished glass Pasteur pipette in BME

(Invitrogen) supplemented with 10 percent FBS (VWR), 0.45 percent glucose (Sigma-Aldrich), 1x sodium pyruvate (Invitrogen), 1x Glutamax (Invitrogen), and 1x penicillin/streptomycin (HyClone). Neurons were counted and plated at a density of 80,000 cells/cm2 in the BME-based buffer on coverslips that had been etched with 70 percent nitric acid (Sigma-Aldrich) before being coated with 1 mg/mL poly-L-lysine (Sigma-Aldrich) in borate buffer. Cells were allowed to adhere for 1-3 hours before media was changed to Neurobasal (Invitrogen) supplemented with 1x B27 (Invitrogen) and 1x Glutamax (Invitrogen). Neurons were kept in a 37°C, 5 percent CO2 incubator and half of the media was replaced with new Neurobasal every 3-4 days until neurons were used for experiments.

Confocal Microscopy

All reactions were carried out at room temperature. Cells were fixed with 4% paraformaldehyde for 10 minutes, then quenched with 0.75% glycine in 200 mM Tris pH 7.4, for 5 minutes. Cells were then permeabilized for 10 minutes in 0.1% Triton-X in PBS and stained with Hoechst (1:12,500 in PBS) for 4 minutes. Cells were finally washed three times in PBS and mounted onto slides with ProLong Diamond Antifade mountant (ThermoFisher). Images were taken on an Olympus FV1000 confocal microscope at 60x, then processed using ImageJ software. Approximately ten images per condition were obtained and representative images are shown.

Electrophysiology Slice Preparation and Recordings

Hippocampal slices were prepared from WT mice (8–12 weeks of age) as described (403). Mice were decapitated, and brains rapidly removed and sectioned into coronal slices (340–400 μm thick) using a vibrating blade microtome in aerated, ice-cold artificial cerebral spinal fluid (aCSF). AAV-YFP-RGS14 (WT or mutant) was injected into CA1 and incubated for one week. For recordings, slices were transferred to a recording chamber in which they were bathed continuously with room temperature aCSF. Extracellular field potential recordings in the stratum radiatum area of CA1 were recorded in response to Schafer collateral inputs. Population excitatory postsynaptic potential (EPSP) output was measured in response to varying input currents to determine baseline

synaptic transmission. For induction of LTP, slices were stimulated 2 × 1 s, 100 Hz, 20-s intervals and postsynaptic neurotransmission was monitored every 15 s for 180 min. Data presented are pooled mean ± SD.

3.4 RESULTS

It was previously shown that recombinant RGS14 shuttles into and out of the nucleus (288) in cell culture. We and others reported a functional nuclear export sequence (NES) embedded within the GPR motif of RGS14 and a functional nuclear localization sequence (NLS) between the RGS domain and the first Ras-binding domain (288, 289) (Figure 3.1A). Furthermore, we recently published a paper showing that RGS14 exists *natively* in the nuclei of striatal neurons (335). The nuclear staining coincided with the discovery of lower molecular weight RGS14-positive bands by western blot, demonstrating the existence of previously speculated splice variants. One of these short splice variants, dubbed RGS14-S, retains an NLS but lacks the NES (409), and may account for the nuclear fraction of RGS14 in primate striatum. We thus wanted to determine whether wild type RGS14 could also shuttle into and out of nuclei in hippocampal neurons. Neurons (DIV 8) transfected with pAAV-hSyn-YFP-RGS14 for 18 hours were treated with Leptomycin B (LMB), a CRM1/nuclear export inhibitor, over two and a half hours and imaged by live cell confocal microscopy. We found that cytoplasmic RGS14 translocated to the nucleus within 40 minutes, and was completely nuclear by two hours (Figure 3.1B). Based on these results, all further LMB treatments were carried out for two hours.

We next wanted to verify co-localization with a nuclear marker, Hoechst, as well as validate the NES box in neurons. We transfected DIV8 neurons with pAAV-YFP-RGS14 WT or NESm (L503A/L504A) for 18 hours. Neurons were then treated with vehicle or LMB for two hours, then fixed and stained with Hoechst, and YFP signal was assessed by confocal microscopy. Vehicle-treated neurons had robust YFP-RGS14 expression that filled the neuronal soma, dendrites, and spines, but did not overlap with the Hoechst-stained nucleus, while YFP-RGS14 colocalized

entirely with Hoechst in LMB-treated neurons (Figure 3.1C), further supporting that cytoplasmic pools of RGS14 are targeted for nuclear localization. Expression of a single band corresponding to the full-length YFP-RGS14 was verified by Western Blot (Figure 3.1.1). LMB strongly and specifically inhibits nuclear export receptor CRM1 (also known as XPO1 or Exportin 1). The CRM1-binding motif is a leucine-rich sequence (410) and we had previously shown that mutating two leucines in the RGS14 GPR motif (LL/AA) inhibited nuclear export of RGS14 in immortal cells (288). Thus, we wanted to verify whether RGS14 nuclear shuttling in neurons was through the same mechanism. We transfected pAAV-hSyn-YFP-RGS14 L503A/L504A (NESm) into DIV 8 neurons for 18 hours, then fixed and stained with Hoechst as before. Again, we verified expression of a single band corresponding to full-length YFP-RGS14 NESm by Western Blot (Figure 3.1.1). We found that under vehicle-treated conditions, YFP-RGS14 NESm was sequestered in the nuclei and colocalized with Hoechst, indistinguishable from the LMB-treated WT RGS14 (Figure 3.1D).

Based on our findings that RGS14 is a nuclear shuttling protein in neurons, and evidence that it utilizes CRM1 as its export receptor, we next wanted to create a structural model of the two interacting. CRM1 recognizes a diverse range of NES motifs, and these motifs can be grouped into ten classes according their unique spacing of hydrophobic residues (411). The NES embedded within RGS14's GPR motif forms an all α-helical secondary structure and matches a Class 3 spacing motif: $\phi_1XX\phi_2XXX\phi_3XX\phi_4$ where ϕ is L, V, I, F, or M, and X is any amino acid (Figure 3.2A). We therefore hypothesized that the RGS14 NES would fit a class 3 binding model to CRM1. The RGS14 GPR peptide, which contains the full NES, was crystallized previously with Gαi1 (296), and a class 3 NES (mDia2) was recently crystallized with CRM1 (411). We therefore created an RGS14-NES/CRM1 model by structurally aligning RGS14's NES with the crystal structure of the mDia2 NES-CRM1 complex (Figure 3.2B). The alignment of the two NES-containing helices reveals optimal positioning of the hydrophobic residues (ϕ) necessary for interaction with CRM1

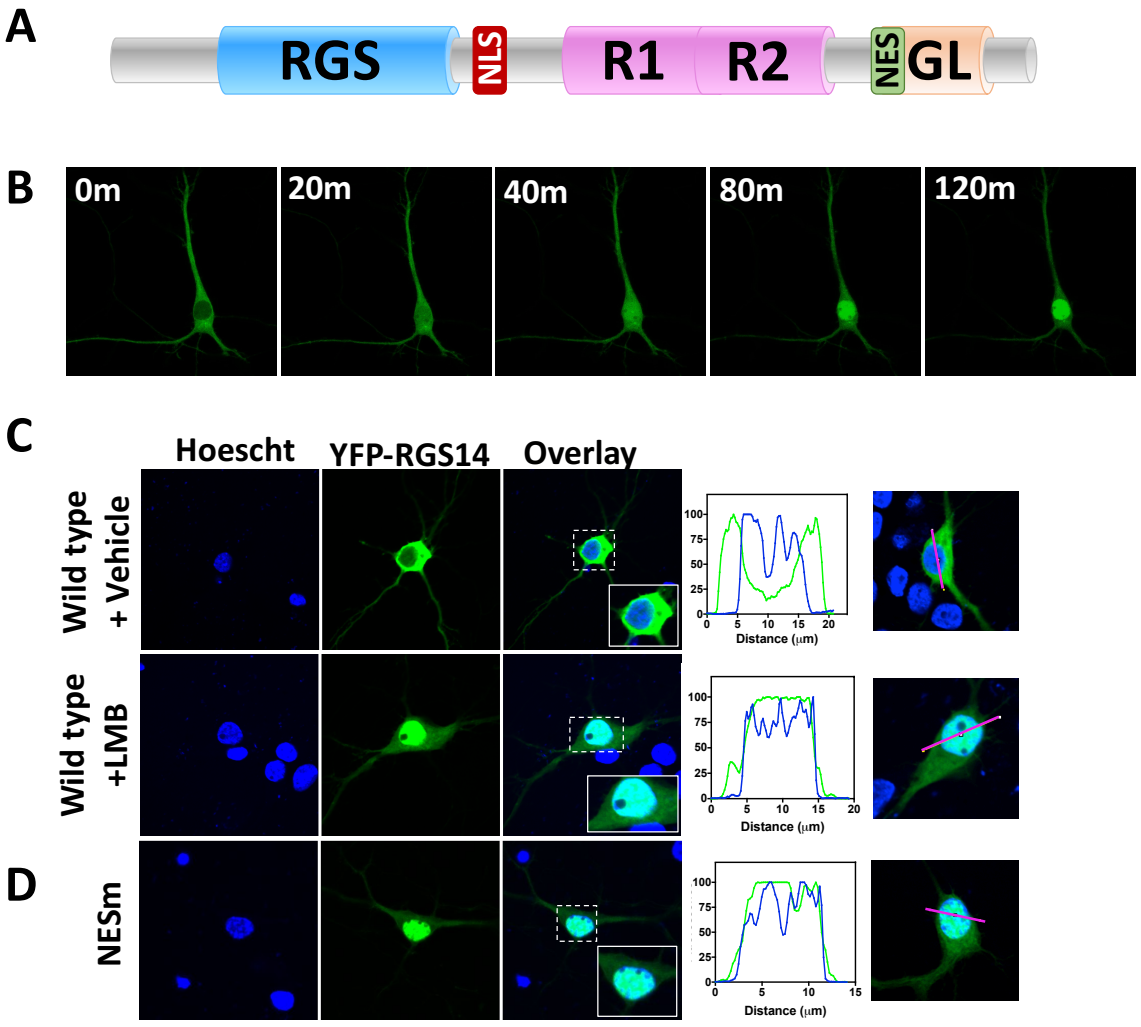

Figure 3.1. RGS14 is a nuclear shuttling protein in neurons.

A) *RGS14 rapidly shuttles into and out of the nucleus in dividing cells via a nuclear localization sequence (NLS) and nuclear export sequence (NES). We thus wanted to validate these cellular dynamics were active in neurons.* ***B)*** *AAV-YFP-RGS14 was transfected and 18 hours later neurons were imaged using live cell confocal microscopy. Leptomycin B (LMB) was added and YFP signal was measured. At 20 minutes, YFP-RGS14 was detectable in the nucleus, at 40 minutes YFP-RSG14 was mostly nuclear, and by 80 minutes YFP-RGS14 was nearly entirely nuclear.* ***C)*** *Wild type RGS14 does not colocalized with Hoechst in vehicle treated conditions, but colocalizes with Hoechst entirely under LMB conditions.* ***D)*** *Mutation of the NES (L503A/L504A, "NESm") in RGS14 sequesters RGS14 entirely in the nucleus under vehicle treated conditions.*

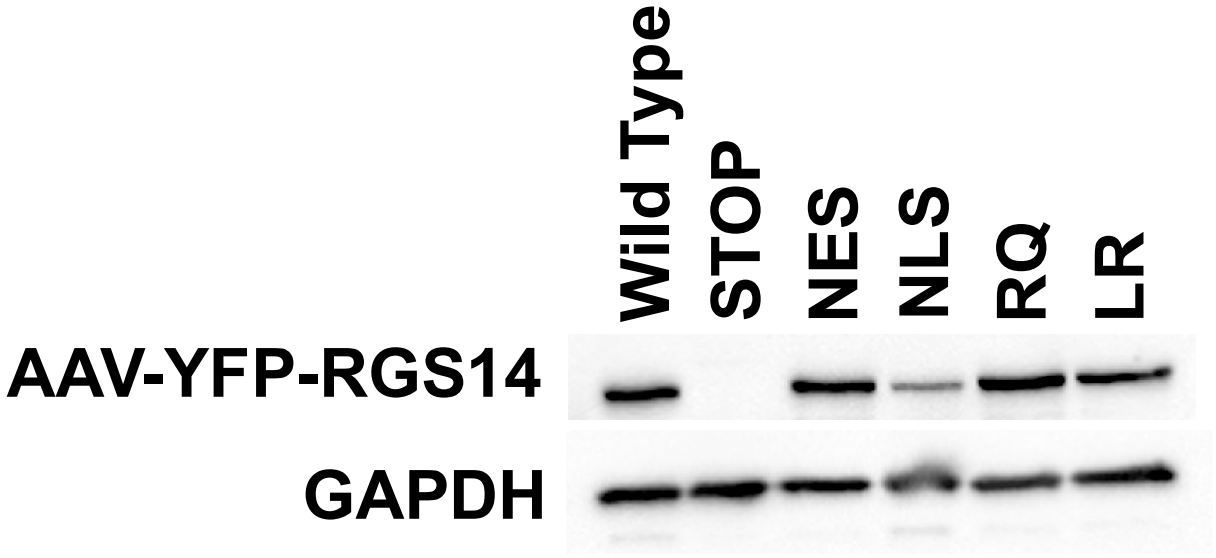

Figure 3.1.1. Expression of RGS14 constructs is verified by western blot.

Wild type RGS14 expressed a single band correlating to the approximate size of YFP-RGS14 (~85 kDa), while the STOP mutation correlating to YFP-STOP-RGS14 produced no detectable RGS14 as expected. The NES, NLS, RQ, and LR mutations similarly produced a single band corresponding to full length YFP-RGS14. GAPDH was used as a loading control.

(Figure 3.2C). These ϕ residues stabilize the RGS14–CRM1 interaction through hydrophobic interactions with CRM1 pockets P0-P3 (Figure 3.2D), mirroring the previously reported mDia2-CRM1 complex (411). Co-immunoprecipitation with RGS14 and Ran-GTP confirmed CRM1 as a binding partner of WT RGS14 but not RGS14 NESm (Figure 3.2E).

We recently reported that RGS14 exists natively in the nuclei of striatal neurons in primate brain (335), although it has been known for quite some time that RGS14 localizes to spines and is a natural suppressor of long term potentiation (LTP), which happens at the level of the spine (338). This suggests a unique role of nuclear-bound RGS14. Based on these findings, and the fact that we can artificially drive it to the nucleus, we next wanted to examine the existence and effect of genetic variants found naturally within the human population. We accessed the Genome Aggregation Database (GnomAD, version 2.0) for all RGS14 missense (amino acid change) and silent (DNA change but no amino acid change) variants. There was a relatively even distribution of missense and silent variants throughout the RGS14 gene (Figure 3.3A, missense on top, silent on bottom). Importantly, multiple human variants were found within the GPR motif, in or near the NES (Figure 3.3A, GPR motif and sequence expanded with variants shown on top in red). To determine the effect on RGS14 trafficking within the cell, we wanted to screen each of these human variants using BRET. The GPR motif binds, in addition to CRM1, inactive Gαi1-GDP, and is subsequently recruited to the plasma membrane (299). RGS14:Gαi1-GDP interactions are robustly detectable by BRET and are indicative of functional trafficking between cellular compartments, and thus provide a convenient screening tool. Wild type RGS14-Luc binds Gαi1-YFP and saturates Net BRET signal (Figure 3.3B, black line). When the GPR motif is mutated such that it cannot bind Gαi1-GDP (GPRm) as previously reported (296, 299), or when the NES is mutated as shown in Figure 3.1B (NESm), RGS14-Luc ceases to bind Gαi1-YFP as measured by BRET, indicating aberrant subcellular trafficking (Figure 3.3B, teal lines). We screened 13 human variants in RGS14's GPR motif by BRET and found that, while the majority did not affect binding to Gαi1-YFP, a handful

did (Figure 3.3.1), of which 2 emerged as especially interesting based on their effect or population frequency (Figure 3.3). The L504R variant, which is extremely rare (found in 0.006% of East Asian population, "East Asian variant") completely ablated binding to Gαi1-YFP compared to wild type (Figure 3.3C), indicative of strongly disrupted cellular trafficking. The R506Q variant, by contrast, is relatively common (found in 1.25% of Ashkenazi Jewish population, "Ashkenazi variant") and had a submaximal reduction in Gαi1-YFP binding, suggesting a more subtle disruption in trafficking between compartments. In this way, these two *naturally occurring* human variants provide biologically relevant tools to study "dose-effect" outcomes with RGS14.

We hypothesized that, based on the reduction in Gαi1-YFP binding and proximity to the NES versus Gα-binding motif, these two variants sequestered RGS14 in the nucleus either entirely (East Asian variant), or partially (Ashkenazi variant). To determine the effect of these variants *in vivo*, we transfected DIV 8 neurons with wild type pAAV-hSyn-YFP-RGS14, RGS14 R506Q (Ashkenazi), or RGS14 L504R (East Asian) for 18 hours, then fixed and stained nuclei with Hoechst. Confocal microscopy captured the position of wild type or variant RGS14 within the neuron. We found that while wild type RGS14 filled the soma, dendrites, and spines, the East Asian variant concentrated entirely within the nucleus, and the Ashkenazi variant had a mixed phenotype (Figure 3.4A and B). This was in agreement with our expectations based on our results in Figure 3.3. In light of these data, the fact that the CRM1- and Gαi1-binding motifs are nearby, and previous studies showing that Gαi1 interactions can affect nuclear localization (288), we wanted to validate that reduction in RGS14-Luc:Gαi1-YFP binding (Figure 3.3) was indeed due to interactions with CRM1 at the NES. We thus generated mutations that disrupted the NLS motif (Figure 3.4.1) and added them to our RGS14-Luc L504R and RGS14-Luc L504R constructs to make RGS14-Luc L504R/NLS and RGS14-Luc R506Q/NLS. These double mutant constructs are unable to translocate to the nucleus (Figure 3.4.1). Therefore, contributions of CRM1 binding should be eliminated, and we should be able to determine the effect of these human variants on Gαi1-YFP

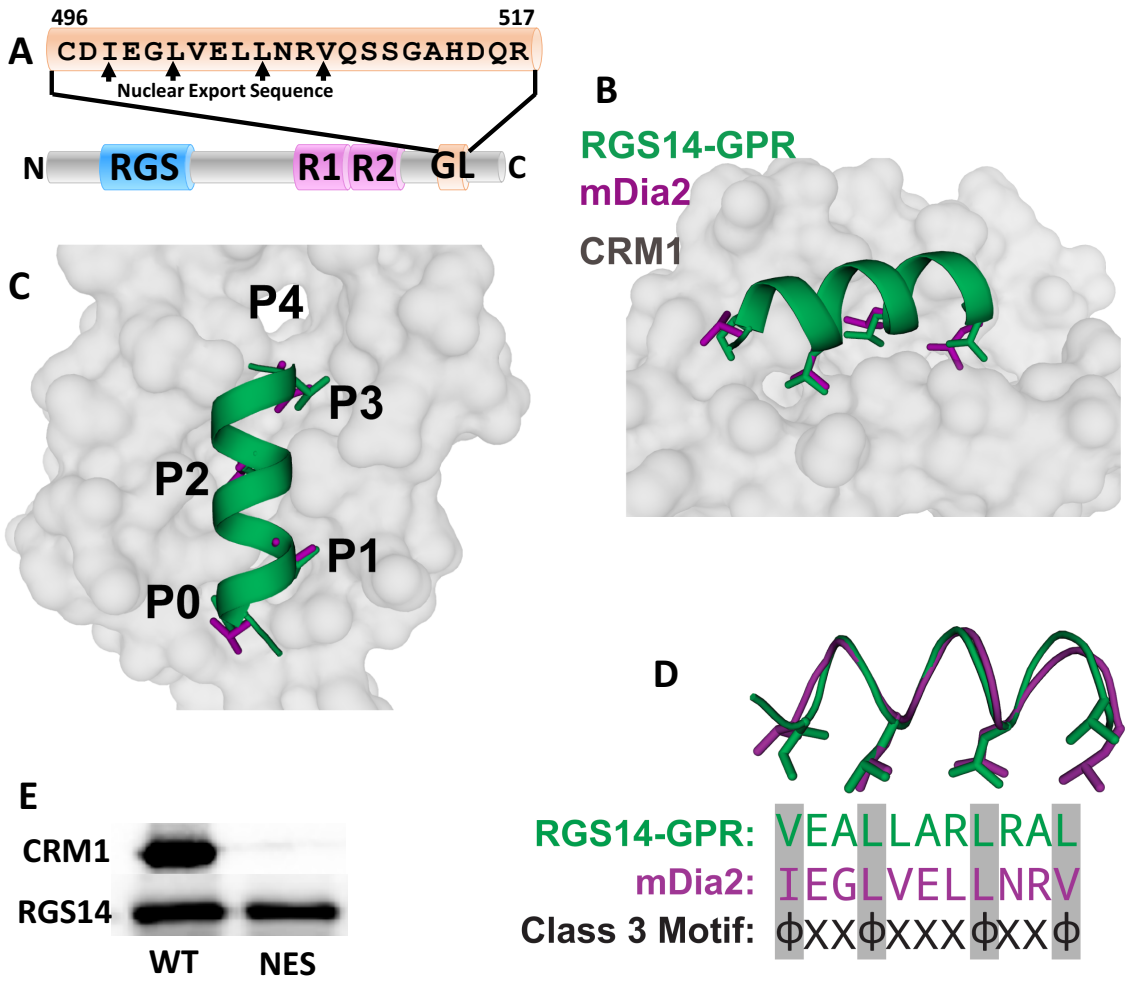

Figure 3.2. RGS14'S GPR (GoLoco, GL) motif contains a class 3 nuclear export sequence that binds CRM1.

A) The NES of RGS14 is embedded within the GPR/GL motif and follows a class 3 pattern: $\phi_1XX\phi_2XXX\phi_3XX\phi_4$. B) The crystallized GPR peptide of RGS14 (1KJY) was structurally aligned with a similar class 3 NES motif, crystallized with CRM1 (mDia2 PDB 5UWP). C-D) The RGS14 NES fits a class 3 binding motif, occupying pockets 0-3, but not pocket 4, as reported previously (411). E) RGS14 WT co-immunoprecipitates with CRM1, but not RGS14 NES.

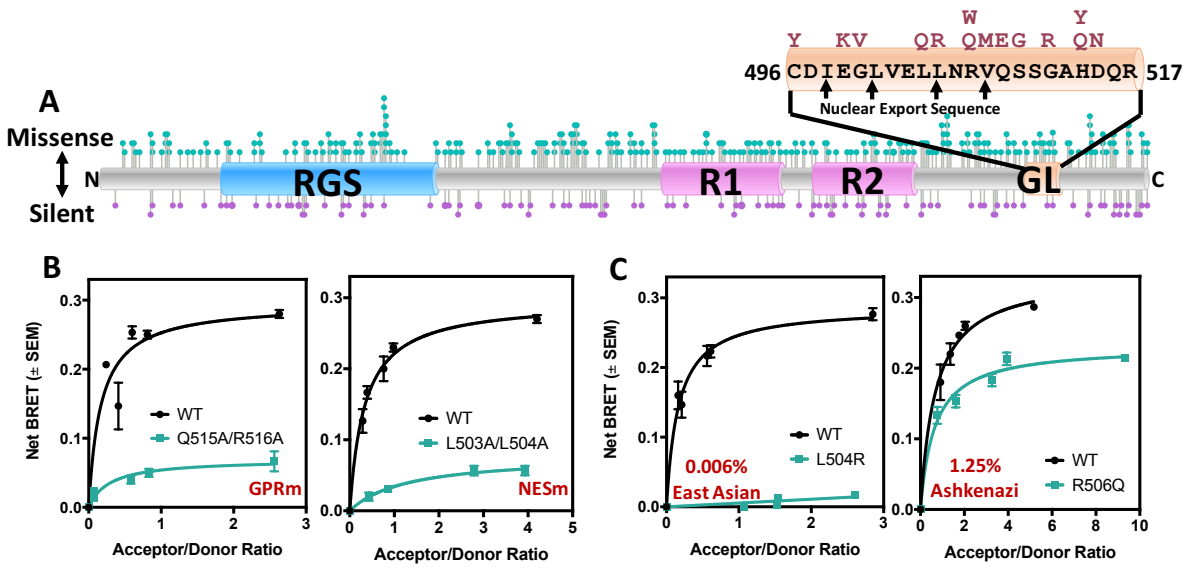

Figure 3.3. RGS14 human rare variants disrupt association with Gαi1-GDP, indicating aberrant cellular trafficking.

A) *RGS14 missense and silent variants were obtained from GnomAD (Broad Institute) and plotted onto the sequence of RGS14 using Lollipops (https://github.com/pbnjay/lollipops). Missense variants are plotted on top in teal, with silent variants on the bottom in purple. The GPR (GoLoco, GL) motif, which contains the NES, has many human variants.* ***B)*** *RGS14 is recruited from the cytoplasm to the plasma membrane by inactive Gαi1-GDP (299). Inactivation of the GPR (Q515A/R516A) prevents Gαi1-GDP binding and recruitment to the plasma membrane. Similarly, inactivation of the NES (L503A/L504A) prevents RGS14 from being accessible for recruitment in the cytoplasm, and therefore cannot associate with Gαi1-GDP at the plasma membrane.* ***C)*** *We tested these variants for their ability to associate with Gαi1-GDP, indicative of proper recruitment to the plasma membrane and found L504R (0.006% of the East Asian population) completely abolished Gαi1-GDP association, while R506Q (1.25% of the Ashkenazi population) saw a more subtle reduction in Gαi1-GDP association.*

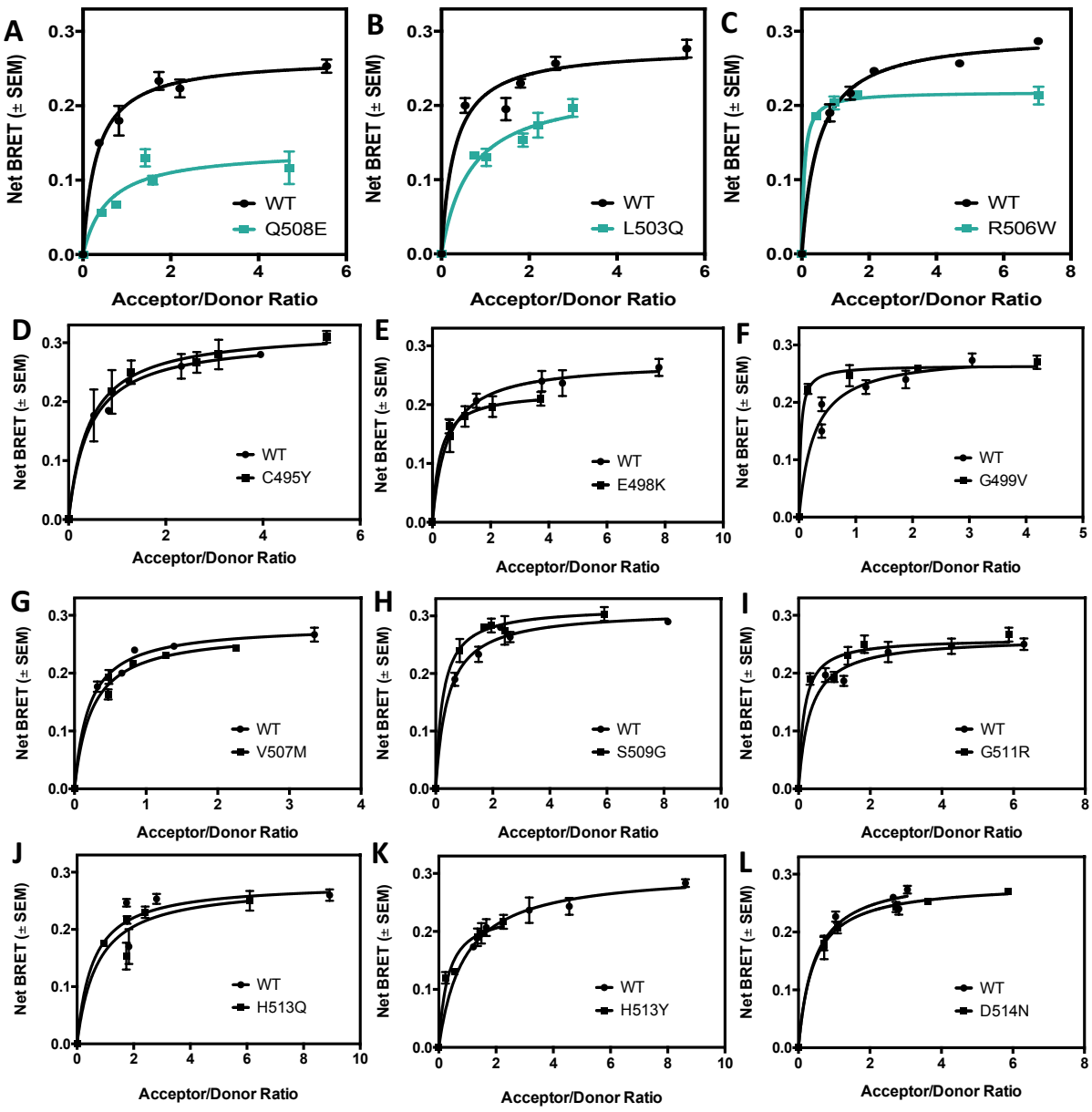

Figure 3.3.1. Most human variants in RGS14 do not affect association with Gαi1-GDP.

Variants from Figure 3.3A were tested for their ability to associate with Gαi1-GDP. There were several variants that saw a reduction in Gαi1-GDP association ***(A-C shown in teal)****, but most had no robust phenotype* ***(D-L)****.*

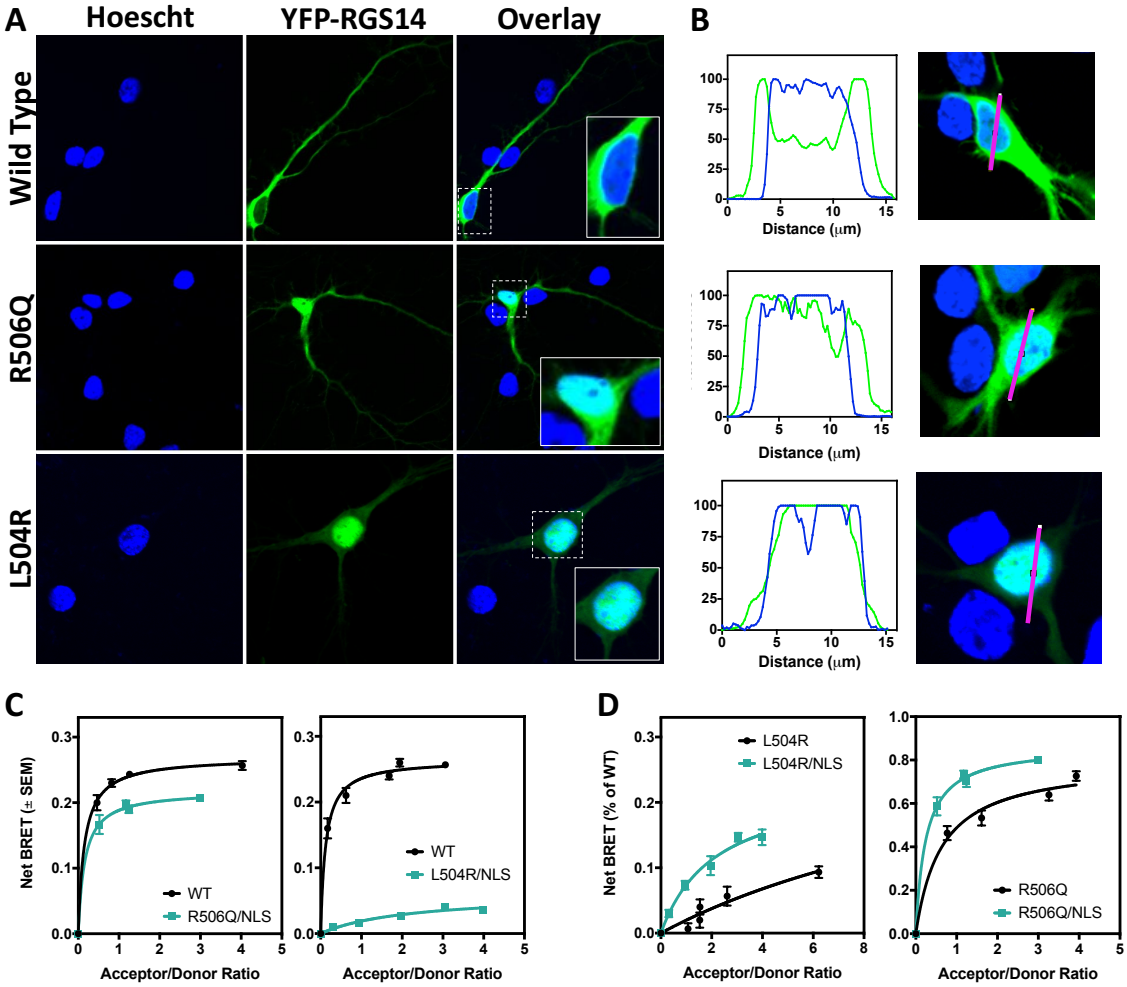

Figure 3.4. RGS14 nucleo-cytoplasmic equilibrium favors the cytoplasm, and human rare variants disrupt this balance.

A) *Wild type RGS14 does not colocalize with Hoechst in neurons under unstimulated conditions, while the R506Q (Ashkenazi) variant occupies both the nucleus and the cytoplasm, and the L504R (East Asian) variant occupies the nucleus entirely.* ***B)*** *Quantification of YFP (RGS14) and Hoechst overlay for WT RGS14 and each of the variants.* ***C)*** *The GPR motif also shares a binding site with Gαi1-GDP, so we introduced an NLS mutation to prevent nuclear localization. Thus any change in Net BRET from wild type is due to effects of Gαi1-GDP binding, independent of mislocalization to the nucleus and interaction with CRM1. Net BRET for both R506Q and L504R is partially (although not fully) restored when an NLS mutation is introduced (compare to Figure 3.3).* ***D)*** *Comparison between L504R to L504R/NLSm, and R506Q to R506Q/NLSm (L504R and R506Q data from Figure 3.3). Adding the NLS mutation enhances Gαi1-GDP association, indicating that at least part of the effect is due to mislocalization to the nucleus via reduced interaction with CRM1.*

binding alone. We found that the L504R/NLS and R506Q/NLS partially, but not fully, restored Gαi1-YFP binding to the GPR motif (Figure 3.4C). We next compared L504R to L504R/NLS, and R506Q to R506Q/NLS as a percentage of wild type (Figure 3.4D) using the data generated in Figure 3.3C. We found a prominent rescue of Gαi1-YFP binding to RGS14 in both the East Asian and Ashkenazi variants when an NLS mutation was added, but not a full rescue, suggesting at least a partial disruption of Gαi1-binding, separate from CRM1. Together, our BRET data and microscopy data indicate aberrant cellular trafficking of RGS14, presumably sequestering it from dendrites and spines, which we predict to be critical for RGS14 inhibition of LTP.

We next utilized the RGS14-NES/CRM1 model, described above, to further explore the mechanism behind the disruption of nuclear export. Based on our model, arginine 506 (R506) in wild-type RGS14 contains a positively charged nitrogen atom that is 5.5 Å away from a negatively charged oxygen atom of glutamic acid in CRM1, which is in line with a possible ionic interaction. We then mutated this residue in our model to the Ashkenazi variant, glutamine 506 (Q506), in order to provide a mechanistic explanation for the decreased nuclear export present in Ashkenazi variant. The variant (Q506) disrupts the ionic interaction that was present between R506 and glutamic acid in CRM1. The distance between Q506 and the glutamic acid in CRM1 is too great for hydrogen bonding, suggesting this variant will reduce affinity of RGS14 for CRM1 (Figure 3.5A). We next wanted to visualize the impact of the East Asian variant, arginine 504 (R504). In wild-type RGS14, leucine 504 (L504) fits nicely within the P2 hydrophobic pocket of CRM1, stabilizing the complex through hydrophobic interactions. The East Asian variant (R504) places a charged arginine within the P2 hydrophobic pocket of CRM1 causing a polar incompatibility that will greatly disrupt the RGS14-CRM1 interaction (Figure 3.5B). This severe mutation within the binding interface of RGS14 and CRM1 explains why the East Asian variant is entirely nuclear.

Based on the findings described presently, we finally wanted to test the contribution of these naturally occurring human variants on RGS14 suppression of LTP. To measure contributions of

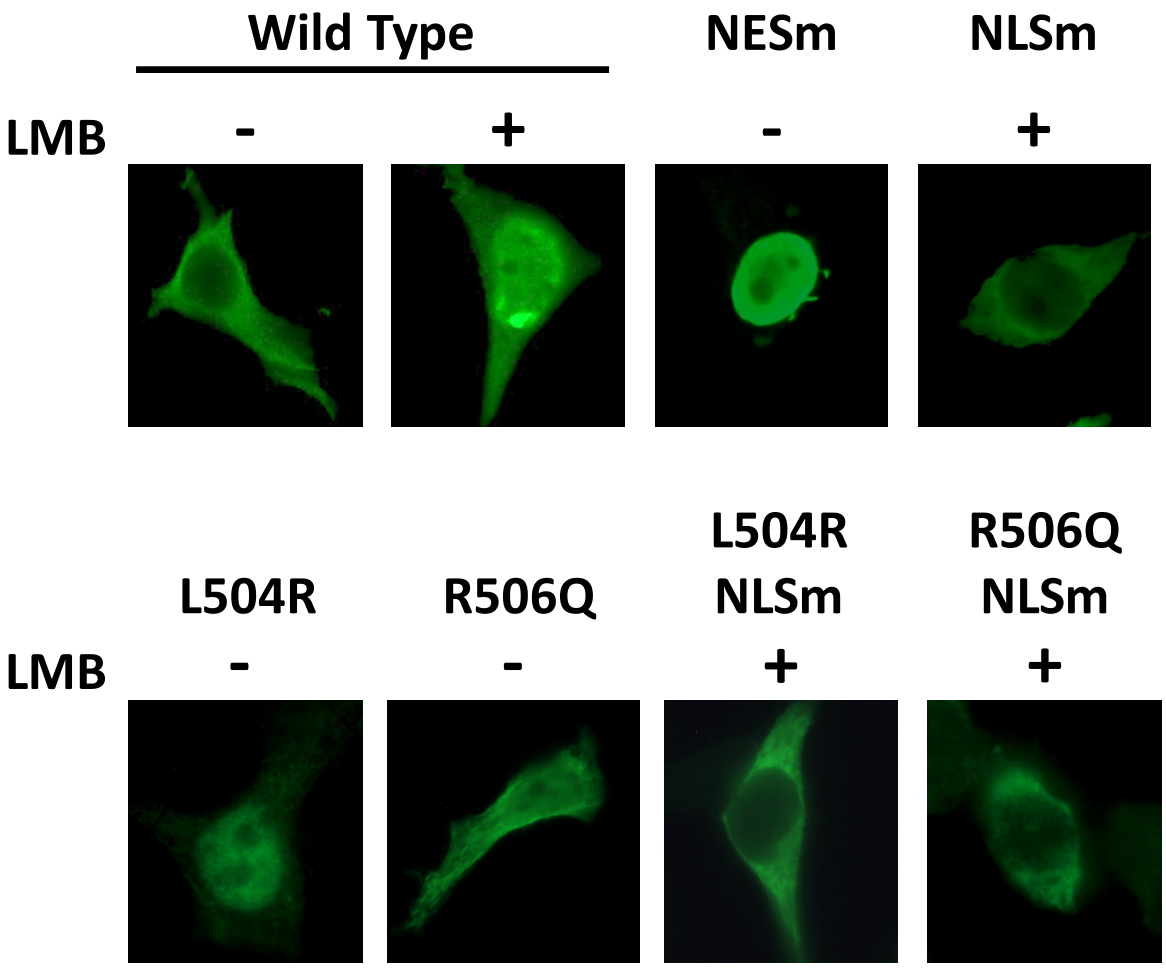

Figure 3.4.1. Nuclear localization mutations control nuclear trafficking and/or export of RGS14.

Wild type RGS14 translocates to the nucleus following LMB treatment (top left). RGS14 NESm is sequestered in the nucleus under vehicle conditions, and NLSm never translocates to the nucleus, even in the presence of LMB (top right). While L504R and R506Q have nuclear localization phenotypes to varying degrees (bottom left), adding an NLS mutation to each construct entirely prevents nuclear localization (bottom right).

experimental RGS14 in a hippocampal region that has robust and readily accessible LTP, we sought to express exogenous RGS14 in CA1. We generated adeno-associated viruses from our wild-type, East Asian, and Ashkenazi constructs, and delivered virus into cultured hippocampal slices (Figure 3.6A). Further, a YFP control was generated by adding a STOP codon at the end of the YFP C terminus, such that RGS14 was not translated (Figure 3.1.1). We found that wild type YFP-RGS14 was detected throughout the soma, dendrites, and spines as found in our dissociated hippocampal neurons (Figure 3.4A). The Ashkenazi variant filled the entire cell, occupying both the nucleus and cytoplasm, while the East Asian variant was entirely nuclear (Figure 3.6A), consistent with our results in dissociated neurons (Figure 3.4A). Next, we recorded excitatory post synaptic currents (EPSCs) at baseline and following an LTP induction protocol. We report that wild type YFP-RGS14 is able to fully block LTP when ectopically expressed in CA1 hippocampal neurons, while YFP alone has no effect on LTP (Figure 3.6B), suggesting that RGS14 is sufficient to suppress LTP. Next, we examined the contribution of the East Asian and Ashkenazi variants on RGS14 suppression of LTP. Consistent with our present data, the East Asian and Ashkenazi variants were unable to fully suppress LTP (Figure 3.6B), both demonstrating a dependence on proper compartmental localization for functional RGS14 actions in the hippocampus. Interestingly, the Ashkenazi variant (R/Q) only failed to suppress LTP for the first ten minutes of recording, whereas the East Asian variant (L/R) was able to fully block LTP for the duration of recording. The degree to which LTP was suppressed (i.e. partially in the case of R/Q and fully in the case of L/R) correlated with the degree of nuclear sequestration, suggesting a graded, rather than binary, relationship between localization and function of RGS14. Taken together, these findings present a compelling role for RGS14's dynamic regulation within its host environment, the effect of this subcellular balance on its role as a regulator of LTP, and the presence of naturally occurring genetic variation that may tip the scale in favor of inhibition or disinhibition of synaptic plasticity and learning.

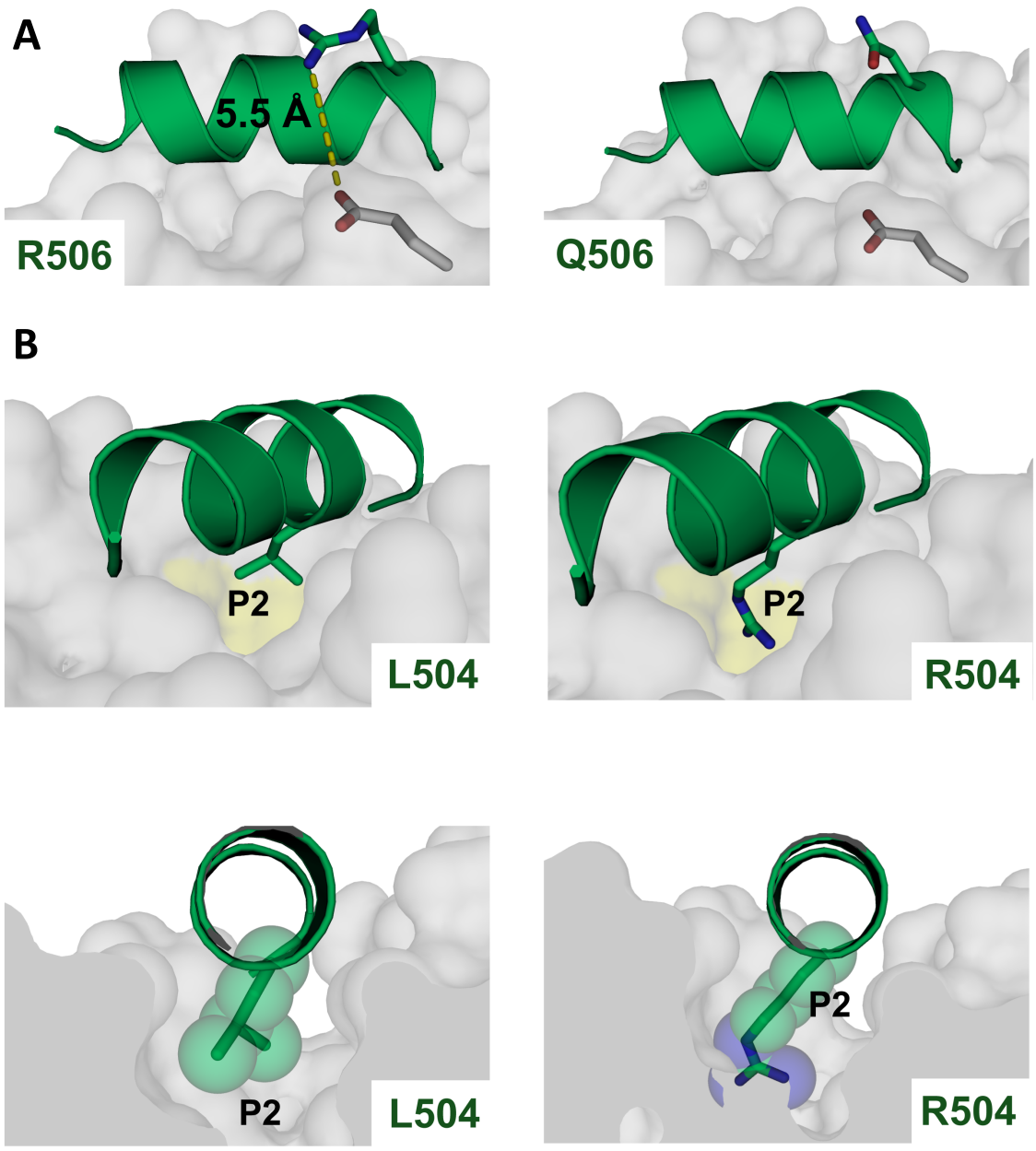

Figure 3.5. RGS14 human rare variants disrupt binding to CRM1 through loss of side chain interactions.

A) *Structural modeling of the Ashkenazi (R506Q) variant onto CRM1. Left panel is the wild type amino acid, arginine, which makes a salt bridge with a nearby glutamate near the binding pocket on CRM1. Mutation to a glutamine (right panel) removes this salt bridge, presumably destabilizing the protein-protein interaction.* ***B)*** *Structural modeling of the East Asian (L504R) variant onto CRM1. The leucine interacts directly with the hydrophobic P2 pocket (left panel). Mutation of this amino acid to an arginine (right panel) introduces a charged side chain into a hydrophobic pocket. These data mechanistically explain the difference in phenotype (R506Q being a subtler phenotype compared to L504R).*

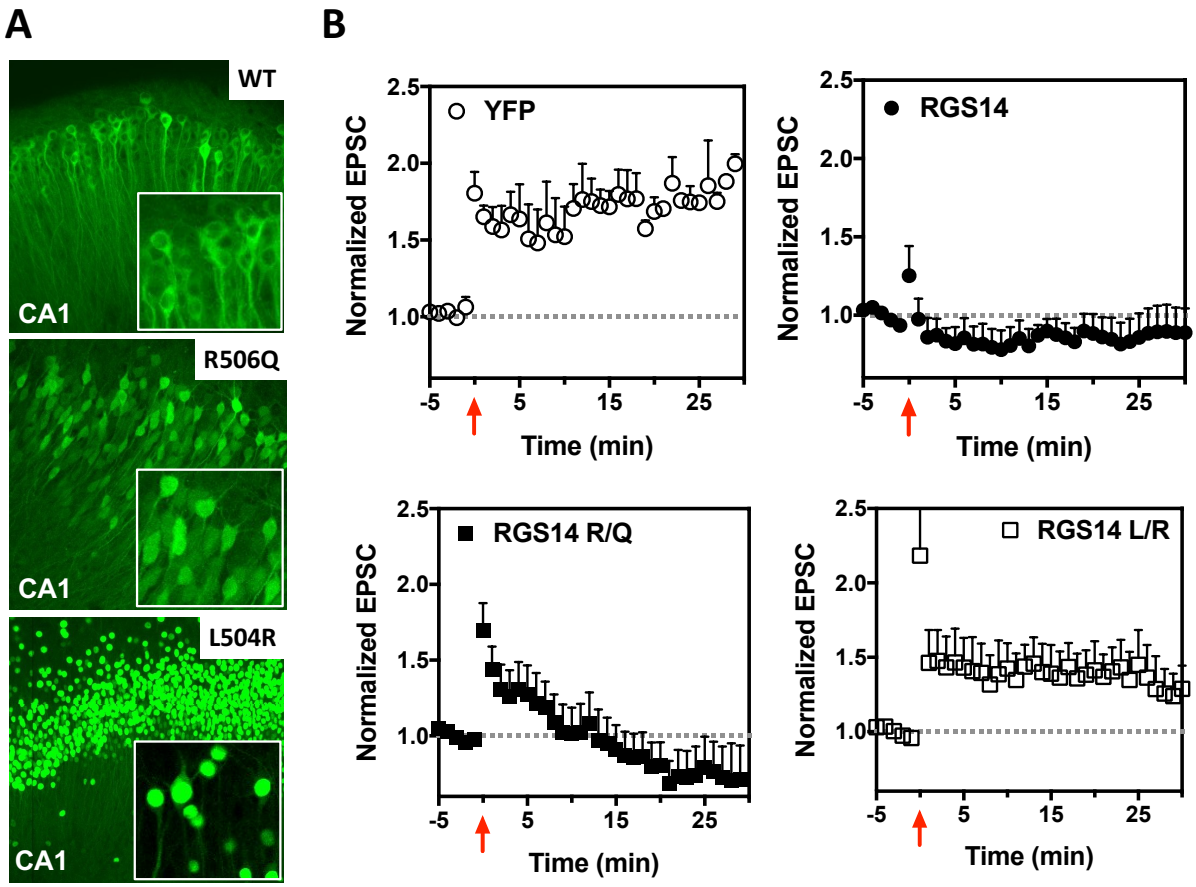

Figure 3.6. Human variants that disrupt RGS14 nuclear equilibrium inhibit RGS14 function and restore long term potentiation.

AAV-YFP-RGS14 was used to make AAV2/9 viruses, including wild type RGS14 as well as human variants R506Q and L504R. Furthermore, a stop codon was generated as follows AAV-YFP-STOP-RGS14, to make a truncated RGS14-lacking YFP virus. Virus was injected into mouse CA1 and incubated for one week, at which point electrophysiological recordings were taken. ***A)*** *Expression of YFP-RGS14 in CA1 brain slices. WT RGS14 fills the cytoplasm of neurons, while R506Q fills both the cytoplasm and nucleus, and L504R is exclusively nuclear, entirely consistent with our data in dissociated neurons.* ***B)*** *Long term potentiation (LTP) was induced by high frequency stimulation of Schaffer collateral input into CA1. While YFP alone had no effect on LTP, WT RGS14 ablates LTP in CA1, a hippocampal region where RGS14 is not natively found. Remarkably, suppression of LTP by RGS14 was restored in R506Q variant-expressing neurons after 10 minutes, while the L504R completely failed to suppress LTP. This suggests that the degree of mislocalization by these variants correlates with ablation of RGS14 function in CA1 neurons.*

DISCUSSION

Long term potentiation and synaptic plasticity are mediated by a complex network of signaling events that drive global changes in connectivity, learning, and behavior. For this network to function properly, signaling proteins must be in the right place, at the right time, for the right amount of time. The importance of each of these conditions is underscored by numerous studies modulating temporal and spatial constituents of plasticity pathways. Here we describe one of these constituents, RGS14, which mediates a type of synaptic plasticity, LTP, and how spatial requirements for RGS14 control its ability to act as a suppressor of LTP.

Previous work has described RGS14 as a natural inhibitor of LTP in CA2 (338), and as a dynamic protein in cell culture (288). We recently published findings detailing the native expression of RGS14 in human and monkey brain, demonstrating not only a broader expression of RGS14, but also a nuclear subpopulation of RGS14 (335). In addition to the hippocampus, RGS14 is robustly expressed in the caudate, putamen, globus pallidus, substantia nigra, and amygdala of primate brain, strongly suggesting a role for RGS14 in movement. Although we do not yet know the significance of RGS14 in these regions, these questions constitute current and ongoing studies. We also found evidence for the existence of putative splice variants in the striatum, some of which are predicted to retain an NLS but lack an NES (412). These data coincided with the discovery of native RGS14 in the nucleus of striatal neurons, prompting us to examine the dynamic regulation of RGS14 is native neuronal populations.

Here we present conclusive evidence showing RGS14 translocates across the nuclear membrane, and does so via interactions with a leucine-rich NES motif and nuclear export receptor CRM1. This NES motif is embedded within the GPR motif and human variants found within certain ethnicities (East Asian and Ashkenazi Jewish) conferred a shift in the nucleo-cytoplasmic equilibrium of RGS14 distribution. Reduced interactions with CRM1 are explainable by structural modeling, although contributions from reduced Gαi1 binding cannot be eliminated, and caused a

loss of function of RGS14 (i.e. a disinhibition or rescue of LTP). This may lead to enhanced or altered plasticity, learning, or other "traits" in carriers of these genetic variants.

The biological significance of nuclear sequestration, including the mediators that drive the nucleo-cytoplasmic balance, is an ongoing investigation in our lab. It is possible that RGS14 is sequestered in the nucleus as a mechanism by the neuron to remove the brake on LTP. Upon LTP induction, the spine undergoes massive remodeling, including phosphorylation state changes, AMPA receptor trafficking, and actin cytoskeleton rearrangement (16). RGS14 being positioned at the spine allows it to participate, biochemically, in regulation of these processes. At least two RGS14 binding partners are strongly linked with regulation of LTP at the spine, including CaM and H-Ras (16, 293, 413). Removing the available pool of RGS14 from spines, or from trafficking to spines, may be one way in which the cell can allow for differential regulation of these LTP-linked pathways.

Another possible explanation for RGS14 nuclear localization is an independent role within the nucleus. The signals that target RGS14 to the nucleus remain unclear. It is possible that LTP stimulation redistributes populations of RGS14 to be more nuclear, as analogous signals do to RGS10 and RGS12 (62, 290, 306). Gene regulation is a key component of LTP maintenance, as opposed to LTP induction. Previous studies indicate that RGS14 inhibits the induction of LTP, so it is unknown what effect if any RGS14 has on LTP maintenance. In the present study, human variants target RGS14 to the nucleus constitutively, so any temporal regulation of gene products by RGS14 is likely dysregulated and may confer a different phenotype than would be captured by two-hour treatment with LMB or normal nuclear shuttling of RGS14. These differences could be teased out in future studies. Although RGS14 does not have a DNA-binding motif, it is possible that through interactions with accessory proteins, RGS14 may be regulating gene expression. This is not entirely unprecedented, as RGS12 (a closely related RGS family member) can translocate to the nucleus and repress transcription of certain genes (290). Identifying genic targets of RGS14 (i.e. transcriptional differences from neurons expressing RGS14-NESm versus RGS14-NLSm)

may elucidate novel mechanisms by which RGS14 regulates neuronal plasticity, and is the focus of current investigation.

Overall, these present studies bring light to the importance of dynamic regulation of signaling proteins in the context of synaptic plasticity and demonstrate the contribution of naturally occurring human genetic variation to this compartmental equilibrium. These data underscore the importance of considering not only "canonical" sequences, but also those representing diverse human populations. Whether these genetic variants confer the emergence of unique traits or attributes to carriers remains an interesting question, particularly within the context of CA2-linked social and contextual memory.

CHAPTER 4:

REGULATOR OF G PROTEIN SIGNALING 14 (RGS14) IS EXPRESSED PRE- AND POSTSYNAPTICALLY IN NEURONS OF HIPPOCAMPUS, BASAL GANGLIA, AND AMYGDALA OF MONKEY AND HUMAN BRAIN[3]

[3] This chapter has been modified from the published manuscript [Squires KE, Gerber KJ, Pare, JF, Branch MR, Smith Y, and Hepler JR (2017) Regulator of G protein signaling 14 (RGS14) is expressed pre- and postsynaptically in neurons of hippocampus, basal ganglia, and amygdala of monkey and human brain. *Brain Struct Funct*.] to comply with formatting standards for this thesis.

4.1 ABSTRACT

Regulator of G protein signaling 14 (RGS14) is a multifunctional signaling protein primarily expressed in mouse pyramidal neurons of hippocampal area CA2 where it regulates synaptic plasticity important for learning and memory. However, very little is known about RGS14 protein expression in the primate brain. Here, we validate the specificity of a new polyclonal RGS14 antibody that recognizes not only full length RGS14 protein in primate, but also lower molecular weight forms of RGS14 protein matching previously predicted human splice variants. These putative RGS14 variants along with full-length RGS14 are expressed in the primate striatum. By contrast, only full length RGS14 is expressed in hippocampus, and shorter variants are completely absent in rodent brain. We report that RGS14 protein immunoreactivity is found both pre- and postsynaptically in multiple neuron populations throughout hippocampal area CA1 and CA2, caudate nucleus, putamen, globus pallidus, substantia nigra, and amygdala in adult rhesus monkeys. A similar cellular expression pattern of RGS14 in the monkey striatum and hippocampus was further confirmed in humans. Our electron microscopy data show for the first time that RGS14 immunostaining localizes within nuclei of striatal neurons in monkeys. Taken together, these findings suggest new pre- and postsynaptic regulatory functions of RGS14 and RGS14 variants, specific to the primate brain, and provide evidence for unconventional roles of RGS14 in the nuclei of striatal neurons potentially important for human neurophysiology and disease.

4.2 INTRODUCTION

Much of neurotransmission is mediated through receptor and heterotrimeric G protein (Gαβγ) signaling near synapses, a process that is tightly regulated by a family of regulators of G protein signaling (RGS) (21) that facilitate the termination of Gαβγ signaling (17, 18, 414). RGS proteins comprise a diverse family of signaling molecules that contain various modular domains, but are defined by a conserved RGS domain that serves as a GTPase activating protein (GAP) to catalyze the conversion of active Gα-GTP into inactive Gα-GDP (15, 18) and limit neurotransmitter signaling. One such RGS family member, RGS14, regulates long-term potentiation (LTP) and synaptic plasticity in mouse pyramidal neurons of hippocampal area CA2 (338). RGS14 specifically binds and regulates Gαi/o proteins (294, 333) and contains additional signaling domains, including tandem Ras/Rap binding domains and a G protein regulatory (GPR; also known as GoLoco, or GL) motif. The first Ras/Rap binding domain (R1) binds active H-Ras-GTP (291-293, 338) and active Rap2A-GTP (294, 415), which have opposing roles in the expression of LTP in the hippocampus (416-420). Though at present, it is currently unknown how RGS14 regulates the balance between these two pathways. While the RGS domain binds active Gαi/o-GTP to catalyze the conversion to Gαi/o-GDP, the GPR motif binds inactive $G\alpha i_{1/3}$-GDP (298). Although the GPR motif was previously reported as a guanine nucleotide dissociation inhibitor (295, 297), more advanced techniques have revealed that it does not prolong $G\alpha i_1$-GDP lifetime (414), but more likely regulates RGS14 membrane localization (288). Of note, RGS14 is capable of interacting with multiple partners simultaneously (299, 415), suggesting that its primary cellular function may be beyond that of a GAP.

Our earlier work reported that RGS14 protein is expressed in hippocampal area CA2 of mouse brain (338, 404), a small, enigmatic substructure of the hippocampus located between areas CA1 and CA3. While CA3 Schaffer collateral inputs into CA1 can undergo LTP in response to high frequency stimulation (421), LTP cannot be induced in CA3 Schaffer collateral projections onto

CA2 under the same conditions (403, 422). However, full expression of LTP at CA3-CA2 Schaffer collateral synapses can be induced by high frequency stimulation upon deletion of RGS14 in mouse. Furthermore, RGS14 knockout mice perform better in a spatial learning task than their wild type counterparts, indicating that RGS14 is a natural suppressor of hippocampal-based learning and memory through blockade of LTP at Schaffer collateral synapses in the mouse CA2 region (338). The restoration of LTP in CA2 by RGS14 ablation was blocked by a selective MEK inhibitor, indicating that RGS14 may suppress LTP by regulating signaling through Ras. Consistent with this idea, RGS14 has been shown to inhibit H-Ras/ERK signaling (292). Although RGS14's role in hippocampal area CA2 is well-established, our understanding of its role and expression outside of the hippocampus remains largely unexplored.

Within the mouse brain, RGS14 protein and mRNA expression is mostly confined to CA2, and behavioral tasks in RGS14 knockout animals confirm its role in hippocampal-mediated functions. We recently characterized a new monoclonal antibody against rodent RGS14, and discovered that hippocampal RGS14 in mice is absent at P0, first detected at P7, and reaches its full expression by early adulthood (404). However, we also noted modest expression of RGS14 in areas outside of CA2, including the piriform cortex, layers II, III, and V of the neocortex, and areas associated with olfaction. Additionally, various reports have suggested RGS14 may be expressed more broadly in the monkey and human brain (173, 197, 326). Although the Allen Mouse Brain Atlas (http://mouse.brain-map.org) confirms that RGS14 mRNA expression is strongest in the hippocampal CA2 region, mRNA expression atlases for human and non-human primate brains (http://human.brain-map.org and http://www.blueprintnhpatlas.org) report RGS14 transcript not only in CA2, but also in the caudate nucleus and putamen. If RGS14 protein is indeed expressed in regions other than CA2, the functions of RGS14 likely extend beyond the regulation of LTP and hippocampal learning in the primate brain as well. In light of reports of other RGS proteins (RGS2, 4, 7, and 9) known to regulate a broad spectrum of synaptic signaling that may be affected in various psychiatric diseases (21, 110-115, 133, 176, 395, 396, 423, 424), an in-depth knowledge of the

pattern of RGS14 protein expression and subcellular localization in the primate brain is needed.

With this goal in mind, the present study characterizes a new specific RGS14 polyclonal antibody that recognizes primate variants of RGS14 and uses this antibody in combination with light and electron microscopy to define in detail the cellular and subcellular localization of RGS14 protein in the human and monkey brain. Our findings demonstrate that RGS14 protein immunoreactivity displays a much broader distribution in the primate brain than in the mouse brain. In addition to being strongly expressed in CA2 and CA1 regions of the hippocampus, robust pre- and postsynaptic labeling was found in basal ganglia nuclei including the caudate nucleus, putamen, globus pallidus, and substantia nigra pars reticulata. Our data also provide evidence for the existence of RGS14 splice variants and their expression in the nucleus of striatal neurons. Altogether, our findings suggest potentially new and diverse functions of RGS14 and RGS14 variants in the primate brain that extend beyond hippocampal learning and memory.

4.3 MATERIALS AND METHODS

RGS14 Constructs and Materials

RGS14 purification

Full-length human RGS14 (Uniprot O43566) was cloned into a pLic-GST vector (pLic-GST-RGS14) and expressed in BL21 (DE3) *Escherichia coli*. Bacterial lysate was passed through a glutathione affinity column, washed with phosphate buffered saline, and bead-bound RGS14 purity was verified by coomassie-stained polyacrylamide gel. Rat RGS14 (Uniprot O08773) was purified as described previously (299). Briefly, full-length RGS14 was cloned into a pLic-MBP vector with a hexahistidine (H6) tag and a tobacco etch virus (TEV) cleavage site (H6-MBP-TEV-RGS14). Lysate was passed through a Ni^{2+} affinity column, cleaved overnight at 4°C with 1:200 TEV protease:RGS14, and finally purified on S75/S200 tandem sizing columns.

RGS14 polyclonal antibody

The RGS14 polyclonal antibody was purchased from Proteintech (Rosemont, Il) and stored at

-20°C until use, and then 4°C after. The immunogen used to generate this antibody is described by Proteintech as KSLPLGVEELGQLPPVEGPGGRPLRKSFRRELGGTANAALRRESQGSLNSSASLDLGFLA FVSSKSESHRKSLGSTEGESESRPGKYCCVYLPDGTASLALARPGLTIRDMLAGICEKRGL SLPDIKVYLVGNEQALVLDQDCTVLADQEVRLENRITFELELTALERVVRISAKPTKRLQ EALQPILEKHGLSPLEVVLHRPGEKQPLDLGKLVSSVAAQRLVLDTLPGVKISKARDKSP CRSQGCPPRTQDKATHPPPASPSSLVKVPSSATGKRQTCDIEGLVELLNRVQSSGAHDQR GLLRKEDLVLPEFLQLPAQGPSSEETPPQTKSAAQPIGGSLNSTTDSAL, which is amino acid 217-566 of human RGS14.

Immunoblotting

Antibody characterization

HEK293 cells were maintained in Dulbecco's modified eagle's medium (DMEM) supplemented with 10% fetal bovine serum (FBS), 100 U/mL penicillin, and 100 mg/mL streptomycin. Truncation mutants in rat FLAG-RGS14 were generated as described previously (288, 404). Cells were transfected in 5% FBS DMEM for 24 hours, then lysed and run on an 11% acrylamide gel at 150V for 2 hours, and transferred overnight onto nitrocellulose membranes. RGS14 antibody was incubated at 1:500 in 5% milk for 2 hours at room temperature, then washed for 30 minutes in 0.1% Tween-TBS. Anti-rabbit secondary antibody conjugated to HRP was incubated for 1 hour at room temperature, and washed for another 30 minutes in 0.1% Tween-TBS. Finally, membranes were incubated with ECL and exposed to X-ray film.

Pre-adsorption immunoblotting

Tissue punches containing RGS14 were taken from hippocampus and striatum of one adult wild-type mouse, and RGS14 expression was verified in this tissue as well as three additional mice by light microscopy (data not shown). Similarly, RGS14-containing tissue punches of hippocampus and striatum were taken from one adult rhesus macaque, and RGS14 expression verified in this

tissue as well as three additional monkeys by light microscopy as described below. Tissue samples were lysed with 50mM Tris, 150mM NaCl, 1mM EDTA, 2mM DTT, 5mM $MgCl_2$, 1% Triton X-100, and protease inhibitors (Roche, Cat# 04693159001). 50 μg of homogenate was loaded into an 11% acrylamide gel and run at 120V for 2 hours, and transferred overnight onto nitrocellulose membranes. 3.3 μg of RGS14 antibody (Proteintech, Cat# 16258-1-AP) was incubated with 33 μg of purified rat RGS14 (Uniprot O08773) and 33 μg of bead-bound purified human RGS14 (Uniprot O43566) overnight in 250 μL TBS. Membranes were incubated in 1:1000 RGS14 antibody, or 1:1000 pre-adsorbed RGS14 antibody in 5% milk for 2 hours. Membranes were washed for 30 minutes in 0.1% Tween-TBS. Secondary antibody (goat anti-rabbit, HRP-conjugated) at 1:25,000 in 0.1% Tween-TBS was incubated for 1 hour at room temperature. Membranes were washed for another 30 minutes in 0.1% Tween-TBS, then incubated with ECL and exposed to X-ray film.

Animals

All animal housings and procedures were approved by the Emory University Institutional Animal Care and Use Committee (IACUC) and all procedures were approved by IACUC protocol. C57BL/6J mouse tissue used in this study was collected following deep anesthesia with isofluorane and rapid decapitation. All applicable international, national, and/or institutional guidelines for the care and use of animals were followed. All procedures performed in studies involving animals were in accordance with the ethical standards of the institution or practice at which the studies were conducted.

The non-human primate tissue was collected from three adult (5-7 years old) rhesus monkeys (2 females, 1 male) from the Yerkes National Primate Center colony. After deep anesthesia with pentobarbital (100 mg/kg), the monkeys were transcardially perfused with an oxygenated Ringer solution followed by 2 liters of fixative (4% paraformaldehyde/0.1% glutaraldehyde in phosphate buffer 0.1M, pH 7.4). After perfusion, the brains were cut in 10 mm-thick blocks in the stereotaxic plane and taken out from the skull. They were then post-fixed for 24 hours in 4% paraformaldehyde

at 4^0C. Following post-fixation, the brains were cut in 60 μm-thick sections with a vibrating microtome. Sections were serially collected and stored in an anti-freeze solution (1.4% NaH_2PO_4-H_20, 2.6% Na_2HPO_4-$7H_2O$, 30% ethylene glycol, 30% glycerol dissolved in distilled water) at -20°C until further use.

Light Microscopy

Monkey tissue

Series of sections (1/24) through the whole brain of three rhesus monkeys were processed to localize RGS14 immunostaining at the light microscopic level as follows: Before any antibody incubations, all sections were treated with a 1% sodium borohydride/PBS solution for 20 minutes and washed in PBS. This was followed by a pre-incubation for 1 hour in a solution containing 1% normal goat serum, 0.3% Triton-X-100, and 1% bovine serum albumin (BSA; Sigma-Aldrich, St. Louis, MO) in PBS. Sections were then incubated for 24 hours at room temperature in a solution containing the rabbit anti-RGS14 antibody (1:4000 dilution) in 1% normal goat serum, 0.3% Triton-X-100, and 1% BSA in PBS. On the following day and after PBS rinses, sections were incubated in a PBS solution containing (secondary) biotinylated horse anti-rabbit IgGs (1:200 dilution; Vector Laboratories, Burlingame, CA) combined with 1% normal goat serum, 0.3% Triton-X-100, and 1% BSA for 90 minutes at room temperature. Sections were exposed to an avidin-biotin-peroxidase complex (ABC; 1:100 dilution, Vector Laboratories) for 90 minutes followed by rinses in PBS and Tris buffer (50mM; pH 7.6). Sections were then incubated with a solution containing 0.025% 3,3'-diaminobenzidine tetrahydrochloride (DAB; Sigma-Aldrich), 10 mM imidazole (Fisher Scientific, Pittsburgh, PA), and 0.006% hydrogen peroxide in Tris buffer for 10 minutes at room temperature. The sections were mounted on slides, air-dried, and dehydrated with increasing dilutions of ethanol followed by xylene, before being being coverslipped with Permount. A ScanScope light microscope (Aperio Technologies; Vista, CA) was used to image the RGS14-immunostained sections.

Human tissue

Post-mortem brain tissue from three individuals (source Emory Alzheimer's Disease Research Center) with no known brain diseases was collected (average age = 81 ± 9.2 years, 2 females, 1 male). Tissue was collected between 5-7 hours post-mortem, fixed with 8% paraformaldehyde for 1-2 weeks, paraffin-embedded, and cut into 8 μm-thick sections on a microtome. Sections were immunolabeled with RGS14 antibody as follows. Endogenous peroxidase in tissue sections was blocked with 3% H_2O_2 in methanol for 5 minutes at 40°C. Sections were microwaved for 5 minutes in Citrate buffer (pH 6.0) and allowed to cool to room temperature for 30 minutes. For immunodetection, nonspecific reagent binding was blocked with normal goat serum in 0.1 M TRIS buffer for 15 minutes at 40°C. Sections were incubated in 1:200 RGS14 antibody (rabbit, Proteintech, Cat# 16258-1-AP) overnight at 4°C. After rinsing, sections were incubated for 30 minutes at 38°C in biotinylated secondary antibody (ABC Elite Kit, Vector Labs, Burlingame, CA), rinsed, incubated for 1 hour at 38°C in avidin-biotin complex (Vector Labs), and then developed with diaminobenzidine (DAB) (Vector Labs). Negative controls consist of sections incubated without primary antibody.

Electron Microscopy

Immunoperoxidase

Brain tissue sections from three rhesus macaque monkeys that included the striatum, globus pallidus, substantia nigra or hippocampus were prepared for immunoperoxidase localization of RGS14 at the electron microscopic (EM) level. The staining protocol was similar to that used for light microscopy, except that Triton-X-100 was omitted from incubation solutions. In brief, sections were first put in a cryoprotectant solution, followed by pre-incubation in a solution containing 1% normal goat serum and 1% BSA in PBS for 1 hour at room temperature, and then, a 48 hours incubation in the primary antibody solution containing rabbit anti-RGS14 antibody (1:4000 dilution). On the following day, sections were incubated for 90 minutes at room

temperature in biotinylated goat anti-rabbit IgGs (1:200; Vector Laboratories), followed by a 90 minute incubation with the ABC complex (1:100, Vector Laboratories), and DAB (Sigma-Aldrich) processing for 10 minutes. After Phosphate Buffer (0.1 M, pH 7.4) rinses, the tissue underwent treatment with 1% osmium for 20 minutes and 1% uranyl acetate in 70% ethanol for 35 minutes, followed by dehydration with decreasing ethanol concentrations. Sections were placed in propylene oxide, embedded in epoxy resin (Durcupan ACM, Fluka, Buchs, Switzerland) for at least 12 hours, and baked in a 60°C oven for 48 hours. As controls, sections were incubated in a solution containing the pre-adsorbed RGS14 antibody prepared as described above. The rest of the immunostaining protocol remained the same as above.

Samples of regions of interest from the resin-embedded sections were cut and glued onto resin blocks, cut into 60 nm ultrathin sections (Leica Ultracut T2), and stained for 5 minutes with lead citrate for examination under the electron microscope (EM; model 1011, Jeol, Peabody, MA). Immunoreactive elements were digitally collected at 40,000x and 60,000x with a Gatan CCD camera (Model 785; Warrendale, PA) controlled by Digital Micrograph software (version 3.11.1). Preliminary electron microscopic observations were made from the striatum in the three monkeys to determine the animal with the best ultrastructural preservation. Representative electron microscopic data from the striatum, hippocampus and amygdala were then collected from this animal and shown in the present study.

Pre-embedding immunogold

Series of 3-5 sections at the level of the striatum or CA1 hippocampal region were processed for the pre-embedding immunogold procedure to further characterize the subcellular localization of RGS14 in these brain regions. After being processed with the cryoprotectant protocol (see above), these sections were pre-incubated in a PBS solution containing 5% milk for 30 min, followed by an overnight incubation at RT in the primary RGS14 antibody solution consisting of RGS14 antibody (1:4000 dilution) and 1% dry milk in TBS-gelatin buffer (0.02 M, 0.1% gelatin, pH 7.6). On the next day, sections were first incubated for 90 min with secondary goat anti-rabbit

Fab' fragments conjugated to 1.4-nm gold particles (1:100; Nanoprobes, Yaphank, NY) and 1% dry milk in TBS-gelatin to limit cross-reactivity of the secondary antibody. Sections underwent incubation for approximately 10 min in the dark with a HQ Silver Kit (Nanoprobes) to increase gold particle sizes to 30-50-nm through silver intensification, in order to optimize RGS14 visualization. The remaining of the electron microscopy procedure was the same as described above for the immunoperoxidase reaction and described in detail in our previous studies (425-427).

4.4 RESULTS

Characterization of the antibody

We recently characterized a monoclonal antibody that recognizes the full-length rodent RGS14 protein to study its postnatal developmental expression in the mouse brain (404). We found that, while the mouse hippocampal area CA2 expression of RGS14 protein increases throughout postnatal development and peaks in adulthood, RGS14 expression can also be found in other brain structures, including the piriform cortex, olfactory regions, and in neocortical layers II, III, and V. Other reports have suggested RGS14 may be expressed both in and out of the hippocampus of monkeys and humans (173, 326). Until recently, technical barriers, including lack of an antibody that recognizes the full-length primate RGS14, have prevented a detailed analysis of RGS14 protein expression in brains of higher mammals. Here, we characterized and assessed the specificity of an RGS14 antibody commercially available from Proteintech (Rosemont, IL). This polyclonal antibody was generated from an immunogen containing the human sequence for the R1 domain through the C-terminus, and therefore was predicted to recognize both primate and rodent RGS14, which share an approximately 90% conserved sequence.

To determine the location of the epitope(s), we generated truncation constructs of rat FLAG-RGS14 (Figure 4.1A). We expressed these mutants in HEK293 cells for 24 hours and then immunoblotted with the RGS14 polyclonal antibody, or a FLAG antibody. We found that constructs containing the R1, R2, and GPR domains, but not those containing only the RGS domain,

were recognized by the RGS14 antibody, while the FLAG antibody detected even expression across constructs (Figure 4.1B). Thus, the RGS14 antibody recognizes the part of the protein that matches the immunogen used to generate it (Figure 4.1C). RGS domains have relatively high sequence conservation, however this immunogen lacks the RGS domain and was therefore predicted to be highly specific to RGS14 over all other RGS proteins. To validate this, we expressed RGS14, RGS10, RGS12 (trans-spliced), RGS2, RGS4, and RGS16 in HEK293 cells, and separated lysates alongside mouse hippocampal lysate by gel electrophoresis (Figure 4.2). While expression of each construct was verified by blotting for each respective tag (Figure 4.2, bottom), the RGS14 antibody recognized only native RGS14 from mouse brain (Figure 4.2, lane 1) and recombinant RGS14 (Figure 4.2, lane 2)—validating the specificity of the antibody. Though the RGS14 sequence is approximately 90% conserved between rat, mouse, and human, the monoclonal antibody we previously characterized (404) does not recognize human RGS14. Therefore, as the synthetic immunogen used to generate the RGS14 antibody was based on the human peptide sequence, we next wanted to verify that the antibody recognized not only rodent RGS14, but also monkey RGS14.

Immunoblot analysis of RGS14 expression

To explore species specificity, as well as regional expression of RGS14 in brain tissue, we used flash-frozen (stored at -80°C) fresh hippocampal and striatal punches from an adult wild-type mouse and a rhesus monkey. We immunoblotted 50 μg of total protein from each sample with anti-RGS14. We found that this antibody labeled full-length RGS14 in mouse hippocampal lysate, as we've previously shown (333, 338, 404) (Figure 4.3A). Reports of mRNA in mouse brain indicate RGS14 is nearly entirely confined to the hippocampus (http://mouse.brain-map.org). Surprisingly, full-length RGS14 was also detected in mouse striatal lysate (Figure 4.3A) and in fixed mouse brain tissue (data not shown), indicating a discrepancy between mRNA and RGS14 protein expression in the mouse striatum, which should be explored in future studies.

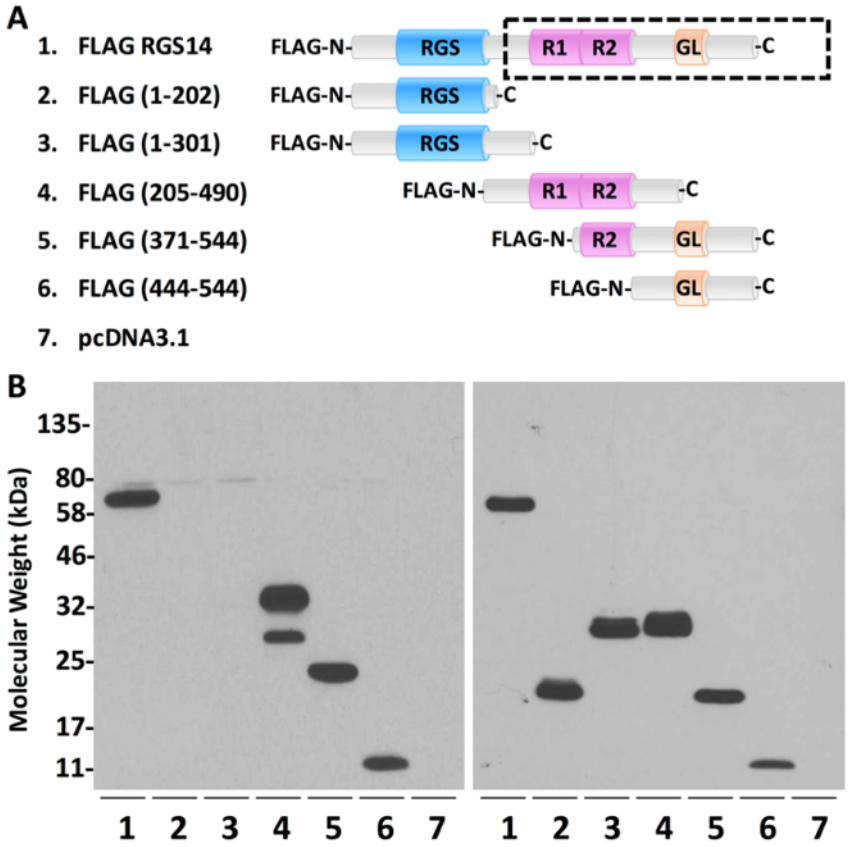

Figure 4.1. Polyclonal RGS14 antibody recognizes epitopes within the carboxy-terminal half of the protein.

(A) *Full-length and truncated forms of FLAG-RGS14 are listed, and their corresponding protein sequences are depicted by cartoon. The human immunogen used to generate this polyclonal antibody is outlined by the dashed box.* ***(B)*** *Constructs in A were cloned into pcDNA3.1, expressed in HEK 293 cells and immunoblotted for RGS14 (left) or FLAG (right). Full-length RGS14 is recognized by the antibody (lane 1). While the front half of the protein (lanes 2-3) is not recognized by the antibody, the back half of RGS14 (lanes 4-6) is, indicating that the epitope(s) are located within the C-terminal end of the protein (from R1 domain to the GPR motif). Expression of each construct is verified by immunoblotting for the FLAG tag, which is universal to all the constructs (right). The epitopes recognized by the polyclonal antibody match the immunogen depicted by the dashed box in* ***(A)****.*

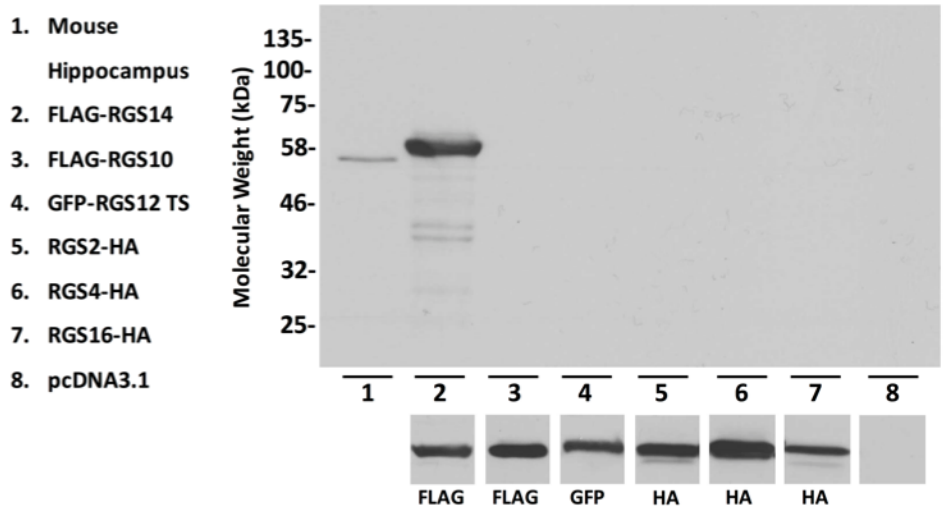

Figure 4.2. RGS14 antibody specifically recognizes RGS14, but not other RGS proteins.

Lysates from hippocampus or HEK 293 cells transfected with RGS2, 4, 10, 12, 14, or 16 were immunoblotted for recognition by the RGS14 antibody or their respective tag. Lane 1: The RGS14 antibody recognizes a band corresponding to full-length RGS14 in the mouse hippocampus. Lanes 2-7: FLAG-RGS14, FLAG-RGS10, GFP-RGS12 trans-spliced (TS), RGS2-HA, RGS4-HA, and RGS16-HA were immunoblotted for RGS14 (top), or their respective tags (bottom). The RGS14 antibody recognized full-length, recombinant FLAG-RGS14 (lane 2), but not the other RGS (lanes 3-7), including RGS10 and RGS12, which are in the same R12 family as RGS14 and thus have a closely related sequence. Immunoblotting for each respective tag confirmed expression of each construct.

In the monkey hippocampus and caudate nucleus, we observed full-length RGS14 (Figure 4.3A), as expected based on the reported mRNA expression in the non-human primate brain atlas (http://www.blueprintnhpatlas.org). Consistent with predicted full-length protein sequences for mouse (547 amino acids; ~60 kDa) and monkey (566 amino acids; ~62 kDa), monkey RGS14 migrated as a slightly higher molecular weight protein than that observed for mouse. Notably, the monkey caudate immunoblots revealed multiple bands of lower molecular weight compared to full-length RGS14 (Figure 4.3A). We hypothesize that these bands may represent splice variants of RGS14 (Figure 4.3A), the existence of which have been suggested, but not demonstrated or characterized (289, 409, 412, 428). To test whether these bands were in fact splice variants of RGS14, we pre-adsorbed the antibody with purified RGS14 protein (both human and rat species) at a 10:1 mass stoichiometry overnight in 250 μL TBS and used it for immunoblots. We found that virtually all immunoreactivity for both mouse and monkey lysates disappeared, following the same immunoblot protocol as before, when the pre-adsorbed antibody was used (Figure 4.3B). This indicates that the bands detected with the RGS14 antibody are specific and likely represent splice variants of the full-length protein. Based on these findings, we used this highly specific antibody to determine the regional expression of RGS14 in the monkey and human brain.

RGS14 localization in Rhesus monkey brain

In the monkey brain, RGS14 immunoreactivity was confined to the caudate nucleus (CD), putamen (PUT), substantia nigra pars reticulata (SNr), globus pallidus (GP), hippocampus (Hp), and amygdala (Am) (Figure 4.4). This pattern of expression was robust and very similar in the three monkey brains used in this study. However, it is strikingly different from the RGS14 labeling pattern described in our previous mouse study (404). Table 4.1 summarizes the relative intensity of RGS14 immunoreactivity in key regions of the monkey and human brains.

To validate the specificity of the polyclonal antibody in these immunohistochemical reactions, we incubated monkey brain tissue with RGS14 antibody pre-adsorbed overnight with purified protein at a 10:1 mass stoichiometry, as we did for the immunoblot experiments, and found that all

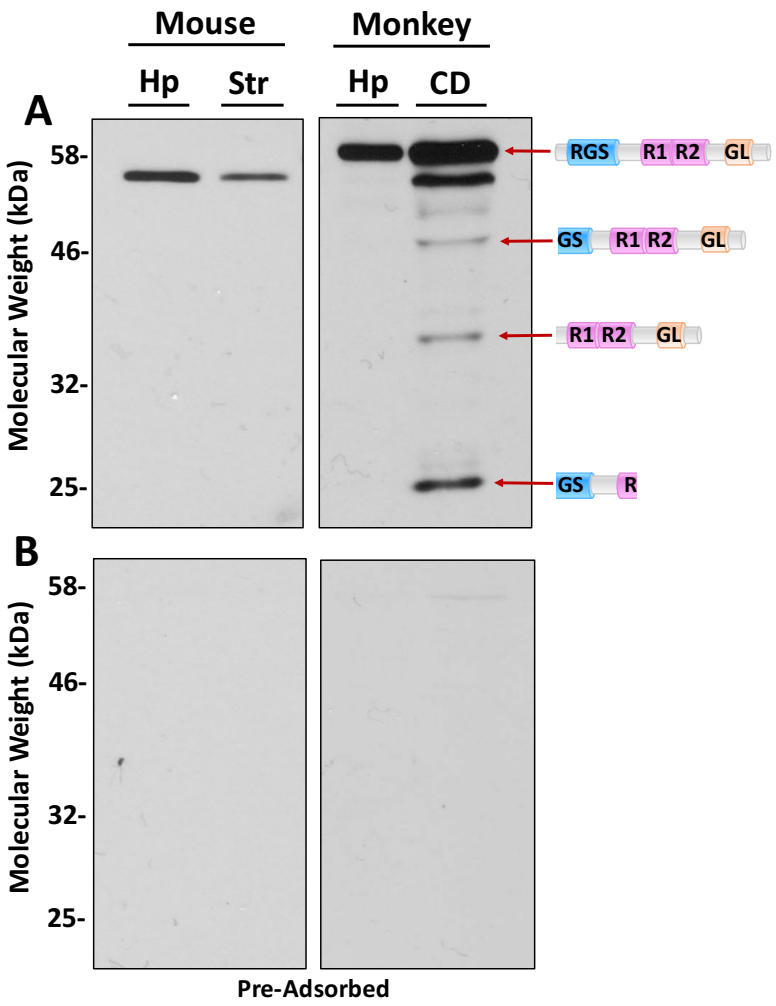

Figure 4.3. RGS14 antibody recognizes endogenous RGS14 in the rodent and primate brain.

Hippocampal (Hp) and Striatal (Str) punches taken from an adult wild type mouse and a rhesus monkey were lysed and processed through the Bradford assay to quantify protein concentration. The striatal punches in the monkey were taken from the caudate nucleus (CD). Fifty micrograms of protein was loaded into each lane and separated on an 11% acrylamide gel. ***(A)*** *RGS14 was detected by immunoblotting with 1:1000 diluted RGS14 antibody. Mouse hippocampal and striatal lysates contain full-length RGS14. Monkey hippocampal lysate contains full-length RGS14, and caudate lysate contains full-length RGS14 and three putative splice variants. The putative splice variants match predicted molecular weights: isoform 1 (canonical/full-length; UniProt O43566-7; GenBank EAW85012.1); isoform 2 (UniProt O43566-4; GenBank AAM12650.1); isoform 3 (UniProt O43566-5; GenBank: AAY26402.1); isoform 4 (UniProt O43566-6; GenBank: BAC85600.1). Their predicted protein sequences (412) are represented by cartoons.* ***(B)*** *RGS14 antibody was pre-adsorbed with purified rat RGS14 and purified human RGS14 proteins (10 µg protein: 1 µg antibody). Membranes were subjected to the same antibody dilution (1:1000) and the same immunoblot protocol. Stained RGS14 bands are absent following pre-adsorption, indicating that the antibody is specific and that all detected bands are RGS14.*

regions enriched in RGS14immunolabeling (CD, PUT, SN, GP, hippocampus, and amygdala) were completely devoid of immunoreactivity when exposed to the pre-adsorbed antibody (Figure 4.5, control sections from Figure 4.4 are next to their pre-adsorbed counterparts for comparison). Note that the molecular layer of the cortex appears labeled in Figure 4.4 and Figure 4.5, even in pre-adsorbed sections, indicating that this staining represents non-specific labeling and is likely a common "edge effect" fixation artefact. These findings provide further evidence for the specificity of the RGS14 antibody when applied to the monkey brain. The overall pattern of cellular and subcellular expression of RGS14 in each of the labeled brain regions is described below.

Hippocampus

Overall, the pattern of RGS14 labeling at light and electron microscopic level was similar between the three monkeys used in the present study. The monkey hippocampus was heavily stained when incubated with the RGS14 antibody (Figure 4.4C-F; 6A). Robust RGS14 expression was found throughout the CA2-CA1 region, but not in the CA3 area nor the dentate gyrus, of the macaque hippocampus. Consistent with our previous report in mice (338, 404), heavy CA2 labeling of pyramidal cell bodies and dendrites was found throughout the whole rostro-caudal extent of the primate hippocampus. Strong RGS14 expression was also found in CA1, but the labeling in this region was mainly confined to the neuropil, although immunoreactive pyramidal cell bodies and proximal dendritic profiles could also be seen (Figure 4.6A). To further determine the cellular make-up of the CA1 neuropil labeling, we used electron microscopy (EM) to characterize the localization of the RGS14 immunoreactivity. Overall, we found that RGS14-positive structures in CA1 comprise both pre- and postsynaptic profiles (Figure 4.6B-D). Axon terminals forming asymmetric (i.e. putatively excitatory) axo-dendritic (Figure 4.6B) or axo-spinous (Figure 4.6C) synapses, dendrites of various sizes, and spines (Figure 4.6D) were the main constituents of the CA1 neuropil immunoreactivity. Based on the known projections from CA2 to CA1 (429) and the restricted expression of RGS14 throughout the brain, it is reasonable to suggest that most of the putative glutamatergic RGS14-immunoreactive axon terminals in CA1 originate from RGS14-

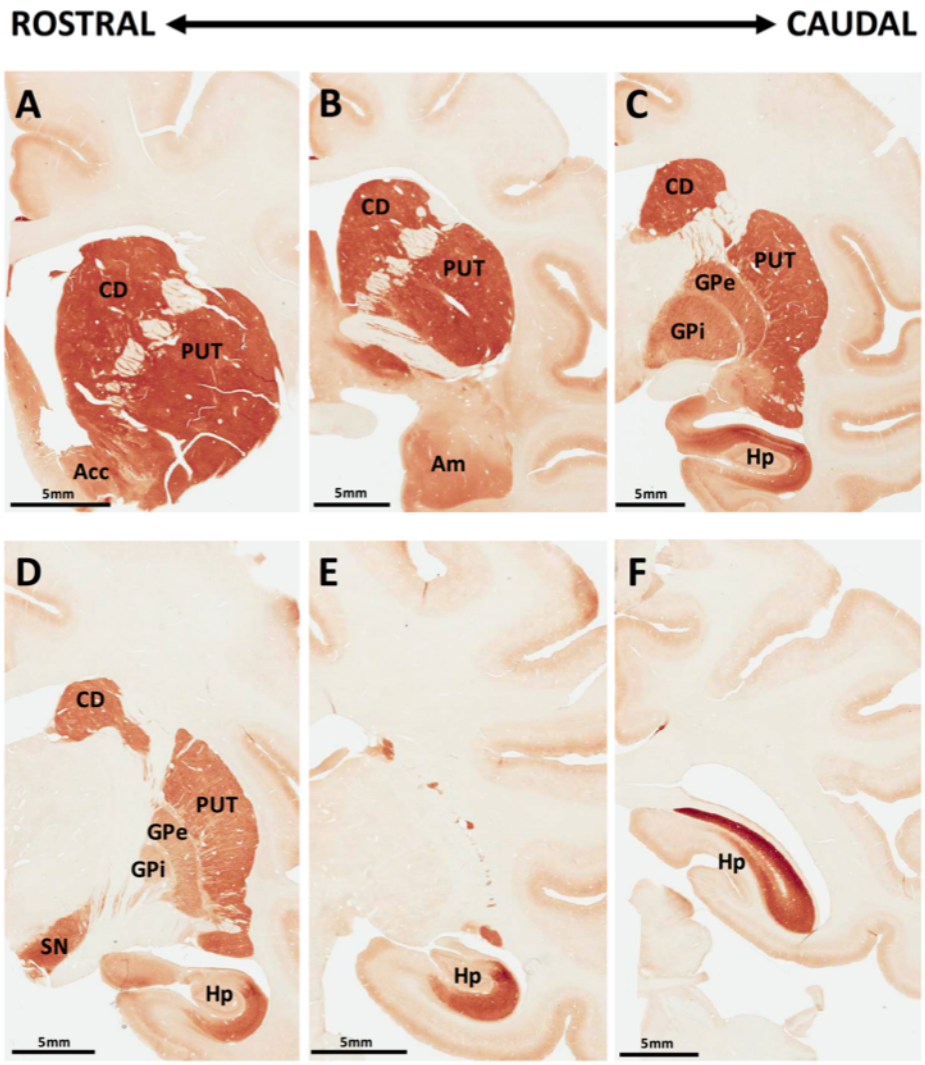

Figure 4.4. RGS14 immunoreactivity is expressed in discrete regions throughout the monkey brain.

(A-F) *Coronal sections through the rostrocaudal extent of the monkey brain show strong RGS14 immunostaining in the caudate nucleus (CD), putamen (PUT), nucleus accumbens (Acc), internal and external globus pallidus (GPi, GPe), substantia nigra (SN), and hippocampus (Hp), while moderate staining was found in the amygdala (Am). Apart from caudal hippocampal labeling, brainstem sections posterior to that displayed in panel F were devoid of RGS14 immunostaining.*

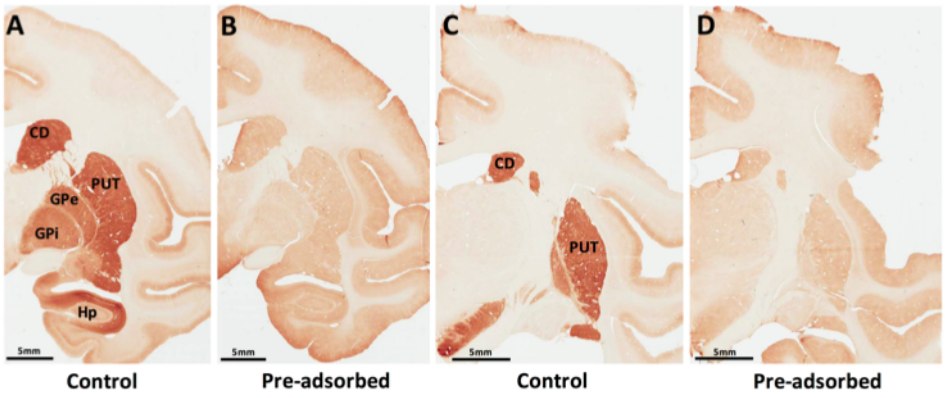

Figure 4.5. RGS14 labeling in monkey brain is specific.

(A-D) *RGS14 immunoreactivity was ablated in all regions of the monkey brain after incubation with RGS14 antibody pre-adsorbed with the synthetic immunogenic peptide against which it was made (**A** versus **B**; **C** versus **D**). Note that brain sections depicted in **A** and **C** are also used in Figure 4.4.*

positive CA2 pyramidal cells.

Striatum

In line with our immunoblot data (Figure 4.3A), both the caudate nucleus and putamen displayed strong cellular and neuropil RGS14 immunoreactivity (Fig 7). The labeling was found throughout the rostro-caudal extent of the caudate nucleus and putamen, and in the nucleus accumbens, albeit to a lower intensity than in the dorsal striatum (Figure 4.4A-E; 7A). The morphology of labeled striatal cell bodies was consistent with that of previously reported striatal projection neurons, i.e. small- to medium-sized soma with large nuclei surrounded by a thin rim of cytoplasm (430). At the electron microscopic level, striatal RGS14 immunoreactivity was largely expressed postsynaptically in dendrites and spines frequently contacted by unlabeled putative glutamatergic terminals (Fig 7B-C). Occasionally, RGS14-immunoreactive terminals forming symmetric axo-dendritic synapses were encountered (Figure 4.7D). Although there was no clear evidence for immunostaining associated with striatal interneurons, such as fast-spiking parvalbumin-positive neurons, this issue remains to be addressed.

Figure 4.3 demonstrates the existence of putative lower molecular weight RGS14 variants in monkey caudate, which match previously predicted splice variants (289, 409, 412, 428). Recombinant RGS14 is a nuclear shuttling protein that contains both a nuclear localization signal (NLS) and a nuclear export signal (NES) (288, 289) , and the smallest of these variants retains an NLS but lacks an NES. Therefore, we hypothesized that the caudate may contain a nuclear subset of a short-form of RGS14. To further characterize the subcellular localization of RGS14 in striatal elements, we processed striatal sections with the pre-embedding immunogold method (Figure 4.8), which provides a higher level of spatial resolution than the immunoperoxidase technique. Overall, the pattern of cellular distribution of gold labeling was similar to that described above using the immunoperoxidase approach, such that most labeling was found in postsynaptic structures, including dendrites, spines, and neuronal cell bodies (Figure 4.8). In general, the bulk of gold labeling was located in the cytosol of immunoreactive elements, often closely associated with

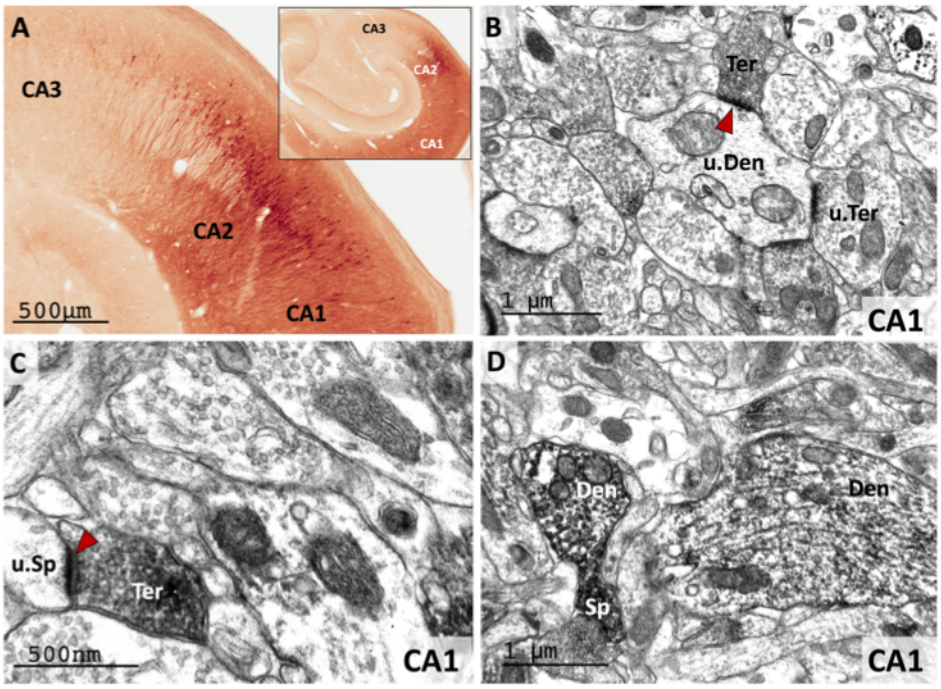

Figure 4.6. RGS14 is expressed in CA1 and CA2 pyramidal cell bodies and neuropil in the monkey hippocampus.

(A) *Light microscopy reveals dense RGS14 labeling of pyramidal cell bodies in CA2. By contrast, there is virtually no labeling in CA3. CA1 displays a lighter RGS14 labeling than CA2, which is preferentially localized in the neuropil.* ***(B and C)*** *Electron micrographs of RGS14-positive terminals (Ter) forming asymmetric axo-dendritic* ***(B)*** *or axo-spinous* ***(C)*** *synapses in CA1. In each micrograph, RGS14-immunoreactive axon terminals (Ter), spines (Sp) and dendrites (Den) are indicated, while u.Ter, u.Sp, and u.Den mark unlabeled corresponding elements. The red arrowheads point at asymmetric synapses that involve RGS14-containing terminals, which likely originate from CA2-CA1 axonal projections.* ***(D)*** *Post-synaptic RGS14 labeling in CA1 dendrites and spines.*

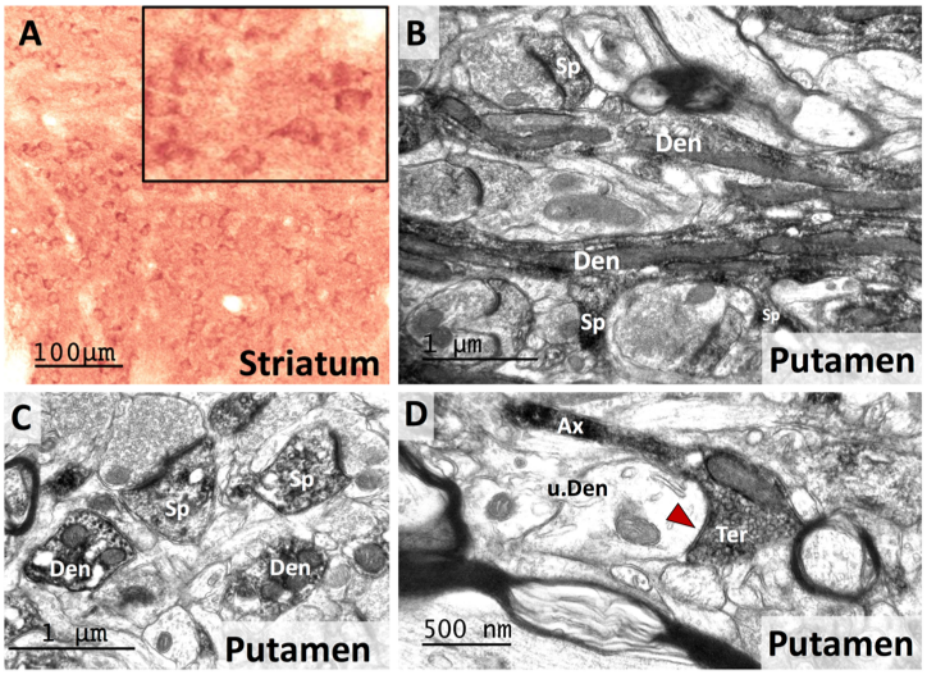

Figure 4.7. RGS14 is localized in dendrites and spines of GABAergic projection neurons in the monkey striatum.

(A) *A light micrograph shows RGS14-immunoreactive cell bodies alongside a dense neuropil labeling in the monkey striatum. The inset shows a high power view of RGS-positive striatal cell bodies that morphologically resemble those of striatal projection neurons.* ***(B-C)*** *Electron micrographs of RGS14-labeled dendrites (Den) and spines (Sp) in the monkey putamen. Note in the lower part of B, the spines coming off a dendritic process, further confirming the RGS14 expression in spiny projection neurons.* ***(D)*** *Electron micrograph of an RGS14-positive axon terminal that forms a symmetric axo-dendritic synapse (red arrow) with an unlabeled dendrite (u.Den) in the putamen. Although the source of these terminals was not characterized, their ultrastructural features suggest that they may originate from recurrent collaterals of GABAergic striatofugal axons (431).*

vesicular and tubular endoplasmic reticulum-like structures (red arrowheads in Figure 4.8). In addition, a significant number of gold particles was also found in the nucleus of labeled cell bodies, suggesting nuclear expression of RGS14 (yellow arrows in Figure 4.8C-D). Only a small subset of gold labeling was associated with the plasma membrane of all immunoreactive structures (Figure 4.8).

Globus pallidus

Both the external and internal segments of the globus pallidus displayed robust RGS14 immunoreactivity (Figure 4.4C-D; 9A). At the light microscopic level, the pallidal labeling was exclusively associated with terminal- and axon-like processes that wrapped around non-immunoreactive dendrites of pallidal neurons (Figure 4.9A), a pattern previously described as "woolly fibers" (432). In light of the previous literature showing that "woolly fibers" originate from striatopallidal GABAergic axons (432), we used electron microscopy to determine if RGS14 neuropil immunoreactivity in both pallidal segments was, indeed, expressed in GABAergic striatal-like terminals. As shown in Figure 4.9, RGS14 immunoreactivity was exclusively expressed presynaptically in small unmyelinated axons and axon terminals that formed symmetric synapses with unlabeled dendrites of pallidal cells (blue arrowheads in Figure 4.9B-D). The ultrastructural features and the symmetric membrane specialization of the synapses formed by these terminals was similar to that described for striatopallidal GABAergic terminals in previous studies (433-435), thereby indicating that these RGS14-immunoreactive terminals likely originate from striatal projection neurons. The dendrites contacted by the immunoreactive axon terminals also received asymmetric synaptic inputs from unlabeled terminals (red arrowheads in Figure 4.9B).

Substantia nigra

Similar to the pallidum, strong RGS14-positive labeling of "woolly fibers" was found in the SNr (Figure 4.10A). In contrast, the pars compacta (SNc) was completely devoid of RGS14 labeling (Figure 4.10A). At the electron microscopic level, the distribution of labeling was the same

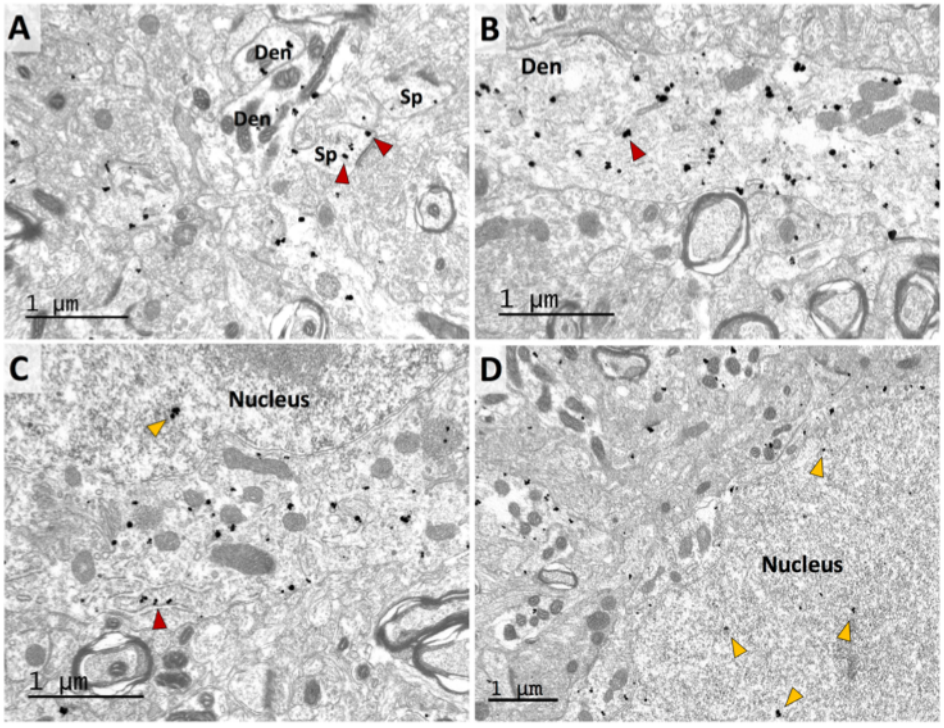

Figure 4.8. RGS14 localizes in the cytosol and the nucleus of striatal projection neurons.
Electron micrographs of RGS14-immunoreactive dendrites (Den) and spines (Sp) ***(A-B)****, and neuronal cell bodies* ***(C-D)*** *in the monkey striatum as revealed with the pre-embedding immunogold method. Note that most gold particles are largely located within the cytosol of immunoreactive structures, with rare instances of plasma membrane labeling. In* ***(A)****, the red arrowheads indicate examples of RGS14 labeling in spines. In* ***(B)****, the red arrowhead indicates an example of RGS14 labeling in dendrites. In* ***(C)*** *and* ***(D)****, the staining is associated with the endoplasmic reticulum (red arrowhead) and vesicular organelles in the cytoplasm of immunoreactive cell bodies, while some gold particles are also found in the nucleus of these labeled neurons (yellow arrowheads).*

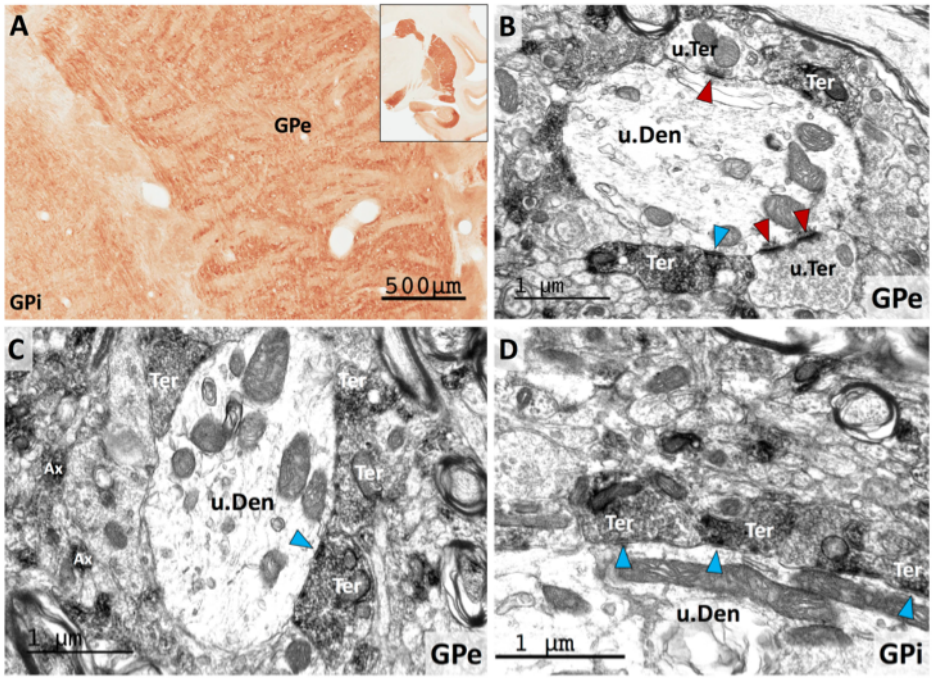

Figure 4.9. RGS14 is localized presynaptically in striatopallidal GABAergic terminals.

(A) *Light micrograph of RGS14-immunoreactive neuropil in both the internal and external globus pallidus (GPi, GPe) displays the "woolly fibers" pattern of labeling previously used to describe the massive striatal GABAergic innervation wrapped around pallidal dendrites (432).* ***(B-D)*** *Electron micrographs of RGS14 labeling in GPe and GPi confirm that most of the immunoreactivity is found in axon terminals (Ter) that display the ultrastructural features of striatal GABAergic terminals and form symmetric synapses (blue arrowheads) with unlabeled dendrites (u.Den) of pallidal neurons. Note that red arrowheads depict asymmetric synapses formed by unlabeled terminals (u.Ter). Labeled unmyelinated axons (Ax) are also found throughout the neuropil in both pallidal segments* ***(C)***.

as in the globus pallidus, i.e. found mostly in putative striatal-like GABAergic terminals that formed symmetric synapses with unlabeled dendrites (Figure 4.10B-D; blue arrowhead in 10C). Consistent with the pattern of "woolly fibers", some SNr dendrites were completely ensheathed by striatal-like RGS14-labeled boutons (Figure 4.10B). In addition to the large amount of putative striatal terminals, another population of RGS14-containing boutons forming asymmetric axo-dendritic synapses (i.e. putatively excitatory) were found in the SNr (red arrowhead in Figure 4.10D). Although the exact source(s) of these terminals remains to be established, the central nucleus of the amygdala is one of the RGS14-enriched brain regions (described below) that may contribute to this innervation (436, 437).

Amygdala

Another RGS14-enriched region of the monkey brain was the amygdala (Figure 4.11). The basomedial (BM), basolateral (BL) and centrolateral (CeL) nuclei were the most strongly immunoreactive amygdala sub-regions (Figure 4.11). In contrast to these regions, the lateral amygdala displayed a far less intense level of RGS14 immunoreactivity (Figure 4.11A). In the BM, BL, and CeL, numerous immunoreactive neuronal cell bodies and proximal dendrites laid within a diffuse lightly immunostained neuropil (Figure 4.11A; 11D). At higher magnification, some of the positive neurons displayed the morphological features of projection cells (Figure 4.11B-C), though double labeling experiments are needed to further characterize their exact chemical phenotype. A dense band of strongly RGS14-immunoreactive cells was also found in the amygdalostriatal transition area (AStr) along the lateral edge of the CeL (Figure 4.11D-E; see arrows in E). In adjacent sections immunostained for the ubiquitous neuronal marker, NeuN, this band of labeling corresponds to a sub-region of the AStr that contains a larger neuronal density than neighboring regions (Figure 4.11F; see arrows). To further extend our analysis of RGS14 expression in primates, we explored the localization of RGS14 immunoreactivity within the human brain.

RGS14 localization in the Human brain

Post-mortem human brain tissue used in this series of experiments was collected from

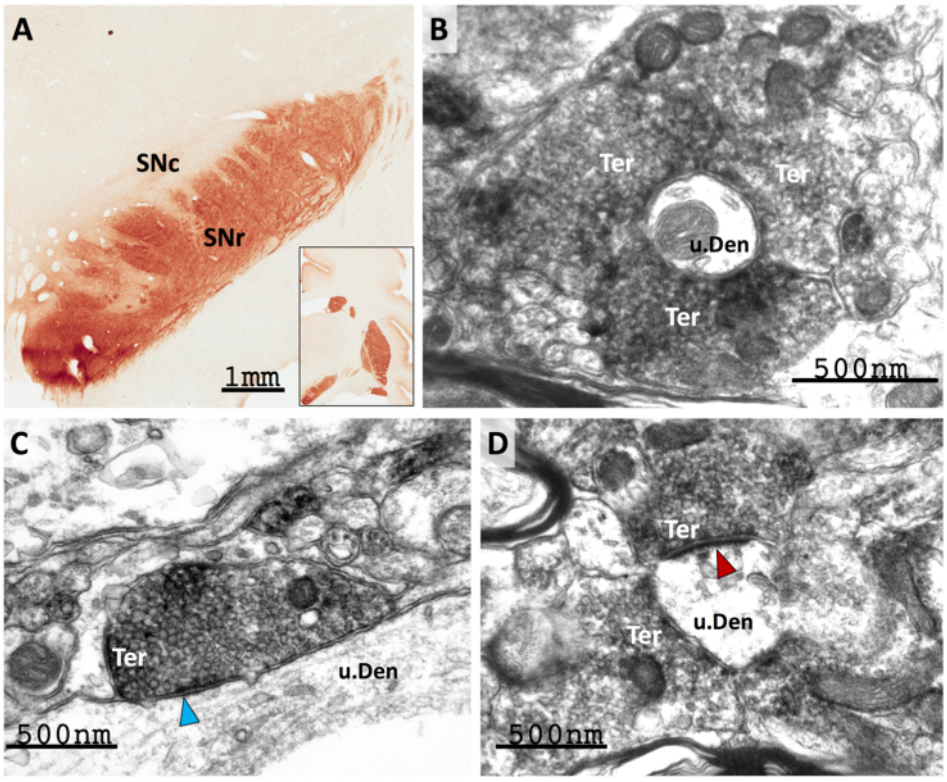

Figure 4.10. RGS14 is localized pre-synaptically in the monkey substantia nigra pars reticulata.

(A) *Light micrograph showing dense RGS14 neuropil labeling in the pars reticulata (SNr) of the monkey substantia nigra, while the pars compacta (SNc) is completely devoid of immunoreactivity. As in GPe and GPi, the SNr labeling is made up of rich plexuses of varicosities that display a woolly fibers-like pattern of innervation of dendritic processes.* ***(B-C)*** *At the electron microscope level, the immunostaining is mainly confined to pre-synaptic terminals (Ter) that display the ultrastructural features of striatonigral GABAergic boutons and form symmetric axo-dendritic synapses (blue arrowhead in* ***C****).* ***(D)*** *illustrates a subset of RGS14-immunoreactive terminals that forms asymmetric axo-dendritic synapses (red arrowheads). The amygdala is a potential source of these putative excitatory terminals.*

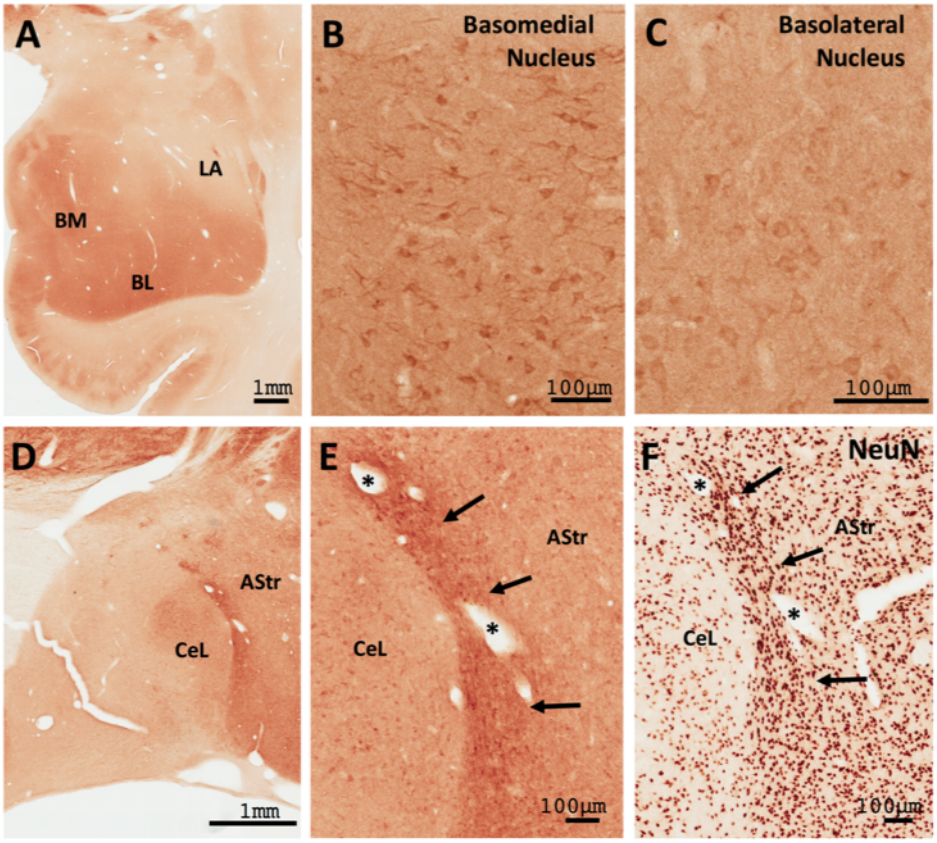

Figure 4.11. RGS14 is expressed throughout the monkey amygdala.

*(**A**) Low power view of the distribution of RGS14 immunoreactivity in the monkey amygdala. **(B-C)** Light microscope images show discrete RGS14 staining of cell bodies and neuropil in the basomedial (BM) and basolateral (BL) nuclei, but not the lateral (LA) nuclei. **(D-E)** RGS14 labeling in the central lateral (CeL) and amygdalostriatal region (AStr). The dense band of labeling adjacent to the CeL corresponds to a sub-region of the AStr (arrows in E and F) that contains a larger neuronal density than neighboring AStr regions as revealed by NeuN immunostaining **(F)**.*

neurologically healthy individuals, immersion-fixed and sectioned (see *Methods* for details). As shown in the mouse and monkey brains, the CA2 and CA1 hippocampal regions contained a large number of RGS14-immunoreactive pyramidal cell bodies, while the CA3 region was devoid of staining in humans (Figure 4.12). The neuropil staining in CA1 and CA2 was considerably lighter in humans than monkeys, likely due to protein degradation during post-mortem delay and immersion (instead of trans-cardiac) fixation of the human tissue. Despite this lower level of immunoreactivity, the general pattern of distribution of RGS14-positive neurons in the human hippocampus was found to be largely consistent with that seen in the monkey and rodent brain.

To confirm that the strong RGS14 expression in the monkey basal ganglia could also be found in humans, we examined the cellular localization of RGS14 in the human striatum and globus pallidus. Reminiscent of the monkey data, a moderate neuropil and cellular expression of RGS14 immunoreactivity in the caudate nucleus (Figure 4.13A) and putamen (Figure 4.13B), combined with a strong woolly fiber-like pattern of axonal labeling in both pallidal segments (Figure 4.13C, D), was also observed in humans.

4.5 DISCUSSION

We and others have previously examined RGS14 protein localization and expression throughout the postnatal development of the mouse brain using different antibodies capable of recognizing only rodent RGS14 (404, 438). Here, we demonstrate the specificity of a new polyclonal antiserum that recognizes the primate RGS14, and used it to map the cellular and subcellular expression of RGS14 and putative RGS14 splice variants in the monkey and human brain (Table 4.1). We show that RGS14 immunoreactivity is selectively found in areas CA1 and CA2 of the hippocampus, striatum, globus pallidus, substantia nigra pars reticulata, and amygdala in rhesus monkeys. Furthermore, we confirm RGS14 expression in the human hippocampus and dorsal striatum, further validating the study of RGS14 in rodent and monkey models as relevant to human health and disease. Figure 4.14 summarizes our findings of RGS14 expression in primate brain.

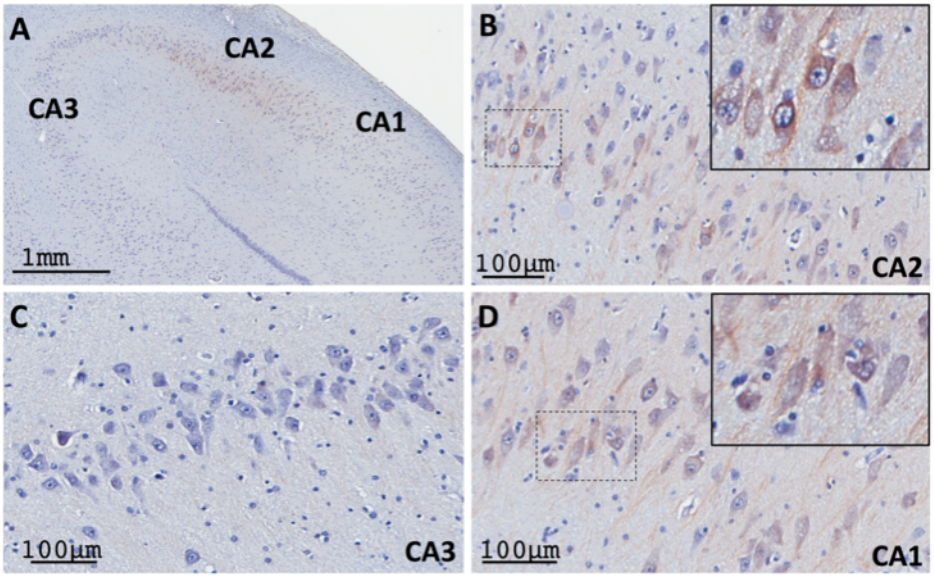

Figure 4.12. RGS14 expression in human hippocampus is comparable to that of monkey and mouse.

Human hippocampi were double stained with Nissl reagent and RGS14 immunolabeling. ***(A)*** *Low power view of RGS14 labeling in CA2 and CA1 subfields, but not in CA3, of human hippocampus.* ***(B, D)*** *Higher magnification of RGS14-immunoreactive pyramidal cell bodies in the CA2* ***(B)*** *and CA1* ***(D)*** *regions, as shown in the monkey and mouse hippocampus. The insets in the upper right corner of each panel show examples of cell body labeling. There is minimal neuropil labeling in both regions.* ***(C)*** *Micrograph showing thionin-stained CA3 neurons devoid of RGS14 immunoreactivity.*

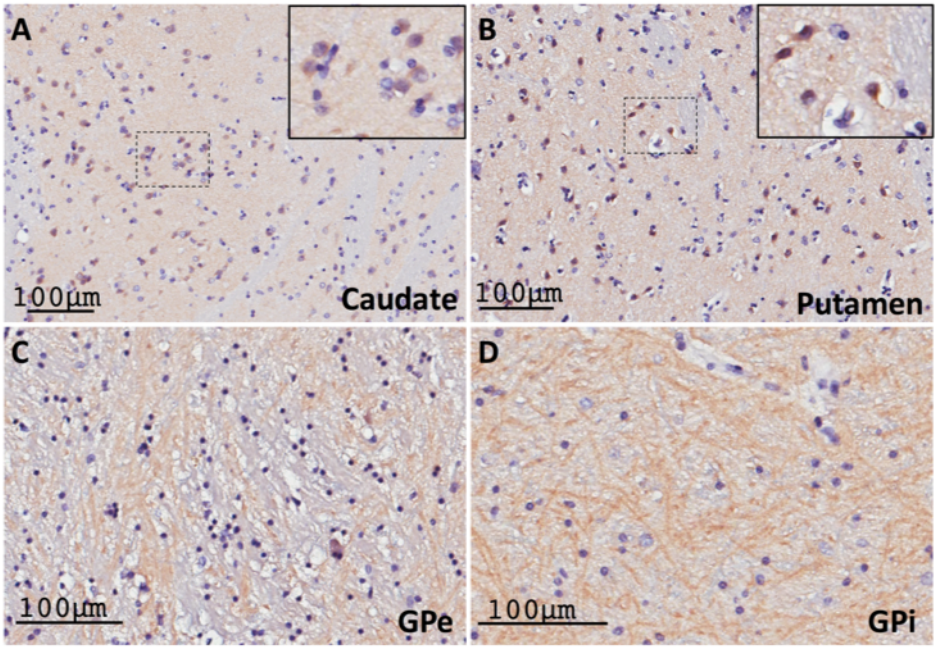

Figure 4.13. RGS14 expression in the human basal ganglia is consistent with labeling in the monkey basal ganglia.

(A-B) *Light micrographs of RGS14-positive neuronal cell bodies, double stained with Nissl reagent, within a lightly labeled neuropil in the human caudate nucleus* ***(A)*** *and putamen* ***(B)****. The insets in the upper right corner of each panel show examples of cell body labeling.* ***(C-D)*** *Dense RGS14-immunoreactive woolly fibers-like neuropil in the human GPe and GPi. The pattern of RGS14 labeling in both the striatum and the globus pallidus in humans is consistent with that described in monkeys.*

Validation of antibody specificity

To confirm our conclusions regarding RGS14 localization in the human and monkey brain, we determined that the polyclonal RGS14 antibody used in our study was specific and only recognized RGS14 (Figure 4.1-3). A previous report described the putative localization of RGS14 in the monkey brain (326). Based on our present findings and others (294, 333, 338, 404, 412), it appears that the antibody used in that study was not specific to RGS14. The predicted size of full-length RGS14 is 60 kDa, which matches the size of the band our antibody detects via immunoblot of lysates from both mouse and monkey brain. However, the previously reported antibody recognized a protein that appeared as a single band at 44 kDa in monkey brain membranes, but not supernatant, thereby suggesting that the labeled protein was not RGS14. In their study, the antibody also detected RGS14 expression in astrocytes, while only neuronal labeling was observed in our study, consistent with our previous findings in mice using a different rodent-specific monoclonal antibody (404). Noticeable differences in labeling between the two studies were also found in the CA1 and CA2 regions of the hippocampus. Although our findings in primates and those from our previous rodent studies provide evidence for strong RGS14 labeling in CA2 pyramidal neurons (338, 404, 429, 439), the previous study reported low RGS14 expression in CA2 neurons compared with the CA1 region (326). Most importantly, the protein immunostaining patterns reported here match exactly the reported mRNA expression patterns for RGS14 in human and non-human primates (http://human.brain-map.org; http://www.blueprintnhpatlas.org). Based on these observations, we are confident that the immunostaining reported here is truly representative of the cellular and subcellular expression RGS14 protein in the monkey and human brains.

RGS14 in the monkey and human hippocampus

RGS14 has previously been shown to suppress synaptic plasticity as well as hippocampal-dependent learning and memory specifically within the CA2 region of the hippocampus in mice (338). Here, we show that RGS14 is also strongly expressed in pyramidal neurons of the CA2 region in both monkey and human hippocampi, but strong cellular and neuropil immunoreactivity

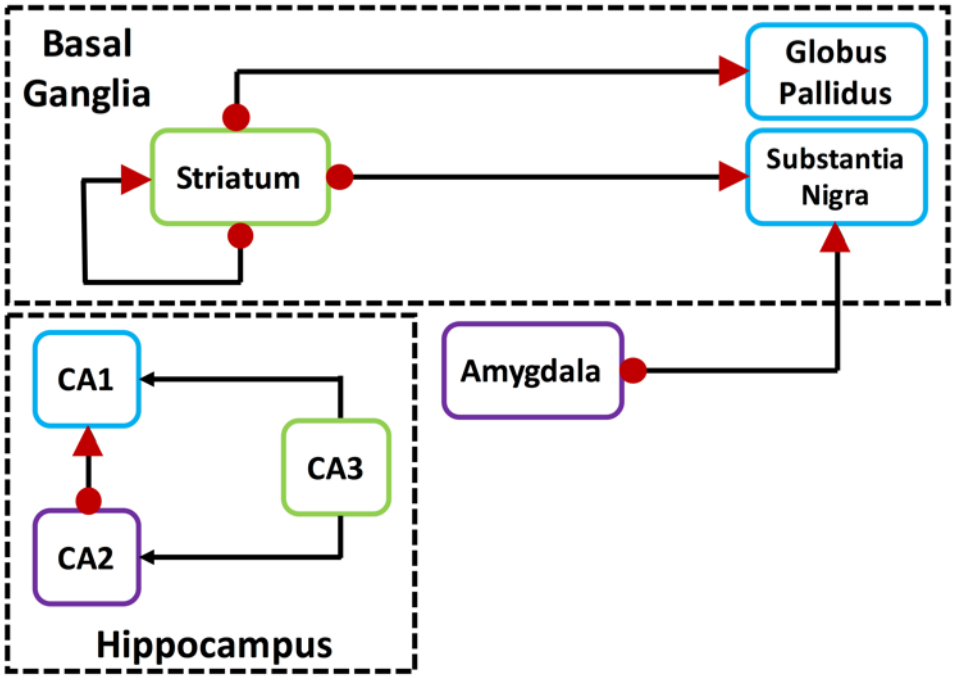

Figure 4.14. Circuitry diagram of RGS14 protein expression in the primate brain.

Circuit diagram of RGS14-positive neurons and their connections within the basal ganglia and hippocampus networks. Red arrowheads indicate pre-synaptic RGS14 labeling in terminals. Red dots depict post-synaptic RGS14 labeling in cell bodies, dendrites, and spines. Axonal projections are designated by black lines.

could also be found in the primate CA1 region. Our ultrastructural analysis revealed that the bulk of CA1 labeling comprises putative glutamatergic terminals that likely originate from CA2 axonal projections and cell bodies/dendrites/spines of CA1 pyramidal neurons. While there is strong evidence that postsynaptic RGS14 in CA2 pyramidal neurons acts as a natural suppressor of LTP at CA3-CA2 glutamatergic synapses (338), the presynaptic function(s) of RGS14 in the CA1 region remains entirely unexplored. Various other RGS proteins have been shown to enhance presynaptic neurotransmitter release by blocking Gβγ-mediated inhibition of Cav2.2 (N-type) calcium channels downstream of GPCRs (21, 154, 424). It is possible that RGS14 acts in a similar fashion as a dedicated GTPase activating protein, or GAP (414), though its presynaptic functions are likely to be more nuanced and complex due to the fact that it contains multiple G protein-binding domains and a growing list of protein binding partners, each with signaling roles. Understanding the presynaptic roles for RGS14 remains a topic of great interest and a focus of ongoing and future studies.

RGS14 in the Basal Ganglia

While the role of RGS14 in the regulation of synaptic physiology in normal and diseased states has largely been centered on its functions in the hippocampus of adult mice (413), our recent study has shown that RGS14 immunoreactivity is also expressed in non-hippocampal regions during early postnatal development of the mouse brain (404). Here, we provide evidence for the first time that RGS14 protein is also expressed in the striatum of adult mice. Furthermore, our light and electron microscopic immunohistochemical findings indicate that RGS14 is heavily expressed postsynaptically in dendrites and spines of striatal GABAergic projection neurons and presynaptically in striatopallidal and striatonigral terminals of primates. Therefore, RGS14 is expressed along both the so-called direct and indirect GABAergic striatofugal pathways of the basal ganglia (440-442). Other RGS proteins, including RGS4, contribute to the dopamine-mediated regulation of long term depression (LTD) of corticostriatal glutamatergic synapses in indirect pathway neurons through modulation of postsynaptic mGluR1/5 and D2 dopamine receptors (153).

RGS9-2 and RGS7, which are also highly expressed in the striatum (438), were similarly found to modulate dopamine signaling (267, 443). RGS14 could possibly regulate synaptic signaling and plasticity in a similar manner to these other RGS proteins. However, multiple GPCRs and their associated downstream signals are implicated in synaptic plasticity in the basal ganglia (442), providing many potential targets at which RGS14 could act in both indirect and direct pathway striatal projection neurons.

RGS14 splice variants in the caudate nucleus

Of great interest is our unexpected observation of multiple specific RGS14 bands in the immunoblots of the monkey caudate nucleus (Figure 4.3A). While we cannot rule out the possibility that these bands represent proteolyzed and degraded RGS14, a more likely scenario is that they label previously speculated human splice variants of RGS14 (289, 409, 412, 428). Notably, these putative splice variants are absent from the monkey hippocampus (Figure 4.3A) and have not been reported in rodents. Of the three reported human variants of RGS14, perhaps the most interesting feature is the lack of a functional RGS domain, suggesting a clear function for these RGS14 variants independent from its canonical role as a GAP for G proteins. Two of these splice variants retain a functional GPR motif, which interacts with inactive $G\alpha i_1$ and $G\alpha i_3$, and these shorter forms of RGS14 exhibit enhanced binding to Gα in the absence of the RGS domain (412), providing a context for RGS14 expression without an RGS domain. Remarkably, RGS proteins from the R4 family (e.g. RGS4) interact directly with the RBD region of truncated RGS14 lacking an RGS domain, enhancing the GAP activity of the secondary RGS protein (412). This could be a mechanism by which splice variants of RGS14 regulate the function of other RGS proteins specifically within the striatum, as expression of these variants is not seen in the hippocampus.

Independent of RGS14 regulation of G protein functions, some of these variants may serve specific, but as yet undefined, roles within the nucleus of striatal output neurons. We and others have previously demonstrated that full-length recombinant RGS14 contains both a nuclear localization sequence (NLS) and a nuclear export sequence (NES) used to shuttle in and out of the

nucleus (288, 289). Of note, the smallest variant (RGS14-S) retains a NLS, but lacks the NES, which is encoded within the GPR motif. Remarkably, our electron microscopy data revealed native RGS14 expression in the nuclei of projection neurons in the monkey caudate nucleus, where the short splice variant is detected by immunoblot. Although this remains to be confirmed, our data suggest that the short splice variant of RGS14 (RGS14-S) might account for RGS14 immunoreactivity within the nucleus of striatal neurons, where it may mediate unique nuclear functions different from the canonical role of RGS14 as a G protein modifier at the plasma membrane. Thus, our findings provide the first evidence for the expression of multiple splice variants of RGS14 in the primate striatum, and suggest for the first time that one or more of these variants displays nuclear localization within striatal projection neurons. Further investigation into the specific roles and localization of these variants within the striatum is of great interest for ongoing and future studies.

RGS14 in the amygdala

We also observed specific RGS14 immunostaining within the basal and centrolateral nuclei of the monkey amygdala. Although this staining was slightly weaker than the robust basal ganglia and hippocampal immunoreactivity, significant cell body and neuropil labeling was expressed in the basomedial, basolateral, and centrolateral nuclei, while the lateral nucleus was largely devoid of immunoreactivity. The amygdala is a central component of the limbic system which plays key roles in the processing of emotional memory, decision making and emotional responses to fear, anxiety and social aggression in primates and rodents (444-447). Because the amygdala is made up of glutamatergic principal neurons and various populations of GABAergic interneurons (448-450), the exact cellular phenotype of RGS14-containing neurons awaits further double labeling studies. However, based on morphological grounds and relative abundance, it is clear that some of the labeled cells belong to the population of amygdalofugal glutamatergic neurons. Whether RGS14 inhibits LTP linked to spatial and contextual learning and memory in the amygdala in a similar fashion as it does in CA2 hippocampal cells (338) is unknown. The possibility that amygdala

RGS14 modulates neuronal plasticity and LTP associated with emotional learning and memory linked to fear conditioning (451), social anxiety, and PTSD (452, 453) remains a topic of great interest for future studies.

4.6 CONCLUSIONS

In this study, we provide conclusive evidence for RGS14 protein expression in the monkey and human hippocampus, amygdala, and basal ganglia (Table 4.1). At the ultrastructural level, our electron microscopy data show that RGS14 displays both a postsynaptic localization in dendrites and spines and a presynaptic localization in terminals of glutamatergic and GABAergic neuronal populations. Furthermore, we provide strong evidence for the existence of predicted human splice variants of RGS14 specifically within the primate striatum. Additionally, we report for the first time electron microscopy data suggesting endogenous RGS14 localization in the nuclei of striatal neurons. Figure 4.14 illustrates, based on our findings, a circuity diagram of regions enriched in RGS14 and their proposed axonal projection targets in the primate brain. Future research must be performed to determine the role of cytosolic and nuclear RGS14 in these neurons and their functional networks. In particular, understanding the role of the pre- and postsynaptic RGS14 expression in both direct and indirect striatofugal pathways is highly relevant because of the importance of these networks in the pathophysiology of basal ganglia disorders such as Parkinson's disease (PD). Further investigations aimed at determining whether RGS14 plays a role in the emergence of disrupted synaptic transmission and plasticity at the striatal, pallidal, and nigral level might set the stage for the development of attractive therapeutic targets that could regulate RGS14 and its downstream signaling events in diseased conditions.

Functional Region	Structure	RGS14 Expression	
		Monkey	Human
Hippocampus	CA1	***	**
	CA2	****	***
	CA3	0	0
Basal Ganglia	Caudate	****	**
	Putamen	****	**
	Globus Pallidus, internal	***	***
	Globus Pallidus, external	***	**
	Substantia Nigra, pars compacta	0	NA
	Substantia Nigra, pars reticulata	***	NA
Amygdala	Amygdala, basolateral	**	NA
	Amygdala, central lateral	**	NA
	Amygdala, basomedial	**	NA
	Amygdala, lateral	0	NA
	Amygdalostriatal transition	**	NA
	Amygdalostriatal transition (peri-CeL)	***	NA

Table 4.1. RGS14 localization within monkey and human brain.

*Structures are grouped by functional region, and RGS14 expression is represented by *, where 0 is no expression, * is low expression, and **** is dense expression. NA represents an area that was not examined.*

CHAPTER 5:

DISCUSSION: RGS14 IS A MULTIFUNCTIONAL NUCLEO-CYTOPLASMIC SHUTTLING PROTEIN WHOSE LOCALIZATION IS DISRUPTED BY HUMAN GENETIC VARIANTS

5.1 INTRODUCTION

RGS14 has been well studied in the context of purified protein interactions (from *Escherichia coli*) (299, 333), mammalian cell culture assays (293, 414, 454), and rodent brain (338, 404). Therefore, the goal of these studies was to expand our knowledge of human-centered RGS14, including: its role in human disease and traits, its unique expression in primate brain, and the diversity of human sequence variation. These studies described above contribute to the field novel methods to identify change-of-function variants from the large databanks of human sequencing variation, novel information into the extended expression of RGS14 in human brain outside of the hippocampus, and novel roles for RGS14 as a nuclear-shuttling protein. Each of these findings will be described in detail below.

Representing the diversity of human RGS proteins

RGS proteins were originally discovered in yeast (10) and have grown over the last twenty years to be appreciated as regulators of critical physiology, giving rise to both diseases and well as traits. While loss of RGS2 is linked with hypertension in both rodents (120, 121) and humans (116, 122), loss of RGS16 seems to have a more subtle phenotype in regulating circadian rhythms in rodents (207, 209) and the "morning person" phenotype in humans (212, 213). Further, while some mutations bear a loss-of-function phenotype, others cause a gain-of-function phenotype. For example, one reported mutation in RGS4 enhances its GAP activity (380), which could have substantial effects on the propensity or prognosis of expression-linked RGS4 diseases such as schizophrenia (142). By contrast, loss-of-function human variants have been linked with hypertensive patients (122), the cause of which has been suggested to be dependent on RGS2 protein degradation (123). Furthermore, a gain-of-function in one context may in fact be a loss-of-function in another context, as many RGS proteins have multifunctional roles (Figure 5.1). For example, in this thesis I demonstrated that RGS14 human variants redirect somatic pools of RGS14 into the nuclei of neurons, leading to a loss-of-function at the spines suppressing LTP. However, roles for RGS14 in the nucleus are currently unknown, and it is not unlikely that sequestering

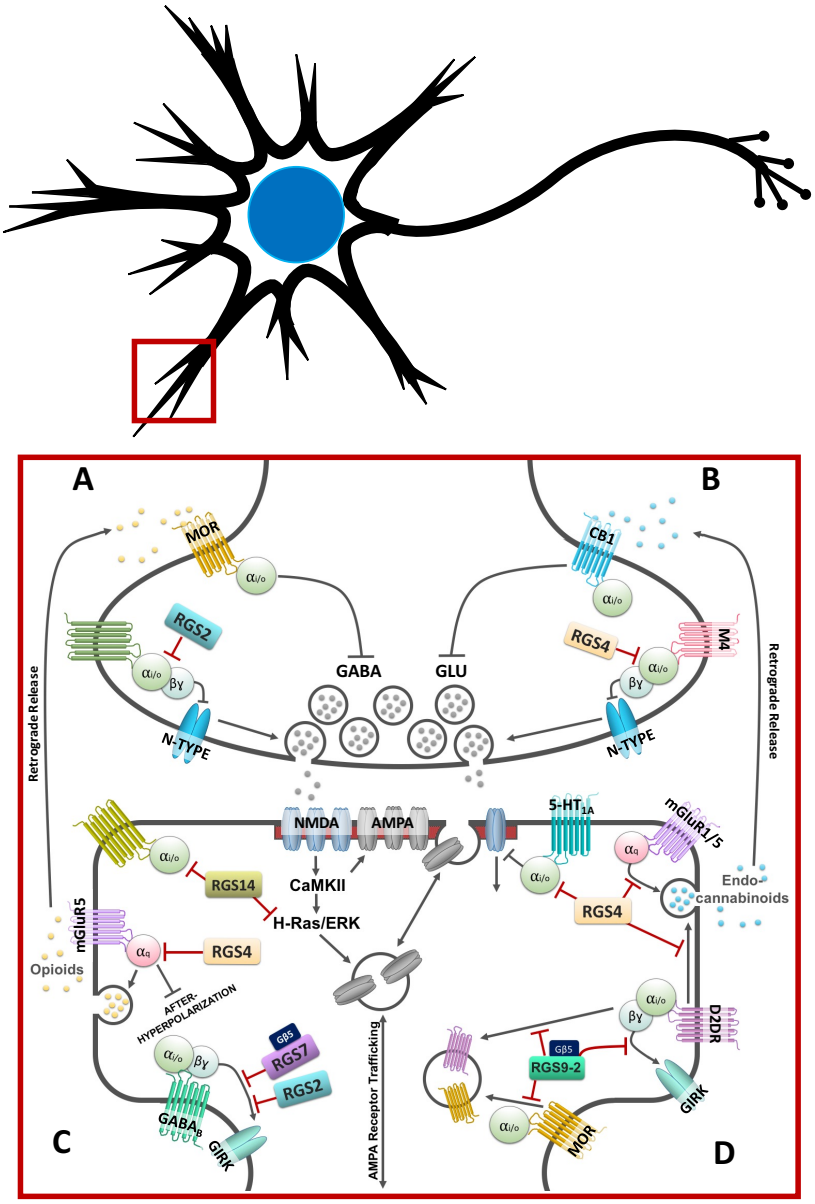

Figure 5.1. Model for multifunctional RGS protein roles in synaptic signaling and plasticity.[4]

RGS proteins regulate many aspects of synaptic signaling. ***A)*** *RGS2 expression disinhibits pre-synaptic CaV2.2 (N-Type) Ca^{2+} channels by decreasing active Gβγ.* ***B)*** *RGS4 diminishes M4 muscarinic acetylcholine autoreceptor signaling, increasing acetylcholine release.* ***C)*** *RGS14 associates with the plasma membrane via Gαi/o, where it regulates CaMKII- and ERK-depedent signaling events that underlie induction of LTP. RGS4 inhibits mGluR5-mediated suppression of the afterhyperpolarization current following action potential firing. Additionally, RGS4 suppresses mGluR5-mediated retrograde opioid release from parvocellular neuroendocrine cells (PNCs) in the hypothalamus, increasing GABA release onto these neurons. RGS2 and the RGS7:Gβ5 complex both inhibit post-synaptic $GABA_B$ receptor-mediated GIRK currents.* ***D)*** *RGS4 blocks post-synaptic serotonin-mediated inhibition of NMDA receptor current. Furthermore, RGS4 inhibits group I mGluR- and D2DR-mediated retrograde release of endocannabinoids, blocking LTD. Finally, the RGS9-2:Gβ5 complex accelerates the off kinetics for D2DR-coupled GIRK channels and inhibits agonist-induced internalization of MORs and D2DRs.*

[4] This figure and legend have been modified from the published manuscript: Gerber KJ, Squires KE, and Hepler JR (2016) Roles for Regulator of G Protein Signaling Proteins in Synaptic Signaling and Plasticity. *Mol. Pharmacol*.

RGS14 in the nucleus actually *enhances* its nuclear-linked tasks.

While functions for RGS proteins are examined in the lab using isogenic mice and canonical sequence recombinant protein, these studies are not representative of the diversity of human sequence variation. Approximately one out of every thousand base pairs differs from human to human, and while most of that variation lives in non-coding regions (although they almost certainly have their own critical function), many variants occur in exonic segments. The rise of population genomics has made this reality all the more obvious by providing high quality "minor allele" data readily available and compiled by the Genome Aggregation Database (GnomAD, Broad Institute) (23). RGS14 alone has 297 reported missense variants, reported by GnomAD, spanning the entire gene, the vast majority of which occur at a frequency of less than 1% of the population. This poses a great challenge to the field in identifying likely change-of-function variants.

Several methods have emerged in response to this challenge, each with a different focus. Combined annotation dependent depletion (CADD) combines multiple *in-silico* measures of "deleteriousness" to produce a combined "C-score" (46). This C-score takes into account side chain properties of the native versus mutated amino acid, sequence conservation, among many other biochemical measures. Missense tolerance ratios have only recently been described, and make predictions about functionally sensitive local segments of a gene based on a comparison of expected genetic variation versus observed genetic variation (47). This method is highly similar to d_N/d_S ratios, but is optimized for intra-species comparisons, as opposed to interspecies evolutionary analysis (50). Finally, post-translational modification sites are likely sensitive to genetic variation, as they control important functions of the RGS protein such as compartmental localization and function (62, 79, 203, 204). We thus combined all three methods, alongside structural considerations when available, to isolate and predict change-of-function variants, and validated our methods using RGS4 as a model. Using these methods, we report here for the first time that human variants precipitate a functional consequence on RGS14, broadening our knowledge of RGS14 as it relates to humans.

5.2 RGS14: CROSSTALK BETWEEN SEQUENCE DIVERSITY AND LOCALIZATION

RGS14 is a multifunctional signaling protein

RGS14 is an R12-subfamily RGS protein, mostly closely related to RGS10 and RGS12. In addition to the canonical RGS domain shared by all RGS family members, RGS14 contains additional signaling domains, including two tandem Ras/Rap binding domains termed R1 and R2, and a G protein regulatory (GPR) motif (Figure 5.2). Although RGS14 is named for its RGS domain, which binds and facilitates GTPase activity of Gαi/o proteins (333), the R1 domain and GPR motif have characteristic roles in signaling. The R1 domain binds both active Rap2A-GTP (294, 415) and H-Ras-GTP (291-293), and has been shown to regulate H-Ras-GTP downstream signaling to ERK (292) and H-Ras-GTP-linked neurite outgrowth (293). The GPR motif, although originally characterized as a guanine dissociation inhibitor (295, 297, 298), is critical for RGS14 compartmental localization within the cell. While recombinant RGS14 alone is mostly cytosolic, co-transfected Gαi1-GDP recruits RGS14 to the plasma membrane (288, 299).

RGS14 is a hippocampal regulator of long term potentiation and spatial learning

Although expressed in select other tissues (294, 333), RGS14 is primarily a brain protein. Expression of RGS14 in the rodent brain has been well-studied, is primarily localized to the CA2 region of the hippocampus (338), and is detectable as early as postnatal day 7 in mice (404). CA2 falls between the CA1 and CA3 regions of the hippocampus, both of which comprise the tri-synaptic pathway (dentate gyrus, CA1, and CA3). While synaptic responses can be reliably and persistently potentiated (called long term potentiation or LTP) within CA3-CA1 Schaffer collateral neurons, CA2 is characteristically unable to maintain LTP (403). However, when RGS14 is genetically ablated from mice, CA2 LTP is comparable to that of CA1, indicating that RGS14 is a natural inhibitor of long term potentiation in the hippocampal CA2 region. Further, as the hippocampus is an important mediator of episodic and spatial memory (455), RGS14 knockout

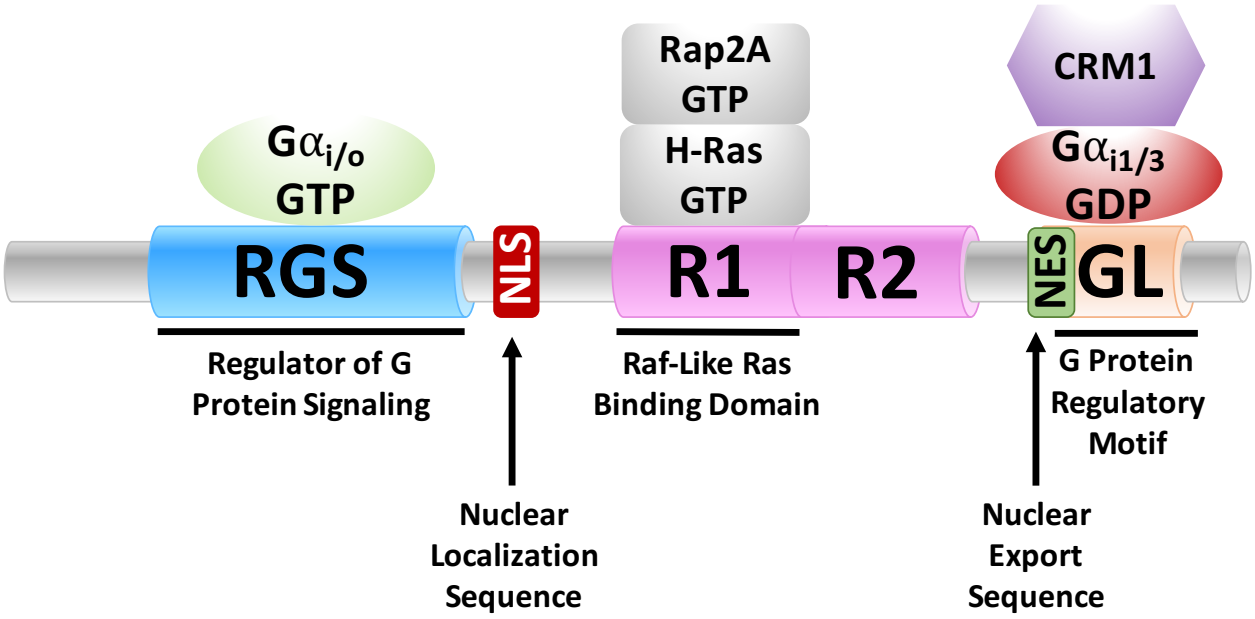

Figure 5.2. Linear structure of RGS14 domains/motifs and associated binding partners.
RGS14 is a multifunctional signaling protein that contains accessory domains and motifs. The regulator of G protein signaling (RGS) domain binds to active Gαi/o-GTP to catalyze the GTPase activity of the Gα subunit. Shortly after the RGS domain is a nuclear localization sequence (NLS) motif, a basic triplet of residues that putatively binds to the importin α/β1 heterodimer to translocate RGS14 into the nucleus. Following the NLS are tandem Ras/Rap binding domains, R1 and R2. While R2's function remains a mystery, the R1 domain binds both active H-Ras-GTP and active Rap2A-GTP. Although the consequence of Rap2A-GTP binding is unknown, RGS14 interaction with H-Ras-GTP can suppress H-Ras signaling to ERK and coordinate plasticity in PC12 cells. Finally, at the C terminus is the nuclear export sequence (NES) and G protein regulatory motif (GoLoco, GL) which overlap in sequence. The NES binds nuclear export receptor CRM1 to translocate RGS14 out of the nucleus, and the GL motif binds inactive Gαi1/3-GDP to direct RGS14 to the plasma membrane.

mice were tested for their ability to learn spatial cues in the Morris Water Maze, and were found to perform better than their wildtype counterparts, with no other overt phenotypes, consistent with its constrained expression pattern (338). Altogether, this suggests that RGS14 has a functional role in the hippocampus suppressing LTP critical for spatial learning.

RGS14 has broader expression within monkey and human brain, with unknown consequences

Just as rodent RGS14 sequence does not represent the complexity of human RGS14 sequence, my work in this thesis demonstrated that rodent RGS14 expression is not fully representative of human and higher mammal RGS14 expression (335). In these studies, I show that, like rat and mouse, RGS14 is expressed in the CA2 region of monkey and human hippocampus (Figure 4.6 and Figure 4.12). However, unlike mouse brain, RGS14 is densely expressed in multiple nuclei of the basal ganglia (Figure 4.4 and Figure 4.14), including the caudate and putamen (Figure 4.7 and Figure 4.8), the internal and external globus pallidus (Figure 4.9), as well as the substantia nigra (Figure 4.10). Together, these nuclei are well known for their role in both purposeful movement as well as movement disorders, such as Parkinson's Disease and dystonia. The strong and specific expression of RGS14 in this circuit points to a potential role in regulating the (patho)physiology of movement. We did not observe any differences in RGS14 expression between MPTP-treated monkeys (an animal model of Parkinson's Disease) and age-matched controls (not shown). However, one study in Parkinson's patients found diminished RGS14 immunoreactivity in dopaminergic cells of the substantia nigra and reduced RGS14 transcript in the putamen (343). Furthermore, the authors found that healthy controls had both nuclear as well as cytoplasmic/membrane pools of RGS14, whereas the Parkinson's patients *lost the nuclear localization* of RGS14 in these same neurons. This is consistent with the hypothesis that RGS14 has a unique role in the basal ganglia and its associated movement disorders.

RGS14 is a nuclear shuttling protein in neurons

Furthermore, my work here suggests that primate RGS14 exists as multiple splice variants in the caudate nucleus (Figure 4.3), which had been speculated but never demonstrated (412).

Importantly, and consistent with the findings in previous human studies, at least one of these splice variants resides natively in the nucleus (Figure 4.8). Upon sequence analysis, both a nuclear localization sequence (NLS) and a nuclear export sequence (NES) were identified and functionally confirmed (Figure 3.1). While most of the splice variants include both the NLS and NES, the smallest variant (identified in the literature as RGS14-S) contains the NLS but lacks the NES, indicating that its subcellular localization would be constrained to the nucleus.

Interestingly, the NES box falls within the GPR motif (Figure 5.2) and upon inhibition of nuclear export receptor CRM1 by Leptomycin B, both endogenous and recombinant RGS14 become entirely nuclear (288, 289, 454). In dissociated hippocampal neurons, RGS14 can be sequestered to the nucleus by LMB treatment or inactivation of the NES (Figure 3.1), indicating that RGS14 translocates to the nucleus in neurons other than those in the basal ganglia. Together, these findings suggest that RGS14 is not only a multifunctional protein, but also a dynamically regulated protein within subcellular compartments. These data indicate that RGS14 has a unique, and potentially independent, role within the nuclei of neurons, not previously studied.

RGS14 human variants tip the nuclear-cytoplasmic balance

Like all RGS proteins, RGS14 is riddled with genetic variants in the human population, many of which are missense and produce an amino acid change. While other domains have unique and important functions, the GPR motif is important for both plasma membrane localization (288, 299) as well as nuclear export (288, 289, 335, 454). I thus sought to define the contribution of human variants on subcellular localization, with a particular focus on the newly appreciated nuclear pool. Under unstimulated conditions, a majority of RGS14 resides in the cytosol of neurons, as shown in dissociated hippocampal cultures (Figure 3.1), hippocampal slices (Figure 3.6A), and native expression in primate brain (335). However, nuclear export inhibition reveals a sequestration of RGS14 in the nucleus, suggesting that it rapidly translocates to and from the nucleus, in a nucleo-cytoplamsic equilibrium, which favors the cytoplasm. In these current studies, I report that at least two human variants (R506Q, found in the Ashkenazi Jewish population and L504R, found in the

East Asian population) disrupt this equilibrium, and tip the balance toward nuclear sequestration, to varying degrees. While a small pool of RGS14 can be found natively in the nuclei of primate neurons (335), these human variants may work to increase the proportion of nuclear RGS14 in humans. RGS14 actions in the nucleus are currently a mystery, as there are no predicted nucleotide binding motifs on RGS14, but related RGS proteins can give clues to its nuclear role.

Many RGS proteins have been shown to shuttle between the cytoplasm and nucleus (456-458), and some RGS proteins are dependent on their N terminus to regulate their subcellular localization (459). RGS3T (an N terminal truncation mutant of RGS3) is predominantly nuclear and leads to apoptosis (460). Similarly, RGS8's nuclear localization is governed by its N terminus, and loss of the N terminus reduces RGS8's ability to desensitize G protein-coupled inwardly rectifying K^+ (GIRK) channel responses (178). R7 subfamily RGS nuclear localization in the brain (461) is governed by its interacting partner, R7BP, via regulation of a C terminal palmitoylation (462-465). RGS13 inhibits CREB-mediated transcription (466). Others have differential subcellular distribution based on alternative splicing. Human RGS6, and in particular certain splice variants are localized to the nucleus (467), similar to the purported role of distinct splice variants in RGS14 (see above). RGS6 translocation to the nucleus appears to be part of the cell's stress response (468). Although no definitive nuclear role has been reported, there is evidence that nuclear RGS proteins can regulate transcription. RGS2 translocates to the nucleus (469) where it inhibits transcription of multiple targets including Nox1 (470), COX2 (471), which may explain, at least in part, its role in hypertension via an immune mechanism (472, 473). RGS12 localizes to the nucleus in a cell-cycle dependent manner (300) and represses transcription (290). Finally, RGS10 localizes to transcriptionally active regions in rodent brain (287). Interestingly, its nuclear localization is regulated by a PKA modification of Ser186, and nuclear RGS10 is unable to regulate Gα (62).

Thus, several possible explanations exist for the purpose of RGS14 nuclear localization: 1) nuclear localization may act to sequester the RGS protein from its intended targets, such as Gα, H-

Ras, CaM, or GIRK, as has been suggested (456); 2) nuclear localization may be a mechanism by which RGS proteins regulate gene transcription; and finally 3) although unlikely, nuclear localization may be a way to regulate a potential nuclear pool of Gα proteins, as has been suggested in the past (458). There is sparse evidence for nuclear Gα proteins (474), and what evidence exists points to a role in dividing cells (475), so is therefore an unlikely contributing factor to RGS14's role in the brain. Of note, a study on RGS2 demonstrated that its nuclear localization did not affect its regulation of Gαq signaling (91), pointing to the indication that nuclear localization of RGS proteins may not be an effective way of limiting conventional GAP signaling.

RGS14 rare variants disrupt inhibition of long term potentiation

RGS14 is a natural inhibitor of long term potentiation (LTP) (338). I hypothesized that its role in LTP suppression was dependent on its localization to dendrites/spines, where its interaction with other proteins (CaM, H-Ras, Gα, etc) was crucial for these effects (Figure 5.3). As such, variants that mislocalize to the nucleus, such as the Ashkenazi and East Asian variants (Figure 3.4), were predicted to have little to no effect on LTP. Accordingly, wild type RGS14 was able to translocate to appropriate compartments (Figures 3.4 and 3.6A) and inhibited LTP in CA1 neurons when ectopically expressed (Figure 3.6B), while LTP is characteristically robust in CA1 where native RGS14 expression is absent (403). Thus, these results contribute, first and foremost, to the idea that RGS14 is alone capable of inhibiting LTP signaling. This is novel and important because it signifies that the mechanistic machinery necessary for LTP exist in CA1 as well as CA2, and that RGS14 is intrinsically suppressing LTP. In line with my prediction, variants that sequester RGS14 in the nucleus (and thus prevent RGS14 localization to crucial LTP-regulating compartments) prevent blockade of LTP in CA1 neurons (Figure 3.6). As LTP is a fundamental mediator of learning (476), and RGS14 knockout mice have both enhanced CA2 LTP as well as hippocampal-based learning (338), these human variants likely play important and previously unappreciated roles in hippocampal-based learning. Particularly within the context of CA2, RGS14 may be acting to

regulate social and/or contextual memory (340), and these dysfunctional human variants may have principal roles in the expression of related social/contextual *traits*.

5.3 WORKING MODEL

My studies presented here indicate that RGS14 is a dynamically regulated nucleo-cytoplasmic protein, that under wild type conditions (Figure 5.3A), exists in three distinct populations: nuclear (indicated by green dots representing RGS14 in blue nucleus), cytoplasm (green dots in soma), and dendrites/spines (green dots in distal processes). This dynamic regulation is accomplished by multiple binding partners, including Gαi and CRM1, among others. Specifically, while other karyopherins such as importin α/β1 may direct RGS14 into the nucleus, CRM1 (also known as XPO1 and Exportin 1) rapidly shuttles it out of the nucleus. From there, although it is presently speculative in neurons, Gαi1-GDP recruits RGS14 to the plasma membrane. I propose the same mechanism accounts for RGS14 association at plasma membranes of dendrites and spines. Although RGS14 is not a PSD-associated protein (335), it is well-positioned in dendrites and spines to regulate signaling important for LTP (Figure 5.3A red box). Here, RGS14 inhibits Gαi/o signaling via its RGS domain and H-Ras/ERK signaling via its Ras binding domains (RBD) (292, 334) to suppress LTP and learning (419, 420, 477, 478). Although inhibition of Gαi/o leading to inhibition of LTP seems unintuitive, a newly hydrolyzed Gαi-GDP may be captured by the GPR motif (GoLoco, GL) (299) which would further solidify its association at the plasma membrane and prolong Gβγ signaling to G protein-coupled inwardly-rectifying K^+ (GIRK) channels, leading to a brake on LTP (479). By contrast, variant forms of RGS14, including human sequence variants as well as splice variants, become sequestered in the nucleus (Figure 5.3B green dots in blue nucleus) via reduced interaction with export receptor CRM1 (Figures 3.4-3.5), resulting in an inability to be recruited to the plasma membrane by Gαi1-GDP. As such, variant RGS14 exists primarily as a nuclear population, and is largely absent from dendrites and spines (Figure 5.3B red box). The lack of RGS14 at the dendrites and spines allows for unabated signaling via GPCRs and

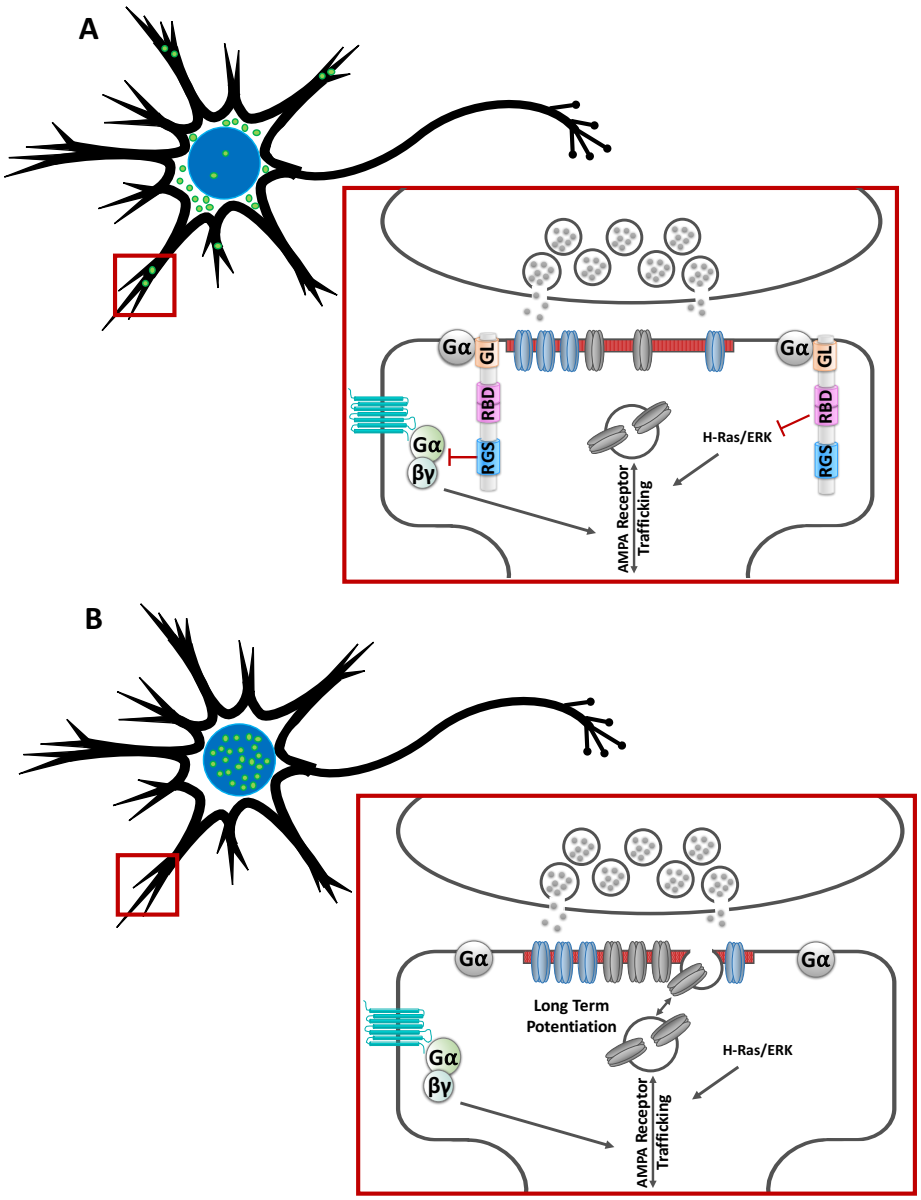

Figure 5.3. Working model for RGS14 subcellular localization and regulation of LTP.

A) *Wild type RGS14 (green dot) is disperse throughout the neuron, occupying multiple compartments including the nucleus, the cytoplasm, and the dendrites (red box). Within a dendrite (expanded red box), Gα-GDP interaction with the G protein regulatory motif (GoLoco, GL) brings RGS14 to the micro-compartment necessary for inhibition of GPCR signaling by the RGS domain and inhibition of H-Ras/ERK signaling by the Ras binding domains (RBD), both of which support LTP.* ***B)*** *Variant forms of RGS14 (green dots) are sequestered in the nucleus and cannot reach dendrites (red box). Due to their mislocalization, they cannot interact with, and be recruited by, Gα-GDP to dendritic compartments (expanded red box). The lack of RGS14 at these micro-compartments allows for unabated GPCR and H-Ras/ERK signaling, removing the block on LTP.*

H-Ras/ERK, leading to the propagation of LTP and learning.

5.4 FUTURE DIRECTIONS

RGS14 function in the nucleus

RGS14 is a nuclear shuttling protein in neurons (Figure 3.1) and is natively found in the nucleus of primate brain (Figure 4.8). Its function in the nucleus, however, remains a mystery. As other family members are capable of repressing transcription (290, 470, 471), one strong possibility is that RGS14 represses transcription, particularly of gene products that are necessary for LTP and learning, its only known function at present. Future studies should be done to measure any changes in transcription products comparing RGS14-NLSm (unable to enter the nucleus) and RGS14-NESm (unable to escape the nucleus). RNA sequencing (RNA-seq) would prime future studies with ideally unbiased information about genes that are up-or-downregulated in response to nuclear RGS14. In these studies, hippocampal neurons from wild type embryonic rats would be plated and incubated with adeno-associated virus containing wild type RG14, RGS14-NLSm, or RGS14-NESm for two weeks (demonstrated by preliminary studies to produce maximal protein expression). Neurons would then be harvested in RNase-free lysis buffer, sonicated to shear DNA, and RNA would be extracted. cDNA converted from RNA would then be sequenced to detect (virtually) actively transcribed gene products. This process would be repeated in triplicate for each condition (wild type, NLSm, NESm) and findings would be pooled within each respective group. From here, data will be ranked by ratio of NESm/NLSm, such that transcribed products that are elevated when RGS14 is exclusively nuclear will be at the top of our list. Wild type RGS14, which crosses the nuclear membrane in a regulated fashion, will be used to verify that differences in transcription from nuclear RGS14 are not due to stress on the cell. Understanding which genes respond to nuclear RGS14 then provides clues into not just whether, but how (e.g. via cooperative binding partner) RGS14 interacts with DNA, as RGS14 does not have any predicted DNA-binding sites and likely must cooperate with accessory proteins.

Next, chromatin immunoprecipitation followed by deep sequencing (ChIP-seq) would confirm any putative RGS14-based regulatory role on gene transcription at the level of the DNA. Based on up-or-downregulated targets identified by RNA-seq, we could make predictions about activator/repressor activity if those regulatory elements are known for target transcripts. As before, comparisons would be made between AAV RGS14 NLSm and AAV RGS14 NESm following two weeks of transduction in hippocampal neurons. Again, where the NESm and wild type RGS14 results converge represents promising DNA targets. Any regulatory regions that co-immunoprecipitate with RGS14 could be validated by luciferase reporter assay. Furthermore, depending on the putative target sites, we could define novel interactions with co-repressors or co-activators, which may provide clues into nuclear roles of RGS14's regulation of long term potentiation. Overall, ChIP-seq would demonstrate whether or not RGS14, likely through a binding partner, is regulating DNA via activator- or repressor-like activity versus regulating an upstream effector that signals to activators/repressors.

Roles of RGS14 beyond the hippocampus

RGS14 expression in rodent brain is relatively constricted to the hippocampus (404), but has much broader expression in primate brain (335). Specifically, RGS14 is strongly expressed in the caudate, putamen, and globus pallidus of both human and monkey brain (Figures 4.7-4.10 and Figure 4.13). The lack of expression in mice makes it a challenge to investigate RGS14 roles in these areas, however expression could be virally introduced and effects could be studied in both whole animal (behavior), in slice (subcellular localization and co-localization with binding partners), and in dissociated striatal neurons (function on excitability, actions on G protein signaling, GPCR association). As a starting point, mice would be bi-laterally microinjected in the striatum with AAV-YFP-RGS14 or AAV-YFP-STOP-RGS14 (a construct that has a premature stop codon between the YFP and the RGS14 sequences so that only YFP is translated). Other striatal-enriched RGS proteins (267, 443) can give us clues into putative roles for striatal RGS14. Loss of RGS9-2 in the striatum leads to coordination deficits (281). Furthermore, viral

overexpression of RGS9-2 reduces locomotor responses to cocaine while RGS9-2 knockout mice have enhanced locomotor responses to cocaine (267). Thus, both the accelerating rotarod test and cocaine-induced locomotor hyperactivity would be assessed in mice with striatal YFP or YFP-RGS14. I predict that striatal RGS14 would elicit similar phenotypes to that of RGS9-2, in particular with respect to regulation of cocaine-induced hyperactivity.

Effect of nuclear mislocalization on behavior

Finally, RGS14 human variants mislocalize RGS14, tipping the nucleo-cytoplasmic equilibrium toward the nucleus (Figure 3.4), and these variants disrupt RGS14's natural ability to inhibit LTP in the hippocampus (Figure 3.6). LTP is believed to be the cellular correlate of, and foundation for, memory (476) and RGS14 knockout mice have both enhanced LTP and enhanced spatial learning (338). Consequently, removing RGS14 inhibition of LTP, as is the case for these human variants, should thereby heighten spatial learning, similar to RGS14 knockout mice. Therefore, new technology such as CRISPR should be used to generate transgenic mice carrying these human variants. The mice should be tested in spatial learning tasks (e.g. the Morris Water Maze), among others, compared to wild type mice. For these experiments, wild type RGS14, RGS14 knockout mice, RGS14 L/R, and RGS14 R/Q would be subjected to the Morris Water Maze. As before, I predict RGS14 knockout mice would perform better than their wild type counterparts. Based on the full versus partial effect on LTP from the L/R and R/Q variants, respectively, I predict that the L/R (East Asian) mice would perform similar to the RGS14 knockout mice, whereas the R/Q (Ashkenazi) mice would perform better than wild type mice, but worse than L/R and knockout mice. Furthermore, as RGS14 is expressed in other brain regions in higher mammals, including those of the basal ganglia, it would be interesting to test these mice on movement-related tasks, as described above. In particular, the native nuclear expression of RGS14 in the caudate, a basal ganglia sub-region, hints at potentially interesting effects of these human-derived mislocalized variants of RGS14, with possible clues into as yet unrecognized roles.

5.5 CONCLUDING REMARKS

Overall, my findings presented in this thesis have progressed our understanding of the relationship between sequence variation, subcellular localization, and function of RGS proteins, with a particular focus on RGS14. Splice variants, present in humans but not rodents, as well as single point variants can have great consequence on subcellular localization, which in turn can have great consequence on functional output. My combination of "big data" analysis, biochemical investigation, and *ex vivo* functional readout has presented for the first time the unique nature of human-centered RGS14: its unique localization, sequence diversity, and unique regional expression. Future experiments will uncover novel roles of RGS14 in the nucleus, in the basal ganglia, and importantly, the relationship between sequence variation, brain distribution, and protein function.

APPENDIX:

REGULATOR OF G PROTEIN SIGNALING 14 (RGS14) FORMS A HETEROMERIC G PROTEIN COMPLEX: INTERACTION BETWEEN RAP2A, H-RAS, AND Gαi1

A.1 INTRODUCTION

Heterotrimeric G proteins, the major target of the past 4 decades of drug discovery, are critical mediators of virtually every functional system in animals, and ablation of these signaling proteins leads to severe deformities or death (28-34). G protein signaling cycles are regulated by a family of proteins called Regulators of G protein Signaling (RGS). RGS proteins have been extensively characterized as modulators of various peripheral (480), immune (26), and neurological (21) processes, via their interactions with G proteins. While some RGS proteins contain only the canonical RGS domain, others such as RGS14 are multifunctional and contain additional signaling domains including tandem Ras-binding domains (R1 and R2) and a G protein regulatory (GPR) motif.

RGS14 is densely expressed in the CA2 region of the hippocampus in mouse, monkey, and human (335, 404) and has been characterized as a native regulator of long term potentiation (LTP) in the CA2 region of the hippocampus (338). Curiously, while hippocampal CA3-CA1 Schaffer collaterals undergo robust and reliable LTP, the CA3-CA2 Schaffer collaterals lack the capacity for LTP in wild type mice. RGS14 knockout mice, however, demonstrate robust LTP in these CA2 synapses, comparable to CA1 (338). Further, RGS14 knockout mice have enhanced spatial learning, a hippocampal-dependent task (338). Interacting partners for RGS14 include active Gαi/o-GTP (RGS domain), active H-Ras-GTP (first Ras-binding domain, R1) (292, 293), and inactive Gαi1/3-GDP (288, 481), both of which have be extensively characterized for their role as signaling partners (299, 412, 414). However, RGS14 was originally discovered as a Rap2A effector (294), and since then very little investigation into this interaction has taken place (415).

RGS14's interaction with a highly similar small G protein, H-Ras, has been well studied. H-Ras binds to the R1 domain at a conserved Ras-binding residue, R333 in rat RGS14 (R335 in human sequence) (293) and RGS14 inhibits H-Ras signaling (292). H-Ras and downstream effectors are strongly linked with synaptic plasticity (477). H-Ras-GTP controls trafficking of GluR1 and

GluR2L AMPA subunits to synapses during LTP (419), enhances AMPA receptor currents (420), and is crucial for learning and memory (478). Thus, RGS14 may be naturally inhibiting LTP by suppressing H-Ras signaling necessary for plasticity. However, Rap2A has been reported to inhibit synaptic plasticity via a process known as depotentiation, or the reversal of LTP (418). Specifically, Rap2A removes GluR1 and GluR2L and reduces AMPA receptor potentiation of currents through its MAP kinase, c-Jun N-terminal kinase (JNK). Furthermore, active Rap2A inhibits spine formation and learning in mice (416, 417, 482). Therefore, RGS14 may be naturally inhibiting LTP via its interaction with Rap2A, either in addition to or in place of RGS14 interactions with H-Ras. Finally, due to their opposing functions and shared interaction surface on RGS14, we hypothesized that RGS14 may have a preferred small G protein and would bind H-Ras or Rap2A competitively.

Here we find that RGS14 binds active, but not inactive Rap2A and colocalizes with active Rap2A at the plasma membrane. RGS14 R333L ablates Rap2A-GTP binding, suggesting it does indeed share a binding interface on RGS14 with H-Ras. The Rap2A:RGS14 complex is facilitated by coexpression of Gαi1-GDP, which binds to the GPR motif on RGS14. Altogether, this suggests that Rap2A-GTP binds and behaves very similar to H-Ras-GTP. We thus hypothesized that Rap2A-GTP and H-Ras-GTP bind to RGS14 in a competitive manner. To our great surprise, H-Ras-GTP did not reduce Rap2A-GTP binding to RGS14. Further, Rap2A-GTP enhanced H-Ras-GTP binding to RGS14, suggesting that perhaps these two small G proteins form a heterotrimeric complex with RGS14. In fact, we report that H-Ras and Rap2A interact independent of RGS14. Small G protein dimerization has been reported previously, however this is the first time, to our knowledge, that a heteromeric complex of small G proteins has been reported.

A.2 MATERIALS AND METHODS

Cell Culture

HEK293 and HeLa cells were kept in DMEM supplemented with 10% FBS and 1%

Penicillin/Streptomycin in a cell culture incubator maintained at 5% CO_2. Transfections were carried out for 18-24 hours in DMEM supplemented with 5% FBS. For immunocytochemistry experiments, 300ng of rRGS14 or rRGS14 R333L was transfected alongside 750ng of Rap2A-Venus (WT, G12V, or S17N) in HeLa cells. All BRET experiments were carried out in HEK293 cells using the following transfection conditions. For RGS14:Rap2A experiments, 5ng RGS14-Luciferace (WT or R333L) was transfected along with 0, 3, 10, 30, 100, or 300 ng Venus-Rap2A (WT, G12V, or S17N). For Gαi1:RGS14:Rap2A experiments, we used the same conditions with 0 or 750ng Gαi1-EE. For Rap2A competition for RGS14:H-Ras we transfected 5ng RGS14-Luciferase with 10, 50, 100, 250, or 500ng of Venus-H-Ras (G12V), 750ng Gαi1-EE, and 0 or 500ng unlabeled Rap2A (G12V). For H-Ras competition for RGS14:Rap2A we transfected 5ng RGS14-Luciferase with 0, 3, 10, 30, 100, or 300ng of Venus-Rap2A (G12V), 500ng Gαi1-EE, and 0 or 600ng unlabeled H-Ras (G12V). Finally, for the Rap2A:H-Ras experiment, we transfected 5ng Luciferase-H-Ras (G12V) with 0, 3, 10, 30, 100, or 300ng Venus-Rap2A (G12V or S17N).

Bioluminescence Resonance Energy Transfer (BRET)

BRET experiments were carried out as described previously (293, 299, 387). Briefly, cells were resuspended in Tyrode's solution (140 mM NaCl, 5 mM KCl, 1 mM MgCl2, 1 mM CaCl2, 0.37 mM NaH2PO4, 24 mM NaHCO3, 10 mM HEPES, and 0.1% glucose, pH 7.4) and plated at 10^5 cells/well in a 96-well Optiplate (PerkinElmer Life Sciences). Initial Venus fluorescence was read at 530nm (485nm excitation) for use in Acceptor/Donor calculations. Next, 5 μM coelenterazine H (Nanolight Technologies) was incubated for 2 minutes and BRET recordings were taken at 485nm and 530nm. Net BRET was calculated as follows: (530nm/485nm) for each increasing Venus condition subtracting baseline (530nm/485nm) where Venus was not expressed. Acceptor/Donor was calculated using the 530nm fluorescence measurement divided by the 485nm bioluminescence measurement.

Immunocytochemistry

HeLa cells were fixed following 18 hours transfection with 4% PFA in PBS for 10 minutes, quenched with 0.75% glycine in 200 mM Tris pH 7.4 for 5 minutes, and then permeabilized with 0.1% Triton-X-PBS. Cells were blocked with 8% BSA-PBS for 1 hour and then exposed to rabbit anti-RGS14 (1:1000, Proteintech) for 2 hours in 4% BSA-PBS. Cells were then washed 3 times in 0.05% Triton-X-PBS and exposed to goat anti-rabbit AlexaFluor 546 (Invitrogen) for 1 hour. Finally, cells were washed 3 times in PBS, incubated with Hoechst stain (1:12,500) for 4 minutes, and fixed onto glass slides with ProLong Diamond Antifade mountant (ThermoFisher). Images were taken on Olympus FV1000 confocal microscope at 100x, then processed using ImageJ software.

Immunoprecipitation and Western Blot

Western blots were performed as previously described (288). Briefly, HeLa cells were transfected with Flag-RGS14 and 3xHA-Rap1A or 3xHA-Rap2A. Cells were lysed in 150 mM NaCl, 50 mM Tris–HCl, pH 8.0, 1 mM EDTA, 1 mM EGTA, 10 mM $MgCl_2$, 1% Triton-X, and protease inhibitors. Lysates were centrifuged and Anti-Flag affinity sepharose (Sigma) was incubated for 2 hours, rotating end over end at 4°C. Beads were washed 4 times with TBS, and then resuspended in Laemmli buffer, boiled for 5 minutes, and separated on 13% SDS-PAGE. Proteins were transferred onto a nitrocellulose membrane, blocked for 1 hour in milk, and then immunoblotted with anti-Flag (Invitrogen), anti-Rap1 (Santa Cruz SC-65), and anti-Rap2 (Santa Cruz SC-164).

A3. RESULTS

RGS14 interacts with H-Ras in an activity-dependent manner. Specifically, H-Ras G12V, which is constitutively active and GTP-bound, co-immunoprecipitates with RGS14 from mammalian cell culture or mouse brain (292, 293). However, RGS14 was identified as a Rap2A-binding partner in a yeast screen (294). Thus, we sought to confirm whether RGS14 bound Rap2A in mammalian cells in a GTP-dependent manner. We expressed Flag-RGS14 with Rap1A/Rap2A

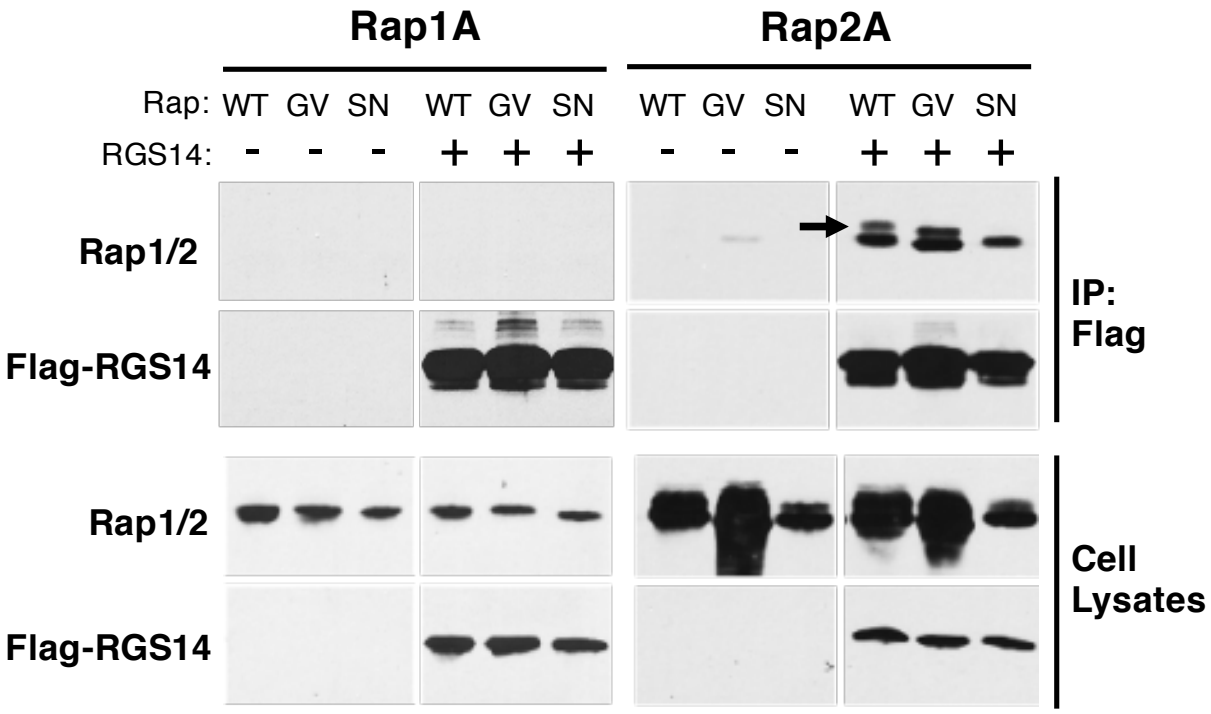

Figure A.1. RGS14 binds Rap2A-GTP, but not Rap2A-GDP and not Rap1A.

HeLa cells were transfected with Flag-RGS14 and Rap1A or Rap2A WT, GV (constitutively active), or SN (constitutively inactive). Flag-RGS14 was immunoprecipitated and Western Blots revealed only Rap2A WT and Rap2A GV (arrow) co-immunoprecipitated with Flag-RGS14. Rap1A did not co-immunoprecipitate in any condition. Altogether, RGS14 interacts with Rap2A-GTP in mammalian cell lysates.

(WT, constitutively active G12V, or constitutively inactive S17N for each Rap) in HeLa cells and immunoprecipitated RGS14 with anti-Flag affinity sepharose. We found that Rap2A WT and Rap2A G12V, but not Rap2A S17N nor Rap1A in any condition co-precipitated with Flag-RGS14 (Figure A.1). This is consistent with previous reports showing WT Rap2A is mostly in its active, GTP-bound state (483), and should thus bind RGS14 in a similar manner to constitutively active Rap2A G12V.

RGS14 interacts with Rap2A-GTP in live cells

Co-immunoprecipitation demonstrates an interaction in cell lysates, but does not account for cellular compartments or interactions in "time and space" (484). We thus turned to bioluminescence resonance energy transfer (BRET), which measures protein-protein interactions in live cells (387). We transfected HEK293 cells with RGS14-Luciferase (RGS14-Luc) and increasing amounts of Venus-Rap2A (Ven-Rap2A). Protein-protein interactions are detected by transfer of energy from Luc to Ven, and plotted as Net BRET. We found that RGS14-Luc and Ven-Rap2A WT formed a complex in live cells, as detected by a robust Net BRET signal (Figure A.2 black circles). Similarly, RGS14-Luc and Ven-Rap2A G12V form a complex in live cells to about the same degree (Figure A.2 grey squares). This is consistent with our co-immunoprecipitation data (Figure A.1) and with previous reports that Rap2A mostly exists in its GTP-bound state (483). Next, we found that Ven-Rap2A S17N formed virtually no detectable interaction with RGS14-Luc (Figure A.2 blue triangles), consistent with our co-immunoprecipitation data (Figure A.1). Finally, H-Ras-GTP binds to a conserved R333 on the first Raf-like Ras-binding domain of RGS14, but not the analogous residue in the second Ras-binding domain (292, 293). Thus, we wanted to explore whether Rap2A bound at the same interface. RGS14-Luc R333L showed virtually no binding to Ven-Rap2A G12V, almost indistinguishable from the Ven-Rap2A S17N BRET signal (Figure A.2 red open circles).

RGS14 is recruited to the plasma membrane by Rap2A-GTP

We next wanted to visualize RGS14 colocalization with Rap2A in cells. In mammalian cells,

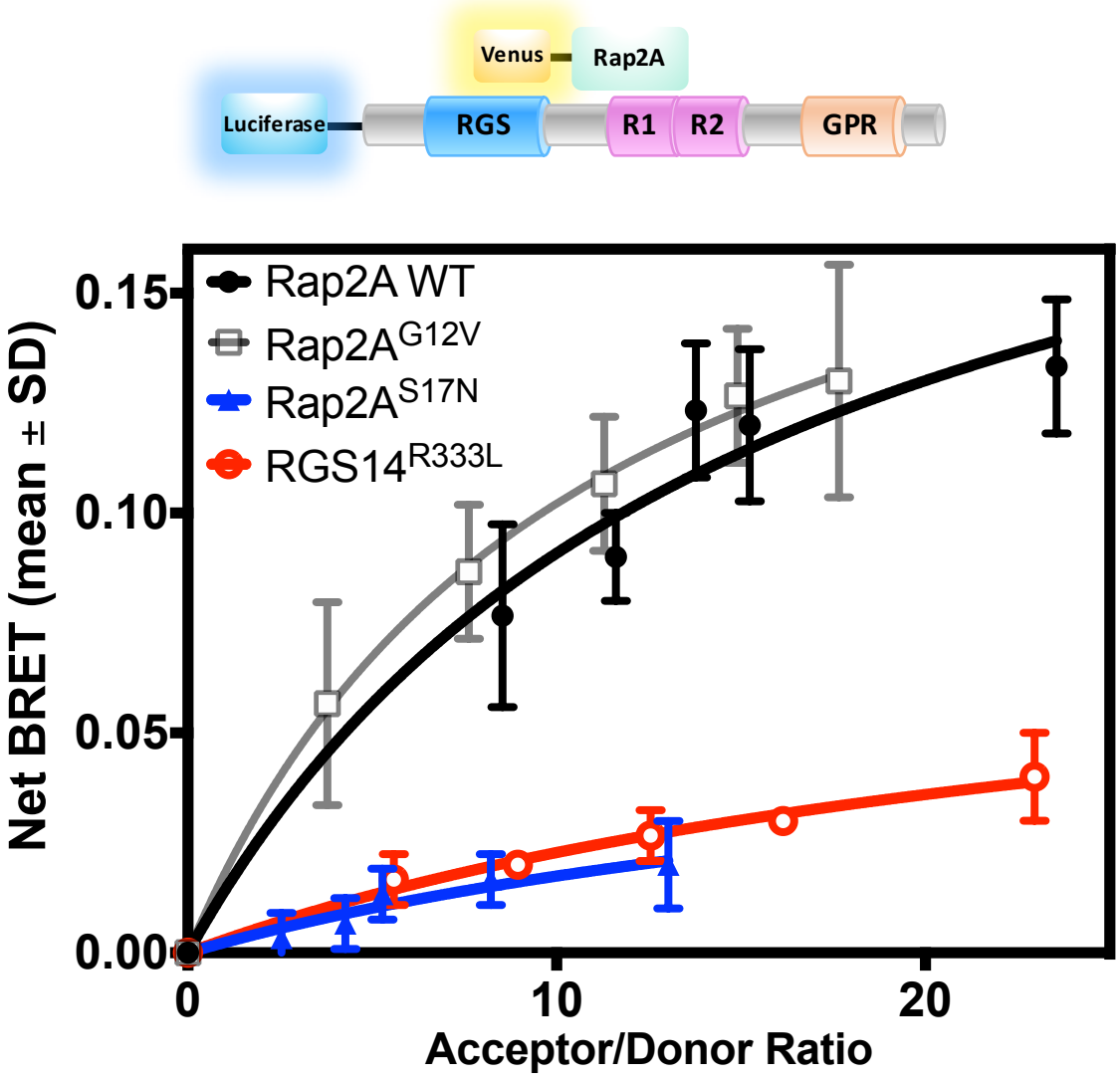

Figure A.2. RGS14 binds Rap2A-GTP in live cells at R333 in the first Ras-binding domain on RGS14.

RGS14-Luc was expressed in HEK293 cells with increasing Ven-Rap2A and energy transfer, indicating closely interacting Luc and Ven, was recorded as Net BRET. RGS14-Luc binds WT and GV Ven-Rap2A, but not SN Ven-Rap2A, indicating that Rap2A must be GTP-bound to interact with RGS14. RGS14-Luc R333L did not interact with GV Ven-Rap2A, indicating that Rap2A binds at the R333 interface of RGS14, in the first Ras-binding domain.

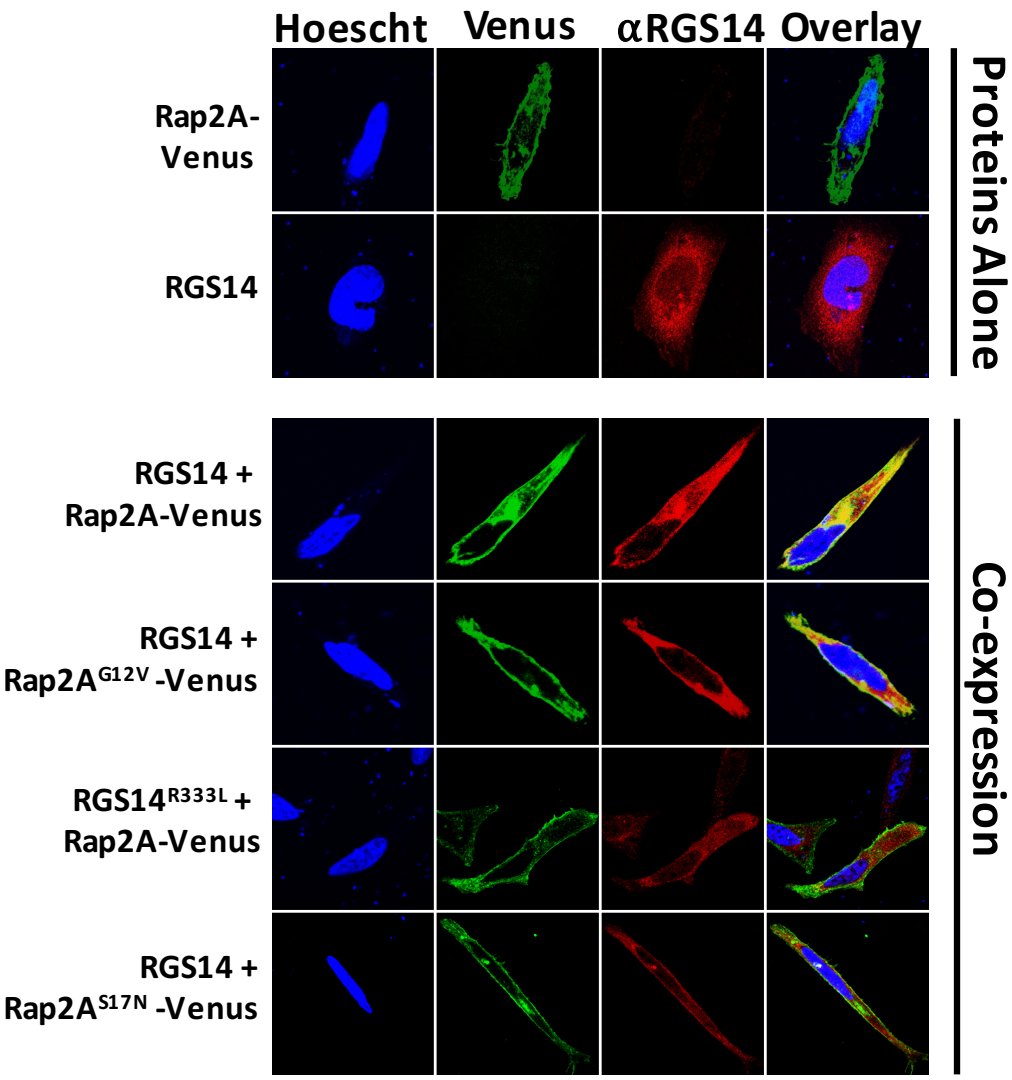

Figure A.3. RGS14 is recruited to the plasma membrane by Rap2A-GTP via interactions at R333 in the R1 domain of RGS14.

RGS14 and Venus-Rap2A were transfected into HeLa cells, fixed, and stained for immunocytochemistry. Rap2A alone is primarily at the plasma membrane, while RGS14 fills the cytoplasm. When transfected together, RGS14 is recruited to the plasma membrane by Rap2A WT and Rap2A G12V (the constitutively active form). When R333 is mutated to R333L on RGS14, there is no longer recruitment to the plasma membrane. Finally, a constitutively inactive form of Rap2A (S17N) does not recruit or colocalize with RGS14.

active H-Ras binds RGS14 at R333 (in the R1 domain) to recruit RGS14 to the plasma membrane (293). As Rap2A is a highly similar GTPase to H-Ras, we hypothesized that Rap2A-GTP binding to RGS14 would have a similar effect in mammalian cells. We therefore transfected HeLa cells with Ven-Rap2A and RGS14-Luc for immunocytochemistry. Under unstimulated conditions, Ven-Rap2A is localized primarily at the plasma membrane. RGS14-Luc alone is primarily dispersed throughout the cytosol (Figure A.3), as was shown previously (293, 299). Wild type Ven-Rap2A is localized to the plasma membrane (Figure A.3), via a CAAX box at its C-terminus (485). Co-expression of wild type Ven-Rap2A and RGS14-Luc shows a great deal of overlay at the plasma membrane (Figure A.3), indicating that RGS14 is recruited to the membrane by Rap2A (which is abundantly GTP-bound under normal conditions (483)). Furthermore, constitutively active Ven-Rap2A G12V colocalizes with RGS14-Luc at the plasma membrane to a similar degree as the wild type Ven-Rap2A (Figure A.3). When R333 in the R1 domain of RGS14 is mutated to a leucine, which abolishes binding as demonstrated by Figure A.2, there is no colocalization at the plasma membrane and no observable overlay. Finally, constitutively inactive Ven-Rap2A S17N also shows no recruitment, and no overlay, of RGS14 at the plasma membrane (Figure A.2). These results are consistent with our binding data in live cells (Figure A.2) and with previous reports on H-Ras binding to RGS14 (293).

The RGS14:Rap2A-GTP complex is facilitated by RGS14 interaction with Gαi1-GDP

The RGS14:H-Ras-GTP complex is much weaker than the RGS14-Rap2A-GTP complex, as measured by Net BRET (compare Figure A.2 to previous reports (293)), and the RGS14:H-Ras-GTP complex is greatly facilitated by inactive Gαi1-GDP interactions with the RGS14 GPR motif (293), presumably bringing RGS14 to the cellular compartment where it can bind H-Ras-GTP (293). Thus, we wanted to determine whether Gαi1-GDP could also facilitate RGS14:Rap2A-GTP interactions. We expressed RGS14-Luc and increasing amounts of WT Ven-Rap2A in HEK293 cells with or without Gαi1 and recorded Net BRET. We found that, although Rap2A and RGS14

form a robust complex alone, the addition of Gαi1 facilitated this complex, as measured by Net BRET (Figure A.4).

Rap2A enhances H-Ras binding to RGS14

Due to the striking similarity between the H-Ras-GTP:RGS14 complex and the Rap2A-GTP:RGS14 complex, and the fact that binding of both GTPases to RGS14 is sensitive to R333L manipulation, we hypothesized that both could not bind at the same time. We thus tested this hypothesis in two ways: 1) can unlabeled H-Ras prevent Rap2A binding to RGS14; 2) can unlabeled Rap2A prevent H-Ras binding to RGS14. We first expressed RGS14-Luc and increasing Ven-Rap2A in HEK293 cells with unlabeled H-Ras G12V at a 2:1 H-Ras:Rap2A stoichiometry. To our surprise, H-Ras was completely unable to block Rap2A binding to RGS14 (Figure A.5A). We hypothesized that Rap2A may have a higher affinity for RGS14, compared to H-Ras, providing an explanation as to why H-Ras was unable to compete off Rap2A. We thus tested the converse, whether unlabeled Rap2A was able to prevent H-Ras-GTP binding to RGS14. Remarkably, we instead found that Rap2A *enhanced* the H-Ras-GTP:RGS14 complex (Figure A.5B).

Rap2A-GTP, but not Rap2A-GDP, forms a 1:1 complex with H-Ras-GTP

Based on these unexpected results, we hypothesized that perhaps either RGS14 was associating with H-Ras via a pre-formed Rap2A:H-Ras complex or that RGS14 was bringing H-Ras and Rap2A together, acting as a scaffold. There is some evidence of small G protein dimerization, although only homodimerization (486, 487). The idea that two different GTPases could interact is novel. Thus, we transfected constitutively active Luc-H-Ras G12V with constitutively active Ven-Rap2A G12V in the presence or absence of RGS14:Gαi1. We found that increasing concentrations of Rap2A-GTP formed a saturable interaction with H-Ras-GTP (Figure A.6A), suggesting that Rap2A and H-Ras for a 1:1 complex. Although we cannot conclude whether the interaction is direct, or whether it is in fact a dimer (versus trimer or multimer), the strength of the energy transfer indicates the Luc and Ven probes are in close proximity (387)and thus suggests the interaction is

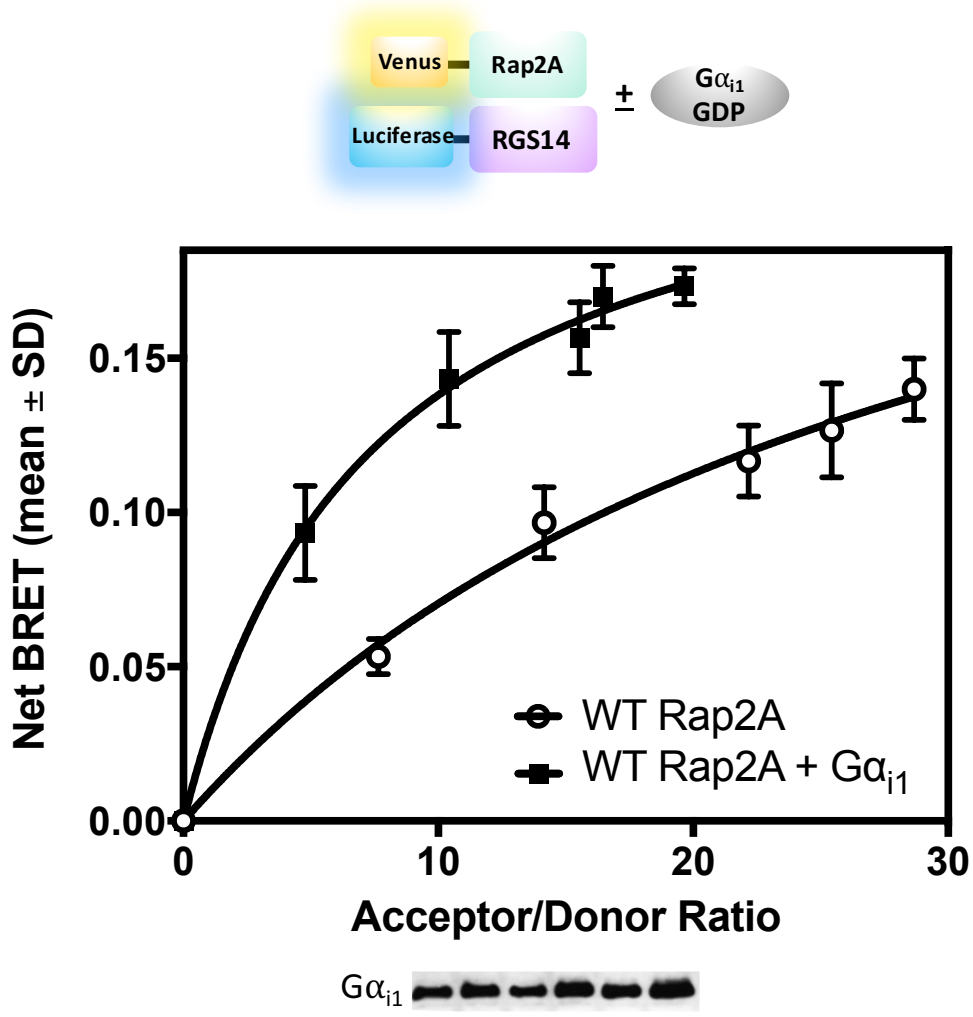

Figure A.4. Rap2A binding to RGS14 is enhanced by Gαi1-GDP.

RGS14-Luc was expressed in HEK293 cells with increasing WT Ven-Rap2A, and with or without untagged Gαi1-GDP. WT Rap2A interacted strongly with RGS14, as measured by Net BRET. Addition of untagged Gαi1-GDP greatly facilitated the interaction between WT Rap2A and RGS14, as measured by Net BRET.

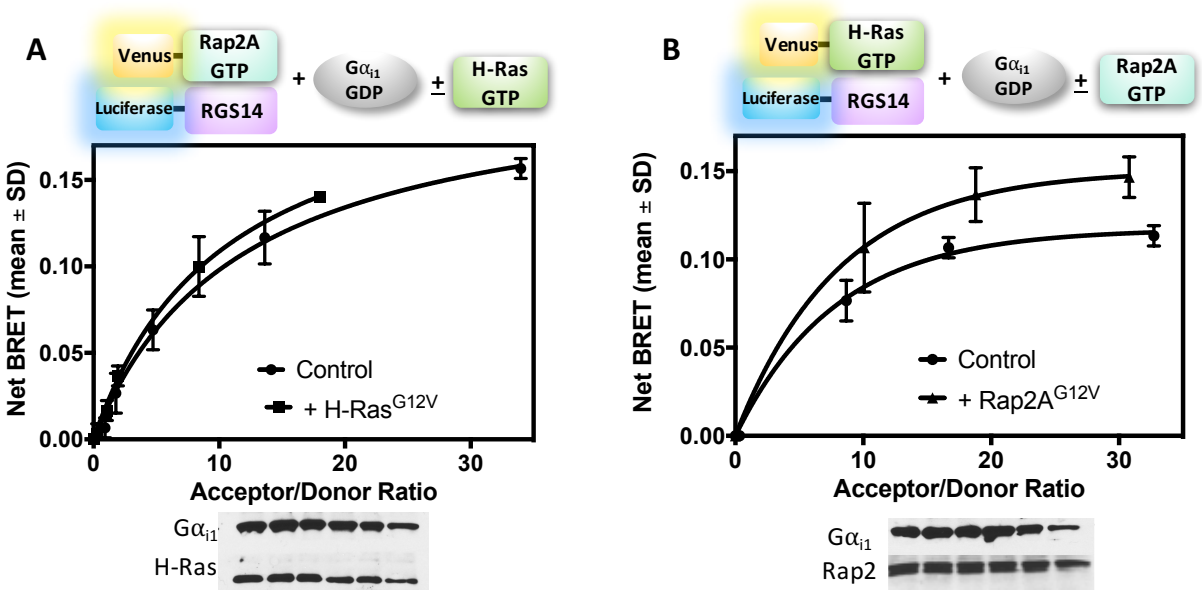

Figure A.5 Rap2A enhances H-Ras binding to RGS14, and H-Ras has no effect on Rap2A:RGS14.

A) *HEK293 cells were transfected with RGS14-Luc and increasing Ven-Rap2A G12V with Gαi1 in the presence or absence of unlabeled H-Ras G12V. Net BRET recordings were taken and Rap2A was found to interact strongly with RGS14 in the absence of H-Ras G12V. Interestingly, there was no effect by BRET of adding H-Ras G12V on Rap2A binding to RGS14.* ***B)*** *HEK293 cells were transfected with RGS14-Luc and increasing Ven-H-Ras G12V with Gαi1 in the presence or absence of Rap2A G12V. While RGS14 formed a complex with H-Ras alone, it was actually enhanced by the addition of Rap2A G12V.*

direct.

Finally, we wanted to test whether the interaction was GTP-dependent, as is the case for K-Ras dimerization (487). We transfected Luc-H-Ras G12V (constitutively active) with Ven-Rap2A G12V (constitutively active) or Ven-Rap2A S17N (constitutively inactive). We found that Rap2A S17N showed greatly reduced associated with H-Ras, indicating that the interaction is dependent on activation state.

A.4 DISCUSSION

These studies presented here advance our knowledge and understanding of the Rap2A:RGS14 complex, first described in 2000 (294). We show that the RGS14:Rap2A interaction is specific to GTP-bound Rap2A, and that Rap2A binds to R333 in the R1 domain (Figure A.2). Further, we show that Rap2A-GTP recruits RGS14 to the plasma membrane. RGS14 interaction with inactive Gαi1-GDP (at the GPR motif) enhances Rap2A interactions. Each of these results is identical to previous findings defining the RGS14:H-Ras interaction. It was thus assumed that H-Ras and Rap2A bound interchangeably at the R333 site. Remarkably, we found the opposite. While H-Ras has no effect on Rap2A binding to RGS14, Rap2A actually *enhanced* H-Ras:RGS14 association. These results were puzzling and pointed to a Rap2A:H-Ras interaction that mediated RGS14 interaction with H-Ras. Although previous results detected an RGS14:H-Ras interaction in the absence of recombinant Rap2A, most cells produce endogenous Rap2A that may mediate those interactions.

RGS14 is an important regulator of long term potentiation (LTP) and learning in the hippocampus (338), where Rap2A is expressed. Rap2A has been shown to mediate the reversal of LTP, known as depotentiation (418), and active Rap2A-GTP suppresses neurite growth (417, 482, 488) and spatial learning (416). Rap2A appears to mediate these effects by a Traf2- and Nck-interacting kinase (TNIK) and c-Jun NH2-terminal kinase (JNK) signaling cascade (418, 488, 489), which results in the removal of AMPA receptors (418). By contrast, H-Ras and its associated

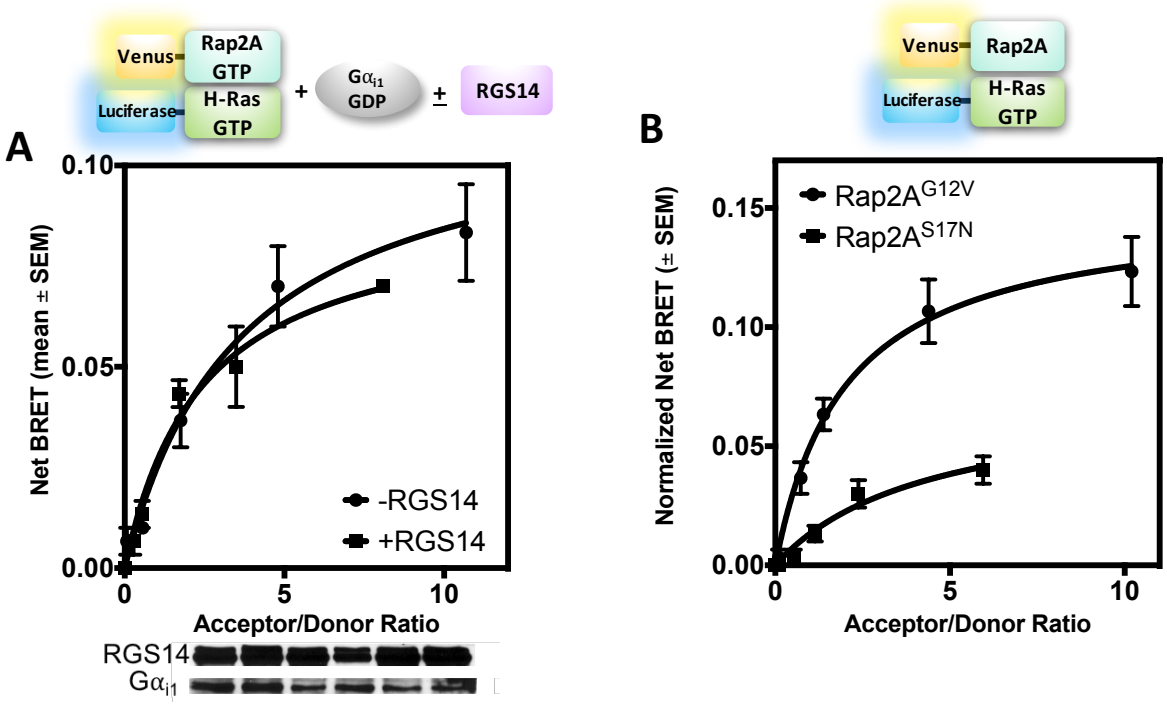

Figure A.6 Rap2A-GTP forms a complex with H-Ras-GTP.

A) *HEK293 cells were transfected with Luc-H-Ras G12V and increasing Ven-Rap2A G12V with or without RGS14 and Gαi1. Net BRET was then measured in the +RGS14 versus –RGS14 condition and no differences were found. Interestingly, a Luc-H-Ras:Ven-Rap2A complex was detected in the presence or absence of RGS14, indicating that these two small G proteins interact independent of RGS14 as a scaffold.* ***B)*** *The H-Ras:Rap2A complex is dependent on the activation state of Rap2A. HEK293 cells were transfected with Luc-H-Ras G12V and increasing Ven-Rap2A G12V or Ven-Rap2A S17N. While Rap2A G12V formed a complex with H-Ras G12V, Rap2A S17N did not. This suggests that the complex is GTP-dependent.*

MEK/ERK signaling support LTP (477). Specifically, activated H-Ras regulates trafficking of AMPA receptors to synapses (419), enhances AMPA receptor currents (420), and is crucial for learning and memory (478). Due to RGS14 inhibition of LTP, RGS14 is either enhancing Rap2A signaling, inhibiting H-Ras signaling, or both. One potential mechanism of the RGS14:Rap2A:H-Ras complex is to sequester H-Ras from its downstream effectors, in line with our previous data (292). Future studies should be done to conclude what, if any, regulatory role RGS14 has on Rap2A/JNK signaling, and furthermore whether the Rap2A:H-Ras complex regulates one or both signaling cascades. Understanding the mechanism behind these interactions will provide new clues into RGS14's interactome in the hippocampus.

REFERENCES

1. Gilman AG (1987) G proteins: transducers of receptor-generated signals. *Annu Rev Biochem* 56:615-649.
2. Hamm HE (1998) The many faces of G protein signaling. *J Biol Chem* 273(2):669-672.
3. Bourne HR, Sanders DA, & McCormick F (1990) The GTPase superfamily: a conserved switch for diverse cell functions. *Nature* 348(6297):125-132.
4. Simon MI, Strathmann MP, & Gautam N (1991) Diversity of G proteins in signal transduction. *Science* 252(5007):802-808.
5. Hepler JR & Gilman AG (1992) G proteins. *Trends Biochem Sci* 17(10):383-387.
6. Vuong TM & Chabre M (1990) Subsecond deactivation of transducin by endogenous GTP hydrolysis. *Nature* 346(6279):71-74.
7. Wagner R, Ryba N, & Uhl R (1988) Rapid transducin deactivation in intact stacks of bovine rod outer segment disks as studied by light scattering techniques. Arrestin requires additional soluble proteins for rapid quenching of rhodopsin catalytic activity. *FEBS Lett* 235(1-2):103-108.
8. Chan RK & Otte CA (1982) Isolation and genetic analysis of Saccharomyces cerevisiae mutants supersensitive to G1 arrest by a factor and alpha factor pheromones. *Mol Cell Biol* 2(1):11-20.
9. Dohlman HG, Apaniesk D, Chen Y, Song J, & Nusskern D (1995) Inhibition of G-protein signaling by dominant gain-of-function mutations in Sst2p, a pheromone desensitization factor in Saccharomyces cerevisiae. *Mol Cell Biol* 15(7):3635-3643.
10. Dohlman HG, Song J, Ma D, Courchesne WE, & Thorner J (1996) Sst2, a negative regulator of pheromone signaling in the yeast Saccharomyces cerevisiae: expression, localization, and genetic interaction and physical association with Gpa1 (the G-protein alpha subunit). *Mol Cell Biol* 16(9):5194-5209.
11. Trahey M & McCormick F (1987) A cytoplasmic protein stimulates normal N-ras p21

GTPase, but does not affect oncogenic mutants. *Science* 238(4826):542-545.

12. Koelle MR & Horvitz HR (1996) EGL-10 regulates G protein signaling in the C. elegans nervous system and shares a conserved domain with many mammalian proteins. *Cell* 84(1):115-125.

13. De Vries L, Mousli M, Wurmser A, & Farquhar MG (1995) GAIP, a protein that specifically interacts with the trimeric G protein G alpha i3, is a member of a protein family with a highly conserved core domain. *Proc Natl Acad Sci U S A* 92(25):11916-11920.

14. Druey KM, Blumer KJ, Kang VH, & Kehrl JH (1996) Inhibition of G-protein-mediated MAP kinase activation by a new mammalian gene family. *Nature* 379(6567):742-746.

15. Willars GB (2006) Mammalian RGS proteins: multifunctional regulators of cellular signalling. *Semin Cell Dev Biol* 17(3):363-376.

16. Evans PR, Dudek SM, & Hepler JR (2015) Regulator of G Protein Signaling 14: A Molecular Brake on Synaptic Plasticity Linked to Learning and Memory. *Prog Mol Biol Transl Sci* 133:169-206.

17. Ross EM & Wilkie TM (2000) GTPase-activating proteins for heterotrimeric G proteins: regulators of G protein signaling (RGS) and RGS-like proteins. *Annu Rev Biochem* 69:795-827.

18. Hollinger S & Hepler JR (2002) Cellular regulation of RGS proteins: modulators and integrators of G protein signaling. *Pharmacol Rev* 54(3):527-559.

19. Tesmer JJ, Berman DM, Gilman AG, & Sprang SR (1997) Structure of RGS4 bound to AlF4--activated G(i alpha1): stabilization of the transition state for GTP hydrolysis. *Cell* 89(2):251-261.

20. Sjogren B (2017) The evolution of regulators of G protein signalling proteins as drug targets - 20 years in the making: IUPHAR Review 21. *Br J Pharmacol* 174(6):427-437.

21. Gerber KJ, Squires KE, & Hepler JR (2016) Roles for Regulator of G Protein Signaling Proteins in Synaptic Signaling and Plasticity. *Mol Pharmacol* 89(2):273-286.

22. Fu W, *et al.* (2013) Analysis of 6,515 exomes reveals the recent origin of most human protein-coding variants. *Nature* 493(7431):216-220.

23. Lek M, *et al.* (2016) Analysis of protein-coding genetic variation in 60,706 humans. *Nature* 536(7616):285-291.

24. Yuan H, Low CM, Moody OA, Jenkins A, & Traynelis SF (2015) Ionotropic GABA and Glutamate Receptor Mutations and Human Neurologic Diseases. *Mol Pharmacol* 88(1):203-217.

25. Ogden KK, *et al.* (2017) Molecular Mechanism of Disease-Associated Mutations in the Pre-M1 Helix of NMDA Receptors and Potential Rescue Pharmacology. *PLoS Genet* 13(1):e1006536.

26. Xie Z, Chan EC, & Druey KM (2016) R4 Regulator of G Protein Signaling (RGS) Proteins in Inflammation and Immunity. *AAPS J* 18(2):294-304.

27. Bansal G, Druey KM, & Xie Z (2007) R4 RGS proteins: regulation of G-protein signaling and beyond. *Pharmacol Ther* 116(3):473-495.

28. Plummer NW, *et al.* (2012) Development of the mammalian axial skeleton requires signaling through the Galpha(i) subfamily of heterotrimeric G proteins. *Proc Natl Acad Sci U S A* 109(52):21366-21371.

29. Moon AM, *et al.* (2014) Disruption of G-protein gamma5 subtype causes embryonic lethality in mice. *PLoS One* 9(3):e90970.

30. Offermanns S, *et al.* (1998) Embryonic cardiomyocyte hypoplasia and craniofacial defects in G alpha q/G alpha 11-mutant mice. *EMBO J* 17(15):4304-4312.

31. Wettschureck N & Offermanns S (2005) Mammalian G proteins and their cell type specific functions. *Physiol Rev* 85(4):1159-1204.

32. Okae H & Iwakura Y (2010) Neural tube defects and impaired neural progenitor cell proliferation in Gbeta1-deficient mice. *Dev Dyn* 239(4):1089-1101.

33. Yu S, *et al.* (1998) Variable and tissue-specific hormone resistance in heterotrimeric Gs

protein alpha-subunit (Gsalpha) knockout mice is due to tissue-specific imprinting of the gsalpha gene. *Proc Natl Acad Sci U S A* 95(15):8715-8720.

34. Offermanns S, Mancino V, Revel JP, & Simon MI (1997) Vascular system defects and impaired cell chemokinesis as a result of Galpha13 deficiency. *Science* 275(5299):533-536.

35. Williams NM*, et al.* (2004) Support for RGS4 as a Susceptibility Gene for Schizophrenia. *BIOL PSYCHIATRY* (55):192-195.

36. Zhang P & Mende U (2014) Functional role, mechanisms of regulation, and therapeutic potential of regulator of G protein signaling 2 in the heart. *Trends Cardiovasc Med* 24(2):85-93.

37. Ganss R (2015) Keeping the Balance Right: Regulator of G Protein Signaling 5 in Vascular Physiology and Pathology. *Prog Mol Biol Transl Sci* 133:93-121.

38. Ahlers KE, Chakravarti B, & Fisher RA (2016) RGS6 as a Novel Therapeutic Target in CNS Diseases and Cancer. *AAPS J* 18(3):560-572.

39. Bomba L, Walter K, & Soranzo N (2017) The impact of rare and low-frequency genetic variants in common disease. *Genome Biol* 18(1):77.

40. Tennessen JA*, et al.* (2012) Evolution and functional impact of rare coding variation from deep sequencing of human exomes. *Science* 337(6090):64-69.

41. Nelson MR*, et al.* (2012) An abundance of rare functional variants in 202 drug target genes sequenced in 14,002 people. *Science* 337(6090):100-104.

42. Park JH*, et al.* (2011) Distribution of allele frequencies and effect sizes and their interrelationships for common genetic susceptibility variants. *Proc Natl Acad Sci U S A* 108(44):18026-18031.

43. Kenakin T & Miller LJ (2010) Seven transmembrane receptors as shapeshifting proteins: the impact of allosteric modulation and functional selectivity on new drug discovery. *Pharmacol Rev* 62(2):265-304.

44. Okamoto N*, et al.* (2017) Novel CLCN7 compound heterozygous mutations in intermediate autosomal recessive osteopetrosis. *Hum Genome Var* 4:17036.

45. Lo Bello M*, et al.* (2017) ALS-Related Mutant FUS Protein Is Mislocalized to Cytoplasm and Is Recruited into Stress Granules of Fibroblasts from Asymptomatic FUS P525L Mutation Carriers. *Neurodegener Dis* 17(6):292-303.

46. Kircher M*, et al.* (2014) A general framework for estimating the relative pathogenicity of human genetic variants. *Nat Genet* 46(3):310-315.

47. Traynelis J*, et al.* (2017) Optimizing genomic medicine in epilepsy through a gene-customized approach to missense variant interpretation. *Genome Res* 27(10):1715-1729.

48. Dewhurst HM, Choudhury S, & Torres MP (2015) Structural Analysis of PTM Hotspots (SAPH-ire)--A Quantitative Informatics Method Enabling the Discovery of Novel Regulatory Elements in Protein Families. *Mol Cell Proteomics* 14(8):2285-2297.

49. Torres MP, Dewhurst H, & Sundararaman N (2016) Proteome-wide Structural Analysis of PTM Hotspots Reveals Regulatory Elements Predicted to Impact Biological Function and Disease. *Mol Cell Proteomics* 15(11):3513-3528.

50. Kimura M (1977) Preponderance of synonymous changes as evidence for the neutral theory of molecular evolution. *Nature* 267(5608):275-276.

51. Hornbeck PV*, et al.* (2012) PhosphoSitePlus: a comprehensive resource for investigating the structure and function of experimentally determined post-translational modifications in man and mouse. *Nucleic Acids Res* 40(Database issue):D261-270.

52. Jensen LJ*, et al.* (2002) Prediction of human protein function from post-translational modifications and localization features. *J Mol Biol* 319(5):1257-1265.

53. Lothrop AP, Torres MP, & Fuchs SM (2013) Deciphering post-translational modification codes. *FEBS Lett* 587(8):1247-1257.

54. Walsh CT, Garneau-Tsodikova S, & Gatto GJ, Jr. (2005) Protein posttranslational modifications: the chemistry of proteome diversifications. *Angew Chem Int Ed Engl*

44(45):7342-7372.

55. Huang KY*, et al.* (2016) dbPTM 2016: 10-year anniversary of a resource for post-translational modification of proteins. *Nucleic Acids Res* 44(D1):D435-446.

56. Li J*, et al.* (2014) SysPTM 2.0: an updated systematic resource for post-translational modification. *Database (Oxford)* 2014:bau025.

57. Prabakaran S, Lippens G, Steen H, & Gunawardena J (2012) Post-translational modification: nature's escape from genetic imprisonment and the basis for dynamic information encoding. *Wiley Interdiscip Rev Syst Biol Med* 4(6):565-583.

58. Alqinyah M & Hooks SB (2017) Regulating the regulators: Epigenetic, transcriptional, and post-translational regulation of RGS proteins. *Cell Signal* 42:77-87.

59. Johnson LN (1992) Glycogen phosphorylase: control by phosphorylation and allosteric effectors. *FASEB J* 6(6):2274-2282.

60. Pearson G*, et al.* (2001) Mitogen-activated protein (MAP) kinase pathways: regulation and physiological functions. *Endocr Rev* 22(2):153-183.

61. Hunter T (2007) The age of crosstalk: phosphorylation, ubiquitination, and beyond. *Mol Cell* 28(5):730-738.

62. Burgon PG, Lee WL, Nixon AB, Peralta EG, & Casey PJ (2001) Phosphorylation and nuclear translocation of a regulator of G protein signaling (RGS10). *J Biol Chem* 276(35):32828-32834.

63. Jenkins MA & Traynelis SF (2012) PKC phosphorylates GluA1-Ser831 to enhance AMPA receptor conductance. *Channels (Austin)* 6(1):60-64.

64. Pickart CM (2001) Mechanisms underlying ubiquitination. *Annu Rev Biochem* 70:503-533.

65. Glickman MH & Ciechanover A (2002) The ubiquitin-proteasome proteolytic pathway: destruction for the sake of construction. *Physiol Rev* 82(2):373-428.

66. Mukhopadhyay D & Riezman H (2007) Proteasome-independent functions of ubiquitin in endocytosis and signaling. *Science* 315(5809):201-205.

67. Schnell JD & Hicke L (2003) Non-traditional functions of ubiquitin and ubiquitin-binding proteins. *J Biol Chem* 278(38):35857-35860.

68. Aka JA, Kim GW, & Yang XJ (2011) K-acetylation and its enzymes: overview and new developments. *Handb Exp Pharmacol* 206:1-12.

69. Arnesen T (2011) Towards a functional understanding of protein N-terminal acetylation. *PLoS Biol* 9(5):e1001074.

70. Yang XJ & Seto E (2008) Lysine acetylation: codified crosstalk with other posttranslational modifications. *Mol Cell* 31(4):449-461.

71. Yuan ZL, Guan YJ, Chatterjee D, & Chin YE (2005) Stat3 dimerization regulated by reversible acetylation of a single lysine residue. *Science* 307(5707):269-273.

72. Hwang CS, Shemorry A, & Varshavsky A (2010) N-terminal acetylation of cellular proteins creates specific degradation signals. *Science* 327(5968):973-977.

73. Tasaki T, Sriram SM, Park KS, & Kwon YT (2012) The N-end rule pathway. *Annu Rev Biochem* 81:261-289.

74. Park SE*, et al.* (2015) Control of mammalian G protein signaling by N-terminal acetylation and the N-end rule pathway. *Science* 347(6227):1249-1252.

75. Linder ME & Deschenes RJ (2007) Palmitoylation: policing protein stability and traffic. *Nat Rev Mol Cell Biol* 8(1):74-84.

76. Wedegaertner PB, Chu DH, Wilson PT, Levis MJ, & Bourne HR (1993) Palmitoylation is required for signaling functions and membrane attachment of Gq alpha and Gs alpha. *J Biol Chem* 268(33):25001-25008.

77. Linder ME*, et al.* (1993) Lipid modifications of G proteins: alpha subunits are palmitoylated. *Proc Natl Acad Sci U S A* 90(8):3675-3679.

78. Seno K & Hayashi F (2017) Palmitoylation is a prerequisite for dimerization-dependent raftophilicity of rhodopsin. *J Biol Chem* 292(37):15321-15328.

79. Tu Y, Popov S, Slaughter C, & Ross EM (1999) Palmitoylation of a conserved cysteine in

the regulator of G protein signaling (RGS) domain modulates the GTPase-activating activity of RGS4 and RGS10. *J Biol Chem* 274(53):38260-38267.

80. Bedford MT & Clarke SG (2009) Protein arginine methylation in mammals: who, what, and why. *Mol Cell* 33(1):1-13.

81. McBride AE & Silver PA (2001) State of the arg: protein methylation at arginine comes of age. *Cell* 106(1):5-8.

82. Hamamoto R, Saloura V, & Nakamura Y (2015) Critical roles of non-histone protein lysine methylation in human tumorigenesis. *Nat Rev Cancer* 15(2):110-124.

83. Heximer SP, Watson N, Linder ME, Blumer KJ, & Hepler JR (1997) RGS2/G0S8 is a selective inhibitor of Gqalpha function. *Proc Natl Acad Sci U S A* 94(26):14389-14393.

84. Heximer SP*, et al.* (1999) G protein selectivity is a determinant of RGS2 function. *J Biol Chem* 274(48):34253-34259.

85. Heximer SP (2004) RGS2-mediated regulation of Gqalpha. *Methods Enzymol* 390:65-82.

86. Huang C, Hepler JR, Gilman AG, & Mumby SM (1997) Attenuation of Gi- and Gq-mediated signaling by expression of RGS4 or GAIP in mammalian cells. *Proc Natl Acad Sci U S A* 94(12):6159-6163.

87. Nance MR*, et al.* (2013) Structural and functional analysis of the regulator of G protein signaling 2-galphaq complex. *Structure* 21(3):438-448.

88. Hepler JR, Berman DM, Gilman AG, & Kozasa T (1997) RGS4 and GAIP are GTPase-activating proteins for Gq alpha and block activation of phospholipase C beta by gamma-thio-GTP-Gq alpha. *Proc Natl Acad Sci U S A* 94(2):428-432.

89. Tu Y, Woodson J, & Ross EM (2001) Binding of regulator of G protein signaling (RGS) proteins to phospholipid bilayers. Contribution of location and/or orientation to Gtpase-activating protein activity. *J Biol Chem* 276(23):20160-20166.

90. Bernstein LS, Grillo AA, Loranger SS, & Linder ME (2000) RGS4 binds to membranes through an amphipathic alpha -helix. *J Biol Chem* 275(24):18520-18526.

91. Heximer SP, Lim H, Bernard JL, & Blumer KJ (2001) Mechanisms governing subcellular localization and function of human RGS2. *J Biol Chem* 276(17):14195-14203.

92. Gu S*, et al.* (2007) Unique hydrophobic extension of the RGS2 amphipathic helix domain imparts increased plasma membrane binding and function relative to other RGS R4/B subfamily members. *J Biol Chem* 282(45):33064-33075.

93. Bernstein LS*, et al.* (2004) RGS2 binds directly and selectively to the M1 muscarinic acetylcholine receptor third intracellular loop to modulate Gq/11alpha signaling. *J Biol Chem* 279(20):21248-21256.

94. Neitzel KL & Hepler JR (2006) Cellular mechanisms that determine selective RGS protein regulation of G protein-coupled receptor signaling. *Semin Cell Dev Biol* 17(3):383-389.

95. Davydov IV & Varshavsky A (2000) RGS4 is arginylated and degraded by the N-end rule pathway in vitro. *J Biol Chem* 275(30):22931-22941.

96. Bodenstein J, Sunahara RK, & Neubig RR (2007) N-terminal residues control proteasomal degradation of RGS2, RGS4, and RGS5 in human embryonic kidney 293 cells. *Mol Pharmacol* 71(4):1040-1050.

97. Hong JX, Wilson GL, Fox CH, & Kehrl JH (1993) Isolation and characterization of a novel B cell activation gene. *J Immunol* 150(9):3895-3904.

98. Hwang IY, Park C, Harrision KA, Huang NN, & Kehrl JH (2010) Variations in Gnai2 and Rgs1 expression affect chemokine receptor signaling and the organization of secondary lymphoid organs. *Genes Immun* 11(5):384-396.

99. Gibbons DL*, et al.* (2011) Cutting Edge: Regulator of G protein signaling-1 selectively regulates gut T cell trafficking and colitic potential. *J Immunol* 187(5):2067-2071.

100. Moratz C, Hayman JR, Gu H, & Kehrl JH (2004) Abnormal B-cell responses to chemokines, disturbed plasma cell localization, and distorted immune tissue architecture in Rgs1-/- mice. *Mol Cell Biol* 24(13):5767-5775.

101. Johnson BA*, et al.* (2010) Multiple sclerosis susceptibility alleles in African Americans.

Genes Immun 11(4):343-350.

102. Smyth DJ*, et al.* (2008) Shared and distinct genetic variants in type 1 diabetes and celiac disease. *N Engl J Med* 359(26):2767-2777.

103. Hunt KA*, et al.* (2008) Newly identified genetic risk variants for celiac disease related to the immune response. *Nat Genet* 40(4):395-402.

104. Patel J*, et al.* (2015) RGS1 regulates myeloid cell accumulation in atherosclerosis and aortic aneurysm rupture through altered chemokine signalling. *Nat Commun* 6:6614.

105. Carreras J*, et al.* (2017) Clinicopathological characteristics and genomic profile of primary sinonasal tract diffuse large B cell lymphoma (DLBCL) reveals gain at 1q31 and RGS1 encoding protein; high RGS1 immunohistochemical expression associates with poor overall survival in DLBCL not otherwise specified (NOS). *Histopathology* 70(4):595-621.

106. Kehrl JH & Sinnarajah S (2002) RGS2: a multifunctional regulator of G-protein signaling. *Int J Biochem Cell Biol* 34(5):432-438.

107. Song L, Zmijewski JW, & Jope RS (2001) RGS2: regulation of expression and nuclear localization. *Biochem Biophys Res Commun* 283(1):102-106.

108. Ingi T*, et al.* (1998) Dynamic regulation of RGS2 suggests a novel mechanism in G-protein signaling and neuronal plasticity. *J Neurosci* 18(18):7178-7188.

109. Oliveira-Dos-Santos AJ*, et al.* (2000) Regulation of T cell activation, anxiety, and male aggression by RGS2. *Proc Natl Acad Sci U S A* 97(22):12272-12277.

110. Hohoff C*, et al.* (2015) RGS2 ggenetic variation: association analysis with panic disorder and dimensional as well as intermediate phenotypes of anxiety. *Am J Med Genet B Neuropsychiatr Genet* 168B(3):211-222.

111. Okimoto N*, et al.* (2012) RGS2 mediates the anxiolytic effect of oxytocin. *Brain Res* 1453:26-33.

112. Lifschytz T*, et al.* (2012) Relationship between Rgs2 gene expression level and anxiety and depression-like behaviour in a mutant mouse model: serotonergic involvement. *Int J*

Neuropsychopharmacol 15(9):1307-1318.

113. Koenen KC, *et al.* (2009) RGS2 and generalized anxiety disorder in an epidemiologic sample of hurricane-exposed adults. *Depress Anxiety* 26(4):309-315.

114. Amstadter AB, *et al.* (2009) Variation in RGS2 is associated with suicidal ideation in an epidemiological study of adults exposed to the 2004 Florida hurricanes. *Arch Suicide Res* 13(4):349-357.

115. Amstadter AB, *et al.* (2009) Variant in RGS2 moderates posttraumatic stress symptoms following potentially traumatic event exposure. *J Anxiety Disord* 23(3):369-373.

116. Semplicini A, *et al.* (2006) Reduced expression of regulator of G-protein signaling 2 (RGS2) in hypertensive patients increases calcium mobilization and ERK1/2 phosphorylation induced by angiotensin II. *J Hypertens* 24(6):1115-1124.

117. Leygraf A, *et al.* (2006) Rgs 2 gene polymorphisms as modulators of anxiety in humans? *J Neural Transm (Vienna)* 113(12):1921-1925.

118. Cui H, *et al.* (2008) Association of RGS2 gene polymorphisms with suicide and increased RGS2 immunoreactivity in the postmortem brain of suicide victims. *Neuropsychopharmacology* 33(7):1537-1544.

119. Sun X, Kaltenbronn KM, Steinberg TH, & Blumer KJ (2005) RGS2 is a mediator of nitric oxide action on blood pressure and vasoconstrictor signaling. *Mol Pharmacol* 67(3):631-639.

120. Tang KM, *et al.* (2003) Regulator of G-protein signaling-2 mediates vascular smooth muscle relaxation and blood pressure. *Nat Med* 9(12):1506-1512.

121. Heximer SP, *et al.* (2003) Hypertension and prolonged vasoconstrictor signaling in RGS2-deficient mice. *J Clin Invest* 111(4):445-452.

122. Yang J, *et al.* (2005) Genetic variations of regulator of G-protein signaling 2 in hypertensive patients and in the general population. *J Hypertens* 23(8):1497-1505.

123. Phan HTN, Sjogren B, & Neubig RR (2017) Human Missense Mutations in Regulator of

G Protein Signaling 2 Affect the Protein Function Through Multiple Mechanisms. *Mol Pharmacol* 92(4):451-458.

124. Nguyen CH*, et al.* (2009) Translational control by RGS2. *J Cell Biol* 186(5):755-765.

125. Zhang S*, et al.* (1998) RGS3 and RGS4 are GTPase activating proteins in the heart. *J Mol Cell Cardiol* 30(2):269-276.

126. Liu Y*, et al.* (2014) Regulator of G protein signaling 3 protects against cardiac hypertrophy in mice. *J Cell Biochem* 115(5):977-986.

127. Qiu R, Wang J, Tsark W, & Lu Q (2010) Essential role of PDZ-RGS3 in the maintenance of neural progenitor cells. *Stem Cells* 28(9):1602-1610.

128. Nishiura H*, et al.* (2009) Pro- and anti-apoptotic dual functions of the C5a receptor: involvement of regulator of G protein signaling 3 and extracellular signal-regulated kinase. *Lab Invest* 89(6):676-694.

129. Shi CS, Huang NN, & Kehrl JH (2012) Regulator of G-protein signaling 3 isoform 1 (PDZ-RGS3) enhances canonical Wnt signaling and promotes epithelial mesenchymal transition. *J Biol Chem* 287(40):33480-33487.

130. Ooe A, Kato K, & Noguchi S (2007) Possible involvement of CCT5, RGS3, and YKT6 genes up-regulated in p53-mutated tumors in resistance to docetaxel in human breast cancers. *Breast Cancer Res Treat* 101(3):305-315.

131. Wang J, Zhou Y, Fei X, Chen X, & Zhu Z (2017) Regulator of G-protein signaling 3 targeted by miR-126 correlates with poor prognosis in gastric cancer patients. *Anticancer Drugs* 28(2):161-169.

132. Chen Z, Wu Y, Meng Q, & Xia Z (2016) Elevated microRNA-25 inhibits cell apoptosis in lung cancer by targeting RGS3. *In Vitro Cell Dev Biol Anim* 52(1):62-67.

133. Ingi T & Aoki Y (2002) Expression of RGS2, RGS4 and RGS7 in the developing postnatal brain. *Eur J Neurosci* 15(5):929-936.

134. Bastin G*, et al.* (2012) Amino-terminal cysteine residues differentially influence RGS4

protein plasma membrane targeting, intracellular trafficking, and function. *J Biol Chem* 287(34):28966-28974.

135. Stewart A, Huang J, & Fisher RA (2012) RGS Proteins in Heart: Brakes on the Vagus. *Front Physiol* 3:95.

136. Jaba IM*, et al.* (2013) NO triggers RGS4 degradation to coordinate angiogenesis and cardiomyocyte growth. *J Clin Invest* 123(4):1718-1731.

137. Lee MJ*, et al.* (2012) Characterization of arginylation branch of N-end rule pathway in G-protein-mediated proliferation and signaling of cardiomyocytes. *J Biol Chem* 287(28):24043-24052.

138. Felkin LE, Lara-Pezzi EA, Hall JL, Birks EJ, & Barton PJ (2011) Reverse remodelling and recovery from heart failure are associated with complex patterns of gene expression. *J Cardiovasc Transl Res* 4(3):321-331.

139. Mittmann C*, et al.* (2002) Expression of ten RGS proteins in human myocardium: functional characterization of an upregulation of RGS4 in heart failure. *Cardiovasc Res* 55(4):778-786.

140. Owen VJ*, et al.* (2001) Expression of RGS3, RGS4 and Gi alpha 2 in acutely failing donor hearts and end-stage heart failure. *Eur Heart J* 22(12):1015-1020.

141. Opel A*, et al.* (2015) Absence of the Regulator of G-protein Signaling, RGS4, Predisposes to Atrial Fibrillation and Is Associated with Abnormal Calcium Handling. *J Biol Chem* 290(31):19233-19244.

142. Mirnics K, Middleton FA, Stanwood GD, Lewis DA, & Levitt P (2001) Disease-specific changes in regulator of G-protein signaling 4 (RGS4) expression in schizophrenia. *Mol Psychiatry* 6(3):293-301.

143. Chen X*, et al.* (2004) Regulator of G-protein signaling 4 (RGS4) gene is associated with schizophrenia in Irish high density families. *Am J Med Genet B Neuropsychiatr Genet* 129B(1):23-26.

144. Prasad KM*, et al.* (2005) Genetic polymorphisms of the RGS4 and dorsolateral prefrontal cortex morphometry among first episode schizophrenia patients. *Mol Psychiatry* 10(2):213-219.

145. Guo S*, et al.* (2006) RGS4 polymorphisms and risk of schizophrenia: an association study in Han Chinese plus meta-analysis. *Neurosci Lett* 406(1-2):122-127.

146. Chowdari KV*, et al.* (2002) Association and linkage analyses of RGS4 polymorphisms in schizophrenia. *Hum Mol Genet* 11(12):1373-1380.

147. Chowdari KV*, et al.* (2008) Linkage disequilibrium patterns and functional analysis of RGS4 polymorphisms in relation to schizophrenia. *Schizophr Bull* 34(1):118-126.

148. Campbell DB*, et al.* (2008) Ethnic stratification of the association of RGS4 variants with antipsychotic treatment response in schizophrenia. *Biol Psychiatry* 63(1):32-41.

149. So HC*, et al.* (2008) An association study of RGS4 polymorphisms with clinical phenotypes of schizophrenia in a Chinese population. *Am J Med Genet B Neuropsychiatr Genet* 147B(1):77-85.

150. Emilsson L, Saetre P, & Jazin E (2006) Low mRNA levels of RGS4 splice variants in Alzheimer's disease: association between a rare haplotype and decreased mRNA expression. *Synapse* 59(3):173-176.

151. Ho AM, MacKay RK, Dodd PR, & Lewohl JM (2010) Association of polymorphisms in RGS4 and expression of RGS transcripts in the brains of human alcoholics. *Brain Res* 1340:1-9.

152. Min C*, et al.* (2012) RGS4 exerts inhibitory activities on the signaling of dopamine D2 receptor and D3 receptor through the N-terminal region. *Pharmacol Res* 65(2):213-220.

153. Lerner TN & Kreitzer AC (2012) RGS4 is required for dopaminergic control of striatal LTD and susceptibility to parkinsonian motor deficits. *Neuron* 73(2):347-359.

154. Ding J*, et al.* (2006) RGS4-dependent attenuation of M4 autoreceptor function in striatal cholinergic interneurons following dopamine depletion. *Nat Neurosci* 9(6):832-842.

155. Ashrafi A*, et al.* (2017) Absence of regulator of G-protein signaling 4 does not protect against dopamine neuron dysfunction and injury in the mouse 6-hydroxydopamine lesion model of Parkinson's disease. *Neurobiol Aging* 58:30-33.

156. Seki N*, et al.* (1998) Isolation, tissue expression, and chromosomal assignment of human RGS5, a novel G-protein signaling regulator gene. *J Hum Genet* 43(3):202-205.

157. Smith EN*, et al.* (2009) Genome-wide association study of bipolar disorder in European American and African American individuals. *Mol Psychiatry* 14(8):755-763.

158. Campbell DB*, et al.* (2008) Association of RGS2 and RGS5 variants with schizophrenia symptom severity. *Schizophr Res* 101(1-3):67-75.

159. Daniel JM*, et al.* (2016) Regulator of G-Protein Signaling 5 Prevents Smooth Muscle Cell Proliferation and Attenuates Neointima Formation. *Arterioscler Thromb Vasc Biol* 36(2):317-327.

160. Holobotovskyy V*, et al.* (2013) Regulator of G-protein signaling 5 controls blood pressure homeostasis and vessel wall remodeling. *Circ Res* 112(5):781-791.

161. Cheng WL*, et al.* (2015) Regulator of G-protein signalling 5 protects against atherosclerosis in apolipoprotein E-deficient mice. *Br J Pharmacol* 172(23):5676-5689.

162. Kirsch T, Wellner M, Luft FC, Haller H, & Lippoldt A (2001) Altered gene expression in cerebral capillaries of stroke-prone spontaneously hypertensive rats. *Brain Res* 910(1-2):106-115.

163. Grayson TH*, et al.* (2007) Vascular microarray profiling in two models of hypertension identifies caveolin-1, Rgs2 and Rgs5 as antihypertensive targets. *BMC Genomics* 8:404.

164. Li J*, et al.* (2004) Regulator of G protein signaling 5 marks peripheral arterial smooth muscle cells and is downregulated in atherosclerotic plaque. *J Vasc Surg* 40(3):519-528.

165. Adams LD, Geary RL, Li J, Rossini A, & Schwartz SM (2006) Expression profiling identifies smooth muscle cell diversity within human intima and plaque fibrous cap: loss of RGS5 distinguishes the cap. *Arterioscler Thromb Vasc Biol* 26(2):319-325.

166. Berger M, Bergers G, Arnold B, Hammerling GJ, & Ganss R (2005) Regulator of G-protein signaling-5 induction in pericytes coincides with active vessel remodeling during neovascularization. *Blood* 105(3):1094-1101.

167. Armulik A, Abramsson A, & Betsholtz C (2005) Endothelial/pericyte interactions. *Circ Res* 97(6):512-523.

168. Wang Z*, et al.* (2016) Regulator of G-protein signaling 5 protects cardiomyocytes against apoptosis during in vitro cardiac ischemia-reperfusion in mice by inhibiting both JNK1/2 and P38 signaling pathways. *Biochem Biophys Res Commun* 473(2):551-557.

169. Hamzah J*, et al.* (2008) Vascular normalization in Rgs5-deficient tumours promotes immune destruction. *Nature* 453(7193):410-414.

170. Nisancioglu MH*, et al.* (2008) Generation and characterization of rgs5 mutant mice. *Mol Cell Biol* 28(7):2324-2331.

171. Cho H*, et al.* (2008) Rgs5 targeting leads to chronic low blood pressure and a lean body habitus. *Mol Cell Biol* 28(8):2590-2597.

172. Chang YP*, et al.* (2007) Multiple genes for essential-hypertension susceptibility on chromosome 1q. *Am J Hum Genet* 80(2):253-264.

173. Larminie C*, et al.* (2004) Selective expression of regulators of G-protein signaling (RGS) in the human central nervous system. *Brain Res Mol Brain Res* 122(1):24-34.

174. Saitoh O & Odagiri M (2003) RGS8 expression in developing cerebellar Purkinje cells. *Biochem Biophys Res Commun* 309(4):836-842.

175. Saitoh O*, et al.* (2003) Distribution of regulator of G protein signaling 8 (RGS8) protein in the cerebellum. *Cerebellum* 2(2):154-160.

176. Gold SJ, Ni YG, Dohlman HG, & Nestler EJ (1997) Regulators of G-protein signaling (RGS) proteins: region-specific expression of nine subtypes in rat brain. *J Neurosci* 17(20):8024-8037.

177. Itoh M, Odagiri M, Abe H, & Saitoh O (2001) RGS8 protein is distributed in dendrites and

cell body of cerebellar Purkinje cell. *Biochem Biophys Res Commun* 287(1):223-228.

178. Saitoh O*, et al.* (2001) Regulator of G protein signaling 8 (RGS8) requires its NH2 terminus for subcellular localization and acute desensitization of G protein-gated K+ channels. *J Biol Chem* 276(7):5052-5058.

179. Ostrovskaya O*, et al.* (2014) RGS7/Gbeta5/R7BP complex regulates synaptic plasticity and memory by modulating hippocampal GABABR-GIRK signaling. *Elife* 3:e02053.

180. Chen IS, Furutani K, Inanobe A, & Kurachi Y (2014) RGS4 regulates partial agonism of the M2 muscarinic receptor-activated K+ currents. *J Physiol* 592(6):1237-1248.

181. Wydeven N, Posokhova E, Xia Z, Martemyanov KA, & Wickman K (2014) RGS6, but not RGS4, is the dominant regulator of G protein signaling (RGS) modulator of the parasympathetic regulation of mouse heart rate. *J Biol Chem* 289(4):2440-2449.

182. Saitoh O, Kubo Y, Miyatani Y, Asano T, & Nakata H (1997) RGS8 accelerates G-protein-mediated modulation of K+ currents. *Nature* 390(6659):525-529.

183. Kuwata H, Nakao K, Harada T, Matsuda I, & Aiba A (2008) Generation of RGS8 null mutant mice by Cre/loxP system. *Kobe J Med Sci* 53(6):275-281.

184. Gold SJ, Heifets BD, Pudiak CM, Potts BW, & Nestler EJ (2002) Regulation of regulators of G protein signaling mRNA expression in rat brain by acute and chronic electroconvulsive seizures. *J Neurochem* 82(4):828-838.

185. Estes JD*, et al.* (2004) Follicular dendritic cell regulation of CXCR4-mediated germinal center CD4 T cell migration. *J Immunol* 173(10):6169-6178.

186. Shi GX, Harrison K, Wilson GL, Moratz C, & Kehrl JH (2002) RGS13 regulates germinal center B lymphocytes responsiveness to CXC chemokine ligand (CXCL)12 and CXCL13. *J Immunol* 169(5):2507-2515.

187. Bansal G, Xie Z, Rao S, Nocka KH, & Druey KM (2008) Suppression of immunoglobulin E-mediated allergic responses by regulator of G protein signaling 13. *Nat Immunol* 9(1):73-80.

188. Bansal G*, et al.* (2008) RGS13 controls g protein-coupled receptor-evoked responses of human mast cells. *J Immunol* 181(11):7882-7890.

189. Han JI, Huang NN, Kim DU, & Kehrl JH (2006) RGS1 and RGS13 mRNA silencing in a human B lymphoma line enhances responsiveness to chemoattractants and impairs desensitization. *J Leukoc Biol* 79(6):1357-1368.

190. Hwang IY, Hwang KS, Park C, Harrison KA, & Kehrl JH (2013) Rgs13 constrains early B cell responses and limits germinal center sizes. *PLoS One* 8(3):e60139.

191. Pise-Masison CA*, et al.* (2009) Gene expression profiling of ATL patients: compilation of disease-related genes and evidence for TCF4 involvement in BIRC5 gene expression and cell viability. *Blood* 113(17):4016-4026.

192. Sethakorn N & Dulin NO (2013) RGS expression in cancer: oncomining the cancer microarray data. *J Recept Signal Transduct Res* 33(3):166-171.

193. Raedler D*, et al.* (2015) Identification of novel immune phenotypes for allergic and nonallergic childhood asthma. *J Allergy Clin Immunol* 135(1):81-91.

194. Natochin M, Granovsky AE, & Artemyev NO (1997) Regulation of transducin GTPase activity by human retinal RGS. *J Biol Chem* 272(28):17444-17449.

195. Chen CK, Wieland T, & Simon MI (1996) RGS-r, a retinal specific RGS protein, binds an intermediate conformation of transducin and enhances recycling. *Proc Natl Acad Sci U S A* 93(23):12885-12889.

196. Patten M*, et al.* (2002) Endotoxin induces desensitization of cardiac endothelin-1 receptor signaling by increased expression of RGS4 and RGS16. *Cardiovasc Res* 53(1):156-164.

197. Grafstein-Dunn E, Young KH, Cockett MI, & Khawaja XZ (2001) Regional distribution of regulators of G-protein signaling (RGS) 1, 2, 13, 14, 16, and GAIP messenger ribonucleic acids by in situ hybridization in rat brain. *Brain Res Mol Brain Res* 88(1-2):113-123.

198. Kurrasch DM, Huang J, Wilkie TM, & Repa JJ (2004) Quantitative real-time polymerase

chain reaction measurement of regulators of G-protein signaling mRNA levels in mouse tissues. *Methods Enzymol* 389:3-15.

199. Kim SD*, et al.* (2006) The expression patterns of RGS transcripts in platelets. *Platelets* 17(7):493-497.

200. Kveberg L, Ryan JC, Rolstad B, & Inngjerdingen M (2005) Expression of regulator of G protein signalling proteins in natural killer cells, and their modulation by Ly49A and Ly49D. *Immunology* 115(3):358-365.

201. Shi GX, Harrison K, Han SB, Moratz C, & Kehrl JH (2004) Toll-like receptor signaling alters the expression of regulator of G protein signaling proteins in dendritic cells: implications for G protein-coupled receptor signaling. *J Immunol* 172(9):5175-5184.

202. Beadling C, Druey KM, Richter G, Kehrl JH, & Smith KA (1999) Regulators of G protein signaling exhibit distinct patterns of gene expression and target G protein specificity in human lymphocytes. *J Immunol* 162(5):2677-2682.

203. Osterhout JL*, et al.* (2003) Palmitoylation regulates regulator of G-protein signaling (RGS) 16 function. II. Palmitoylation of a cysteine residue in the RGS box is critical for RGS16 GTPase accelerating activity and regulation of Gi-coupled signalling. *J Biol Chem* 278(21):19309-19316.

204. Hiol A*, et al.* (2003) Palmitoylation regulates regulators of G-protein signaling (RGS) 16 function. I. Mutation of amino-terminal cysteine residues on RGS16 prevents its targeting to lipid rafts and palmitoylation of an internal cysteine residue. *J Biol Chem* 278(21):19301-19308.

205. Lippert E*, et al.* (2003) Role of regulator of G protein signaling 16 in inflammation-induced T lymphocyte migration and activation. *J Immunol* 171(3):1542-1555.

206. Shankar SP*, et al.* (2012) RGS16 attenuates pulmonary Th2/Th17 inflammatory responses. *J Immunol* 188(12):6347-6356.

207. Goto K*, et al.* (2017) G-protein-coupled receptor signaling through Gpr176, Gz, and

RGS16 tunes time in the center of the circadian clock [Review]. *Endocr J* 64(6):571-579.

208. Ueda HR*, et al.* (2002) A transcription factor response element for gene expression during circadian night. *Nature* 418(6897):534-539.

209. Hayasaka N*, et al.* (2011) Attenuated food anticipatory activity and abnormal circadian locomotor rhythms in Rgs16 knockdown mice. *PLoS One* 6(3):e17655.

210. Doi M*, et al.* (2011) Circadian regulation of intracellular G-protein signalling mediates intercellular synchrony and rhythmicity in the suprachiasmatic nucleus. *Nat Commun* 2:327.

211. Pashkov V*, et al.* (2011) Regulator of G protein signaling (RGS16) inhibits hepatic fatty acid oxidation in a carbohydrate response element-binding protein (ChREBP)-dependent manner. *J Biol Chem* 286(17):15116-15125.

212. Jones SE*, et al.* (2016) Genome-Wide Association Analyses in 128,266 Individuals Identifies New Morningness and Sleep Duration Loci. *PLoS Genet* 12(8):e1006125.

213. Hu Y*, et al.* (2016) GWAS of 89,283 individuals identifies genetic variants associated with self-reporting of being a morning person. *Nat Commun* 7:10448.

214. Carper MB, Denvir J, Boskovic G, Primerano DA, & Claudio PP (2014) RGS16, a novel p53 and pRb cross-talk candidate inhibits migration and invasion of pancreatic cancer cells. *Genes Cancer* 5(11-12):420-435.

215. Miyoshi N, Ishii H, Sekimoto M, Doki Y, & Mori M (2009) RGS16 is a marker for prognosis in colorectal cancer. *Ann Surg Oncol* 16(12):3507-3514.

216. Liang G, Bansal G, Xie Z, & Druey KM (2009) RGS16 inhibits breast cancer cell growth by mitigating phosphatidylinositol 3-kinase signaling. *J Biol Chem* 284(32):21719-21727.

217. Nagata Y*, et al.* (2001) A novel regulator of G-protein signaling bearing GAP activity for Galphai and Galphaq in megakaryocytes. *Blood* 97(10):3051-3060.

218. Park IK*, et al.* (2001) Molecular cloning and characterization of a novel regulator of G-protein signaling from mouse hematopoietic stem cells. *J Biol Chem* 276(2):915-923.

219. Yowe D*, et al.* (2001) RGS18 is a myeloerythroid lineage-specific regulator of G-protein-signalling molecule highly expressed in megakaryocytes. *Biochem J* 359(Pt 1):109-118.

220. Gagnon AW, Murray DL, & Leadley RJ (2002) Cloning and characterization of a novel regulator of G protein signalling in human platelets. *Cell Signal* 14(7):595-606.

221. Ma P*, et al.* (2012) A newly identified complex of spinophilin and the tyrosine phosphatase, SHP-1, modulates platelet activation by regulating G protein-dependent signaling. *Blood* 119(8):1935-1945.

222. Gegenbauer K, Elia G, Blanco-Fernandez A, & Smolenski A (2012) Regulator of G-protein signaling 18 integrates activating and inhibitory signaling in platelets. *Blood* 119(16):3799-3807.

223. Alshbool FZ*, et al.* (2015) The regulator of G-protein signaling 18 regulates platelet aggregation, hemostasis and thrombosis. *Biochem Biophys Res Commun* 462(4):378-382.

224. Delesque-Touchard N*, et al.* (2014) Regulator of G-protein signaling 18 controls both platelet generation and function. *PLoS One* 9(11):e113215.

225. Mao Y*, et al.* (2014) Regulators of G protein signaling are up-regulated in aspirin-resistant platelets from patients with metabolic syndrome. *Pharmazie* 69(5):371-373.

226. Haggmark A*, et al.* (2014) Plasma profiling reveals three proteins associated to amyotrophic lateral sclerosis. *Ann Clin Transl Neurol* 1(8):544-553.

227. Schosser A*, et al.* (2011) Genomewide association scan of suicidal thoughts and behaviour in major depression. *PLoS One* 6(7):e20690.

228. von Buchholtz L*, et al.* (2004) RGS21 is a novel regulator of G protein signalling selectively expressed in subpopulations of taste bud cells. *Eur J Neurosci* 19(6):1535-1544.

229. Li X*, et al.* (2005) Isolation and expression pattern of RGS21 gene, a novel RGS member. *Acta Biochim Pol* 52(4):943-946.

230. Cohen SP*, et al.* (2012) Regulator of G-protein signaling-21 (RGS21) is an inhibitor of bitter gustatory signaling found in lingual and airway epithelia. *J Biol Chem*

287(50):41706-41719.

231. Sharma A*, et al.* (2016) Identification of Non-HLA Genes Associated with Celiac Disease and Country-Specific Differences in a Large, International Pediatric Cohort. *PLoS One* 11(3):e0152476.

232. Anderson GR, Posokhova E, & Martemyanov KA (2009) The R7 RGS protein family: multi-subunit regulators of neuronal G protein signaling. *Cell Biochem Biophys* 54(1-3):33-46.

233. Sjogren B (2011) Regulator of G protein signaling proteins as drug targets: current state and future possibilities. *Adv Pharmacol* 62:315-347.

234. Snow BE*, et al.* (1998) A G protein gamma subunit-like domain shared between RGS11 and other RGS proteins specifies binding to Gbeta5 subunits. *Proc Natl Acad Sci U S A* 95(22):13307-13312.

235. Masuho I, Xie K, & Martemyanov KA (2013) Macromolecular composition dictates receptor and G protein selectivity of regulator of G protein signaling (RGS) 7 and 9-2 protein complexes in living cells. *J Biol Chem* 288(35):25129-25142.

236. Stewart A*, et al.* (2015) Regulator of G protein signaling 6 is a critical mediator of both reward-related behavioral and pathological responses to alcohol. *Proc Natl Acad Sci U S A* 112(7):E786-795.

237. Posner BA, Gilman AG, & Harris BA (1999) Regulators of G protein signaling 6 and 7. Purification of complexes with gbeta5 and assessment of their effects on g protein-mediated signaling pathways. *J Biol Chem* 274(43):31087-31093.

238. Hooks SB*, et al.* (2003) RGS6, RGS7, RGS9, and RGS11 stimulate GTPase activity of Gi family G-proteins with differential selectivity and maximal activity. *J Biol Chem* 278(12):10087-10093.

239. He W*, et al.* (2000) Modules in the photoreceptor RGS9-1.Gbeta 5L GTPase-accelerating protein complex control effector coupling, GTPase acceleration, protein folding, and

stability. *J Biol Chem* 275(47):37093-37100.

240. Martemyanov KA & Arshavsky VY (2004) Kinetic approaches to study the function of RGS9 isoforms. *Methods Enzymol* 390:196-209.

241. Yang J*, et al.* (2010) RGS6, a modulator of parasympathetic activation in heart. *Circ Res* 107(11):1345-1349.

242. Stewart A*, et al.* (2014) Regulator of G-protein signaling 6 (RGS6) promotes anxiety and depression by attenuating serotonin-mediated activation of the 5-HT(1A) receptor-adenylyl cyclase axis. *FASEB J* 28(4):1735-1744.

243. Bifsha P, Yang J, Fisher RA, & Drouin J (2014) Rgs6 is required for adult maintenance of dopaminergic neurons in the ventral substantia nigra. *PLoS Genet* 10(12):e1004863.

244. Moon SW*, et al.* (2015) Structural Neuroimaging Genetics Interactions in Alzheimer's Disease. *J Alzheimers Dis* 48(4):1051-1063.

245. Schizophrenia Working Group of the Psychiatric Genomics C (2014) Biological insights from 108 schizophrenia-associated genetic loci. *Nature* 511(7510):421-427.

246. Chograni M, Alkuraya FS, Maazoul F, Lariani I, & Chaabouni-Bouhamed H (2014) RGS6: a novel gene associated with congenital cataract, mental retardation, and microcephaly in a Tunisian family. *Invest Ophthalmol Vis Sci* 56(2):1261-1266.

247. Li J, Dani JA, & Le W (2009) The role of transcription factor Pitx3 in dopamine neuron development and Parkinson's disease. *Curr Top Med Chem* 9(10):855-859.

248. Kuusisto J, Mykkanen L, Kervinen K, Kesaniemi YA, & Laakso M (1995) Apolipoprotein E4 phenotype is not an important risk factor for coronary heart disease or stroke in elderly subjects. *Arterioscler Thromb Vasc Biol* 15(9):1280-1286.

249. Verghese PB, Castellano JM, & Holtzman DM (2011) Apolipoprotein E in Alzheimer's disease and other neurological disorders. *Lancet Neurol* 10(3):241-252.

250. Berman DM*, et al.* (2004) A functional polymorphism in RGS6 modulates the risk of bladder cancer. *Cancer Res* 64(18):6820-6826.

251. Maity B, *et al.* (2013) Regulator of G protein signaling 6 is a novel suppressor of breast tumor initiation and progression. *Carcinogenesis* 34(8):1747-1755.

252. Maity B, *et al.* (2011) Regulator of G protein signaling 6 (RGS6) induces apoptosis via a mitochondrial-dependent pathway not involving its GTPase-activating protein activity. *J Biol Chem* 286(2):1409-1419.

253. Hohoff C, *et al.* (2009) Association analysis of Rgs7 variants with panic disorder. *J Neural Transm (Vienna)* 116(11):1523-1528.

254. Sutton LP, *et al.* (2016) Regulator of G-Protein Signaling 7 Regulates Reward Behavior by Controlling Opioid Signaling in the Striatum. *Biol Psychiatry* 80(3):235-245.

255. Crowe RR, *et al.* (2001) Genomewide survey of panic disorder. *Am J Med Genet* 105(1):105-109.

256. Gelernter J, *et al.* (2001) Linkage genome scan for loci predisposing to panic disorder or agoraphobia. *Am J Med Genet* 105(6):548-557.

257. McCauley JL, *et al.* (2009) Follow-up examination of linkage and association to chromosome 1q43 in multiple sclerosis. *Genes Immun* 10(7):624-630.

258. He W, Cowan CW, & Wensel TG (1998) RGS9, a GTPase accelerator for phototransduction. *Neuron* 20(1):95-102.

259. Zhang K, *et al.* (1999) Structure, alternative splicing, and expression of the human RGS9 gene. *Gene* 240(1):23-34.

260. Traynor JR, Terzi D, Caldarone BJ, & Zachariou V (2009) RGS9-2: probing an intracellular modulator of behavior as a drug target. *Trends Pharmacol Sci* 30(3):105-111.

261. Michaelides M, *et al.* (2010) Novel mutations and electrophysiologic findings in RGS9- and R9AP-associated retinal dysfunction (Bradyopsia). *Ophthalmology* 117(1):120-127 e121.

262. Nishiguchi KM, *et al.* (2004) Defects in RGS9 or its anchor protein R9AP in patients with slow photoreceptor deactivation. *Nature* 427(6969):75-78.

263. Cheng JY*, et al.* (2007) Bradyopsia in an Asian man. *Arch Ophthalmol* 125(8):1138-1140.

264. Hartong DT, Pott JW, & Kooijman AC (2007) Six patients with bradyopsia (slow vision): clinical features and course of the disease. *Ophthalmology* 114(12):2323-2331.

265. Stockman A*, et al.* (2008) The loss of the PDE6 deactivating enzyme, RGS9, results in precocious light adaptation at low light levels. *J Vis* 8(1):10 11-10.

266. Thomas EA, Danielson PE, & Sutcliffe JG (1998) RGS9: a regulator of G-protein signalling with specific expression in rat and mouse striatum. *J Neurosci Res* 52(1):118-124.

267. Rahman Z*, et al.* (2003) RGS9 modulates dopamine signaling in the basal ganglia. *Neuron* 38(6):941-952.

268. Liou YJ*, et al.* (2009) Analysis of genetic variations in the RGS9 gene and antipsychotic-induced tardive dyskinesia in schizophrenia. *Am J Med Genet B Neuropsychiatr Genet* 150B(2):239-242.

269. Kovoor A*, et al.* (2005) D2 dopamine receptors colocalize regulator of G-protein signaling 9-2 (RGS9-2) via the RGS9 DEP domain, and RGS9 knock-out mice develop dyskinesias associated with dopamine pathways. *J Neurosci* 25(8):2157-2165.

270. Celver J, Sharma M, & Kovoor A (2010) RGS9-2 mediates specific inhibition of agonist-induced internalization of D2-dopamine receptors. *J Neurochem* 114(3):739-749.

271. Cabrera-Vera TM*, et al.* (2004) RGS9-2 modulates D2 dopamine receptor-mediated Ca2+ channel inhibition in rat striatal cholinergic interneurons. *Proc Natl Acad Sci U S A* 101(46):16339-16344.

272. Waugh JL*, et al.* (2011) Association between regulator of G protein signaling 9-2 and body weight. *PLoS One* 6(11):e27984.

273. Zachariou V*, et al.* (2003) Essential role for RGS9 in opiate action. *Proc Natl Acad Sci U S A* 100(23):13656-13661.

274. Psifogeorgou K*, et al.* (2007) RGS9-2 is a negative modulator of mu-opioid receptor

function. *J Neurochem* 103(2):617-625.

275. Psifogeorgou K*, et al.* (2011) A unique role of RGS9-2 in the striatum as a positive or negative regulator of opiate analgesia. *J Neurosci* 31(15):5617-5624.

276. Hooks SB, Martemyanov K, & Zachariou V (2008) A role of RGS proteins in drug addiction. *Biochem Pharmacol* 75(1):76-84.

277. Bodnar RJ (2004) Endogenous opioids and feeding behavior: a 30-year historical perspective. *Peptides* 25(4):697-725.

278. Gainetdinov RR (2007) Mesolimbic dopamine in obesity and diabetes. *Am J Physiol Regul Integr Comp Physiol* 293(2):R601-602.

279. Johnson PM & Kenny PJ (2010) Dopamine D2 receptors in addiction-like reward dysfunction and compulsive eating in obese rats. *Nat Neurosci* 13(5):635-641.

280. Le Merrer J, Becker JA, Befort K, & Kieffer BL (2009) Reward processing by the opioid system in the brain. *Physiol Rev* 89(4):1379-1412.

281. Blundell J, Hoang CV, Potts B, Gold SJ, & Powell CM (2008) Motor coordination deficits in mice lacking RGS9. *Brain Res* 1190:78-85.

282. Shim H*, et al.* (2012) Defective retinal depolarizing bipolar cells in regulators of G protein signaling (RGS) 7 and 11 double null mice. *J Biol Chem* 287(18):14873-14879.

283. Rao A, Dallman R, Henderson S, & Chen CK (2007) Gbeta5 is required for normal light responses and morphology of retinal ON-bipolar cells. *J Neurosci* 27(51):14199-14204.

284. Cao Y*, et al.* (2012) Regulators of G protein signaling RGS7 and RGS11 determine the onset of the light response in ON bipolar neurons. *Proc Natl Acad Sci U S A* 109(20):7905-7910.

285. Yang SH*, et al.* (2016) Overexpression of regulator of G protein signaling 11 promotes cell migration and associates with advanced stages and aggressiveness of lung adenocarcinoma. *Oncotarget* 7(21):31122-31136.

286. Martinez-Cardus A*, et al.* (2009) Pharmacogenomic approach for the identification of

novel determinants of acquired resistance to oxaliplatin in colorectal cancer. *Mol Cancer Ther* 8(1):194-202.

287. Waugh JL*, et al.* (2005) Regional, cellular, and subcellular localization of RGS10 in rodent brain. *J Comp Neurol* 481(3):299-313.

288. Shu FJ, Ramineni S, Amyot W, & Hepler JR (2007) Selective interactions between Gi alpha1 and Gi alpha3 and the GoLoco/GPR domain of RGS14 influence its dynamic subcellular localization. *Cell Signal* 19(1):163-176.

289. Cho H, Kim DU, & Kehrl JH (2005) RGS14 is a centrosomal and nuclear cytoplasmic shuttling protein that traffics to promyelocytic leukemia nuclear bodies following heat shock. *J Biol Chem* 280(1):805-814.

290. Chatterjee TK & Fisher RA (2002) RGS12TS-S localizes at nuclear matrix-associated subnuclear structures and represses transcription: structural requirements for subnuclear targeting and transcriptional repression. *Mol Cell Biol* 22(12):4334-4345.

291. Willard FS*, et al.* (2009) Regulator of G-protein signaling 14 (RGS14) is a selective H-Ras effector. *PLoS One* 4(3):e4884.

292. Shu FJ, Ramineni S, & Hepler JR (2010) RGS14 is a multifunctional scaffold that integrates G protein and Ras/Raf MAPkinase signalling pathways. *Cell Signal* 22(3):366-376.

293. Vellano CP, Brown NE, Blumer JB, & Hepler JR (2013) Assembly and function of the regulator of G protein signaling 14 (RGS14).H-Ras signaling complex in live cells are regulated by Galphai1 and Galphai-linked G protein-coupled receptors. *J Biol Chem* 288(5):3620-3631.

294. Traver S*, et al.* (2000) RGS14 is a novel Rap effector that preferentially regulates the GTPase activity of galphao. *Biochem J* 350 Pt 1:19-29.

295. Kimple RJ*, et al.* (2001) RGS12 and RGS14 GoLoco motifs are G alpha(i) interaction sites with guanine nucleotide dissociation inhibitor Activity. *J Biol Chem* 276(31):29275-

29281.

296. Kimple RJ, Kimple ME, Betts L, Sondek J, & Siderovski DP (2002) Structural determinants for GoLoco-induced inhibition of nucleotide release by Galpha subunits. *Nature* 416(6883):878-881.

297. Kimple RJ, Willard FS, & Siderovski DP (2004) Purification and in vitro functional analyses of RGS12 and RGS14 GoLoco motif peptides. *Methods Enzymol* 390:416-436.

298. Mittal V & Linder ME (2004) The RGS14 GoLoco domain discriminates among Galphai isoforms. *J Biol Chem* 279(45):46772-46778.

299. Brown NE, *et al.* (2015) Integration of G protein alpha (Galpha) signaling by the regulator of G protein signaling 14 (RGS14). *J Biol Chem* 290(14):9037-9049.

300. Chatterjee TK & Fisher RA (2000) Novel alternative splicing and nuclear localization of human RGS12 gene products. *J Biol Chem* 275(38):29660-29671.

301. Dunn HA & Ferguson SS (2015) PDZ Protein Regulation of G Protein-Coupled Receptor Trafficking and Signaling Pathways. *Mol Pharmacol* 88(4):624-639.

302. Snow BE, *et al.* (1998) GTPase activating specificity of RGS12 and binding specificity of an alternatively spliced PDZ (PSD-95/Dlg/ZO-1) domain. *J Biol Chem* 273(28):17749-17755.

303. Sambi BS, *et al.* (2006) The effect of RGS12 on PDGFbeta receptor signalling to p42/p44 mitogen activated protein kinase in mammalian cells. *Cell Signal* 18(7):971-981.

304. Haller C, Fillatreau S, Hoffmann R, & Agenes F (2002) Structure, chromosomal localization and expression of the mouse regulator of G-protein signaling10 gene (mRGS10). *Gene* 297(1-2):39-49.

305. Ajit SK & Young KH (2005) Analysis of chimeric RGS proteins in yeast for the functional evaluation of protein domains and their potential use in drug target validation. *Cell Signal* 17(7):817-825.

306. Lee JK, *et al.* (2008) Regulator of G-protein signaling 10 promotes dopaminergic neuron

survival via regulation of the microglial inflammatory response. *J Neurosci* 28(34):8517-8528.

307. Lee JK, Chung J, McAlpine FE, & Tansey MG (2011) Regulator of G-protein signaling-10 negatively regulates NF-kappaB in microglia and neuroprotects dopaminergic neurons in hemiparkinsonian rats. *J Neurosci* 31(33):11879-11888.

308. Tansey MG & Goldberg MS (2010) Neuroinflammation in Parkinson's disease: its role in neuronal death and implications for therapeutic intervention. *Neurobiol Dis* 37(3):510-518.

309. Hishimoto A*, et al.* (2004) Novel missense polymorphism in the regulator of G-protein signaling 10 gene: analysis of association with schizophrenia. *Psychiatry Clin Neurosci* 58(5):579-581.

310. Lee JK, Chung J, Kannarkat GT, & Tansey MG (2013) Critical role of regulator G-protein signaling 10 (RGS10) in modulating macrophage M1/M2 activation. *PLoS One* 8(11):e81785.

311. Hensch NR, Karim ZA, Druey KM, Tansey MG, & Khasawneh FT (2016) RGS10 Negatively Regulates Platelet Activation and Thrombogenesis. *PLoS One* 11(11):e0165984.

312. Lee JK*, et al.* (2016) RGS10 deficiency ameliorates the severity of disease in experimental autoimmune encephalomyelitis. *J Neuroinflammation* 13:24.

313. Kannarkat GT*, et al.* (2015) Age-related changes in regulator of G-protein signaling (RGS)-10 expression in peripheral and central immune cells may influence the risk for age-related degeneration. *Neurobiol Aging* 36(5):1982-1993.

314. Hooks SB & Murph MM (2015) Cellular deficiency in the RGS10 protein facilitates chemoresistant ovarian cancer. *Future Med Chem* 7(12):1483-1489.

315. Cacan E, Ali MW, Boyd NH, Hooks SB, & Greer SF (2014) Inhibition of HDAC1 and DNMT1 modulate RGS10 expression and decrease ovarian cancer chemoresistance. *PLoS One* 9(1):e87455.

316. Ali MW*, et al.* (2013) Transcriptional suppression, DNA methylation, and histone deacetylation of the regulator of G-protein signaling 10 (RGS10) gene in ovarian cancer cells. *PLoS One* 8(3):e60185.

317. Hooks SB*, et al.* (2010) Regulators of G-Protein signaling RGS10 and RGS17 regulate chemoresistance in ovarian cancer cells. *Mol Cancer* 9:289.

318. Altman MK*, et al.* (2015) Suppression of the GTPase-activating protein RGS10 increases Rheb-GTP and mTOR signaling in ovarian cancer cells. *Cancer Lett* 369(1):175-183.

319. Lee JK & Tansey MG (2015) Physiology of RGS10 in Neurons and Immune Cells. *Prog Mol Biol Transl Sci* 133:153-167.

320. Snow BE, Antonio L, Suggs S, Gutstein HB, & Siderovski DP (1997) Molecular cloning and expression analysis of rat Rgs12 and Rgs14. *Biochem Biophys Res Commun* 233(3):770-777.

321. Ponting CP (1999) Raf-like Ras/Rap-binding domains in RGS12- and still-life-like signalling proteins. *J Mol Med (Berl)* 77(10):695-698.

322. Richman RW*, et al.* (2005) RGS12 interacts with the SNARE-binding region of the Cav2.2 calcium channel. *J Biol Chem* 280(2):1521-1528.

323. Schiff ML*, et al.* (2000) Tyrosine-kinase-dependent recruitment of RGS12 to the N-type calcium channel. *Nature* 408(6813):723-727.

324. Xu B*, et al.* (2011) Exome sequencing supports a de novo mutational paradigm for schizophrenia. *Nat Genet* 43(9):864-868.

325. Doupnik CA, Xu T, & Shinaman JM (2001) Profile of RGS expression in single rat atrial myocytes. *Biochim Biophys Acta* 1522(2):97-107.

326. Lopez-Aranda MF, Acevedo MJ, Carballo FJ, Gutierrez A, & Khan ZU (2006) Localization of the GoLoco motif carrier regulator of G-protein signalling 12 and 14 proteins in monkey and rat brain. *Eur J Neurosci* 23(11):2971-2982.

327. Yang S & Li YP (2007) RGS12 is essential for RANKL-evoked signaling for terminal

differentiation of osteoclasts in vitro. *J Bone Miner Res* 22(1):45-54.

328. Yang S*, et al.* (2013) Mx1-cre mediated Rgs12 conditional knockout mice exhibit increased bone mass phenotype. *Genesis* 51(3):201-209.

329. Yuan X*, et al.* (2015) Regulators of G protein signaling 12 promotes osteoclastogenesis in bone remodeling and pathological bone loss. *Cell Death Differ* 22(12):2046-2057.

330. Huang J*, et al.* (2016) Pivotal Role of Regulator of G-protein Signaling 12 in Pathological Cardiac Hypertrophy. *Hypertension* 67(6):1228-1236.

331. Dai J*, et al.* (2011) Genetic variations in the regulator of G-protein signaling genes are associated with survival in late-stage non-small cell lung cancer. *PLoS One* 6(6):e21120.

332. Wang Y*, et al.* (2017) RGS12 Is a Novel Tumor-Suppressor Gene in African American Prostate Cancer That Represses AKT and MNX1 Expression. *Cancer Res* 77(16):4247-4257.

333. Hollinger S, Taylor JB, Goldman EH, & Hepler JR (2001) RGS14 is a bifunctional regulator of Galphai/o activity that exists in multiple populations in brain. *J Neurochem* 79(5):941-949.

334. Li Y*, et al.* (2016) Regulator of G protein signalling 14 attenuates cardiac remodelling through the MEK-ERK1/2 signalling pathway. *Basic Res Cardiol* 111(4):47.

335. Squires KE*, et al.* (2017) Regulator of G protein signaling 14 (RGS14) is expressed pre- and postsynaptically in neurons of hippocampus, basal ganglia, and amygdala of monkey and human brain. *Brain Struct Funct*.

336. Ryu J*, et al.* (2014) Profile of differential promoter activity by nucleotide substitution at GWAS signals for multiple sclerosis. *Medicine (Baltimore)* 93(28):e281.

337. Sevastou I, Pryce G, Baker D, & Selwood DL (2016) Characterisation of Transcriptional Changes in the Spinal Cord of the Progressive Experimental Autoimmune Encephalomyelitis Biozzi ABH Mouse Model by RNA Sequencing. *PLoS One* 11(6):e0157754.

338. Lee SE, *et al.* (2010) RGS14 is a natural suppressor of both synaptic plasticity in CA2 neurons and hippocampal-based learning and memory. *Proc Natl Acad Sci U S A* 107(39):16994-16998.

339. Dudek SM, Alexander GM, & Farris S (2016) Rediscovering area CA2: unique properties and functions. *Nat Rev Neurosci* 17(2):89-102.

340. Alexander GM, *et al.* (2016) Social and novel contexts modify hippocampal CA2 representations of space. *Nat Commun* 7:10300.

341. Hitti FL & Siegelbaum SA (2014) The hippocampal CA2 region is essential for social memory. *Nature* 508(7494):88-92.

342. Piskorowski RA, *et al.* (2016) Age-Dependent Specific Changes in Area CA2 of the Hippocampus and Social Memory Deficit in a Mouse Model of the 22q11.2 Deletion Syndrome. *Neuron* 89(1):163-176.

343. Vogt IR, *et al.* (2006) Transcriptional changes in multiple system atrophy and Parkinson's disease putamen. *Exp Neurol* 199(2):465-478.

344. Mahajan A, *et al.* (2016) Trans-ethnic Fine Mapping Highlights Kidney-Function Genes Linked to Salt Sensitivity. *Am J Hum Genet* 99(3):636-646.

345. Yasui T, *et al.* (2013) A replication study for three nephrolithiasis loci at 5q35.3, 7p14.3 and 13q14.1 in the Japanese population. *J Hum Genet* 58(9):588-593.

346. Urabe Y, *et al.* (2012) A genome-wide association study of nephrolithiasis in the Japanese population identifies novel susceptible Loci at 5q35.3, 7p14.3, and 13q14.1. *PLoS Genet* 8(3):e1002541.

347. Robinson-Cohen C, *et al.* (2017) Genetic Variants Associated with Circulating Parathyroid Hormone. *J Am Soc Nephrol* 28(5):1553-1565.

348. Kestenbaum B, *et al.* (2010) Common genetic variants associate with serum phosphorus concentration. *J Am Soc Nephrol* 21(7):1223-1232.

349. Nunn C, Mao H, Chidiac P, & Albert PR (2006) RGS17/RGSZ2 and the RZ/A family of

regulators of G-protein signaling. *Semin Cell Dev Biol* 17(3):390-399.

350. De Vries L, Elenko E, Hubler L, Jones TL, & Farquhar MG (1996) GAIP is membrane-anchored by palmitoylation and interacts with the activated (GTP-bound) form of G alpha i subunits. *Proc Natl Acad Sci U S A* 93(26):15203-15208.

351. Mao H*, et al.* (2004) RGS17/RGSZ2, a novel regulator of Gi/o, Gz, and Gq signaling. *J Biol Chem* 279(25):26314-26322.

352. Sierra DA*, et al.* (2002) Evolution of the regulators of G-protein signaling multigene family in mouse and human. *Genomics* 79(2):177-185.

353. Glick JL, Meigs TE, Miron A, & Casey PJ (1998) RGSZ1, a Gz-selective regulator of G protein signaling whose action is sensitive to the phosphorylation state of Gzalpha. *J Biol Chem* 273(40):26008-26013.

354. Tu Y, Wang J, & Ross EM (1997) Inhibition of brain Gz GAP and other RGS proteins by palmitoylation of G protein alpha subunits. *Science* 278(5340):1132-1135.

355. James MA, Lu Y, Liu Y, Vikis HG, & You M (2009) RGS17, an overexpressed gene in human lung and prostate cancer, induces tumor cell proliferation through the cyclic AMP-PKA-CREB pathway. *Cancer Res* 69(5):2108-2116.

356. Hayes MP & Roman DL (2016) Regulator of G Protein Signaling 17 as a Negative Modulator of GPCR Signaling in Multiple Human Cancers. *AAPS J* 18(3):550-559.

357. You M*, et al.* (2009) Fine mapping of chromosome 6q23-25 region in familial lung cancer families reveals RGS17 as a likely candidate gene. *Clin Cancer Res* 15(8):2666-2674.

358. Shelton RC*, et al.* (2011) Altered expression of genes involved in inflammation and apoptosis in frontal cortex in major depression. *Mol Psychiatry* 16(7):751-762.

359. Zhang H, Wang F, Kranzler HR, Anton RF, & Gelernter J (2012) Variation in regulator of G-protein signaling 17 gene (RGS17) is associated with multiple substance dependence diagnoses. *Behav Brain Funct* 8:23.

360. Yoon D*, et al.* (2012) Large-scale genome-wide association study of Asian population

reveals genetic factors in FRMD4A and other loci influencing smoking initiation and nicotine dependence. *Hum Genet* 131(6):1009-1021.

361. Ji YR*, et al.* (2015) Critical role of Rgs19 in mouse embryonic stem cell proliferation and differentiation. *Differentiation* 89(1-2):42-50.

362. Garzon J, Rodriguez-Munoz M, Lopez-Fando A, Garcia-Espana A, & Sanchez-Blazquez P (2004) RGSZ1 and GAIP regulate mu- but not delta-opioid receptors in mouse CNS: role in tachyphylaxis and acute tolerance. *Neuropsychopharmacology* 29(6):1091-1104.

363. Igci M*, et al.* (2016) Gene expression profiles of autophagy-related genes in multiple sclerosis. *Gene* 588(1):38-46.

364. Tso PH, Yung LY, Wang Y, & Wong YH (2011) RGS19 stimulates cell proliferation by deregulating cell cycle control and enhancing Akt signaling. *Cancer Lett* 309(2):199-208.

365. Wang Q & Traynor JR (2013) Modulation of mu-opioid receptor signaling by RGS19 in SH-SY5Y cells. *Mol Pharmacol* 83(2):512-520.

366. Wang Y, Tong Y, Tso PH, & Wong YH (2013) Regulator of G protein signaling 19 suppresses Ras-induced neoplastic transformation and tumorigenesis. *Cancer Lett* 339(1):33-41.

367. Ji YR*, et al.* (2010) Effects of regulator of G protein signaling 19 (RGS19) on heart development and function. *J Biol Chem* 285(37):28627-28634.

368. Wang J*, et al.* (1998) RGSZ1, a Gz-selective RGS protein in brain. Structure, membrane association, regulation by Galphaz phosphorylation, and relationship to a Gz gtpase-activating protein subfamily. *J Biol Chem* 273(40):26014-26025.

369. Wang Y*, et al.* (2002) Regulator of G protein signaling Z1 (RGSZ1) interacts with Galpha i subunits and regulates Galpha i-mediated cell signaling. *J Biol Chem* 277(50):48325-48332.

370. Yang L, Lee MM, Leung MM, & Wong YH (2016) Regulator of G protein signaling 20 enhances cancer cell aggregation, migration, invasion and adhesion. *Cell Signal*

28(11):1663-1672.

371. Barker SA, Wang J, Sierra DA, & Ross EM (2001) RGSZ1 and Ret RGS: two of several splice variants from the gene RGS20. *Genomics* 78(3):223-229.

372. Li Q*, et al.* (2017) Regulator of G protein signaling 20 correlates with clinicopathological features and prognosis in triple-negative breast cancer. *Biochem Biophys Res Commun* 485(3):693-697.

373. Kohara K*, et al.* (2008) Identification of hypertension-susceptibility genes and pathways by a systemic multiple candidate gene approach: the millennium genome project for hypertension. *Hypertens Res* 31(2):203-212.

374. Lundstrom K (2009) An overview on GPCRs and drug discovery: structure-based drug design and structural biology on GPCRs. *Methods Mol Biol* 552:51-66.

375. Bologna Z, Teoh JP, Bayoumi AS, Tang Y, & Kim IM (2017) Biased G Protein-Coupled Receptor Signaling: New Player in Modulating Physiology and Pathology. *Biomol Ther (Seoul)* 25(1):12-25.

376. Sjogren B, Blazer LL, & Neubig RR (2010) Regulators of G protein signaling proteins as targets for drug discovery. *Prog Mol Biol Transl Sci* 91:81-119.

377. Neubig RR & Siderovski DP (2002) Regulators of G-protein signalling as new central nervous system drug targets. *Nat Rev Drug Discov* 1(3):187-197.

378. Hayes MP, Bodle CR, & Roman DL (2018) Evaluation of the Selectivity and Cysteine Dependence of Inhibitors across the Regulator of G Protein-Signaling Family. *Mol Pharmacol* 93(1):25-35.

379. Cardon LR & Harris T (2016) Precision medicine, genomics and drug discovery. *Hum Mol Genet* 25(R2):R166-R172.

380. Hill C, Brownlie Z, Davey J, Milligan G, & Ladds G (2008) Isolation and characterization of a novel human RGS mutant displaying gain-of-function activity. *Cell Signal* 20(2):323-336.

381. Blazer LL, *et al.* (2015) Selectivity and anti-Parkinson's potential of thiadiazolidinone RGS4 inhibitors. *ACS Chem Neurosci* 6(6):911-919.

382. Drenan RM, *et al.* (2006) R7BP augments the function of RGS7*Gbeta5 complexes by a plasma membrane-targeting mechanism. *J Biol Chem* 281(38):28222-28231.

383. Chen CK, *et al.* (2003) Instability of GGL domain-containing RGS proteins in mice lacking the G protein beta-subunit Gbeta5. *Proc Natl Acad Sci U S A* 100(11):6604-6609.

384. Ding L & Hegde AN (2009) Expression of RGS4 splice variants in dorsolateral prefrontal cortex of schizophrenic and bipolar disorder patients. *Biol Psychiatry* 65(6):541-545.

385. Vural A, *et al.* (2013) Normal autophagic activity in macrophages from mice lacking Galphai3, AGS3, or RGS19. *PLoS One* 8(11):e81886.

386. Dewhurst HM & Torres MP (2017) Systematic analysis of non-structural protein features for the prediction of PTM function potential by artificial neural networks. *PLoS One* 12(2):e0172572.

387. Brown NE, Blumer JB, & Hepler JR (2015) Bioluminescence resonance energy transfer to detect protein-protein interactions in live cells. *Methods Mol Biol* 1278:457-465.

388. Hunter S, *et al.* (2009) InterPro: the integrative protein signature database. *Nucleic Acids Res* 37(Database issue):D211-215.

389. Edgar RC (2004) MUSCLE: a multiple sequence alignment method with reduced time and space complexity. *BMC Bioinformatics* 5:113.

390. Hornbeck PV, *et al.* (2015) PhosphoSitePlus, 2014: mutations, PTMs and recalibrations. *Nucleic Acids Res* 43(Database issue):D512-520.

391. Bairoch A, *et al.* (2005) The Universal Protein Resource (UniProt). *Nucleic Acids Res* 33(Database issue):D154-159.

392. Ding L, Mychaleckyj JC, & Hegde AN (2007) Full length cloning and expression analysis of splice variants of regulator of G-protein signaling RGS4 in human and murine brain. *Gene* 401(1-2):46-60.

393. Slep KC*, et al.* (2001) Structural determinants for regulation of phosphodiesterase by a G protein at 2.0 A. *Nature* 409(6823):1071-1077.

394. Skiba NP, Yang CS, Huang T, Bae H, & Hamm HE (1999) The alpha-helical domain of Galphat determines specific interaction with regulator of G protein signaling 9. *J Biol Chem* 274(13):8770-8778.

395. Rahman Z*, et al.* (1999) Cloning and characterization of RGS9-2: a striatal-enriched alternatively spliced product of the RGS9 gene. *J Neurosci* 19(6):2016-2026.

396. Seeman P, Ko F, Jack E, Greenstein R, & Dean B (2007) Consistent with dopamine supersensitivity, RGS9 expression is diminished in the amphetamine-treated animal model of schizophrenia and in postmortem schizophrenia brain. *Synapse* 61(5):303-309.

397. Anderson GR, Semenov A, Song JH, & Martemyanov KA (2007) The membrane anchor R7BP controls the proteolytic stability of the striatal specific RGS protein, RGS9-2. *J Biol Chem* 282(7):4772-4781.

398. Soundararajan M*, et al.* (2008) Structural diversity in the RGS domain and its interaction with heterotrimeric G protein alpha-subunits. *Proc Natl Acad Sci U S A* 105(17):6457-6462.

399. Rivero G*, et al.* (2010) Characterization of regulators of G-protein signaling RGS4 and RGS10 proteins in the postmortem human brain. *Neurochem Int* 57(7):722-729.

400. Betke KM, Wells CA, & Hamm HE (2012) GPCR mediated regulation of synaptic transmission. *Prog Neurobiol* 96(3):304-321.

401. Gong B & Wang YT (2012) Directional gating of synaptic plasticity by GPCRs and their distinct downstream signalling pathways. *EMBO J* 31(4):783-785.

402. Lopez de Maturana R & Sanchez-Pernaute R (2010) Regulation of corticostriatal synaptic plasticity by G protein-coupled receptors. *CNS Neurol Disord Drug Targets* 9(5):601-615.

403. Zhao M, Choi YS, Obrietan K, & Dudek SM (2007) Synaptic plasticity (and the lack thereof) in hippocampal CA2 neurons. *J Neurosci* 27(44):12025-12032.

404. Evans PR, Lee SE, Smith Y, & Hepler JR (2014) Postnatal developmental expression of regulator of G protein signaling 14 (RGS14) in the mouse brain. *J Comp Neurol* 522(1):186-203.

405. Fung HY, Fu SC, Brautigam CA, & Chook YM (2015) Structural determinants of nuclear export signal orientation in binding to exportin CRM1. *Elife* 4.

406. Jay JJ & Brouwer C (2016) Lollipops in the Clinic: Information Dense Mutation Plots for Precision Medicine. *PLoS One* 11(8):e0160519.

407. Gibson SK & Gilman AG (2006) Gialpha and Gbeta subunits both define selectivity of G protein activation by alpha2-adrenergic receptors. *Proc Natl Acad Sci U S A* 103(1):212-217.

408. Beaudoin GM, 3rd*, et al.* (2012) Culturing pyramidal neurons from the early postnatal mouse hippocampus and cortex. *Nat Protoc* 7(9):1741-1754.

409. Martin-McCaffrey L*, et al.* (2004) RGS14 is a mitotic spindle protein essential from the first division of the mammalian zygote. *Dev Cell* 7(5):763-769.

410. Dong X*, et al.* (2009) Structural basis for leucine-rich nuclear export signal recognition by CRM1. *Nature* 458(7242):1136-1141.

411. Fung HY, Fu SC, & Chook YM (2017) Nuclear export receptor CRM1 recognizes diverse conformations in nuclear export signals. *Elife* 6.

412. Zhao P, Nunn C, Ramineni S, Hepler JR, & Chidiac P (2013) The Ras-binding domain region of RGS14 regulates its functional interactions with heterotrimeric G proteins. *J Cell Biochem* 114(6):1414-1423.

413. Vellano CP, Lee SE, Dudek SM, & Hepler JR (2011) RGS14 at the interface of hippocampal signaling and synaptic plasticity. *Trends Pharmacol Sci* 32(11):666-674.

414. Brown NE, Lambert NA, & Hepler JR (2016) RGS14 regulates the lifetime of Galpha-GTP signaling but does not prolong Gbetagamma signaling following receptor activation in live cells. *Pharmacol Res Perspect* 4(5):e00249.

415. Mittal V & Linder ME (2006) Biochemical characterization of RGS14: RGS14 activity towards G-protein alpha subunits is independent of its binding to Rap2A. *Biochem J* 394(Pt 1):309-315.

416. Ryu J, Futai K, Feliu M, Weinberg R, & Sheng M (2008) Constitutively active Rap2 transgenic mice display fewer dendritic spines, reduced extracellular signal-regulated kinase signaling, enhanced long-term depression, and impaired spatial learning and fear extinction. *J Neurosci* 28(33):8178-8188.

417. Fu Z*, et al.* (2007) Differential roles of Rap1 and Rap2 small GTPases in neurite retraction and synapse elimination in hippocampal spiny neurons. *J Neurochem* 100(1):118-131.

418. Zhu Y*, et al.* (2005) Rap2-JNK removes synaptic AMPA receptors during depotentiation. *Neuron* 46(6):905-916.

419. Qin Y*, et al.* (2005) State-dependent Ras signaling and AMPA receptor trafficking. *Genes Dev* 19(17):2000-2015.

420. Zhu JJ, Qin Y, Zhao M, Van Aelst L, & Malinow R (2002) Ras and Rap control AMPA receptor trafficking during synaptic plasticity. *Cell* 110(4):443-455.

421. Florian C & Roullet P (2004) Hippocampal CA3-region is crucial for acquisition and memory consolidation in Morris water maze task in mice. *Behav Brain Res* 154(2):365-374.

422. Simons SB, Caruana DA, Zhao M, & Dudek SM (2011) Caffeine-induced synaptic potentiation in hippocampal CA2 neurons. *Nat Neurosci* 15(1):23-25.

423. Labouebe G*, et al.* (2007) RGS2 modulates coupling between GABAB receptors and GIRK channels in dopamine neurons of the ventral tegmental area. *Nat Neurosci* 10(12):1559-1568.

424. Han J*, et al.* (2006) RGS2 determines short-term synaptic plasticity in hippocampal neurons by regulating Gi/o-mediated inhibition of presynaptic Ca2+ channels. *Neuron* 51(5):575-586.

425. Gonzales KK, Pare JF, Wichmann T, & Smith Y (2013) GABAergic inputs from direct and indirect striatal projection neurons onto cholinergic interneurons in the primate putamen. *J Comp Neurol* 521(11):2502-2522.

426. Mitrano DA, Pare JF, & Smith Y (2010) Ultrastructural relationships between cortical, thalamic, and amygdala glutamatergic inputs and group I metabotropic glutamate receptors in the rat accumbens. *J Comp Neurol* 518(8):1315-1329.

427. Kuwajima M*, et al.* (2007) Localization and expression of group I metabotropic glutamate receptors in the mouse striatum, globus pallidus, and subthalamic nucleus: regulatory effects of MPTP treatment and constitutive Homer deletion. *J Neurosci* 27(23):6249-6260.

428. Martin-McCaffrey L*, et al.* (2005) RGS14 is a microtubule-associated protein. *Cell Cycle* 4(7):953-960.

429. Kohara K*, et al.* (2014) Cell type-specific genetic and optogenetic tools reveal hippocampal CA2 circuits. *Nat Neurosci* 17(2):269-279.

430. Graveland GA & DiFiglia M (1985) The frequency and distribution of medium-sized neurons with indented nuclei in the primate and rodent neostriatum. *Brain Res* 327(1-2):307-311.

431. Wilson CJ & Groves PM (1980) Fine structure and synaptic connections of the common spiny neuron of the rat neostriatum: a study employing intracellular inject of horseradish peroxidase. *J Comp Neurol* 194(3):599-615.

432. Haber SN & Nauta WJ (1983) Ramifications of the globus pallidus in the rat as indicated by patterns of immunohistochemistry. *Neuroscience* 9(2):245-260.

433. Shink E & Smith Y (1995) Differential synaptic innervation of neurons in the internal and external segments of the globus pallidus by the GABA- and glutamate-containing terminals in the squirrel monkey. *J Comp Neurol* 358(1):119-141.

434. Smith Y, Bevan MD, Shink E, & Bolam JP (1998) Microcircuitry of the direct and indirect pathways of the basal ganglia. *Neuroscience* 86(2):353-387.

435. Difiglia M, Pasik P, & Pasik T (1982) A Golgi and ultrastructural study of the monkey globus pallidus. *J Comp Neurol* 212(1):53-75.

436. Vankova M, Arluison M, Leviel V, & Tramu G (1992) Afferent connections of the rat substantia nigra pars lateralis with special reference to peptide-containing neurons of the amygdalo-nigral pathway. *J Chem Neuroanat* 5(1):39-50.

437. Lee HJ*, et al.* (2005) Role of amygdalo-nigral circuitry in conditioning of a visual stimulus paired with food. *J Neurosci* 25(15):3881-3888.

438. Anderson GR, Lujan R, & Martemyanov KA (2009) Changes in striatal signaling induce remodeling of RGS complexes containing Gbeta5 and R7BP subunits. *Mol Cell Biol* 29(11):3033-3044.

439. Haussler U, Rinas K, Kilias A, Egert U, & Haas CA (2016) Mossy fiber sprouting and pyramidal cell dispersion in the hippocampal CA2 region in a mouse model of temporal lobe epilepsy. *Hippocampus* 26(5):577-588.

440. Gerfen CR*, et al.* (1990) D1 and D2 dopamine receptor-regulated gene expression of striatonigral and striatopallidal neurons. *Science* 250(4986):1429-1432.

441. Albin RL, Young AB, & Penney JB (1989) The functional anatomy of basal ganglia disorders. *Trends Neurosci* 12(10):366-375.

442. Kreitzer AC & Malenka RC (2008) Striatal plasticity and basal ganglia circuit function. *Neuron* 60(4):543-554.

443. Anderson GR*, et al.* (2010) R7BP complexes with RGS9-2 and RGS7 in the striatum differentially control motor learning and locomotor responses to cocaine. *Neuropsychopharmacology* 35(4):1040-1050.

444. Knox D (2016) The role of basal forebrain cholinergic neurons in fear and extinction memory. *Neurobiol Learn Mem* 133:39-52.

445. Bocchio M, McHugh SB, Bannerman DM, Sharp T, & Capogna M (2016) Serotonin, Amygdala and Fear: Assembling the Puzzle. *Front Neural Circuits* 10:24.

446. Lamprecht R (2016) The Role of Actin Cytoskeleton in Memory Formation in Amygdala. *Front Mol Neurosci* 9:23.

447. Lee JH, Lee S, & Kim JH (2016) Amygdala Circuits for Fear Memory: A Key Role for Dopamine Regulation. *Neuroscientist*.

448. Muller JF, Mascagni F, & McDonald AJ (2006) Pyramidal cells of the rat basolateral amygdala: synaptology and innervation by parvalbumin-immunoreactive interneurons. *J Comp Neurol* 494(4):635-650.

449. Mascagni F & McDonald AJ (2003) Immunohistochemical characterization of cholecystokinin containing neurons in the rat basolateral amygdala. *Brain Res* 976(2):171-184.

450. McDonald AJ & Mascagni F (2001) Colocalization of calcium-binding proteins and GABA in neurons of the rat basolateral amygdala. *Neuroscience* 105(3):681-693.

451. Parker CC, Sokoloff G, Cheng R, & Palmer AA (2012) Genome-wide association for fear conditioning in an advanced intercross mouse line. *Behav Genet* 42(3):437-448.

452. Sheynin J & Liberzon I (2017) Circuit dysregulation and circuit-based treatments in posttraumatic stress disorder. *Neurosci Lett* 649:133-138.

453. Minkova L*, et al.* (2017) Task-dependent modulation of amygdala connectivity in social anxiety disorder. *Psychiatry Res* 262:39-46.

454. Branch MR & Hepler JR (2017) Endogenous RGS14 is a cytoplasmic-nuclear shuttling protein that localizes to juxtanuclear membranes and chromatin-rich regions of the nucleus. *PLoS One* 12(9):e0184497.

455. Burgess N, Maguire EA, & O'Keefe J (2002) The human hippocampus and spatial and episodic memory. *Neuron* 35(4):625-641.

456. Sethakorn N, Yau DM, & Dulin NO (2010) Non-canonical functions of RGS proteins. *Cell Signal* 22(9):1274-1281.

457. Huang J & Fisher RA (2009) Nuclear trafficking of regulator of G protein signaling

proteins and their roles in the nucleus. *Prog Mol Biol Transl Sci* 86:115-156.

458. Burchett SA (2003) In through the out door: nuclear localization of the regulators of G protein signaling. *J Neurochem* 87(3):551-559.

459. Chatterjee TK & Fisher RA (2000) Cytoplasmic, nuclear, and golgi localization of RGS proteins. Evidence for N-terminal and RGS domain sequences as intracellular targeting motifs. *J Biol Chem* 275(31):24013-24021.

460. Dulin NO*, et al.* (2000) Regulator of G protein signaling RGS3T is localized to the nucleus and induces apoptosis. *J Biol Chem* 275(28):21317-21323.

461. Zhang JH*, et al.* (2001) Nuclear localization of G protein beta 5 and regulator of G protein signaling 7 in neurons and brain. *J Biol Chem* 276(13):10284-10289.

462. Panicker LM*, et al.* (2010) Nuclear localization of the G protein beta 5/R7-regulator of G protein signaling protein complex is dependent on R7 binding protein. *J Neurochem* 113(5):1101-1112.

463. Song JH, Waataja JJ, & Martemyanov KA (2006) Subcellular targeting of RGS9-2 is controlled by multiple molecular determinants on its membrane anchor, R7BP. *J Biol Chem* 281(22):15361-15369.

464. Hepler JR (2005) R7BP: a surprising new link between G proteins, RGS proteins, and nuclear signaling in the brain. *Sci STKE* 2005(294):pe38.

465. Drenan RM*, et al.* (2005) Palmitoylation regulates plasma membrane-nuclear shuttling of R7BP, a novel membrane anchor for the RGS7 family. *J Cell Biol* 169(4):623-633.

466. Xie Z, Geiger TR, Johnson EN, Nyborg JK, & Druey KM (2008) RGS13 acts as a nuclear repressor of CREB. *Mol Cell* 31(5):660-670.

467. Chatterjee TK, Liu Z, & Fisher RA (2003) Human RGS6 gene structure, complex alternative splicing, and role of N terminus and G protein gamma-subunit-like (GGL) domain in subcellular localization of RGS6 splice variants. *J Biol Chem* 278(32):30261-30271.

468. Chatterjee TK & Fisher RA (2003) Mild heat and proteotoxic stress promote unique subcellular trafficking and nucleolar accumulation of RGS6 and other RGS proteins. Role of the RGS domain in stress-induced trafficking of RGS proteins. *J Biol Chem* 278(32):30272-30282.

469. Rimler A, Jockers R, Lupowitz Z, Sampson SR, & Zisapel N (2006) Differential effects of melatonin and its downstream effector PKCalpha on subcellular localization of RGS proteins. *J Pineal Res* 40(2):144-152.

470. Lee HK*, et al.* (2012) RGS2 is a negative regulator of STAT3-mediated Nox1 expression. *Cell Signal* 24(3):803-809.

471. Wu YL*, et al.* (2008) Regulation of LH receptor and PGF2alpha receptor signaling by the regulator of G protein signaling 2 (RGS2) in human and mouse granulosa cells. *Chin J Physiol* 51(5):282-291.

472. Lee JG*, et al.* (2008) A combination of Lox-1 and Nox1 regulates TLR9-mediated foam cell formation. *Cell Signal* 20(12):2266-2275.

473. Lee HK*, et al.* (2010) Protein kinase C-eta and phospholipase D2 pathway regulates foam cell formation via regulator of G protein signaling 2. *Mol Pharmacol* 78(3):478-485.

474. Willard FS & Crouch MF (2000) Nuclear and cytoskeletal translocation and localization of heterotrimeric G-proteins. *Immunol Cell Biol* 78(4):387-394.

475. Crouch MF, Osborne GW, & Willard FS (2000) The GTP-binding protein G(ialpha) translocates to kinetochores and regulates the M-G(1) cell cycle transition of Swiss 3T3 cells. *Cell Signal* 12(3):153-163.

476. Nicoll RA (2017) A Brief History of Long-Term Potentiation. *Neuron* 93(2):281-290.

477. Thomas GM & Huganir RL (2004) MAPK cascade signalling and synaptic plasticity. *Nat Rev Neurosci* 5(3):173-183.

478. Brambilla R*, et al.* (1997) A role for the Ras signalling pathway in synaptic transmission and long-term memory. *Nature* 390(6657):281-286.

479. Kim CS & Johnston D (2015) A1 adenosine receptor-mediated GIRK channels contribute to the resting conductance of CA1 neurons in the dorsal hippocampus. *J Neurophysiol* 113(7):2511-2523.

480. Gu S, Cifelli C, Wang S, & Heximer SP (2009) RGS proteins: identifying new GAPs in the understanding of blood pressure regulation and cardiovascular function. *Clin Sci (Lond)* 116(5):391-399.

481. Hepler JR, Cladman W, Ramineni S, Hollinger S, & Chidiac P (2005) Novel activity of RGS14 on Goalpha and Gialpha nucleotide binding and hydrolysis distinct from its RGS domain and GDI activity. *Biochemistry* 44(14):5495-5502.

482. Kawabe H*, et al.* (2010) Regulation of Rap2A by the ubiquitin ligase Nedd4-1 controls neurite development. *Neuron* 65(3):358-372.

483. Ohba Y*, et al.* (2000) Rap2 as a slowly responding molecular switch in the Rap1 signaling cascade. *Mol Cell Biol* 20(16):6074-6083.

484. Hepler JR (2014) G protein coupled receptor signaling complexes in live cells. *Cell Logist* 4:e29392.

485. Farrell FX, Yamamoto K, & Lapetina EG (1993) Prenyl group identification of rap2 proteins: a ras superfamily member other than ras that is farnesylated. *Biochem J* 289 (Pt 2):349-355.

486. Lin WC*, et al.* (2014) H-Ras forms dimers on membrane surfaces via a protein-protein interface. *Proc Natl Acad Sci U S A* 111(8):2996-3001.

487. Muratcioglu S*, et al.* (2015) GTP-Dependent K-Ras Dimerization. *Structure* 23(7):1325-1335.

488. Hussain NK, Hsin H, Huganir RL, & Sheng M (2010) MINK and TNIK differentially act on Rap2-mediated signal transduction to regulate neuronal structure and AMPA receptor function. *J Neurosci* 30(44):14786-14794.

489. Taira K*, et al.* (2004) The Traf2- and Nck-interacting kinase as a putative effector of Rap2

to regulate actin cytoskeleton. *J Biol Chem* 279(47):49488-49496.